

University of Warwick institutional repository: <http://go.warwick.ac.uk/wrap>

A Thesis Submitted for the Degree of PhD at the University of Warwick

<http://go.warwick.ac.uk/wrap/62707>

This thesis is made available online and is protected by original copyright.

Please scroll down to view the document itself.

Please refer to the repository record for this item for information to help you to cite it. Our policy information is available from the repository home page.

Screening for Novel Inhibitors of Phospho-MurNAc-pentapeptide Translocase MraY

Agnes Mihalyi

A thesis submitted in partial fulfilment of the requirements
for the degree of

Doctor of Philosophy in Chemistry

University of Warwick

Department of Chemistry

April 2014

Table of Contents

List of Figures	vii
List of Tables.....	xviii
List of Figures in Appendices	xx
List of Abbreviations.....	xxiii
Acknowledgements	xxvii
Declaration	xxviii
Abstract	xxix
1 Introduction	1
1.1 Peptidoglycan biosynthesis and inhibitors	9
1.1.1 Cytoplasmic steps	9
1.1.2 The lipid-linked steps of peptidoglycan biosynthesis	23
1.1.3 Periplasmic steps.....	30
1.2 Enzymology of translocase MraY	36
1.2.1 Initial studies of the MraY reaction	36
1.2.2 Topological model for MraY	38
1.2.3 Catalytic mechanism for the MraY reaction	39
1.2.4 Crystal structure for <i>Aquifex aeolicus</i> MraY	41
1.2.5 Solubilisation, expression and purification of MraY	46
1.2.6 MraY assays	48
1.3 Known inhibitors of MraY	53
1.3.1 Uridyl-peptide inhibitors of MraY	53
1.3.2 Inhibition of MraY by E lysis protein from phage ϕ X174	63
1.3.3 Inhibition of MraY by cyclic peptides and small molecules.....	65
1.4 Aims and objectives of the project	67
2 Development of assay methods for screening MraY	69
2.1 MraY enzymes from various organisms	70

2.2	Development of the fluorescence assay for MraY	75
2.2.1	Preparation of UDP-N-acetylmuramyl-L-Ala- γ -D-Glu- <i>m</i> -Dap -D-Ala-D-Ala (UDPMurNAc-pentapeptide).....	75
2.2.2	Preparation of UDP-N-acetylmuramyl-L-Ala- γ -D-Glu-(N ^e -dansyl)- <i>m</i> -Dap-D-Ala-D-Ala (dansyl-labelled UDPMurNAc-pentapeptide).....	77
2.2.3	Optimisation of the continuous fluorescence assay	83
2.2.4	Continuous fluorescence assays with MraY enzymes from bacteria other than <i>E. coli</i>	93
2.2.5	Specific activity of recombinant MraY enzymes in the fluorescence assay	98
2.2.6	Determination of IC ₅₀ values of potential MraY inhibitors	100
2.2.7	K _M determination for the dansyl-labelled UDPMurNAc-pentapeptide in the fluorescence MraY assay	104
2.3	Attempted HPLC-based MraY assay	110
2.3.1	Preparation of N-labelled UDPMurNAc-pentapeptides	110
2.3.2	HPLC assay methods	113
2.4	Development of the radiochemical MraY assay	120
2.4.1	Radiochemical synthesis of [¹⁴ C]-UDPMurNAc-pentapeptide	120
2.4.2	Radiochemical MraY assay development.....	123
3	Screening of the Diversity Set of the National Cancer Institute	134
3.1	Initial screening data for the diversity set of the National Cancer Institute	135
3.2	Testing of Low Fluorescence compounds with the radiochemical assay	143
3.3	Testing of high fluorescence (HF) and low fluorescence with activity (LFA) natural products with the radiochemical assay	145
3.3.1	Testing michellamine B against MraY	146
3.3.2	Michellamine family of natural products.....	151

3.4	Summary of screening the NCI diversity set.....	156
3.5	Future work in the field of naphthylisoquinoline alkaloids	158
4	Screening for new natural product inhibitors.....	161
4.1	Assay of culture supernatants	164
4.1.1	Screening <i>Streptomyces</i> culture supernatants	166
4.2	Assay of <i>Streptomyces</i> cell extracts from John Sidda.....	166
4.3	Screening <i>Streptomyces</i> cell extracts from solid media	170
5	Assay of novel and known MraY inhibitors	173
5.1	Inhibition of translocase MraY by uridyl-peptide natural products and their synthetic analogues	173
5.1.1	Inhibition by a synthetic muraymycin derivative.....	173
5.1.2	Inhibition by caprazamycin derivatives	177
5.1.3	Inhibition by pacidamycin derivatives	182
5.1.4	Inhibition by tunicamycin	184
5.1.5	Inhibition by capuramycin derivatives.....	185
5.2	Inhibition of MraY by vancomycin	189
5.3	Inhibition by E peptide, antimicrobial peptides and P1 peptide.....	193
5.3.1	Testing E peptide against <i>E. coli</i> , <i>S. aureus</i> , <i>P. aeruginosa</i> , <i>B. subtilis</i> and <i>M. flavus</i> MraYs	193
5.3.2	Testing antimicrobial peptides against MraY	196
5.3.3	Testing the P1 lytic peptide from phage AP205 against MraY	199
5.3.4	Testing the P1 lytic peptide against MurG.....	201
5.4	Testing of halogenated fluorescein derivatives versus MraY and MurG	204
5.4.1	Conclusion	211
6	Conclusions	213
7	Experimental methods.....	219

7.1	Preparation of <i>E. coli</i> C43 <i>MraY</i> membranes, overexpressed with either <i>E. coli</i> , or <i>S. aureus</i> or <i>B. subtilis</i> <i>MraY</i>	219
7.2	Preparation of <i>E. coli</i> C43 membranes.....	220
7.3	Preparation of <i>P. aeruginosa</i> HMS174 pMON2320 membranes (<i>MraY</i> overexpression)	221
7.4	Preparation of <i>M. flavus</i> membranes	222
7.5	Preparation of UDPMurNAc-pentapeptide from <i>Bacillus subtilis</i> cells	223
7.6	Conditions for high resolution LC-MS (HR LC-MS)	224
7.7	Conditions for LC-MS analysis.....	225
7.8	Preparation of UDP-N-acetylmuramyl-L-Ala- γ -D-Glu-(N ^ε -dansyl)- <i>m</i> -Dap-D-Ala-D-Ala (dansyl-labelled UDPMurNAc-pentapeptide)	228
7.9	Incubation of the dansyl-labelled UDPMurNAc-pentapeptide with <i>MraY</i> membranes	228
7.10	General procedure for the continuous fluorescence enhancement <i>MraY</i> assays	229
7.10.1	Time-course of the <i>MraY</i> reaction.....	231
7.10.2	Experiment with inactivated <i>MraY</i> membranes	231
7.10.3	Reverse <i>MraY</i> reaction with UMP addition.....	231
7.10.4	Effect of added heptaprenyl phosphate to the fluorescence substrate incubated with <i>MraY</i> membranes	232
7.11	IC ₅₀ determination of pacidamycins by the continuous fluorescence assays	232
7.12	K _M determination for the dansyl-labelled UDPMurNAc-pentapeptide with <i>P. aeruginosa</i> <i>MraY</i> membranes	233
7.13	Evidence for the presence of the dansyl-labelled lipid I by LC-MS	234
7.14	Preparation of UDP-N-acetylmuramyl-L-Ala- γ -D-Glu-(N ^ε -2,4-dinitrophenyl)- <i>m</i> -Dap-D-Ala-D-Ala (DNP-labelled UDPMurNAc-pentapeptide).....	235

7.15	Preparation of UDP-N-acetylmuramyl-L-Ala- γ -D-Glu-(N ⁶ -fluorescamine)- <i>m</i> -Dap-D-Ala-D-Ala (fluorescamine-labelled UDPMurNAc-pentapeptide).....	235
7.16	Attempt to make an HPLC-based <i>MraY</i> assay	236
7.17	Conversion of UDPMurNAc-tripeptide to UDPMurNAc-pentapeptide (before optimising the procedure).....	237
7.18	Radiochemical synthesis of the [¹⁴ C]-UDPMurNAc-pentapeptide (optimised version).....	239
7.19	General radiochemical <i>MraY</i> assay procedure	240
7.19.1	Radiochemical assay for the wild type <i>E. coli</i> <i>MraY</i>	242
7.19.2	Investigation of D, D-carboxypeptidase activity	242
7.19.3	Background activity from the endogenous undecaprenyl phosphate in <i>E. coli</i> C43 membranes	243
7.19.4	The time-course of the <i>MraY</i> reaction by the radiochemical assay	243
7.19.5	Overproduction of enzyme activity in the <i>E. coli</i> <i>MraY</i> membranes and comparison with the wild type <i>M. flavus</i>	244
7.20	Fluorescence plate reader assays	244
7.21	Testing hits from the initial fluorescence screen of the NCI diversity set by the continuous fluorescence assay	246
7.22	Testing low fluorescence and high fluorescence compounds from the NCI diversity set by the radiochemical <i>MraY</i> assay.....	247
7.23	Testing michellamine B by the radiochemical <i>MraY</i> assay	247
7.24	Antibacterial testing, microtitre broth dilution and agar plate filter disc methods	248
7.24.1	Microtitre broth dilution.....	248
7.24.2	Agar plate filter disc method.....	249
7.25	Assay of <i>Streptomyces</i> culture supernatants	249
7.25.1	<i>Streptomyces</i> culture supernatants	249

7.25.2	Preparation of <i>Streptomyces</i> cell extracts	251
7.26	Assay of P1 protein and halogenated fluorescein analogues by the radiochemical <i>MraY</i> assay	252
7.27	Radiochemical <i>MurG</i> assay procedure	253
7.27.1	<i>E. coli</i> <i>MraY</i> - <i>MurG</i> procedure.....	253
7.27.2	<i>M. flavus</i> <i>MraY</i> - <i>MurG</i> assay procedure.....	254
Appendices.....		255
Appendix 1: Preparation of the dansyl-labelled UDP <i>MurNAc</i> -pentapeptide (Figures A 1 - A 3).....		255
Appendix 2: LC-MS results for the attempted HPLC-based <i>MraY</i> assay (Figures A 4 - A 18).....		257
Appendix 3: Radiochemical synthesis of the [¹⁴ C]-UDP <i>MurNAc</i> -pentapeptide (Figures A 19 -A 22).....		264
Appendix 4: Results from the NCI diversity set		267
Appendix 5a: Inhibition of <i>E. coli</i> and <i>S. aureus</i> <i>MraY</i> by a synthetic muraymycin analogue (Figures A 23 and A 24).....		275
Appendix 5b: Inhibition of <i>E. coli</i> <i>MraY</i> by caprazamycin analogues (Figures A 25 - A 30)		276
Appendix 5c: Inhibition of <i>E. coli</i> and <i>P. aeruginosa</i> <i>MraY</i> by pacidamycin 1,2 and pacidamycin D (Figures A 31 - A 34).....		279
Appendix 5d: Inhibition of <i>P. aeruginosa</i> <i>MraY</i> by tunicamycin (Figure A 35)		281
Appendix 5e: Inhibition of <i>E. coli</i> and <i>B. subtilis</i> <i>MraY</i> by capuramycin analogues (Figures A 36 and A 37).....		282
Appendix 6: Inhibition of <i>E. coli</i> , <i>S. aureus</i> and <i>P. aeruginosa</i> <i>MraY</i> s by the glycopeptide vancomycin (Figures A 38 - A 40).....		283
Appendix 7: Inhibition of <i>E. coli</i> , <i>S. aureus</i> , <i>B. subtilis</i> , <i>P. aeruginosa</i> and <i>M. flavus</i> <i>MraY</i> s by phloxine B (Figures A 41 - A 46)		285
8	References	288

List of Figures

Figure 1-1: Differences in the Gram-negative and Gram-positive cell wall; prepared in Microsoft PowerPoint based on a similar figure in Maliničová <i>et al.</i> (2010).....	3
Figure 1-2: Representation of the forming peptidoglycan heteropolymer for <i>E. coli</i> , β -(1,4)-glycosidic bond between GlcNAc and MurNAc and lactyl linkage between MurNAc and L-Ala.....	4
Figure 1-3: Examples of diamino acids at the third position of the peptide chains in peptidoglycan, AA: amino acid	5
Figure 1-4: <i>S. aureus</i> peptidoglycan	5
Figure 1-5: <i>B. subtilis</i> peptidoglycan	6
Figure 1-6: Peptidoglycan hydrolases	7
Figure 1-7: Peptidoglycan biosynthetic pathway adapted to <i>E. coli</i>	8
Figure 1-8: The reaction catalysed by MurA	10
Figure 1-9: Chemical structures of MurA inhibitors: fosfomycin, terreic acid, 2-aminotetralone analogue and cnicin where fosfomycin, terreic acid and the most potent 2-aminotetralone analogue (MIC: 8 μ g/ml against <i>S. aureus</i>) covalently bind to Cys-115 of MurA.....	11
Figure 1-10: Examples of MurB inhibitors.....	12
Figure 1-11: Proposed mechanism of ATP-dependent Mur ligases (C to F): the reaction begins with the attack of the carboxylate end of the MurNAc peptide (MurNAc for MurC) on the γ -phosphate of ATP to produce an acyl-phosphate intermediate, followed by the attack of the amino group of the amino acid to be added to yield a tetrahedral adduct. Then the elimination of inorganic phosphate leads to the formation of the new peptide bond	13
Figure 1-12: Chemical structure of the most potent analogues of benzofuran acyl sulfonamides	13
Figure 1-13: The most potent pyrazolopyrimidinediones inhibitor of glutamate racemase.....	14
Figure 1-14: Chemical structure of MurD inhibitors, the most potent phosphinate analogue (phosphinoalanine derivative), the most potent benzylidenethiazolidine-	

4-one analogue and the most potent of the macrocyclic inhibitors with an IC ₅₀ of 0.7 ± 0.3 µM against <i>E. coli</i> MurD	15
Figure 1-15: Chemical structure of 3-methoxynordomesticine analogues	16
Figure 1-16: Inhibitors of alanine racemase: D-cycloserine, O-carbamoyl-D-serine and an example for the thiadiazolidinone analogues	17
Figure 1-17: Chemical structure of the tetrahedral adduct formed during D-Ala-D-Ala formation (A), transition state analogue phosphinate inhibitor (B) and phosphinophosphate (C)	17
Figure 1-18: <i>E. coli</i> DdlB co-crystallized with ATP and a phosphinate inhibitor, Tyr-216, Ser-150 and Glu-15 residues in blue, red spheres are Mg ²⁺ ions; figure was prepared using PyMOL molecular graphics software	18
Figure 1-19: Chemical structure of hydroxyethylamines, inhibitors of DdlB and VanA, R: MeO or F.....	19
Figure 1-20: Chemical structure of UDPMurNAc-pentapeptide containing <i>meso</i> -diaminopimelic acid at the third position.....	20
Figure 1-21: Chemical structure of MurF inhibitors, one of the arylsulfonamide lead compounds (IC ₅₀ : 1 µM), 4-phenylpiperidine and diarylquinolines analogues	20
Figure 1-22: <i>E. coli</i> MurF (left) and <i>S. pneumonia</i> MurF co-crystallized with a small molecule inhibitor (right), C-domains in blue, central domains in green and N-domains in red; figures were prepared using PyMOL molecular graphics software.....	21
Figure 1-23: Chemical structure of undecaprenyl phosphate (C ₅₅ -P).....	22
Figure 1-24: Chemical structure of bacitracin	22
Figure 1-25: Schematic representation of the lipid-linked steps of the peptidoglycan biosynthetic pathway, catalysed by MraY and MurG	23
Figure 1-26: Chemical structure of lipid I (C ₅₅) with <i>meso</i> -diaminopimelic acid at the third position of the pentapeptide unit	24
Figure 1-27: Chemical structure of lipid II (C ₅₅) with <i>meso</i> -diaminopimelic acid at the third position of the pentapeptide unit	25
Figure 1-28: Suggested mechanism of action for MurG, R=-C(CH ₃)CO-pentapeptide	26

Figure 1-29: Crystal structure of MurG dimer with its substrate UDPGlcNAc in the active conformation, residues of the hydrophobic patch for membrane interaction in dark blue; figure was prepared using PyMOL molecular graphics software.....	27
Figure 1-30: MurG inhibitors, diphosphate mimic containing a five-membered heterocyclic core, and the most active uridine-linked proline-containing transition state mimic	28
Figure 1-31: 2'deoxyadenosine phosphonate inhibitor of MurM and aminoacyl-tRNA analogue inhibitor of FemX.....	30
Figure 1-32: Proposed mechanism of the transglycosylation reaction of lipid II monomers.....	31
Figure 1-33: Chemical structure of moenomycin A	32
Figure 1-34: Chemical structure of the most potent iminocyclitol-based pyrophosphate mimic inhibiting transglycosylase activity	32
Figure 1-35: Mechanism of the transpeptidation reaction: acylation of the catalytic serine residue of TP by D-Ala at position 4 of the first stem peptide, then the acyl-enzyme intermediate is attacked by the amine of the L-Lys or <i>m</i> -Dap residue at position 3 of the adjacent stem peptide, mode of action of the β -lactam antibiotics: the active site serine residue of TP forms a covalent bond with the β -lactam ring	34
Figure 1-36: The “transfer” reaction (translocase MraY reaction)	36
Figure 1-37: The “exchange” reaction	36
Figure 1-38: Membrane topology of MraY, PL: periplasmic loop, CL: cytoplasmic loop, H: transmembrane helix.....	38
Figure 1-39: Two-step catalytic mechanism for MraY	39
Figure 1-40: One-step catalytic mechanism for MraY	41
Figure 1-41: Structure of the MraY dimer from <i>Aquifex aeolicus</i> , view from within the membrane (top) and cytoplasmic view (bottom), only the transmembrane helices of one protomer are coloured, red spheres are Mg^{2+} , transmembrane helices are numbered (1-10); figures were prepared using PyMOL molecular graphics software	42
Figure 1-42: Membrane topology of <i>A. aeolicus</i> MraY, transmembrane helices are numbered, cytoplasmic loops have letters (A-E), IH: interfacial helix, PB: periplasmic β hairpin, PH: periplasmic helix ¹³⁷	43

Figure 1-43: MraY active site, suggested active site mechanism by Lloyd <i>et al.</i> for <i>E. coli</i> MraY (left) and distance between Mg ²⁺ and the conserved active site residues Asp ¹¹⁷ , Asp ¹¹⁸ and Asp ²⁶⁵ of <i>Aquifex aeolicus</i> MraY (right); figure on the right was prepared using PyMOL molecular graphics software	44
Figure 1-44: HHH motif on loop E and the conserved aspartate residues as sticks, red spheres are Mg ²⁺ ; figure was prepared using PyMOL molecular graphics software	45
Figure 1-45: transmembrane helix 9b, loop E and the active site of MraY with the three conserved aspartate residues as sticks, red sphere Mg ²⁺ ; figure was prepared using PyMOL molecular graphics software	45
Figure 1-46: Representation of the hydrophobic groove by dashed lines (right), yellow sphere: Mg ²⁺ , Asp-117 in red, transmembrane (TM) helices 3 and 9b are also shown ¹³⁷	46
Figure 1-47: The “transfer” radiochemical MraY assay	48
Figure 1-48: The “exchange” radiochemical MraY assay	49
Figure 1-49: Fluorescence MraY assays	50
Figure 1-50: Fluorescent labels introduced into UDPMurNAc-pentapeptide	51
Figure 1-51: Schematic representation of the coupled radiochemical MraY-MurG assays	52
Figure 1-52: Chemical structure of tunicamycins, n: 7-11	54
Figure 1-53: Biosynthesis of dolichyl-pyrophosphoryl-GlcNAc in mammalian N-linked glycoprotein biosynthesis.....	54
Figure 1-54: Structure-activity relationship studies on pacidamycins	58
Figure 1-55: Chemical structure of the caprazamycins and the liposidomycins ..	59
Figure 1-56: Chemical structure of the caprazene core structure (no antibacterial activity) and the antibacterial drug candidate CPZEN-45, a 4-butylanilide derivative of caprazene	60
Figure 1-57: Chemical structure of the muraymycins.....	61
Figure 1-58: Chemical structure of the capuramycins	62
Figure 1-59: Position of the phenylalanine residue of helix 9 of <i>Aquifex aeolicus</i> MraY, essential for E protein inhibition of MraY at the periplasmic phase of the membranes, proposed catalytic active site with three conserved aspartate residues,	

Asp-117, Asp-118 and Asp-265, red sphere Mg^{2+} ; figure was prepared using PyMOL molecular graphics software	64
Figure 1-60: Chemical structure of amphomycin	65
Figure 1-61: Halogenated fluorescein analogues from the combined <i>MraY</i> - <i>MurG</i> screen of Zawadzke <i>et al.</i> (2003)	68
Figure 2-1: Schematic representation of the radiochemical <i>MraY</i> assay	69
Figure 2-2: Schematic representation of the fluorescence <i>MraY</i> assay	70
Figure 2-3: From top to bottom: <i>E. coli</i> , <i>P. aeruginosa</i> , <i>S. aureus</i> , <i>B. subtilis</i> and <i>M. flavus</i> <i>MraY</i> sequence alignment, colour of the amino acids: small and hydrophobic: AVFPMILW, acidic: DE, basic: RK, hydroxyl + sulfhydryl + amine + G: STYHCNGQ.....	74
Figure 2-4: Isotopic pattern for the doubly and negatively charged ion of the UDPMurNAc-pentapeptide.....	77
Figure 2-5: Dansylation of the UDPMurNAc pentapeptide, 1.: formation of the dansyl-labelled UDPMurNAc-pentapeptide, 2.: formation of dansyl amide with ammonium acetate, 3.: formation of the by-product, dansic acid with water.....	78
Figure 2-6: UV-Vis absorbance spectrum of the dansyl-labelled UDPMurNAc-pentapeptide (in blue) and dansic acid (in red)	79
Figure 2-7: Fluorescence emission spectrum of the dansyl-labelled UDPMurNAc-pentapeptide (in blue) and dansic acid (in red), excitation: 340 nm	80
Figure 2-8: HR LC-MS results, 1: Base Peak Chromatogram 2: Extracted Ion Chromatogram for the negatively and doubly charged dansyl-labelled UDPMurNAc-pentapeptide (m/z : 712.19), 2: Extracted Ion Chromatogram for dansic acid (m/z : 250.06) and 3: Extracted Ion Chromatogram for the negatively and doubly charged didansyl-labelled UDPMurNAc-pentapeptide (m/z : 828.71)	81
Figure 2-9: The extracted ion chromatogram and the doubly and negatively charged ion for the dansyl-labelled UDPMurNAc-pentapeptide.....	82
Figure 2-10: Suggested chemical structure (second label in red), the isotopic pattern for the negatively and doubly charged ion of the didansyl-labelled UDPMurNAc pentapeptide.....	82
Figure 2-11: Emission spectrum of the dansyl-labelled UDPMurNAc pentapeptide incubated with <i>E. coli</i> <i>MraY</i> membranes recorded twice over 30 minutes and the	

effect of UMP addition, A: sample without inhibitor, B: sample with 83 µg/ml tunicamycin, λ_{ex} : 340 nm	84
Figure 2-12: Observed small blue shift in the fluorescence emission spectrum associated with dansyl-labelled lipid I formation, same experiment as in Figure 2-11, (the two graphs are combined in one graph), λ_{ex} : 340 nm.....	85
Figure 2-13: Gradual increase in fluorescence associated with the formation of dansyl-labelled lipid I following addition of 90 µg <i>E. coli</i> MraY membranes and 83 µg/ml tunicamycin inhibition, λ_{ex} : 340nm, λ_{em} : 530 nm.....	86
Figure 2-14: No fluorescence changes were observed with 90 µg inactivated MraY enzyme, λ_{ex} : 340nm, λ_{em} : 530 nm.....	87
Figure 2-15: Schematic representation of the reversible fluorescence MraY assay	88
Figure 2-16: Decrease in fluorescence following 0.1 mM UMP addition to the <i>E. coli</i> MraY reaction, λ_{ex} : 340nm, λ_{em} : 530 nm.....	88
Figure 2-17: Effect of heptaprenyl phosphate on the MraY reaction, λ_{ex} : 340nm, λ_{em} : 530 nm	90
Figure 2-18: Isotopic pattern of the negatively and doubly charged ion for the dansyl-labelled C ₅₅ lipid I and the chemical structure	91
Figure 2-19: Isotopic pattern for the negatively and doubly charged ion for the dansyl-labelled C ₃₅ lipid I and the chemical structure	92
Figure 2-20: Isotopic pattern for the negatively and doubly charged ion for the dansyl-labelled C ₅₅ lipid I formed with endogenous undecaprenyl phosphate.....	92
Figure 2-21: Fluorescence MraY assay with wild type 90 µg <i>E. coli</i> membranes (MraY is not overexpressed) λ_{ex} : 340 nm, λ_{em} : 530 nm.....	93
Figure 2-22: <i>P. aeruginosa</i> MraY assay, pacidamycin D concentration 0-180 ng/ml, 90 µg protein, λ_{ex} : 340 nm, λ_{em} : 530 nm.....	95
Figure 2-23: <i>S. aureus</i> MraY assay, testing a muraymycin analogue between 0-80 µM, 90 µg protein, λ_{ex} : 340nm, λ_{em} : 530 nm	96
Figure 2-24: Inhibition of a capuramycin analogue, A-503083 B, against <i>B. subtilis</i> MraY, concentrations of the inhibitor ranging from 0-2.5 µg/ml, 60 µg protein, λ_{ex} : 340nm, λ_{em} : 530 nm	97
Figure 2-25: <i>M. flavus</i> MraY reaction and 83 µg/ml tunicamycin inhibition, 90 µg protein containing membranes, λ_{ex} : 340nm, λ_{em} : 530 nm	98

Figure 2-26: Example for the fluorescence <i>MraY</i> assay: Pacidamycin 1,2 inhibition against <i>E. coli</i> <i>MraY</i> , 60 μ g protein, showing only one curve for each inhibitor concentration, λ_{ex} : 340 nm, λ_{em} : 530 nm	101
Figure 2-27: IC ₅₀ for pacidamycin 1,2 inhibition of <i>MraY</i>	103
Figure 2-28: dansyl-labelled UDPMurNAc-pentapeptide concentrations [s] versus initial rates (v)	106
Figure 2-29: Eadie-Hofstee plot for K_M of the dansyl-labelled UDPMurNAc-pentapeptide in the <i>P. aeruginosa</i> <i>MraY</i> assay	107
Figure 2-30: Lineweaver-Burk plot for K_M of the dansyl-labelled UDPMurNAc-pentapeptide for <i>P. aeruginosa</i> <i>MraY</i>	108
Figure 2-31: Hanes-Woolf method for the dansyl-labelled UDPMurNAc-pentapeptide K_M determination for <i>P. aeruginosa</i> <i>MraY</i>	109
Figure 2-32: UV-Vis absorbance spectrum of the DNP-labelled UDPMurNAc-pentapeptide	111
Figure 2-33: UV-Vis absorbance spectrum of the fluorescamine-labelled UDPMurNAc-pentapeptide	112
Figure 2-34: Possible DNP-labelled UDPMurNAc-pentapeptide fragment (m/z [M-H] ⁺ : 972.3213 corresponding to predicted 972.3512)	113
Figure 2-35: No peak detected for the DNP-labelled C ₃₅ lipid I at 210, 260 and 360 nm, EIC: 1608.7	115
Figure 2-36: Absorbance at 210, 260 and 390 nm for the fluorescamine-labelled lipid I (C ₃₅)- H ₂ O EIC: 1702.8	116
Figure 2-37: Extracted ion chromatograms of the dansyl-labelled lipid Is, the C ₅₅ analogue eluting from the C18 column 2-3 minutes later than the C ₃₅ analogue formed by overexpressed <i>S. aureus</i> <i>MraY</i> membranes (<i>E. coli</i>)	117
Figure 2-38: Lipid I and lipid II (C ₃₅) with <i>M. flavus</i> membranes	118
Figure 2-39: An example for sodium adducts, C ₃₅ lipid I formed with <i>E. coli</i> <i>MraY</i>	118
Figure 2-40: Absorbance at 210, 250 and 330 nm of the dansyl-labelled lipid I (C ₃₅), EIC: 1675.8	119
Figure 2-41: Steps of the radiochemical synthesis of the [¹⁴ C]-UDPMurNAc-pentapeptide, the product is ¹⁴ C-labelled at the D-Ala residues at position 4 and 5 (in red)	121

Figure 2-42: UDPMurNAc tripeptide and pentapeptide by LC-MS at 2 minute retention time	122
Figure 2-43: Schematic representation of the radiochemical MraY assay	124
Figure 2-44: Inhibition of MraY and activity in the wild type <i>E. coli</i> membranes with the radiochemical MraY assay	125
Figure 2-45: No significant D,D-carboxypeptidase activity in the membranes..	128
Figure 2-46: low background activity from endogenous undecaprenyl phosphate from <i>E. coli</i> C43 MraY membranes	129
Figure 2-47: Time-course profile of the MraY reaction by the radiochemical assay, 40 µg protein overexpressed <i>E. coli</i> and <i>B. subtilis</i> , 35 µg protein overexpressed <i>S. aureus</i> and 20 µg protein overexpressed <i>P. aeruginosa</i> in <i>E. coli</i> (C43) membranes and 40 µg <i>M. flavus</i> membranes.....	130
Figure 3-1: Arrangements of the test compounds (wells A2-H6 from a diversity set plate) and controls (no inhibitor, 100 µg/ml tunicamycin and no membranes) in 96-well plate format	136
Figure 3-2: Eliminating compounds with high fluorescence from the wells before the MraY reaction, compounds A4 (3130 FAU), A5 (6,445 FAU), E2 (44,153), E4 (6,844), F6 (4,789 FAU), G3 (3,023) and H5 (13,007) with higher fluorescence had to be removed from the assay λ_{ex} : 340 nm, λ_{em} : 535 nm	137
Figure 3-3: Time-course of the fluorescence MraY assay in microtitre plate format (0, 5, 10, 15 and 20 minutes).....	139
Figure 3-4: Screening compounds with lower fluorescence enhancement activity than 80 %	140
Figure 3-5: The hits tested at 60 µM from the initial screen of the diversity set interfered with fluorescence: low fluorescence (LF) compounds and low fluorescence compounds with fluorescence enhancement activity (LFA), 15 µM dansyl pentapeptide, 35 µg/ml heptaprenyl phosphate, 60 µg protein, λ_{ex} : 340 nm, λ_{em} : 530 nm	141
Figure 3-6: Testing low fluorescence compounds (LF) by the radiochemical MraY assay	144
Figure 3-7: Testing high fluorescence and LFA compounds from the NCI diversity set plate 13091251, LSD calculated in GenStat: 162.5 dpm for the	

highest and lowest means at 5 % level, compound F8 in yellow, tunicamycin in red.....	145
Figure 3-8: Chemical structure of Michellamine B as defined by the National Cancer Institute, Exact mass: 876.38	146
Figure 3-9: IC ₅₀ for Michellamine B against <i>MraY</i> : 400 ± 50 µg/ml.....	147
Figure 3-10: Michellamine B inhibition against <i>B. subtilis</i> <i>MraY</i> , IC ₅₀ : 338 ± 54 µg/ml.....	149
Figure 3-11: Picture of michellamine B inhibition of <i>B. subtilis</i> , from the top clockwise: 25 µl DMSO, 25 µl of 2.5, 1,25 and 0.05 mg/ml stock solutions of michellamine B (M), 25 µl of 2 mg/ml kanamycin and 25 µl 1 mg/ml ampicillin	150
Figure 3-12: Chemical structures of michellamines A, B and C, six elements of chirality	152
Figure 3-13: Chemical structure of michellamine B and korupensamine A and B	152
Figure 3-14: Chemical structure of monomeric naphthylisoquinoline alkaloids, three elements of chirality in the monomer units.....	153
Figure 3-15: Chemical structure of jozimine A ₂ , the structurally related shuangancistroretorine and mbandakamine A and B, the seventh element of chirality is the rotationally hindered biaryl axis between the two monomer units (in red).....	159
Figure 4-1: Antibiotic droplet from a <i>Streptomyces</i> colony (Higher Education and Research Opportunities, the John Innes Centre)	162
Figure 4-2: Chemical structures of A-94964 and A-90289 A and B	162
Figure 4-3: <i>S. coeruleorubidus</i> grown in Lac-MM (left) and ISP2 media (right) and tested by the continuous fluorescence <i>MraY</i> assay after 8 days incubation at 30 °C, λ _{ex} : 340 nm, λ _{em} : 530 nm.....	165
Figure 4-4: <i>Streptomyces</i> strains grown in Lac-MM media, tested in the fluorescence <i>MraY</i> assay, λ _{ex} : 340 nm, λ _{em} : 535 nm	166
Figure 4-5: Chemical structure of gaburedin A, the conserved GABA fragment is shown in the red box	167
Figure 4-6: John's Sidda's cell extracts tested by the microtitre plate fluorescence assay (left) and the radiochemical assay (right) against <i>E. coli</i> <i>MraY</i>	168

Figure 4-7: Testing the fractionated JDS374 cell extract by the microtitre plate fluorescence assay, fractions collected from 5 to 31 minutes (5f-31f)	169
Figure 4-8: Streptomyces cell extracts from solid media tested by the radiochemical assay against <i>E. coli</i> MraY, all the strains were grown for 3 days on SMMS media and <i>S. coeruleorubidus</i> and <i>S. venezuelae</i> were grown on MS agar plates as well, the control contains 10 % methanol/water (1:1).....	171
Figure 5-1: Chemical structure of the synthetic muraymycin analogue, Mw: 1012.5973 and the parent compound with the aminosugar (muraymycin D2)...	174
Figure 5-2: Muraymycin analogue inhibition against <i>E. coli</i> MraY, λ_{ex} : 340 nm, λ_{em} : 530 nm, 90 μg protein (left), IC_{50} : $1.6 \pm 0.3 \mu\text{M}$ (right).....	175
Figure 5-3: Muraymycin analogue inhibition against <i>P. aeruginosa</i> , <i>B. subtilis</i> and <i>M. flavus</i> MraY, 40-90 μg protein, λ_{ex} : 340 nm, λ_{em} : 530 nm	176
Figure 5-4: Chemical structure of caprazamycin A on the left (Exact mass: 1145.58) and caprazamycin E on the right (Exact mass: 1117.55), the additional unit compared to hydroxyacyl-caprazol A and E are circled in red.....	177
Figure 5-5: Chemical structure of caprazamycin analogues, the additional groups compared to hydroxyacyl-caprazol E and A are circled in red.....	179
Figure 5-6: Hydroxyacyl-caprazol E-acetate inhibition against <i>E. coli</i> MraY, IC_{50} : $1.21 \pm 0.13 \mu\text{g/ml}$	180
Figure 5-7: Chemical structure for pacidamycin 1, 2 and D.....	182
Figure 5-8: Pacidamycin 1,2 inhibition against <i>P. aeruginosa</i> MraY tested between 0-0.88 $\mu\text{g/ml}$, 90 μg protein, , λ_{ex} : 340 nm, λ_{em} : 530 nm, IC_{50} : $114 \pm 5 \text{ ng/ml}$	183
Figure 5-9: Chemical structure of tunicamycins, n: 7-11, and the reaction they inhibit in mammalian N-linked glycoprotein biosynthesis	184
Figure 5-10: Chemical structures of the capuramycin analogues, A-500359 F and B, and A-503083 F and B	186
Figure 5-11: A-503083 inhibition against <i>B. subtilis</i> MraY, IC_{50} : $62 \pm 6 \text{ ng/ml}$	188
Figure 5-12: Representation of the vancomycin : <i>N</i> -acyl-D-Ala-D-Ala complex (left), and vancomycin : <i>N</i> -acyl-D-Ala-D-Lac complex in vancomycin resistant bacteria (right), dashed lines represent H-bonds ²⁴⁵	190
Figure 5-13: Vancomycin inhibition against <i>E. coli</i> MraY.....	191

Figure 5-14: E peptide inhibition against <i>E. coli</i> MraY, IC ₅₀ : 17.2 ± 2.11 µg/ml	194
Figure 5-15: Position of F288 of <i>E. coli</i> MraY compared to <i>S. aureus</i> , <i>B. subtilis</i> , <i>P. aeruginosa</i> and <i>M. flavus</i> MraYs.....	194
Figure 5-16: E peptide inhibition against <i>S. aureus</i> , <i>B. subtilis</i> , <i>P. aeruginosa</i> and <i>M. flavus</i> MraYs, control (no inhibitor) in blue, 125 µg/ml E peptide in orange, 40-90 µg protein, λ _{ex} : 340 nm, λ _{em} : 530 nm.....	195
Figure 5-17: Major structural conformations of natural antimicrobial peptides, charged regions in blue and hydrophobic residues in green, A: β-structures with 2-4 β-strands, stabilized by two to four disulphide bridges, B: α-helical peptides, C: loop structures with one disulphide bridge, D: extended structures ²⁵⁵	196
Figure 5-18: P1 peptide inhibition against <i>E. coli</i> MraY (radiochemical assay) IC ₅₀ : 157 ± 9 µg/ml	200
Figure 5-19: Schematic representation of the coupled radiochemical MraY-MurG assay	201
Figure 5-20: P1 against <i>E. coli</i> MurG	202
Figure 5-21: P1 against <i>M. flavus</i> MurG.....	203
Figure 5-22: Halogenated fluorescein analogues from the hits of the combined MraY-MurG screen of Zawadzke <i>et al</i> , di-iodo fluorescein (Mw: 584.10) on the left and tetra-bromo fluorescein analogue (Mw: 697.93) on the right.....	204
Figure 5-23: 2,7-dichloro fluorescein analogue (Mw: 401.20) and 2,7-dibromo fluorescein analogue (Mw: 490.10) synthesised by Justin Slikas.....	205
Figure 5-24: Testing halogenated fluorescein analogues against <i>E. coli</i> MraY .	206
Figure 5-25: Testing halogenated fluorescein analogues against <i>E. coli</i> MurG .	207
Figure 5-26: Chemical structure of phloxine B, Mw: 829.63	208
Figure 5-27: Phloxine B inhibition against <i>E. coli</i> MraY, IC ₅₀ : 26.4 ± 1.0.....	209
Figure 5-28: Inhibition of phloxine B in the combined <i>M. flavus</i> MraY-MurG assay	211
Figure 6-1: Chemical structures of novel MraY inhibitors, michellamine B and phloxine B	218

List of Tables

Table 1-1: Chemical structure of mureidomycins, pacidamycins, napsamycins and sansanmycins	56
Table 2-1: MraY enzymes aligned in pairs, sequence identity and similarity (%)	73
Table 2-2: Increase in specific activity by the fluorescence MraY assay in the membranes by overexpressing MraY.....	99
Table 2-3 : Calculation of % activity versus inhibitor concentration	102
Table 2-4: K_M determination for the dansyl-labelled UDPMurNAc-pentapeptide with <i>P. aeruginosa</i> MraY by graphical methods	109
Table 2-5: Lipid I derivatives of the MraY reaction	114
Table 2-6: % inhibition of known inhibitors against MraY by the radiochemical assay	127
Table 2-7: Comparison of the level of radiolabelled lipid I production for 1 mg protein containing <i>E. coli</i> membranes overexpressed with MraY from <i>E. coli</i> , <i>S. aureus</i> , <i>B. subtilis</i> and <i>P. aeruginosa</i> with the wild type <i>E. coli</i> membranes and radiolabelled lipid I production for <i>M. flavus</i> membranes over 30 minutes reaction time by the radiochemical assay	132
Table 3-1: Categories of test compounds from the NCI diversity set.....	142
Table 3-2: Michellamine B inhibition against <i>S. aureus</i> , <i>P. aeruginosa</i> , <i>B. subtilis</i> and <i>M. flavus</i> MraYs at 500 µg/ml concentration and comparison with two known inhibitors of MraY, tested by the radiochemical MraY assay	148
Table 3-3: Summary of screen	157
Table 4-1: Examples for antibacterial agents produced by <i>Antinomycetes</i> ²³⁵	163
Table 5-1: IC ₅₀ s of caprazamycin analogues against <i>E. coli</i> MraY	180
Table 5-2: Pacidamycin 1,2 and D inhibition against <i>E. coli</i> and <i>P. aeruginosa</i> MraYs, IC ₅₀ s	183
Table 5-3: Tunicamycin inhibition by a fluorescence assay against MraYs from <i>E. coli</i> , <i>P. aeruginosa</i> , <i>S. aureus</i> , <i>B. subtilis</i> and <i>M. flavus</i> , a: determined by P. Brandish ¹⁴³ , b: determined by A. O'Reilly	185
Table 5-4: Inhibition and IC ₅₀ s of capuramycin analogues against <i>E. coli</i> and <i>B. subtilis</i> MraYs.....	187

Table 5-5: Vancomycin inhibition against <i>E. coli</i> , <i>S. aureus</i> and <i>P. aeruginosa</i> MraYs.....	191
Table 5-6: Inhibition against <i>E. coli</i> MraY by antimicrobial peptides determined by a radiochemical MraY assay ²⁶⁵	198
Table 5-7: Phloxine B inhibition against <i>S. aureus</i> , <i>B. subtilis</i> , <i>P. aeruginosa</i> , <i>M. flavus</i> and <i>E. coli</i> MraY	210
Table 7-1: CWSM medium.....	224
Table 7-2: LC conditions for HR LC-MS	225
Table 7-3: LC conditions for LC-MS analysis of the UDPMurNAc-pentapeptide and the dansyl-labelled UDPMurNAc-pentapeptide	227
Table 7-4: LC conditions for the LC–MS analysis of lipid products.....	227
Table 7-5: Composition of the MraY assay mixture for the continuous fluorescence assays	230
Table 7-6: Calculations for K_M determination with graphical methods.....	234
Table 7-7: Reaction mixture (400 μ l + 50 μ l enzymes):.....	239
Table 7-8: Radioactivity in fractions	240
Table 7-9: Composition of a 30 ml master mix for the fluorescence MraY plate reader assays.....	245

List of Figures in Appendices

A 1: Isotopic pattern for dansic acid by HR LC-MS	255
A 2: Isotopic pattern for the negatively charged ion of the dansyl-labelled UDPMurNAc-pentapeptide by LC-MS	256
A 3: Isotopic pattern for the negatively charged ion of the didansyl-labelled UDPMurNAc-pentapeptide by LC-MS	256
A 4: Isotopic pattern for the DNP-labelled UDPMurNAc-pentapeptide by HR LC-MS	257
A 5: Isotopic pattern for the DNP-labelled UDPMurNAc-pentapeptide by HR-LC-MS (two DNP labels)	257
A 6: Isotopic pattern for the DNP-labelled UDPMurNAc-pentapeptide (three labels) by HR LC-MS	258
A 7: Isotopic pattern for a DNP-labelled UDPMurNAc-pentapeptide fragment	258
A 8: Isotopic pattern by HR LC-MS for the fluorescamine-labelled UDPMurAc-pentapeptide	259
A 9: Isotopic pattern for the DNP-labelled C ₃₅ lipid I	259
A 10: Chemical structure for the DNP-labelled C ₃₅ lipid I	260
A 11: Isotopic pattern for the fluorescamine-labelled lipid I (-H ₂ O) by LC-MS	260
A 12: Isotopic pattern of the negatively and doubly charged ion of the fluorescamine-labelled lipid I (C ₃₅) by HR LC-MS and the computer simulated isotopic pattern	261
A 13: Chemical structure of the fluorescamine-labelled C ₃₅ lipid I	261
A 14: Isotopic pattern for dansyl-labelled lipid I (C ₅₅) formed with MraY	262
A 15: Isotopic pattern for the dansyl-labelled lipid I (C ₃₅) formed with MraY ..	262
A 16: Isotopic pattern for lipid I (C ₃₅)	263
A 17: Isotopic pattern for lipid II (C ₃₅)	263
A 18: Control lacking the unlabelled or labelled UDPMurNAc-pentapeptides, no sign for the masses of lipid products (EICs)	264
A 19: Isotopic pattern for the UDPMurNAc-tripeptide	264
A 20: Isotopic pattern for the UDPMurNAc-pentapeptide	265
A 21: Isotopic pattern for the UDPMurNAc-pentapeptide by HR LC-MS	265

A 22: ESI-MS for ^{14}C -labelled UDPMurNAc-pentapeptide m/z $[\text{M}-2\text{H}]^{2-}$: 595.70 for predicted 595.66, and sodium adducts, analysis was performed by Susan Slade	266
A 23: Muraymycin analogue inhibition against <i>E. coli</i> MraY, 50 μM muraymycin gave 15 ± 2 % activity in the assay (missing from graph), IC_{50} : 1.6 ± 0.3 μM ..	275
A 24: Muraymycin analogue inhibition against <i>S. aureus</i> MraY, 50 μM gave 4.5 ± 0.5 % activity in the assay (missing from graph), IC_{50} : 1.6 ± 0.2 μM	275
A 25: Hydroxyacyl-caprazol A inhibition against <i>E. coli</i> MraY, IC_{50} : 339 ± 35 ng/ml, 0.41 μM	276
A 26: Hydroxyacyl-caprazol E inhibition against <i>E. coli</i> MraY, IC_{50} : 602 ± 19 ng/ml, 0.75 μM	276
A 27: Hydroxyacyl-caprazol E-acetate inhibition against <i>E. coli</i> MraY, IC_{50} : 1.21 ± 0.13 $\mu\text{g/ml}$, 1.4 μM	277
A 28: Hydroxyacyl-caprazol E-butyrate inhibition against <i>E. coli</i> MraY, IC_{50} : 5.78 ± 0.41 $\mu\text{g/ml}$, 6.6 μM	277
A 29: Sulphated CPZ-Aglycon A inhibition against <i>E. coli</i> MraY, IC_{50} : 250 ± 35 ng/ml, 0.24 μM	278
A 30: Sulphated CPZ-Aglycon E inhibition against <i>E. coli</i> MraY, IC_{50} : 314 ± 42 ng/ml, 0.31 μM	278
A 31: Pacidamycin 1,2 inhibition against <i>E. coli</i> MraY, IC_{50} : 83 ± 7 ng/ml.....	279
A 32: Pacidamycin 1,2 inhibition against <i>P. aeruginosa</i> MraY, IC_{50} : 114 ± 5 ng/ml	279
A 33: Pacidamycin D inhibition against <i>E. coli</i> MraY, IC_{50} : 46 ± 7 ng/ml.....	280
A 34: Pacidamycin D inhibition against <i>P. aeruginosa</i> MraY, IC_{50} : 27 ± 4 ng/ml	280
A 35: <i>P. aeruginosa</i> MraY inhibition by tunicamycin, IC_{50} : 4.44 ± 1.38 $\mu\text{g/ml}$	281
A 36: A-503083 B inhibition against <i>E. coli</i> MraY, IC_{50} : 139 ± 16 ng/ml.....	282
A 37: A-503083 F inhibition against <i>E. coli</i> MraY, IC_{50} : 4.8 ± 0.6 $\mu\text{g/ml}$	282
A 38: Vancomycin inhibition against <i>E. coli</i> MraY, IC_{50} : 61.6 ± 8 $\mu\text{g/ml}$	283
A 39: Vancomycin inhibition against <i>S. aureus</i> MraY, IC_{50} : 130 ± 12 $\mu\text{g/ml}$...	283
A 40: Vancomycin against <i>P. aeruginosa</i> MraY, IC_{50} : 288 ± 44 $\mu\text{g/ml}$	284
A 41: Phloxine B inhibition of <i>E. coli</i> MraY, IC_{50} : 26.4 ± 1.0 $\mu\text{g/ml}$	285
A 42: Phloxine B inhibition against <i>S. aureus</i> MraY, IC_{50} : 211 ± 29 $\mu\text{g/ml}$	285

A 43: Phloxine B inhibition against <i>B. subtilis</i> Mray, IC ₅₀ : 137 ± 20 µg/ml.....	286
A 44: Phloxine B inhibition against <i>P. aeruginosa</i> Mray, IC ₅₀ : 106 ± 23 µg/ml	286
A 45: Phloxine B inhibition against <i>M. flavus</i> Mray, IC ₅₀ : 162 ± 25 µg/ml.....	287
A 46: Phloxine B inhibition against <i>E. coli</i> Mray in the dark, IC ₅₀ : 24.2 ± 1.7 µg/ml.....	287

List of Abbreviations

Ac	acetyl
ADP	adenosine 5'-diphosphate
<i>A. aeolicus</i>	<i>Aquifex aeolicus</i>
Arg	arginine
Asp	aspartic acid
ATP	adenosine 5'-triphosphate
<i>B. subtilis</i>	<i>Bacillus subtilis</i>
CHAPS	3-[(3-chloramidopropyl)dimethylammonio]-1-propanesulfonate hydrate
cpm	counts per minute
CWSM	cell wall synthesis medium
Ci	curie
Cys	cysteine
DABA	2,3-diaminobutyric acid
<i>m</i>-DAP	<i>meso</i> -diaminopimelic acid
dpm	disintegration per minute
DMSO	dimethyl sulfoxide
DNA	deoxyribonucleic acid
DNP-labelled	2,4-dinitrophenyl-labelled
DTT	dithiothreitol
EC₅₀	half maximal effective concentration
<i>E. coli</i>	<i>Escherichia coli</i>

EDTA	ethylenediaminetetraacetic acid
EIC	extracted ion chromatogram
ELSD	evaporative light scattering detector
ESI-MS	electrospray ionisation mass spectrometry
FAU	fluorescence arbitrary units
FRET	fluorescence energy transfer
x g	multiple of the earth's gravitational acceleration
GlcNAc	<i>N</i> -acetyl glucosamine
Glu	glutamic acid
Gly	glycine
GT	glycosyltransferase
GTP	guanosine 5'-triphosphate
HF	high fluorescence
(His)₆	hexahistidine
HIV	human immunodeficiency virus
HPLC	high performance liquid chromatography
HR LC-MS	high resolution liquid chromatography–mass spectrometry
IC₅₀	half maximal inhibitory concentration
IH	interfacial helix
IPTG	isopropyl-β-D-thiogalactopyranoside
LB	Luria Broth
LC-MS	liquid chromatography–mass spectrometry

LF	low fluorescence
LFA	low fluorescence with fluorescence enhancement activity
Lipid I	MurNAc-(pentapeptide)-pyrophosphoryl undecaprenol
Lipid II	GlcNAc-MurNAc-(pentapeptide)-pyrophosphoryl undecaprenol
Lys	lysine
MALDI-TOF	matrix-assisted laser desorptive/ionization time of flight
MBP	maltose-binding protein
Met	methionine
<i>M. flavus</i>	<i>Micrococcus flavus</i>
MRSA	methicillin-resistant <i>Staphylococcus aureus</i>
Mw	molecular weight
MurNAc	<i>N</i> -acetyl muramic acid
NCBI	National Center for Biotechnology Information
nCi	nanocurie
NCI	National Cancer Institute
NMR	nuclear magnetic resonance
OD₆₀₀	optical density at 600 nm
<i>P. aeruginosa</i>	<i>Pseudomonas aeruginosa</i>
PH	periplasmic β hairpin
PBP	penicillin binding protein

PH	periplasmic helix
Phe	phenylalanine
P_i	inorganic phosphate
PKC	protein kinase C
Pro	proline
rpm	revolutions per minute
<i>S. aureus</i>	<i>Staphylococcus aureus</i>
SDS-PAGE	sodium dodecyl sulphate polyacrylamide gel electrophoresis
SMMS	supplemented minimal agar medium
TCA	trichloroacetic acid
TP	transpeptidase
tRNA	transfer ribonucleic acid
Tyr	tyrosine
UDP	uridine 5'-diphosphate
UDPGlcNAc	uridine 5'-diphosphate- <i>N</i> -acetylglucosamine
UDPMurNAc	uridine 5'-diphosphate- <i>N</i> -acetylmuramic acid
UMP	uridine 5'-monophosphate
UV/Vis	ultra-violet-visible
μCi	micocurie
Val	valine
VRE	vancomycin-resistant <i>Enterococci</i>

Acknowledgements

Most importantly, I would like to thank my supervisor, Professor Tim Bugg for giving me the opportunity to work on this research project, for his support, supervision and advice over the last four years.

I would also like to thank every single member of the Bugg group for their help and support. Special thanks to Dr. Liz Hardiman for introducing me into biological work, Dr. Darren Braddick, Dr. Sandeep Sandhu, Maria Rodolis and Ioanna Tasiopoulou for their advice and support in the area of peptidoglycan and Amy O'Reilly for cloning *MraY* constructs. I would like to thank Anne Smith and Eddie Ryan for their help and support whenever it was needed. I also benefited from much help from the Challis Group. I would like to thank Dr. Yuki Inahashi and John Sidda for their help with *Streptomyces* cell extracts.

I would like to thank the members of my academic advisory panel: Dr. Ann Dixon and Dr. Claudia Blindauer for their suggestions during my research. I would also like to thank Dr. David Roper from Life Sciences for his advice and for the purified enzymes that he generously provided and Anita Catherwood for sharing her experiences in the field of radiochemical synthesis. I would like to thank Dr. Julie Jones from QuBic for the curve fitting programs and her explanations about the statistical software GenStat.

I owe a great debt to Philip Aston and Dr. Lijiang Song for carrying out the high resolution mass spectrometry featured in this thesis and for training me to use the LC-MS and interpret data.

Finally, I would like to thank my family for their support and encouragement over the past four years.

Declaration

The experimental work reported in this thesis is original research carried out by the author, unless otherwise stated, in the Department of Chemistry, University of Warwick, between February 2010 and December 2013.

No part of this work has previously been submitted for any other degree, or qualification at any other institution.

All sources of information have been specifically acknowledged in the form of references.

Date:

Agnes Mihalyi

Abstract

Bacterial drug resistance is an increasingly serious problem that threatens public health and researchers need to develop new drugs. The biosynthetic pathway of the bacterial peptidoglycan is a known and good target for the development of novel antibacterial agents.

This research project focused on the first lipid-linked step of peptidoglycan biosynthesis. The enzyme required for this step is Phospho-MurNAc-pentapeptide Translocase *MraY*. Our aim was to screen for novel inhibitors of *MraY*. A continuous fluorescence *MraY* assay was developed and optimised to test known and potential inhibitors such as nucleoside natural products, antimicrobial peptides and structurally new small molecule potential inhibitors.

The fluorescence assay was adapted to a high-throughput fluorescence assay in microtitre plate format and around 2,000 compounds were screened from the diversity set of the National Cancer Institute (NCI) against *MraY* in order to identify novel inhibitors. However, around 22 % of the test compounds from the diversity set interfered with fluorescence. Therefore, a radiochemical *MraY* assay was developed as an independent method. We eventually identified one potential *MraY* inhibitor from the diversity set, the naphthylisoquinoline alkaloid, michellamine B, with IC_{50} values of 400 and 340 $\mu\text{g/ml}$ against *E. coli* and *B. subtilis* *MraY* respectively. The compound showed antibacterial activity against *B. subtilis* with an MIC value of 16 $\mu\text{g/ml}$.

It was established that *MraY* inhibition from the pacidamycin producer, *S. coeruleorubidus*, was detectable directly from culture supernatants by the fluorescence and by the radiochemical *MraY* assays. Therefore, we tested culture supernatants and cell extracts from various *Streptomyces* strains. *MraY* inhibition was observed using cell extracts from *Streptomyces venezuelae*, and higher levels of inhibition were observed from a *gbnB/gbnR* *S. venezuelae* mutant, though it was not possible to identify the active species present.

Following an earlier report of halogenated fluoresceins identified from a combined *MraY*/MurG screen, we also tested several halogenated fluoresceins, and found that phloxine B, a tetra-bromo fluorescein analogue, was an inhibitor of *E. coli* *MraY* with an IC_{50} value of 32 μM , and also inhibited *MraY* from *P. aeruginosa*, *B. subtilis*, *M. flavus* and *S. aureus* with IC_{50} values ranging between 100 and 210 $\mu\text{g/ml}$.

1 Introduction

Modern medicine seemed to fight successfully against bacterial infections over the last century, however the appearance of bacterial resistance to commonly used antibiotics is constantly increasing. Methicillin-resistant *Staphylococcus aureus*¹, vancomycin-resistant *Enterococcus faecium*² and fluoroquinolone-resistant *Pseudomonas aeruginosa*³ represent a serious threat to public health while in the developing world, bacterial infections still count as a major cause of death, and even tuberculosis has returned⁴. There is a need for developing novel antibacterial agents with new mechanisms of action as some bacteria have the worrying ability to adapt and gain resistance. New alternatives to treat bacterial infections could be derived from bacteriophages, antimicrobial peptides and monoclonal antibodies⁵. One way to search for new antibacterial agents is screening structurally diverse compound libraries of several thousands of compounds against potential targets such as proteins, enzymes and receptors⁶.

The success of antibacterial agents is due to the fact that bacterial and animal cells have important differences in their structure and biosynthetic pathways, thus they can act selectively against bacteria. Important differences between prokaryotic and eukaryotic cells are that the bacterial cell does not have a defined nucleus or organelles, has to synthesise enzymes to produce vitamins and they possess a cell wall⁴. Bacteria can be divided into two groups by Hans Christian Gram's dye staining method (1884); Gram-positive and Gram-negative bacteria. Gram-positive bacteria retain the dye while Gram-negative bacteria do not. The differences in the staining response are due to structural differences in their cell wall⁷(Figure 1-1).

The cell wall, located at the outer side of the cytoplasmic phospholipid membrane, is one of the most important elements of a bacterial cell because it provides rigidity and structural strength to bacteria and also maintains the osmotic pressure of the cytoplasm. Gram-negative bacteria have a thin peptidoglycan layer and an outer membrane that contains lipoproteins, phospholipids and lipopolysaccharides facing into the outer side of the cell wall, and porins for passive nutrient transport. On the other hand, Gram-positive bacteria have a significantly thicker peptidoglycan layer and thus retain the Gram-staining dye. The cell wall of Gram-positive bacteria contains polysaccharides, anionic polymers called teichoic acids within the peptidoglycan layer, and lipoteichoic acids which are linked to the lipids from the cytoplasmic membrane and most importantly, Gram-positive bacteria lack the outer membrane⁸ (Figure 1-1).

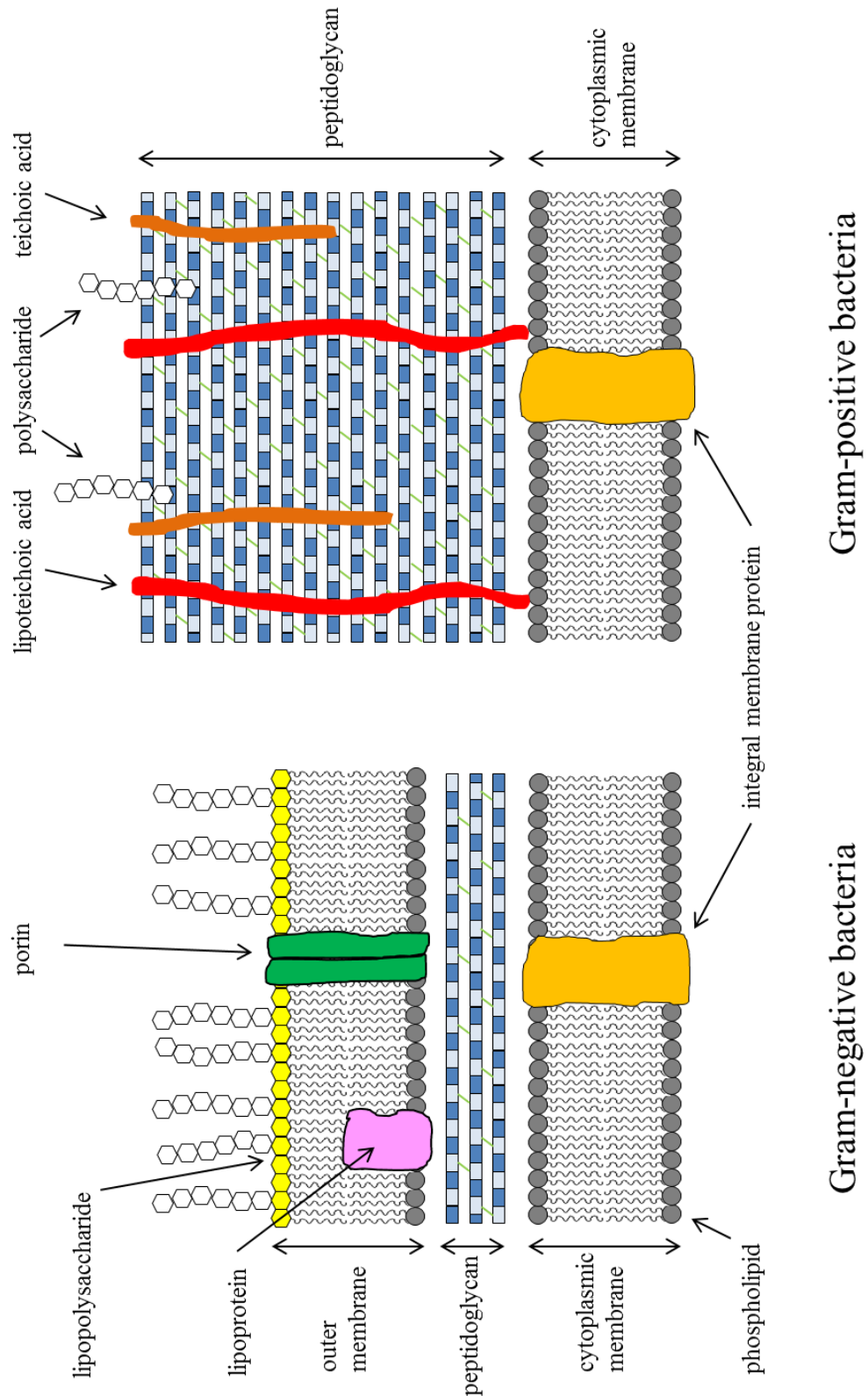


Figure 1-1: Differences in the Gram-negative and Gram-positive cell wall; prepared in Microsoft PowerPoint based on a similar figure in Maliničová *et al.* (2010)

Peptidoglycan (Figure 1-2) is a major heteropolymer of the cell wall of bacteria consisting of linear glycan chains of alternating N-acetylmuramoyl-peptides (MurNAc-peptides) and N-acetylglucosamine (GlcNAc) that are cross-linked by peptide chains²⁹. The linear chains of alternating N-acetylglucosamine and N-acetylmuramic acid sugars are linked by a β -(1,4)-glycosidic bond. The N-acetylmuramic acid moieties are linked via a lactyl group to the pentapeptide L-Ala- γ -D-Glu-X-D-Ala-D-Ala; where X at the third position is a diamino acid, either *meso*-diaminopimelic acid (*m*-Dap), lysine (L-Lys), or rarely ornithine (Orn), depending on the bacterial species (Figure 1-3). Most Gram-negative bacteria have *m*-Dap while Gram-positive bacteria have L-Lys at the third position of the pentapeptide chain. These peptide chains are cross-linked in the final transpeptidation step between the ϵ -amino group of the third position amino acid (*m*-Dap or L-Lys) and the carboxyl group of the fourth position amino acid (D-Ala) of the next strand¹⁰. Figure 1-2 shows the example for the Gram-negative *E. coli* peptidoglycan.

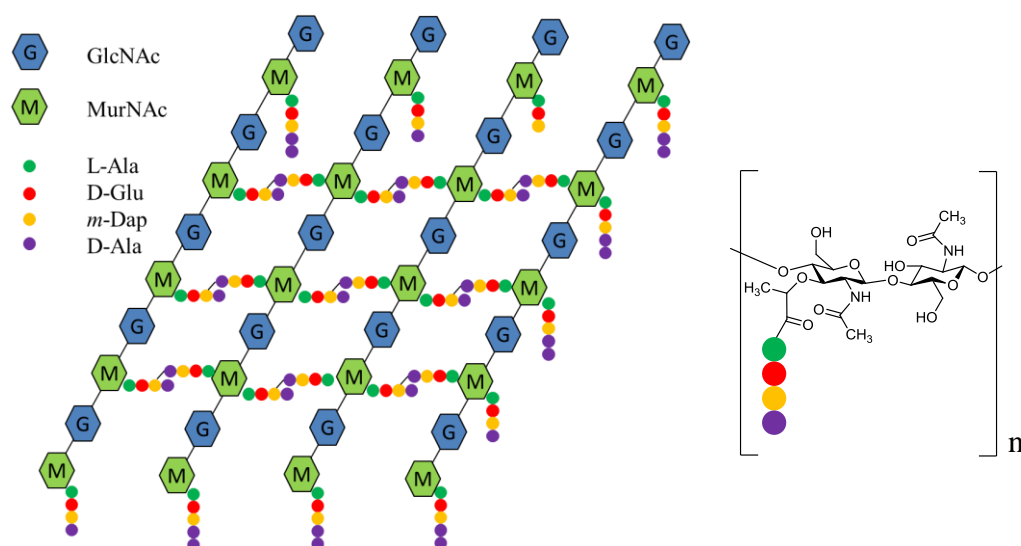


Figure 1-2: Representation of the forming peptidoglycan heteropolymer for *E. coli*, β -(1,4)-glycosidic bond between GlcNAc and MurNAc and lactyl linkage between MurNAc and L-Ala

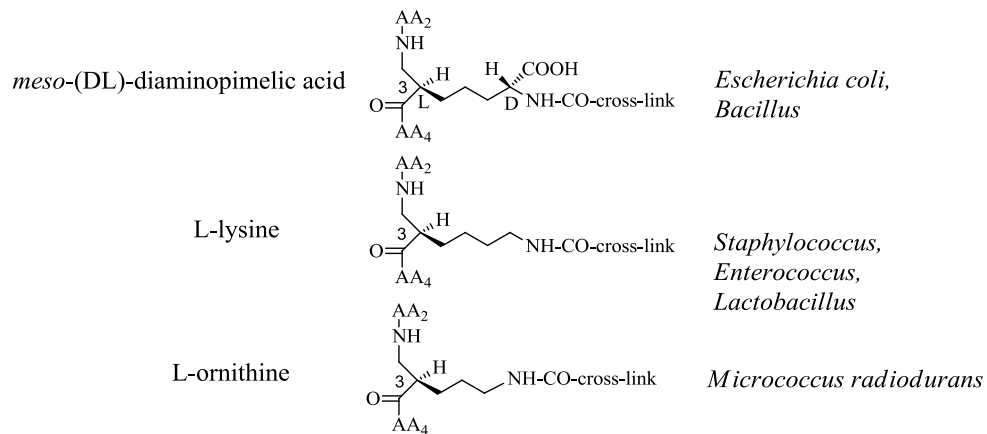


Figure 1-3: Examples of diamino acids at the third position of the peptide chains in peptidoglycan, AA: amino acid

Some bacteria also have interstrand linkages made up of one or more amino acids. The Gram-positive *S. aureus* peptidoglycan (Figure 1-4) contains pentaglycine bridges between the pentapeptides of the glycan chains. The ϵ -amino group of L-lysine is bonded to the carboxy-terminal glycine residue of the interchain pentaglycine peptide bridge by FemX. The subsequent glycine residues are added by FemA and FemB. Finally, the fifth glycine residue is linked to the carboxy-terminus of the fourth position D-Ala of the next strand by transpeptidases while D-Ala at the fifth position is released¹¹.

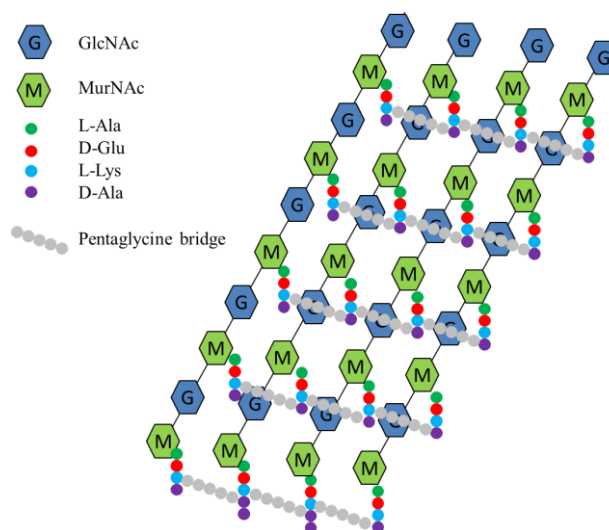


Figure 1-4: *S. aureus* peptidoglycan

Although *B. subtilis* belongs to the Gram-positive bacteria, its peptidoglycan cell wall (Figure 1-5) unusually contains *meso*-diaminopimelic acid at position 3 instead of L-lysine¹².

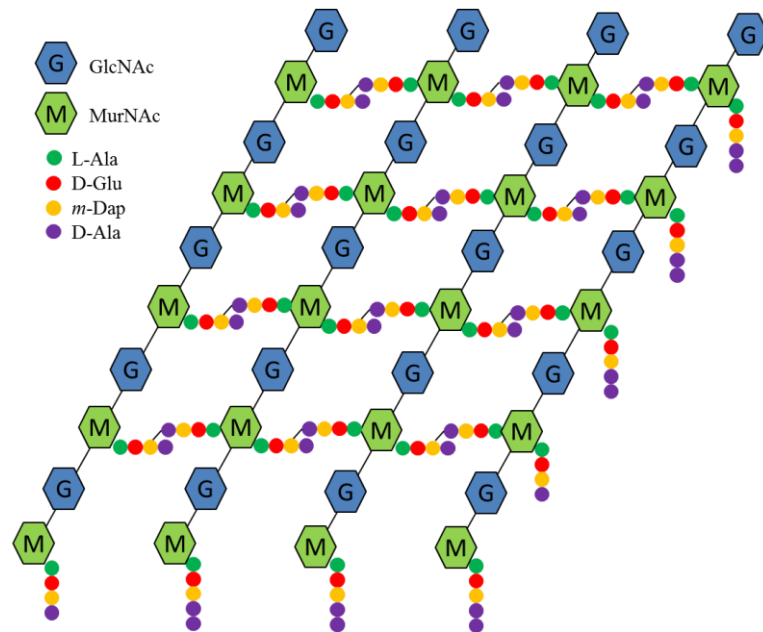


Figure 1-5: *B. subtilis* peptidoglycan

While the peptidoglycan heteropolymer grows, it is synthesised and broken down at the same time by synthases and hydrolases. Peptidoglycan hydrolases are a numerous group of enzymes that are able to cleave chemical bonds in peptidoglycan and take part in the regulation and turnover of peptidoglycan cell wall growth, cell division and autolysis⁸. Glycosidases, N-acetylmuramidase and N-acetylglucosaminidase hydrolyse the β -(1,4) glycosidic bonds between MurNAc and GlcNAc sugars to give 1,8-dehydromuramyl units¹³, while carboxypeptidases and endopeptidases cleave amide bonds between amino acids in peptide chains and bridges. Carboxypeptidases remove a C-terminal amino acid, D,D-peptidases cleave between two D-amino acids while D,L- or L,D-peptidases cleave between an L- and a D-amino acid. Endopeptidases cleave

within the peptide. D,D-carboxypeptidases cleave the fifth position D-alanine from the peptide chain and this changes the substrate properties because tetrapeptides can only be acceptors while pentapeptides containing the terminal D-Ala-D-Ala moiety can be donors and acceptors as well for a peptidoglycan transpeptidation reaction. N-acetylmuramoyl-L-alanine amidases hydrolyse the amide bond between MurNAc and L-alanine of the peptide cross-bridge^{8, 14, 15}.

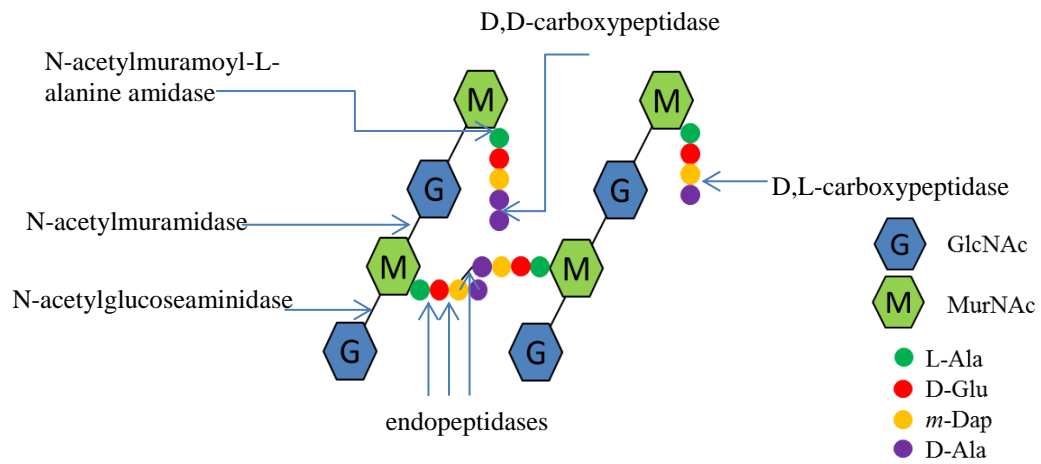


Figure 1-6: Peptidoglycan hydrolases

Maintaining the balance between the constructive activities of peptidoglycan synthases (see Figure 1-7) and the destructive activities of the above mentioned peptidoglycan hydrolases is crucial for the survival of the bacterial cell, or the process results in cell lysis. However, the mechanism of their regulation is yet unknown¹⁵.

1.1 Peptidoglycan biosynthesis and inhibitors

Since the bacterial cell wall is a crucial component for the survival of bacteria but eukaryotic cells do not possess a peptidoglycan cell wall, enzymes involved in peptidoglycan biosynthesis are highly desirable and selective targets for antibacterial agents.

The peptidoglycan biosynthetic pathway can be divided into three major stages, the cytoplasmic steps where UDPMurNAc-pentapeptide assembles following a series of steps catalysed by the Mur enzymes A-F, the lipid linked steps where the monomeric peptidoglycan building blocks lipid I and II are formed by MraY and MurG, and finally the periplasmic steps where the polymerisation reactions take place catalysed by transglycosylase and transpeptidase enzymes¹⁶ (Figure 1-7).

This section summarises the function of the enzymes of the peptidoglycan biosynthetic pathway and their published inhibitors.

1.1.1 Cytoplasmic steps

The cytoplasmic steps have been targets for high-throughput screening by several companies and academic groups because of the availability of spectrophotometric assays and three-dimensional structures of the enzymes determined by X-ray crystallography¹⁶.

1.1.1.1 MurA

The first step in peptidoglycan biosynthesis is catalysed by UDPGlcNAc enolpyruvoyl transferase, the transfer of an enolpyruvyl unit from phosphoenolpyruvate (PEP) to UDPGlcNAc¹⁷ (Figure 1-8).

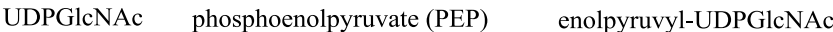


Figure 1-8: The reaction catalysed by MurA

Some Gram-positive bacteria, such as *S. aureus*, have two distinct genes encoding these enzymes, *murA* and *murZ*^{18, 19}. Fosfomycin (Figure 1-9) was shown to irreversibly inhibit UDPGlcNAc enolpyruvyl transferase by forming a covalent bond with the active site cysteine residue, Cys-115^{20, 21}, and kinetic studies showed that fosfomycin inhibited MurA and MurZ from *S. aureus* with IC₅₀ values of 1.36 μ M and 1.37 μ M respectively¹⁹. However, fosfomycin resistant bacteria express the Asp-115 variant of MurA²². The quinone ring of the fungal terreic acid (Figure 1-9) was also found to be covalently attached to the thiol group of Cys-115 by X-ray crystallography (IC₅₀: 15 μ M)²³. In addition, synthetic 2-aminotetralones were identified as inhibitors of MurA and its homologue MurZ (IC₅₀: 3-28 μ M) with some antimicrobial activity against *S. aureus* (MIC: 8-128 μ g/ml)²⁴. The sesquiterpene lactone cnicin (Figure 1-9) was found to form an adduct with enolpyruvyl-UDPGlcNAc as a noncovalent suicide inhibitor (IC₅₀: 17 μ M) and was suggested to have the potential to inhibit the Asp-115 mutant as well.²⁵ Figure 1-9 shows the chemical structures of MurA inhibitors and the formation of the covalent adducts with the Cys-115 residue of *E. coli* MurA.

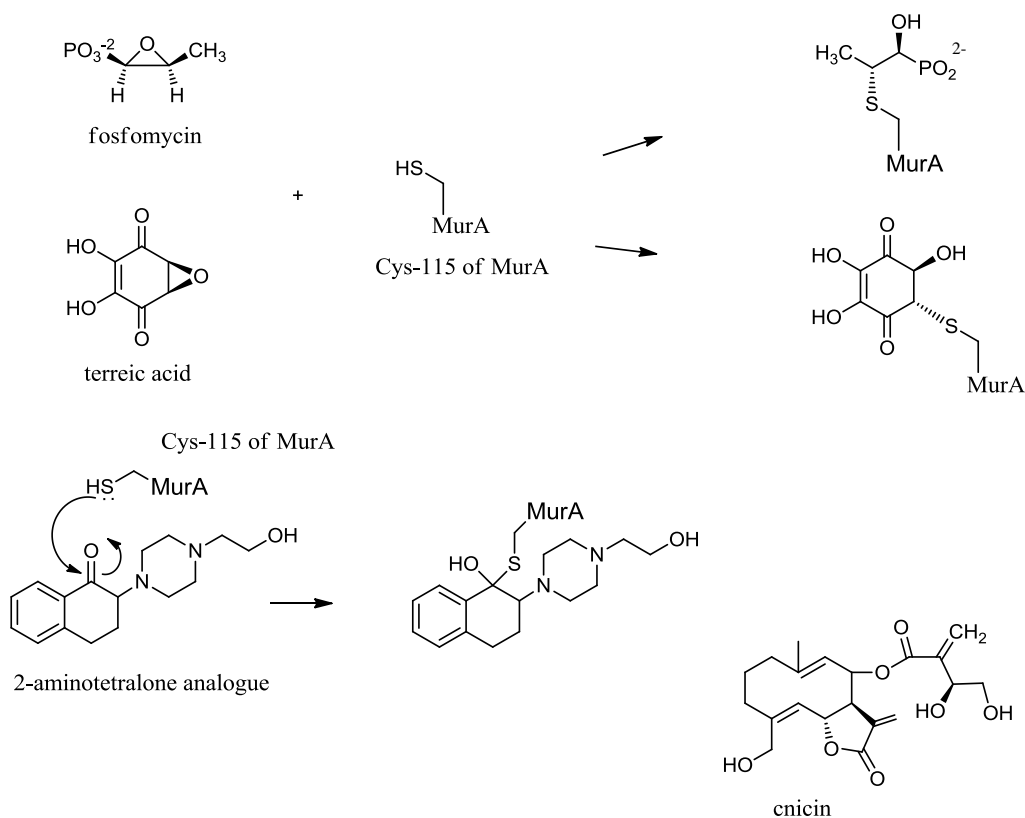


Figure 1-9: Chemical structures of MurA inhibitors: fosfomycin, terreic acid, 2-aminotetralone analogue and cnicin where fosfomycin, terreic acid and the most potent 2-aminotetralone analogue (MIC: 8 $\mu\text{g/ml}$ against *S. aureus*) covalently bind to Cys-115 of MurA

Peptide inhibitors of MurA emerged from phage display library screens, the most potent synthetic peptide (HESFWYLP HHQSY) was a competitive inhibitor of UDPGlcNAc and had an IC_{50} value of 200 μM ²⁶.

1.1.1.2 MurB

MurB, a NADPH dependant enolpyruvyl reductase, is responsible for the second committed step of bacterial peptidoglycan biosynthesis, reducing the carbon-carbon double bond of UDP-enolpyruvate to give UDPMurNAc. A series of imidazolinone analogues (Figure 1-10) with IC_{50} values ranging between 12-49 μM and MICs ranging between 2-4 $\mu\text{g/ml}$ against *S. aureus* were discovered²⁷.

4-Thiazolidinones (Figure 1-10) were identified as possible diphosphate mimics with IC_{50} s ranging between 7.7 and 28.4 μM ²⁸. Pyrazolidine-3,5-dione analogues (Figure 1-10) with IC_{50} values in the low micromolar range were reported to act as MurB inhibitors and they also possessed antibacterial activity against *S. aureus*. The pyrazolidine-3,5-dione analogue in Figure 1-10 has an IC_{50} of 25.1 μM and an MIC value of 8 $\mu g/ml$ against both *S. aureus* and *E. faecalis* and 4 and 32 $\mu g/ml$ against *S. pneumoniae* and *E. coli*^{16, 29}.

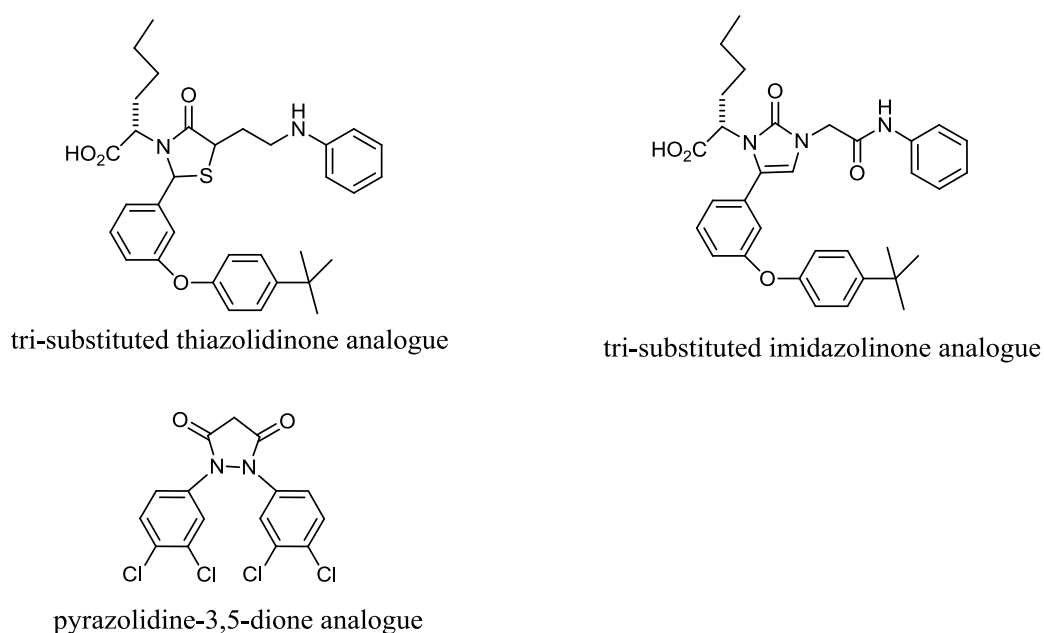


Figure 1-10: Examples of MurB inhibitors

1.1.1.3 MurC

MurC catalyses the ATP-dependent ligation of UDPMurNAc with L-Ala to form UDPMurNAc-L-Ala. The reaction begins with the attack of the carboxylate end of MurNAc on the γ -phosphate of ATP to produce an acyl-phosphate intermediate, followed by the attack of the amino group of L-Ala to yield a tetrahedral adduct. Then the elimination of inorganic phosphate leads to the

formation of the new peptide bond. All the ATP-dependent Mur ligases were suggested to follow a similar mechanism³⁰ (Figure 1-11).

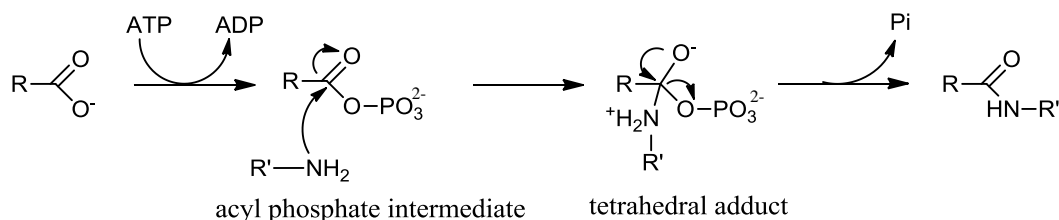


Figure 1-11: Proposed mechanism of ATP-dependent Mur ligases (C to F): the reaction begins with the attack of the carboxylate end of the MurNAc peptide (MurNAc for MurC) on the γ -phosphate of ATP to produce an acyl-phosphate intermediate, followed by the attack of the amino group of the amino acid to be added to yield a tetrahedral adduct. Then the elimination of inorganic phosphate leads to the formation of the new peptide bond

High-throughput screening of compound libraries and structure-based design have led to the discovery of new lead-compounds against MurC³¹. Benzofuran acyl-sulphonamides (Figure 1-12) were shown to be potent MurC inhibitors with an IC_{50} value of 2.3 μ M for the most active compound, competing with both ATP and UDPMurNAc and a competitive inhibitor of ATP, and the possibility of acting via compound aggregation was excluded³². A quinoxaline analogue (Figure 1-12) was published with IC_{50} values of 30.2, 26.4 and 41.6 μ M against MurC from *E. coli*, *Klebsiella pneumoniae* and *Proteus mirabilis* respectively, and it was shown to be a competitive inhibitor of ATP^{16, 33}.

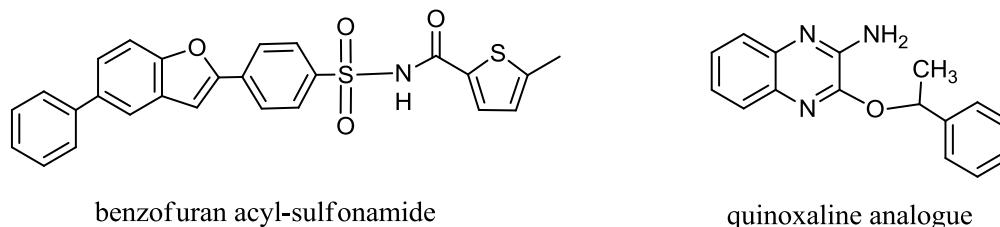


Figure 1-12: Chemical structure of the most potent analogues of benzofuran acyl sulfonamides

1.1.1.4 Glutamate racemase (MurI inhibition)

The enzyme glutamate racemase is responsible for the biosynthesis of D-glutamic acid from L-glutamic acid in many bacteria. From a high-throughput screen, a group of pyrazolopyrimidinediones were identified with selective activity against *Helicobacter pylori* with MIC values ranging between 0.5-16 $\mu\text{g/ml}$. The most potent of the series had an elevated MIC for a strain overexpressing MurI showing that inhibition was achieved by targeting MurI³⁴ (Figure 1-13).

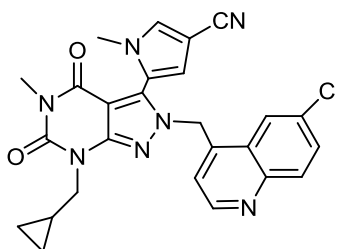


Figure 1-13: The most potent pyrazolopyrimidinediones inhibitor of glutamate racemase

1.1.1.5 MurD

MurD is the second ATP-dependent ligase of the cycle adding D-glutamic acid to UDPMurNAc-L-Ala. Phosphinate inhibitors have been designed which mimic a tetrahedral reaction intermediate, the most potent compound (Figure 1-14), containing a mixture of diastereoisomers, had an IC_{50} of 78 μM ³⁵. A series of glutamic acid-containing 5-benzylidenethiazolidine and 5-benzylidenethiazolidine-2,4-dione inhibitors were designed based on the crystal structure of a MurD-thiazolidine-2,4-dione inhibitor complex with the most potent (Figure 1-14) having an IC_{50} of 28 μM ³⁶. Moreover, macrocyclic inhibitors developed by computer-based molecular design based on X-ray crystallographic data were

found to inhibit *E. coli* MurD by binding to the active site with IC₅₀ values in the low-micromolar range (0.7-9 μM)³⁷ (Figure 1-14).

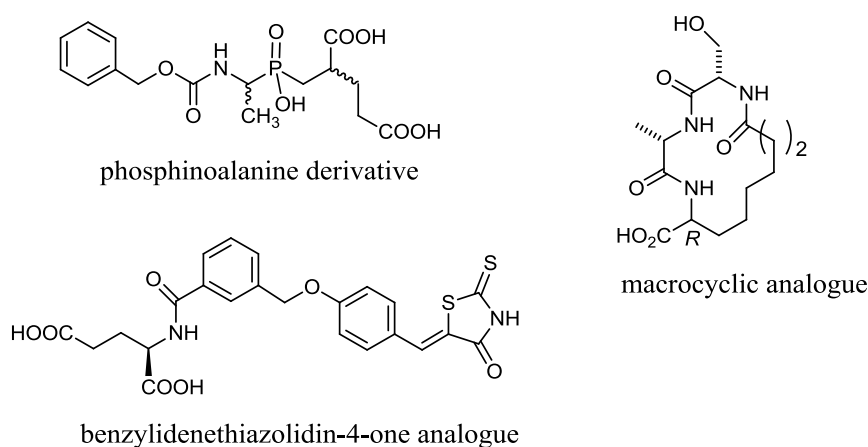


Figure 1-14: Chemical structure of MurD inhibitors, the most potent phosphinate analogue (phosphinoalanine derivative), the most potent benzylidenethiazolidine-4-one analogue and the most potent of the macrocyclic inhibitors with an IC₅₀ of 0.7 ± 0.3 μM against *E. coli* MurD

1.1.1.6 MurE

MurE, another ATP-dependent ligase of the series, is responsible for the addition of the third amino acid, most commonly L-lysine or *meso*-diaminopimelic acid to UDPMurNAc-L-Ala-D-Glu³¹. Aporphine alkaloids, 3-methoxynordomesticine analogues (Figure 1-15) showed inhibition against *M. tuberculosis* MurE with IC₅₀ values in the micromolar range and 3-methoxynordomesticine hydrochloride also showed potent anti-tuberculosis activity (MIC: 4-16 μg/ml)³⁸. Figure 1-15 shows the chemical structure of the 3-methoxynordomesticine analogues, compounds 1 and 2 were isolated from *O. macrophylla* and 3-methoxynordomesticine hydrochloride (3) was obtained from 1 by HCl treatment in ethanol³⁸.

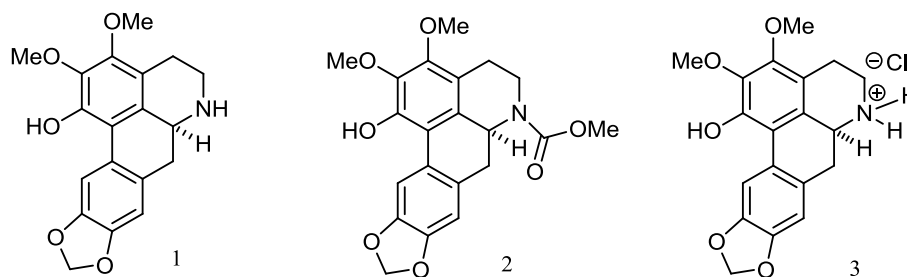


Figure 1-15: Chemical structure of 3-methoxynordomesticine analogues

In addition, a peptide inhibitor (NHNMHRTTQWPL) with an IC_{50} of 500 μ M was also identified as the most potent sequence from a phage display library screen³⁹.

1.1.1.7 Alanine racemase

Alanine racemase is a pyridoxal 5'-phosphate-dependent enzyme that catalyses the racemization of L-alanine to D-alanine⁴⁰⁻⁴⁵. D-cycloserine (K_i of 6.5×10^{-4} M) is a well-known irreversible inhibitor of *E. coli* alanine racemase⁴⁶, and O-carbamoyl-D-serine was shown to inhibit (K_i of 4.8×10^{-4} M) alanine racemase of *Streptococcus faecalis*^{47, 48}. L-cycloserine acts reversibly and is less active with a K_i value of 2.1×10^{-3} M⁴⁶. In addition, thiadiazolidinones analogues were found to inhibit alanine racemase irreversibly with IC_{50} s ranging from 0.36 to 6.4 μ M. The series also had growth inhibitory activity against *S. aureus*, including MRSA strains, with MICs values ranging from 6.25 to 100 μ g/ml⁴⁹ (Figure 1-16).

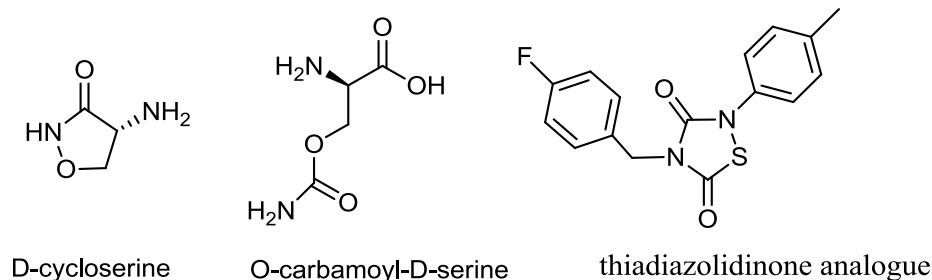


Figure 1-16: Inhibitors of alanine racemase: D-cycloserine, O-carbamoyl-D-serine and an example for the thiadiazolidinone analogues

1.1.1.8 D-Ala-D-Ala ligase (DdlB)

DdlB is another ATP-dependant ligase that assists the addition of D-Ala to D-Ala. The proposed mechanism (Figure 1-17) for the D-Ala-D-Ala dipeptide formation begins with attack of the first D-Ala on the γ -phosphate of ATP to produce an acyl-phosphate intermediate, followed by the attack of the amino group of the second D-Ala to yield a tetrahedral adduct. Then the elimination of inorganic phosphate leads to the formation of the D-Ala-D-Ala dipeptide^{50, 51}. The mechanism is similar to that of the Mur ligases (Figure 1-11).

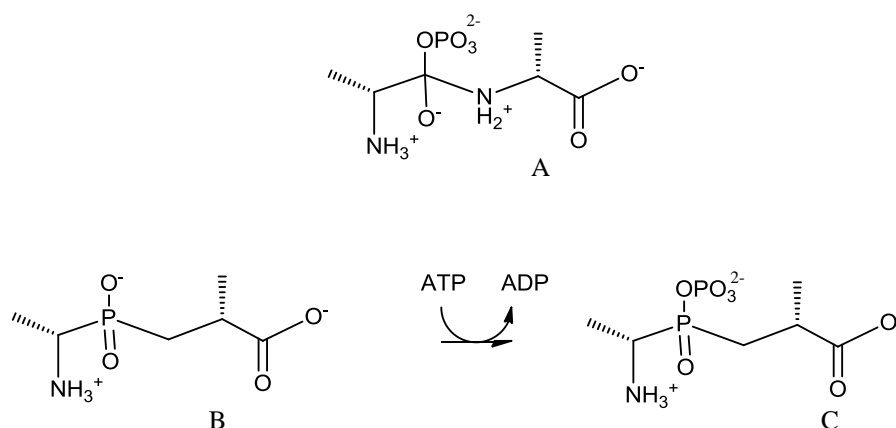


Figure 1-17: Chemical structure of the tetrahedral adduct formed during D-Ala-D-Ala formation (A), transition state analogue phosphinate inhibitor (B) and phosphinophosphate (C)

Phosphinate and phosphonate transition state analogues of the tetrahedral adduct showing time-dependant inhibition had K_i values ranging between 2-13 nM by binding to the free *E. coli* DdlB enzyme⁵². An *S,R*-methylphosphinate and adenosine triphosphate were co-crystallized with *E. coli* DdlB^{50, 53} and the structures are shown in Figure 1-18.

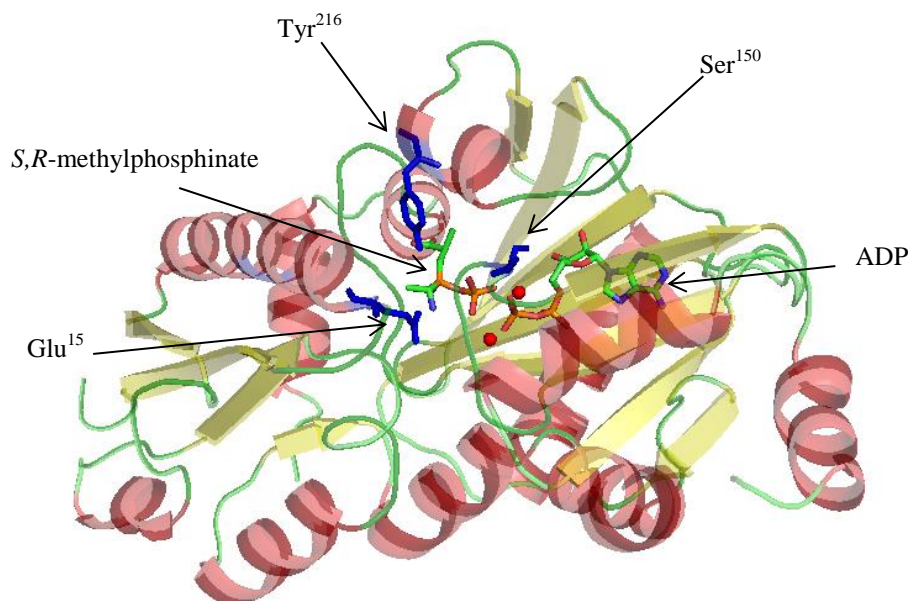


Figure 1-18: *E. coli* DdlB co-crystallized with ATP and a phosphinate inhibitor, Tyr-216, Ser-150 and Glu-15 residues in blue, red spheres are Mg²⁺ ions; figure was prepared using PyMOL molecular graphics software

The important role of a hydrogen-bonded triad of tyrosine, serine, and glutamate residues and a helix dipole was suggested to be involved in catalysing the binding and deprotonating steps of D-Ala-D-Ala formation⁵⁰.

D-cycloserine inhibits D-Ala-D-Ala ligase as an analogue of D-alanine⁵⁴. Studies on *M. tuberculosis* DdlB showed that the inhibition is reversible and competitive versus D-Ala with K_i values of 25 and 14 μ M for the C- and the N-terminal D-Ala

respectively, but uncompetitive against ATP. It was also shown that ATP binds first and ADP dissociates last from the active site⁵⁵.

Moreover, a series of hydroxyethylamines as analogues of tetrahedral intermediates of proteases were synthesised based on computer-aided design for DdlB and VanA responsible for D-Ala-D-Lac formation in vancomycin resistant bacteria (Section 5.2). The two most successful compounds had IC₅₀ values in the micromolar range against both *E. coli* DdlB and *E. faecium* VanA. Figure 1-19 shows these two compounds. The compound with R: MeO is a slightly better inhibitor, may be due to the ability of the methoxy group to accept hydrogen bond, had IC₅₀ values of 224 ± 19 µM against DdlB and 110 ± 28 µM against VanA. The compound with R: F had IC₅₀ values of 290 ± 23 µM and 136 ± 12 µM against DdlB and VanA respectively⁵³.

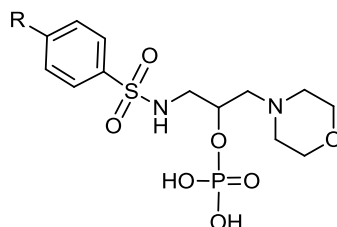


Figure 1-19: Chemical structure of hydroxyethylamines, inhibitors of DdlB and VanA, R: MeO or F

1.1.1.9 MurF

MurF, the last ATP-dependent ligase of the series of Mur synthetases, assists the addition of D-Ala-D-Ala unit to UDPMurNAc tripeptide to form UDPMurNAc-pentapeptide (Figure 1-20)³¹.

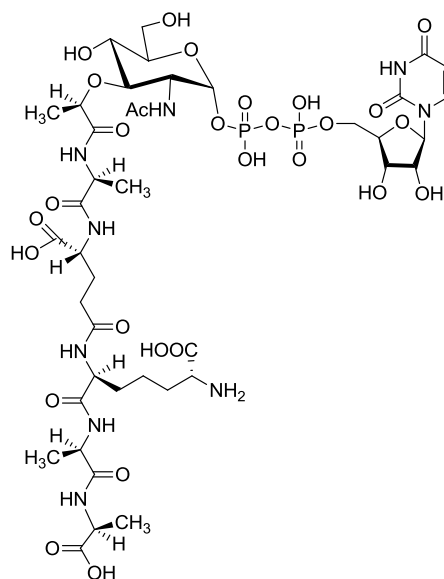


Figure 1-20: Chemical structure of UDPMurNAc-pentapeptide containing *meso*-diaminopimelic acid at the third position

A series of arylsulfonamide inhibitors (Figure 1-21) were reported with IC_{50} s in the range of 22-70 nM but they lacked antibacterial activity⁵⁶. However, a 4-phenylpiperidine (IC_{50} : 26 μ M) also showed growth inhibition against *S. aureus* with MIC values ranging between 8-16 μ g/ml⁵⁷ (Figure 1-21). In addition, diarylquinolines were identified as MurF inhibitors with an IC_{50} values ranging between 24-30 μ M and growth inhibition against *S. aureus* with an MIC of 8 μ g/ml and against *E. faecalis*^{58, 59} (Figure 1-21).

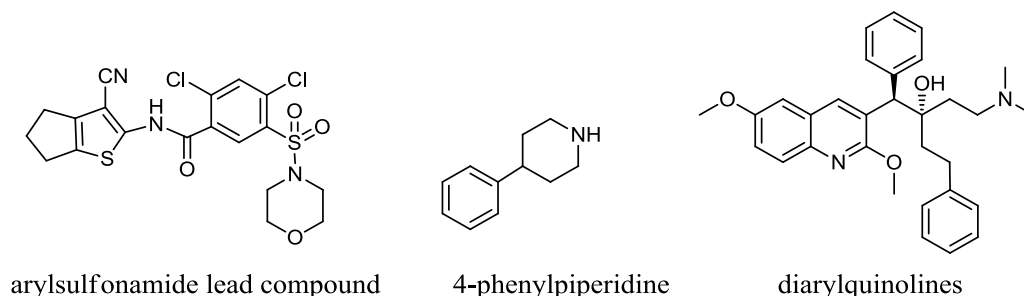


Figure 1-21: Chemical structure of MurF inhibitors, one of the arylsulfonamide lead compounds (IC_{50} : 1 μ M), 4-phenylpiperidine and diarylquinolines analogues

Phage display screening identified the peptide sequence TMGFTAPRFPHY (MurFp1) with half maximal inhibitory activity of 250 μM ⁶⁰.

Figure 1-22 shows the crystal structure of the *E. coli* apo enzyme⁶¹ and MurF from *S. pneumonia* co-crystallised with an arylsulfonamide inhibitor⁶².

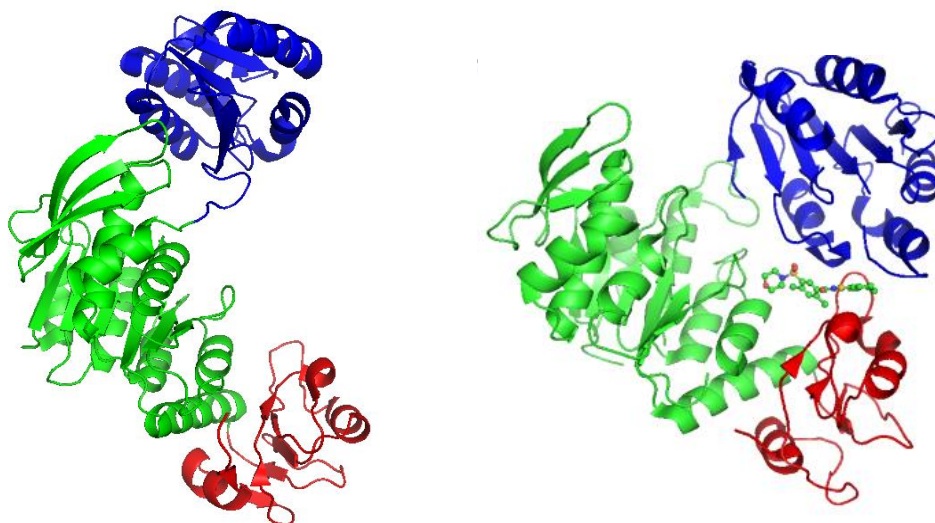


Figure 1-22: *E. coli* MurF (left) and *S. pneumonia* MurF co-crystallized with a small molecule inhibitor (right), C-domains in blue, central domains in green and N-domains in red; figures were prepared using PyMOL molecular graphics software

A considerable difference can be observed in the conformation of the open and the inhibitor bound enzyme as the C-domain moves towards the N-domain which is thought to be induced following binding by the compound⁶². Similar domain closure behaviour was observed for MurD upon ATP binding⁶³.

1.1.1.10 Synthesis of undecaprenyl phosphate

The polyisoprenoid undecaprenyl phosphate ($\text{C}_{55}\text{-P}$, chemical structure in Figure 1-23 and peptidoglycan biosynthetic pathway in Figure 1-7) is the lipid carrier molecule in bacteria that assists the translocation of hydrophilic cell wall intermediates across the hydrophobic membrane bilayer⁶⁴. In the cytoplasm, undecaprenyl pyrophosphate synthase generates undecaprenyl pyrophosphate

containing a mixed *cis*, *trans* isoprenoid chain⁶⁵. At the cytoplasmic membrane undecaprenyl pyrophosphatase dephosphorylates it to yield undecaprenyl phosphate. Undecaprenyl phosphate transfers the glycan components of the acceptor molecules to the periplasmic phase of the membranes where undecaprenyl pyrophosphate is regenerated, and it was also suggested to be recycled by recycling pyrophosphatases to undecaprenyl phosphate^{65, 66}.

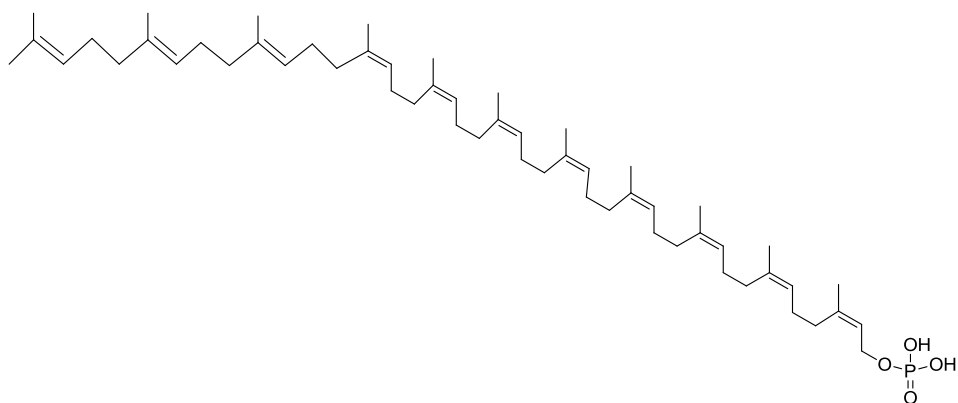


Figure 1-23: Chemical structure of undecaprenyl phosphate (C₅₅-P)

Bacitracin (Figure 1-24), a cyclic peptide natural product, which was isolated from *Bacillus subtilis*, is known to inhibit peptidoglycan biosynthesis in Gram-positive bacteria by forming a complex with undecaprenyl pyrophosphate in the presence of divalent metal ions^{67, 68}.

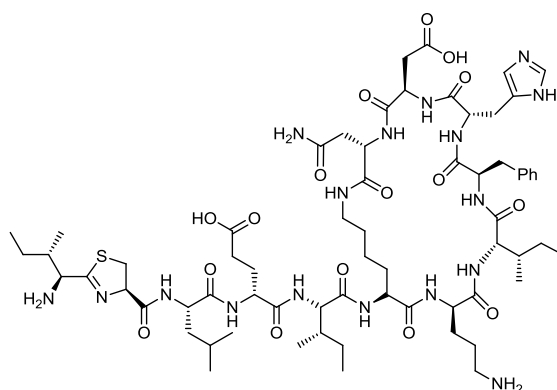


Figure 1-24: Chemical structure of bacitracin

1.1.2 The lipid-linked steps of peptidoglycan biosynthesis

Fluorescence-based and radiochemical assays have been developed for screening the lipid-linked steps (Figure 1-25), however very few inhibitor screens have been published. One example is a screen using a combined MraY-MurG assay which resulted in the identification of chemical structures of new inhibitors⁶⁹. The inhibitory potential and selectivity of the halogenated fluorescein hits from the above mentioned screen was investigated further in Section 5.4.

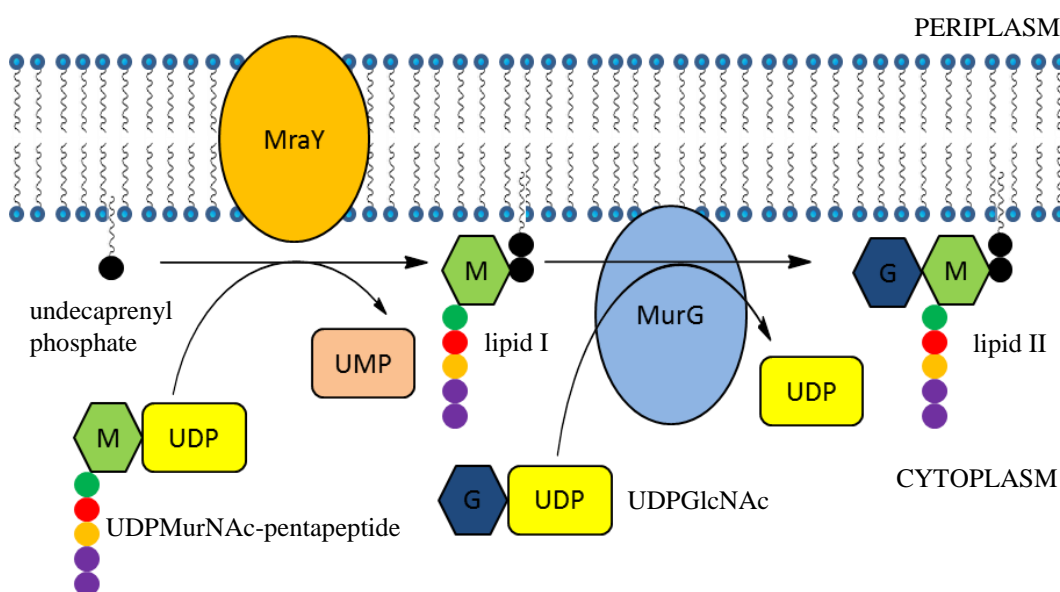


Figure 1-25: Schematic representation of the lipid-linked steps of the peptidoglycan biosynthetic pathway, catalysed by MraY and MurG

1.1.2.1 MraY

The first lipid-linked step of the peptidoglycan biosynthetic pathway is catalysed by the integral membrane protein phospho-MurNAc-pentapeptide translocase MraY. More specifically, the MraY enzyme catalyses the phospho-transfer reaction between UDPMurNAc-pentapeptide and the lipid carrier undecaprenyl phosphate (Figure 1-25). The reversible reaction generates undecaprenyl-diphospho-MurNAc-pentapeptide referred to as lipid I (Figure 1-26) and UMP.

Thus, the MurNAc-pentapeptide is transferred from the water soluble UDP moiety to a membrane component, undecaprenyl phosphate¹⁶. The *MraY* enzyme is described in more detail in Section 1.2.

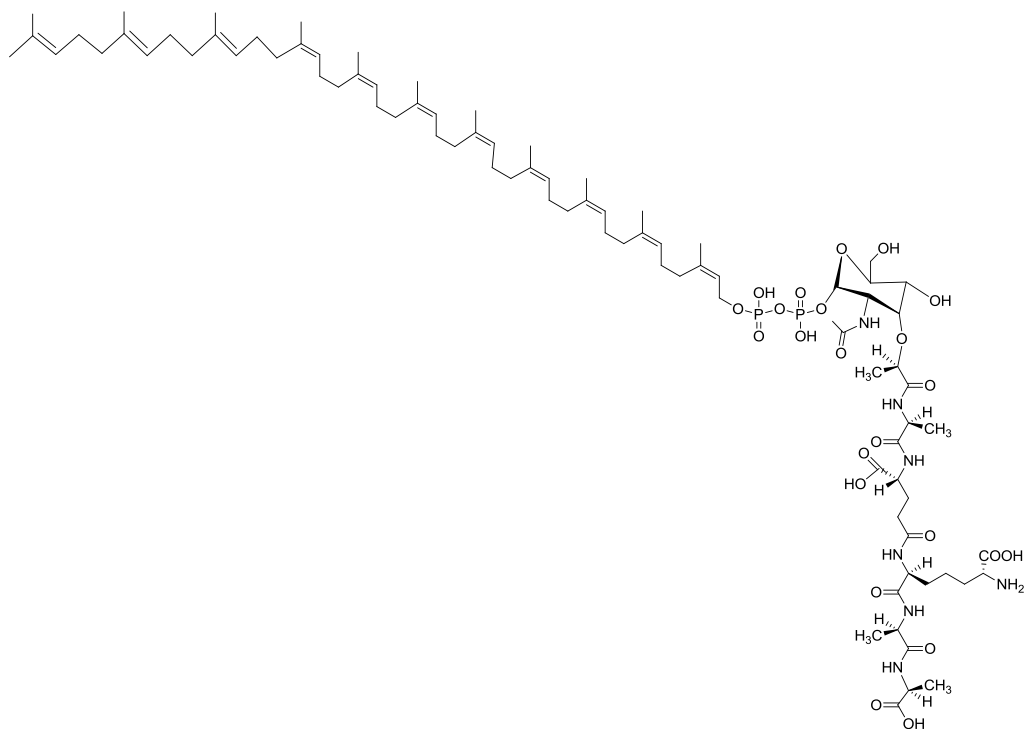


Figure 1-26: Chemical structure of lipid I (C₅₅) with *meso*-diaminopimelic acid at the third position of the pentapeptide unit

1.1.2.2 MurG

The second lipid-linked step of the cycle, the transfer of N-acetyl-D-glucosamine (GlcNAc) from UDPGlcNAc to the C-4 hydroxyl group of lipid I to form lipid II is catalysed by glycosyltransferase MurG (Figure 1-25 and Figure 1-27)^{9, 70}.

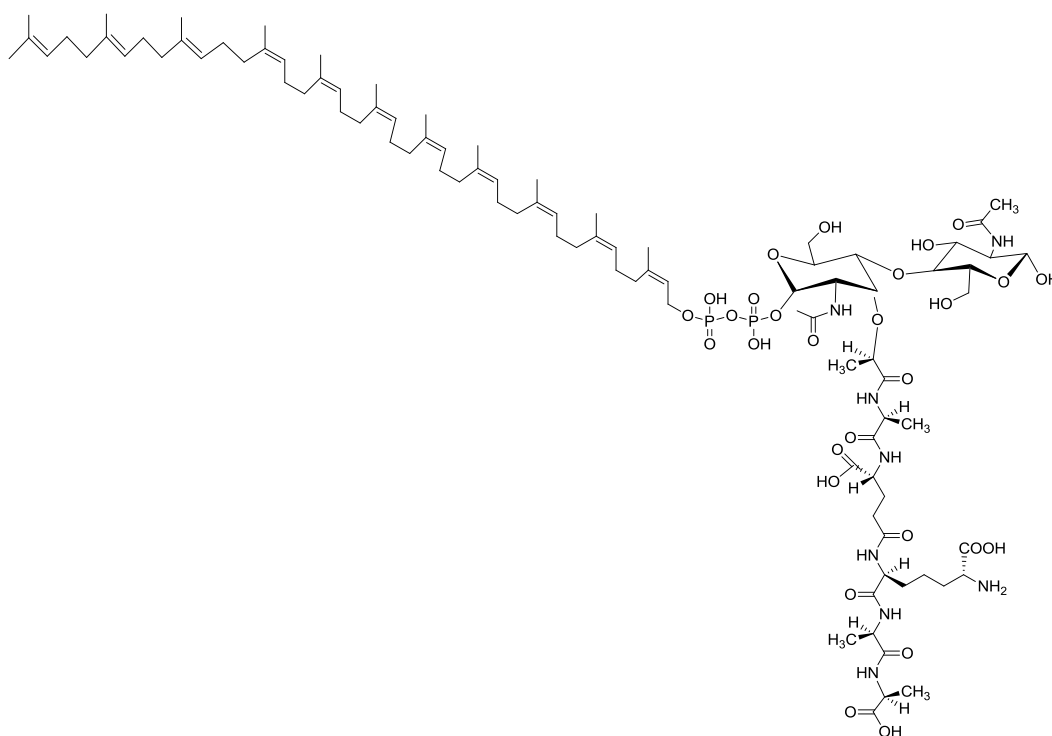


Figure 1-27: Chemical structure of lipid II (C₅₅) with *meso*-diaminopimelic acid at the third position of the pentapeptide unit

MurG is an extrinsic membrane protein and was first overproduced, solubilized from membranes, and purified by Crouvoisier *et al.* using anion exchange chromatography⁷¹. The MurG reaction was suggested to follow an ordered bisubstrate (Bi-Bi) mechanism in which the sugar substrate binds first⁷² and the process is thought to go through an oxocarbenium-ion-like transition state just like for the other enzymes of the GT-B glycosyltransferase superfamily. The reaction (Figure 1-28) was suggested to start with the deprotonation of the C-4 hydroxyl group of MurNAc from lipid I by an active site residue of MurG, possibly His-19 of *E. coli* MurG. The generated oxyanion then attacks C-1 of GlcNAc to form the oxocarbenium-ion-like transition state and during the final step UDP is released to generate lipid II⁹.

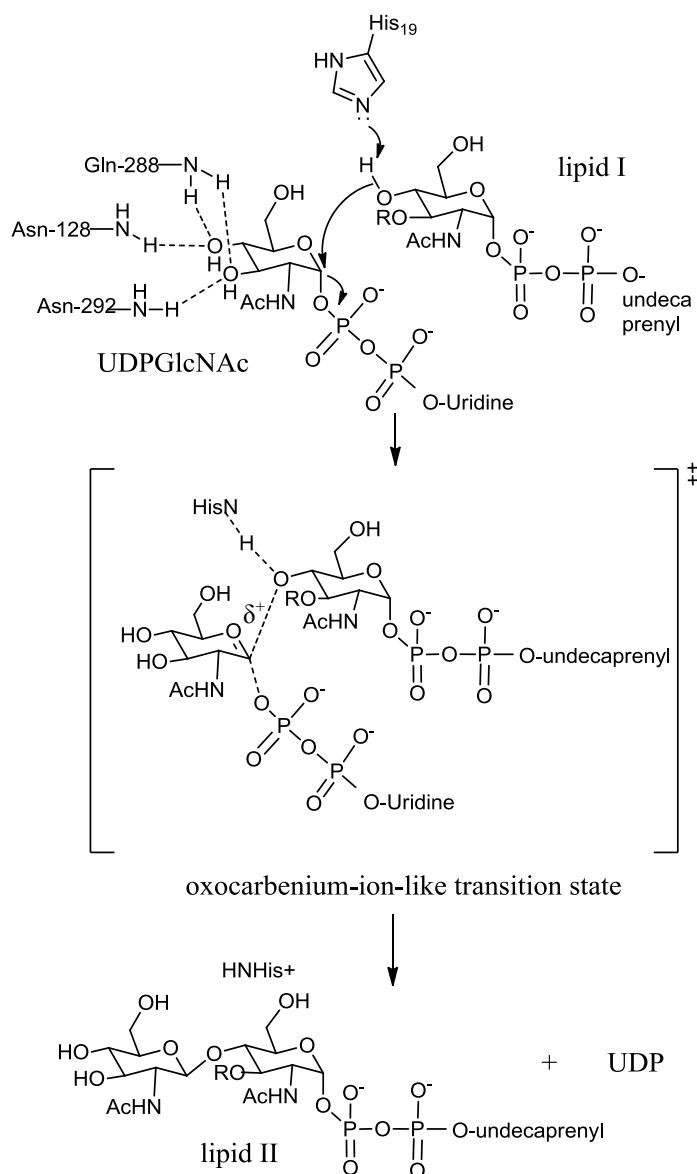


Figure 1-28: Suggested mechanism of action for MurG, R=-C(CH₃)CO-pentapeptide

An 1.9 Å crystal structure of *E. coli* MurG revealed two protein molecules in an asymmetric unit each containing an N-terminal and a C-terminal domain with minimal sequence but high structural homology separated by a deep cleft⁷³. Another 2.5 Å crystal structure of *E. coli* MurG, co-crystallized with its substrate UDPGlcNAc, showed that only one of the substrate molecules of the dimer was in the right orientation for catalytic activity⁷⁴. Interestingly, a hydrophobic patch was identified in the enzyme which could be the interaction site of this extrinsic

membrane protein with the membranes⁷³. Figure 1-29 shows the *E. coli* MurG dimer UDPGlcNAc complex.

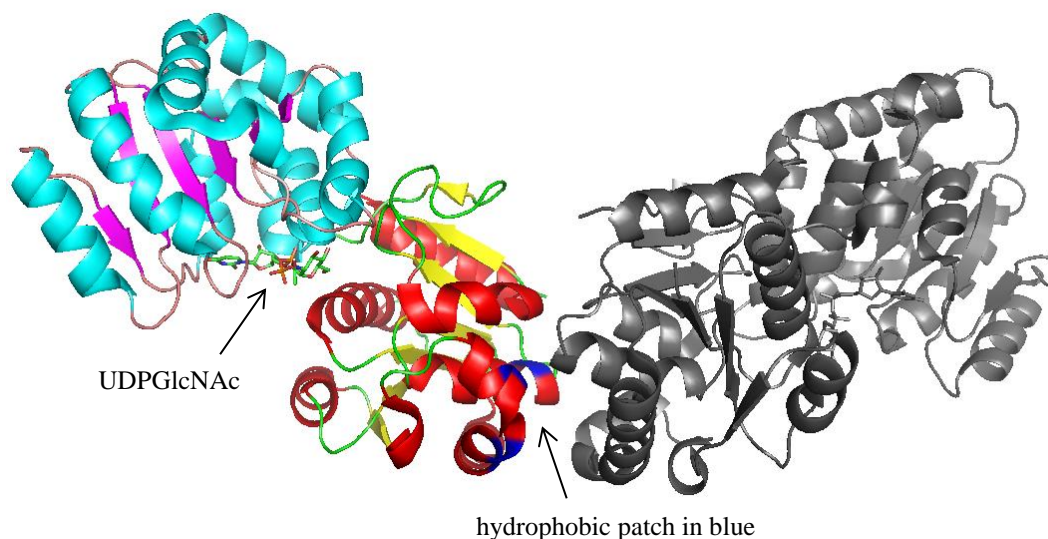


Figure 1-29: Crystal structure of MurG dimer with its substrate UDPGlcNAc in the active conformation, residues of the hydrophobic patch for membrane interaction in dark blue; figure was prepared using PyMOL molecular graphics software

The 2.2 Å crystal structure of *P. aeruginosa* MurG with UDPGlcNAc was also published recently. The authors compared it with the *E. coli* MurG complex and found a close overlap in the structural superposition of the two enzyme complexes despite their moderate, 45 % sequence similarity⁷⁵.

Ramoplanin and the structurally related enduracidin are cyclic lipoglycopeptides that were shown to inhibit MurG and the transglycosylases by forming complexes with lipid I and II^{76, 77} but ramoplanin was also suggested to interact with MurG directly and an IC₅₀ of 20 µM was measured by Helm *et al.*⁷⁸. Moreover, ramoplanin has excellent antibacterial activity against Gram-positives, such as VRE (MIC: 0.39-1.6 µg/ml)⁷⁹, MRSA (killed 99.9 % at 20 µg/ml)⁸⁰ and *Clostridium difficile* (MIC < 0.5 µg/ml)^{81, 82}.

A high-throughput MurG assay using a fluoresceinated UDPGlcNAc analogue was used to screen a 50,000 member compound library at 25 $\mu\text{g/ml}$ and led to the identification of a family of inhibitors containing a five-membered heterocyclic core (Figure 1-30) that appears to function as a diphosphate mimic of UDPGlcNAc⁸³. Further compound libraries were tested by the same method with hits showing more than 40 % inhibition at 2.5 $\mu\text{g/ml}$, however no antibacterial activity has been reported⁸⁴. Trunkfield *et al.* synthesised a series of uridine-linked proline-containing transition state mimics, the most potent showed inhibition against *E. coli* MurG with an IC_{50} value of 400 μM ⁸⁵. Figure 1-30 shows the chemical structure of a diphosphate mimic with an IC_{50} value of 1.4 μM and K_i value of 1.3 μM , and the most potent compound from the series of synthetic uridine linked proline-containing transition state mimics.

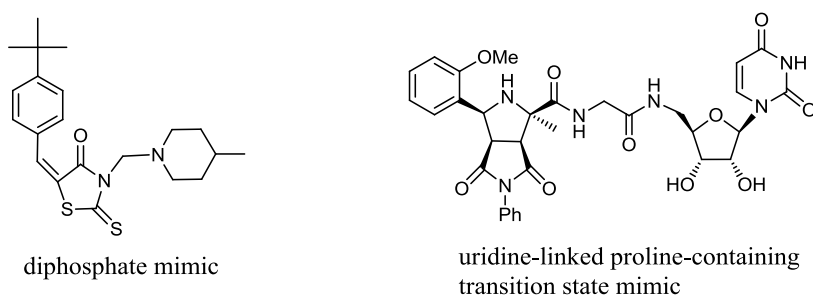


Figure 1-30: MurG inhibitors, diphosphate mimic containing a five-membered heterocyclic core, and the most active uridine-linked proline-containing transition state mimic

In order to screen compound libraries against MurG a fluorescence resonance energy transfer (FRET) assay was developed with the potential to be adapted to microtitre plate format. FRET means the transfer of fluorescence energy from a donor substrate to an acceptor substrate or reaction product. The assay used dansyl-labelled lipid I (λ_{ex} : 340 nm, λ_{em} : 500 nm) and an indole-3-acetic acid fluorophore for UDPGlcNAc (λ_{em} : 345 nm)⁸⁶.

Colicin M, a protein produced by some strains of *E. coli* to kill competitors from the same species was shown to block the biosynthesis of peptidoglycan, by presumably hydrolysing the phosphoester bond of lipid II in the periplasm^{87, 88}. The membrane-permeabilizing 34-amino-acid polycyclic peptide antibiotic nisin was shown to use lipid II as a receptor molecule for increasing its antimicrobial activity (Gram-positives) and based on experiments with pyrene-labelled lipid II it was suggested that lipid II also plays a role in pore formation⁸⁹. Another antibiotic that was suggested to act by binding to lipid II by forming an equimolar stoichiometric complex is the fungal defensin peptide containing 40-amino acids called plectasin with antimicrobial activity against Gram-positive bacteria^{90, 91}.

1.1.2.3 FemABX, MurM and MurN ligases, non-ribosomal peptide bond-forming enzymes

In the case of some Gram-positive bacteria peptide cross-bridges are formed by additional amino acids to the third position L-lysine residue of the pentapeptide linked to the fourth position D-Ala residue of the next strand. Such cases are the addition of pentaglycine bridges to *S. aureus* peptidoglycan monomers by the Fem ligases (Figure 1-4) or Ala/Ser and Ala additions by MurM⁹² and MurN⁹³ to the monomer units from *S. pneumoniae*. These peptide cross-bridge transferases were suggested to play a role in methicillin resistance and utilize aminoacyl-tRNA as a substrate^{94, 95}. A deoxyadenosine phosphonate transition state analogue was found to inhibit MurM with an IC₅₀ value of 100 µM but did not show growth inhibition against penicillin-resistant *S. pneumoniae* at 1 mM concentration and did not affect the MIC of penicillin⁹⁶. Furthermore, an aminoacyl-tRNA based analogue containing an 1,2,4-oxadiazol ring was reported to inhibit FemX with an IC₅₀

value of 1.4 μM but without antimicrobial activity or synergistic effects with penicillin^{16, 97} (Figure 1-31).

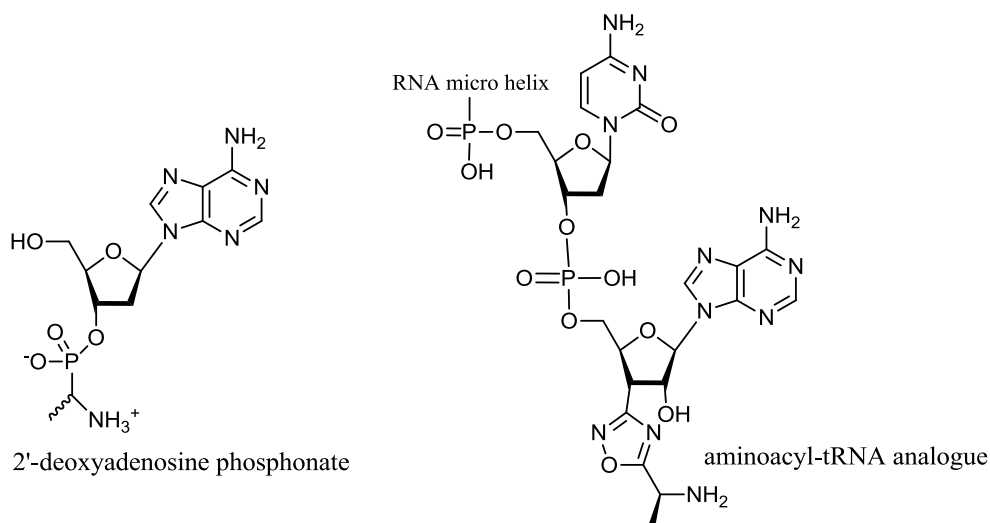


Figure 1-31: 2'-deoxyadenosine phosphonate inhibitor of MurM and aminoacyl-tRNA analogue inhibitor of FemX

1.1.3 Periplasmic steps

The lipid II monomer unit that was synthesised at the cytoplasmic face of the membrane gets flipped across the membranes by a possible ‘flippase’ protein (Figure 1-7), activity of which was suggested to be linked to transglycosylase activity⁹⁸. At the periplasmic face of the membranes, the bifunctional penicillin binding proteins (PBBs) carry out the transglycosylation and transpeptidation reactions using the modified or unmodified lipid II monomer units. However, due to the complicated nature of these reactions and the difficulties of enzyme and substrate preparations, the development of high-throughput assays for these steps has proved to be very challenging so far¹⁶.

1.1.3.1 Transglycosylases (glycosyltransferases)

Glycosyltransferases can be present as monofunctional or more often bifunctional proteins with N-terminal glycosyltransferase (GT) and C-terminal transpeptidase (TP) domains separated by a small linker region. The membrane-bound GT domain polymerises lipid II into β -(1,4)-linked MurNAc-peptide – GlcNAc polymers⁹⁹. During the reaction undecaprenyl pyrophosphate is released (see Section 1.1.1.10). Lovering *et al.* proposed a mechanism for the GT₅₁ domain of *S. aureus* PBP2, according to which E-114 (Enz B⁻) acts as a base to deprotonate the C-4 OH of GlcNAc of the acceptor lipid II, which attacks C-1 of MurNAc of the donor. E-171 may assist this process by direct protonation of the phosphate-sugar bond (Enz A-H) or by coordinating the pyrophosphate group⁹⁹ (Figure 1-32).

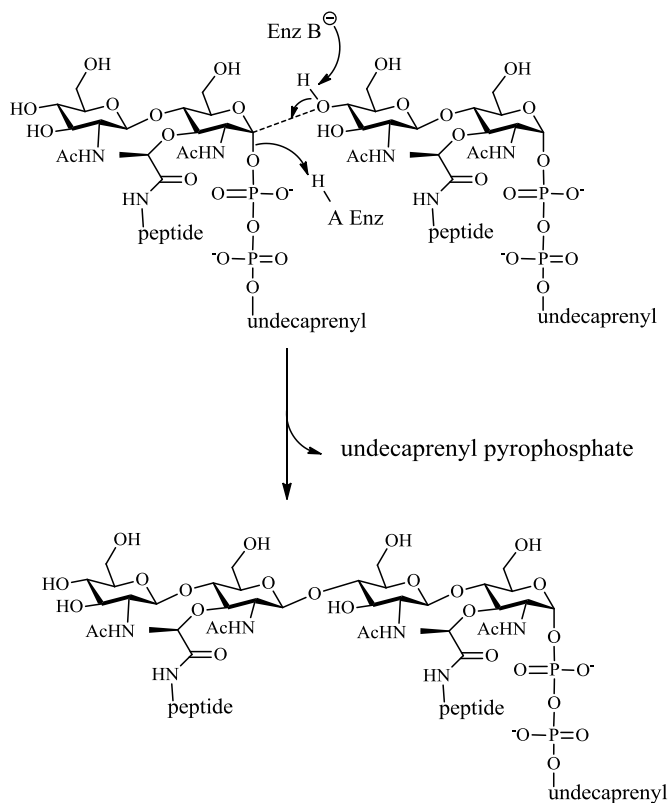


Figure 1-32: Proposed mechanism of the transglycosylation reaction of lipid II monomers

The natural product moenomycin (Figure 1-33) from *Streptomyces* is a well characterized inhibitor of the transglycosylase reaction (IC_{50} : 31 nM¹⁰⁰, and MIC: 5-300 ng/ml against Gram-positive bacteria¹⁰¹) mimicking the forming glycan chain but does not inhibit the monofunctional transglycosylase from *E. coli* or *M. flavus*^{100, 102, 103}. Unfortunately, moenomycin is not useful for clinical drug development because it is poorly absorbed by the human body⁹⁹.

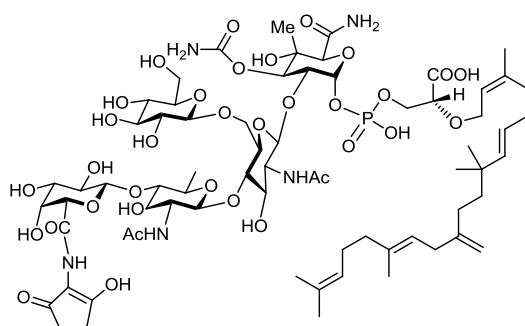


Figure 1-33: Chemical structure of moenomycin A

An iminocyclitol-based pyrophosphate mimic inhibitor was developed for the GT active site of *E. coli* PBP1b by structure-based design with > 80 % inhibition at 100 μ M concentration, also showed > 80 % inhibition at the same concentration against *C. difficile*, *S. aureus* and *H. pylori* transglycosylases but it only showed weak antibacterial activity against *S. aureus* with an MIC value of 125 μ M¹⁰² (Figure 1-34).

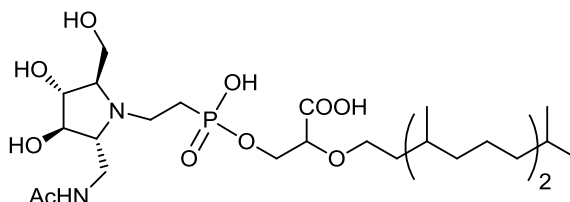


Figure 1-34: Chemical structure of the most potent iminocyclitol-based pyrophosphate mimic inhibiting transglycosylase activity

It was proposed that the natural product vancomycin (see chemical structure in Section 5.2 Figure 5-12) complexes the D-Ala-D-Ala termini of lipid II which leads to the inhibition of utilization of these substrates by transglycosylases^{104, 105}, and an IC₅₀ value of 0.38 μ M was determined against *E. coli* PBP1b¹⁰⁶. In addition, semisynthetic vancomycin analogues incorporating hydrophobic sugar substituents were suggested to interact directly with bacterial membrane proteins, such as transglycosylases, since they exhibit activity against D-Ala-D-Lac containing vancomycin-resistant *Enterococci*¹⁰⁷.

1.1.3.2 Transpeptidases

Transpeptidation is the ultimate enzymatic reaction of the peptidoglycan biosynthetic pathway giving more strength and rigidity to the peptidoglycan heteropolymer. These reactions are catalysed by either monofunctional transpeptidases or the solvent exposed TP domain of the bifunctional penicillin binding proteins⁹⁹. Most commonly the peptide chains of the glycan strands are cross-linked between the ϵ -amino group of the third position amino acid (*m*-Dap or L-Lys) and the carboxyl group of the fourth position amino acid (D-Ala) of the next strand¹⁰. Figure 1-2 illustrates the *E. coli* peptidoglycan structure while Figure 1-5 shows the example of the cross-linked *B. subtilis* peptidoglycan. However, there could be some rare *m*-Dap-*m*-Dap linkages in *E. coli* peptidoglycan¹⁰⁸. Some Gram-positive bacteria have interstrand linkages made up of one or more amino acids. The Gram-positive *S. aureus* peptidoglycan (Figure 1-4) contains pentaglycin bridges between the pentapeptides of the glycan chains¹¹.

During the transpeptidation reaction the active-site serine residue of TP attacks the C-terminal D-Ala-D-Ala peptide bond forming an acyl-enzyme intermediate and the terminal D-Ala is released. The acyl-enzyme intermediate is either hydrolysed to form a shortened peptide chain for the carboxypeptidases reaction or cross-linked with the amino group of the amino acid of the neighbouring strand⁷⁰. The transpeptidation reaction is the target of the β -lactam antibiotics such as penicillin and cephalosporin analogues since the β -lactam-thiazolidine rings have a steric analogy with D-alanyl-D-alanine¹⁰⁹ (Figure 1-35).

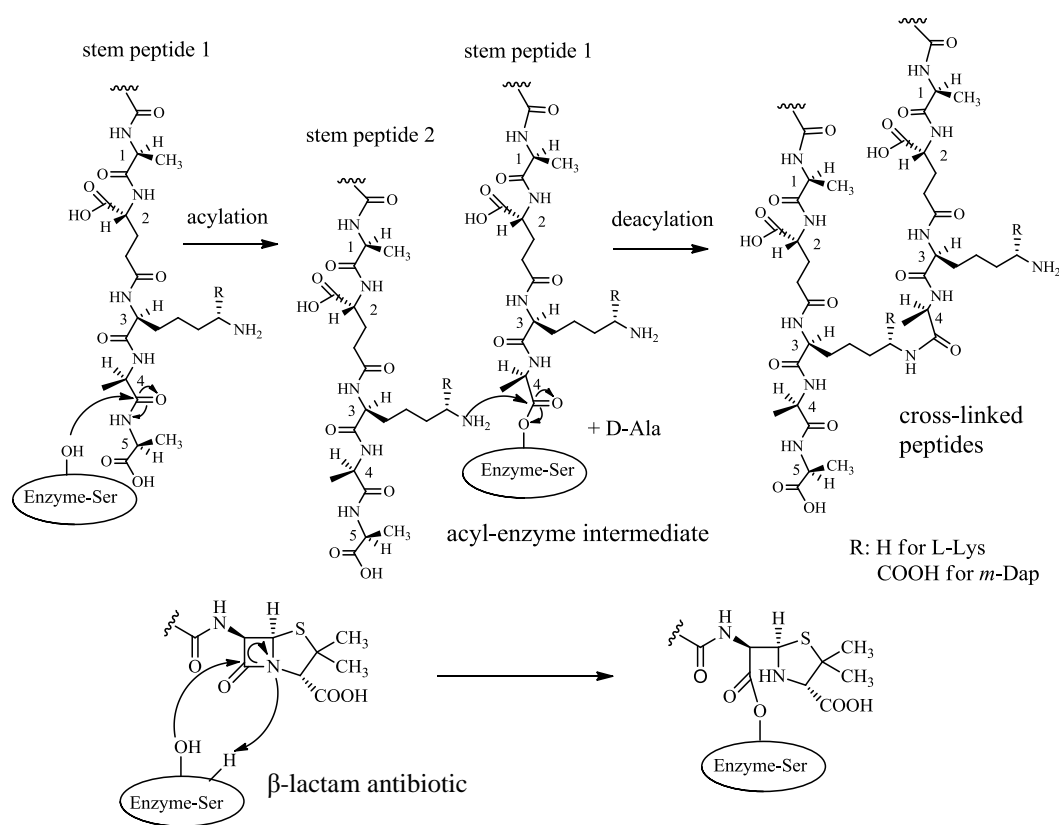


Figure 1-35: Mechanism of the transpeptidation reaction: acylation of the catalytic serine residue of TP by D-Ala at position 4 of the first stem peptide, then the acyl-enzyme intermediate is attacked by the amine of the L-Lys or *m*-Dap residue at position 3 of the adjacent stem peptide, mode of action of the β -lactam antibiotics: the active site serine residue of TP forms a covalent bond with the β -lactam ring

Unfortunately, there are several forms of bacterial resistance against the β -lactam antibiotics, such as producing modified versions of PBPs with lower affinity to β -lactam antibiotics¹¹⁰ or β -lactamase enzymes that deactivate the antibiotic by hydrolysing the β -lactam ring¹¹¹. Still, these reactions are very attractive targets for drug design because their inhibitors do not need to cross the phospholipid bilayer of the cytoplasmic membrane¹⁶.

Vancomycin is thought to prevent transpeptidases from completing the cross-linking process by binding to the D-Ala-D-Ala terminus of the peptidoglycan precursors¹¹².

A few assays have been reported, one of them is an HPLC assay to follow the transpeptidation reaction by incorporating D-Cys-D-Ala into peptidoglycan followed by fluorescent labelling and enzymatic digestion¹¹³. However, further input is necessary to develop quantitative assays that are amenable for high-throughput screening as well¹⁶.

In summary, the majority of antibiotic drugs in clinical use target the cytoplasmic and periplasmic steps of the peptidoglycan biosynthetic pathway¹⁶. The aim of this project is to find novel inhibitors for the first lipid-linked step of the cycle catalysed by the MraY enzyme which is discussed in the following section.

1.2 Enzymology of translocase MraY

Translocase MraY catalyses the reversible phospho-transfer reaction between UDPMurNAc-pentapeptide and the lipid carrier undecaprenyl phosphate with the simultaneous release of UMP (Figure 1-25)⁹.

1.2.1 Initial studies of the MraY reaction

It was first shown by the research groups of Strominger and Neuhaus that membranes from *S. aureus* and *M. lysodeikticus* in the presence of Mg^{2+} were able to transfer phospho-MurNAc-pentapeptide from the soluble cytoplasmic precursor, UDPMurNAc-pentapeptide to the lipid carrier, undecaprenyl phosphate, and generate undecaprenyl-phospho-MurNAc pentapeptide, more recently referred to as lipid I^{114, 115}.

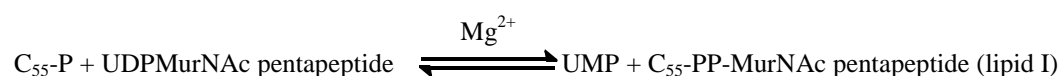


Figure 1-36: The “transfer” reaction (translocase MraY reaction)

Moreover, translocase MraY was shown to be able to exchange ³H-labelled UMP with the unlabelled UMP moiety of UDPMurNAc-pentapeptide^{115, 116}:

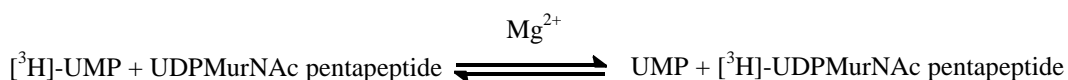


Figure 1-37: The “exchange” reaction

Ikeda *et al* successfully identified the *E. coli mraY* gene within a large cluster of genes (*mra*) where all the tightly packed genes encode proteins involved in peptidoglycan biosynthesis and cell division. The overexpression of this gene was shown to lead to an increase in phospho-MurNAc-pentapeptide translocase

activity¹¹⁷. One copy of the *mraY* gene was found in all bacteria apart from archaeobacteria¹¹⁷ and eukaryotic organisms with the exception of the eukaryotic *Arabidopsis thaliana* where a similar gene was identified¹¹⁸. In addition, the Mray activity was shown to be essential for cell wall growth and survival of the Gram-negative *E. coli*¹¹⁹ and the Gram-positive pathogen *Streptococcus pneumoniae*¹²⁰ by gene knockout studies.

Levels of Mray are very low in the bacterial cell, there are not more than 700 and 2,000 cell copies for lipid I and II respectively in Gram-negative bacteria such as *E. coli* because of their thin cell wall¹²¹. However, in Gram-positive bacteria such as *Micrococcus flavus* where the cell wall is much thicker, there are higher levels of Mray and MurG, so membranes of *M. flavus* can be used to generate lipid I and II in up to 50 mg quantities⁸⁹.

Sequence alignment analysis revealed that the Mray enzyme is part of a superfamily of enzymes called polyisoprenyl-phosphate *N*-acetylhexosamine-1-phosphate transferases¹⁰. Other prokaryotic members of this family are WecA, WbcO, TagO, WbpL and RgpG, involved in the biosynthesis of bacterial exopolysaccharides, and catalyse reactions involved in the membrane-associated polyprenol phosphate acceptor (undecaprenyl phosphate) and a UDP-*N*-acetylhexosamine donor from the cytoplasm^{122, 123}. These bacterial enzymes show more specificity towards the use of the sugar nucleotide donor, while Mray uses UDPMurNAc-pentapeptide; the other enzymes use UDPGlcNAc^{9, 124}. There are similar lipid-linked steps in the eukaryotic asparagine-linked glycoprotein synthesis where a paralogue enzyme uses UDPGlcNAc as the sugar nucleotide

donor and dolichyl phosphate as a lipid carrier¹²⁵⁻¹²⁷ (Figure 1-53 in Section 1.3.1.1).

1.2.2 Topological model for MraY

The presence of alternating hydrophobic and hydrophilic units in the primary structure of MraY¹¹⁷, and the requirement of lipid microenvironment for activity¹²⁸ indicated that MraY protein spanned the cytoplasmic membrane ten times⁹. Sequence alignment of the MraY prokaryotic orthologues revealed 14 conserved polar residues of the family on five hydrophilic sequences¹²⁹. Bouhss *et al.* studied the secondary structure of *E. coli* and *S. aureus* MraY by β -lactamase fusions and developed a topological model for the enzyme as an integral membrane protein (Figure 1-38) containing 10 transmembrane helices, five cytoplasmic and four periplasmic loops with both N- and C-termini located at the periplasmic face of the cytoplasmic membrane¹²⁹.

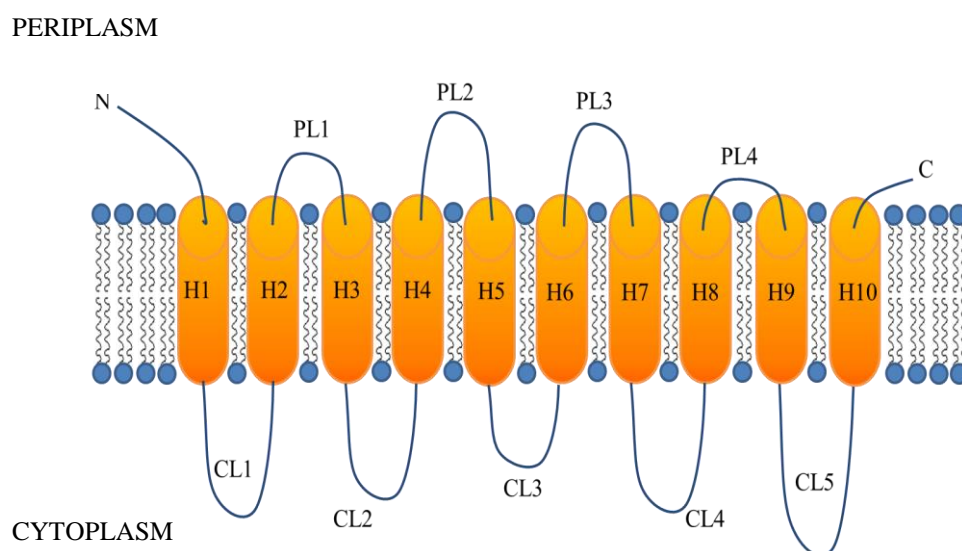


Figure 1-38: Membrane topology of MraY, PL: periplasmic loop, CL: cytoplasmic loop, H: transmembrane helix

Sequence alignment and membrane topology studies suggested that the invariant residues of the polyisoprenyl-phosphate *N*-acetylhexosamine-1-phosphate transferase superfamily were all located at the cytoplasmic face of the membranes^{123, 129, 130}.

1.2.3 Catalytic mechanism for the *MraY* reaction

Heydanek *et al.* proposed a two-step mechanism (Figure 1-39) for the *MraY* catalysed phospho-transfer reaction based on kinetic evidence¹³¹. According to this two-step mechanism, the reaction starts with the attack of an active site nucleophile of *MraY* on the β -phosphate of UDPMurNAc-pentapeptide and forms a covalent enzyme-phospho-MurNAc-pentapeptide intermediate while UMP is released. The second step consists of the attack of an oxyanion from undecaprenyl phosphate on the phosphate of the covalent intermediate leading to the formation of the native form of *MraY* and lipid I^{9, 131}.

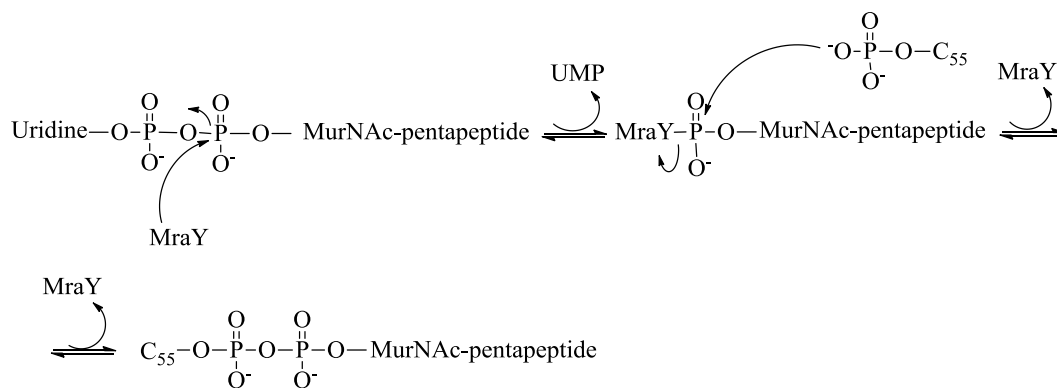


Figure 1-39: Two-step catalytic mechanism for *MraY*

Since only three amino acid residues with nucleophilic side chains were found by sequence alignments, Asp-115, Asp-116, and Asp-267 in *E. coli*, which are completely conserved in *MraY* and its related prokaryotic and eukaryotic

homologues, Lloyd *et al.* performed site-directed mutagenesis on the three conserved residues and proposed that Asp-267 could play the role of the catalytic active site nucleophile¹³⁰. The MraY activity has an absolute requirement for Mg^{2+} at 5-40 mM concentrations which could be replaced by Mn^{2+} but with significant loss of activity^{132, 133}. Lloyd *et al.* suggested that Asp-115 and Asp-116 could be involved in Mg^{2+} coordination which itself is involved with binding the pyrophosphate bridge of UDPMurNAc-pentapeptide¹⁰⁸ (see Figure 1-43 in Section 1.2.4). This suggestion was based on the fact that there are examples for a DDXXD motif to be involved in coordination of Mg^{2+} in the family of prenyl transferases^{130, 134}.

The two-step catalytic mechanism is supported by the exchange reaction (Figure 1-37) experiments of Pless and Neuhaus using *S. aureus* MraY confirming that ³H-labelled UMP can be exchanged into UDPMurNAc-pentapeptide via isotope exchange in the absence of the lipid acceptor undecaprenyl phosphate. Phospho-MurNAc-pentapeptide was formed during the reaction indicating that the enzyme-phospho-MurNAc-pentapeptide intermediate forms first during the transfer reaction. Addition of undecaprenyl phosphate stimulated the forward reaction while addition of the radiolabelled UMP or dodecylamine favoured the reverse reaction by inhibiting lipid I synthesis^{9, 135}. However, the non-purified enzyme preparation of Pless and Neuhaus could have contained phosphatases and endogenous undecaprenyl phosphate⁹.

An alternative one-step mechanism (Figure 1-40) was also proposed for the MraY reaction consisting of a direct attack of the phosphate oxyanion of undecaprenyl

phosphate onto the β -phosphate of UDPMurNAc-pentapeptide leading to the formation of lipid I and UMP in one step⁹.

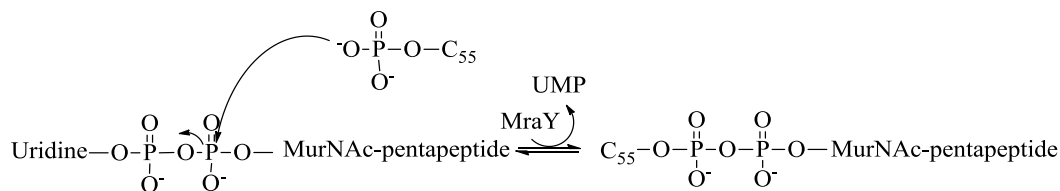


Figure 1-40: One-step catalytic mechanism for MraY

Al-Dabbagh *et al.* have carried out site-directed mutagenesis studies using purified *B. subtilis* MraY and favour the one-step mechanism in the interpretation of their data, suggesting that the Asp-98 invariant residue corresponding to Asp-115 in *E. coli* MraY, plays an important role in catalysis¹³⁶.

1.2.4 Crystal structure for *Aquifex aeolicus* MraY

Chung *et al.* have recently overexpressed, purified and crystallized recombinant MraY from a rod-shaped thermophilic bacterium, *Aquifex aeolicus*. It was shown that MraY crystallizes in both detergent micelles and in the membranes as a dimer in an asymmetric unit, which was confirmed by cross-linking studies, and the axis is perpendicular to the plane of the membrane¹³⁷. Figure 1-41 shows the 3.3 Å MraY dimer structure as seen from the membranes and from the cytoplasm with an oval-shaped tunnel at the centre of the dimer surrounded by hydrophobic amino acids¹³⁷.

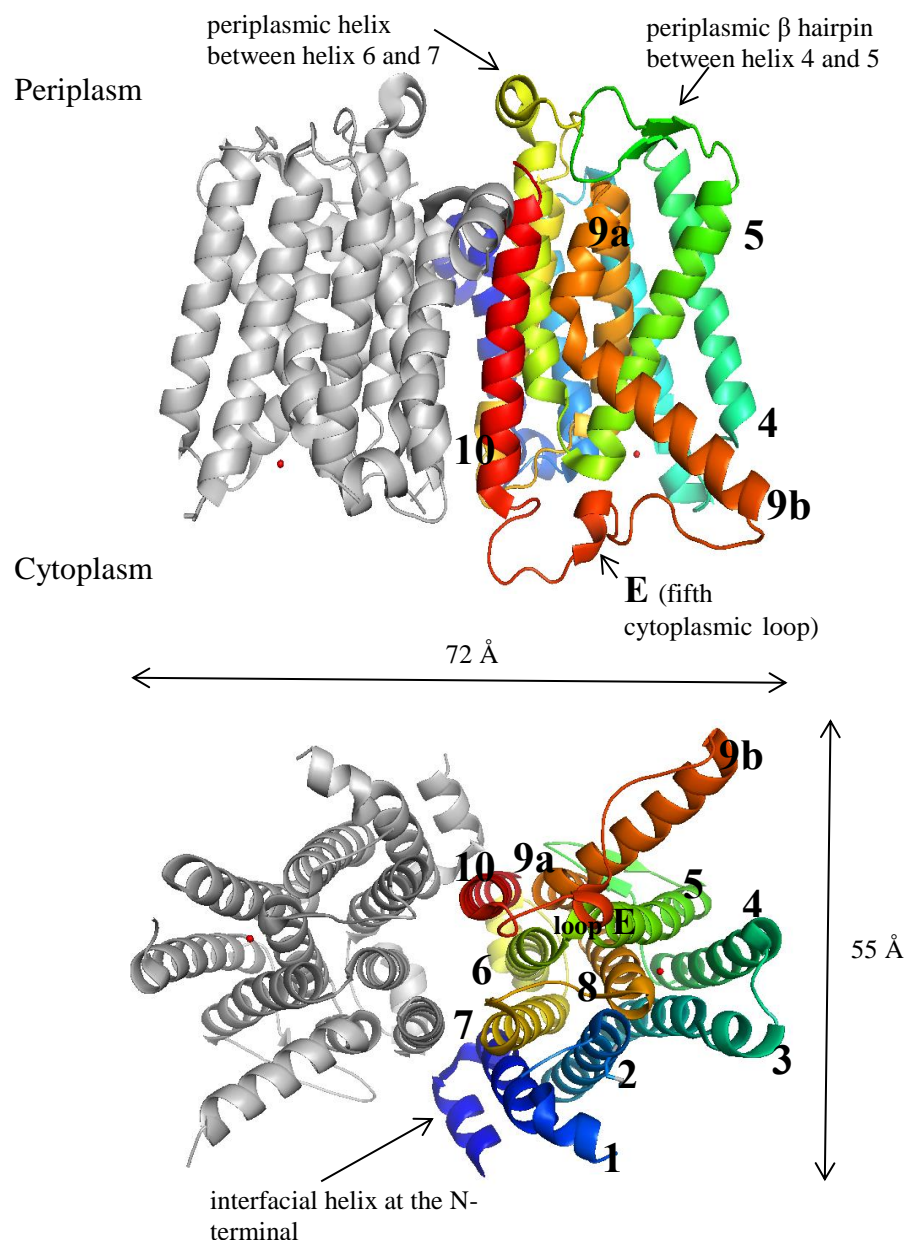


Figure 1-41: Structure of the MraY dimer from *Aquifex aeolicus*, view from within the membrane (top) and cytoplasmic view (bottom), only the transmembrane helices of one protomer are coloured, red spheres are Mg^{2+} , transmembrane helices are numbered (1-10); figures were prepared using PyMOL molecular graphics software

Each monomer contains ten transmembrane helices and five cytoplasmic loops (A to E) with both termini located on the periplasmic side of the membrane as it was suggested by Bouhss *et al.* In addition there is an N-terminal interfacial helix (IH), a periplasmic β hairpin (PB between helices 4 and 5) and a periplasmic helix (PH between helices 6 and 7). Transmembrane helix 9 breaks into two fragments (9a

and 9b) with 9b showing a significant bend in the middle of the membrane and protruding ~20 Å into the membrane (Figure 1-41 and Figure 1-42)¹³⁷.

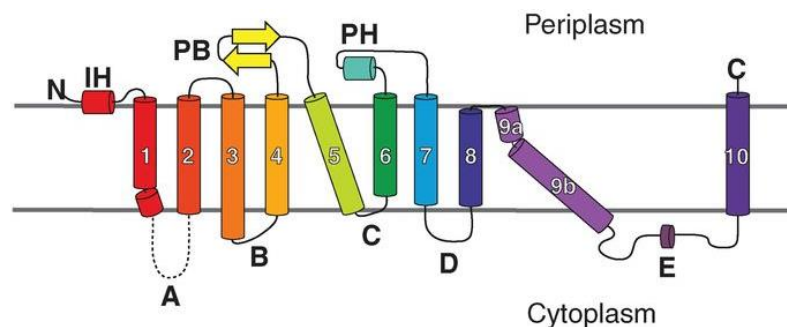


Figure 1-42: Membrane topology of *A. aeolicus* MraY, transmembrane helices are numbered, cytoplasmic loops have letters (A-E), IH: interfacial helix, PB: periplasmic β hairpin, PH: periplasmic helix¹³⁷

According to Lloyd *et al.* the conserved Asp-115 and Asp-116 residues are involved in Mg^{2+} chelation while Asp-267 is an active site nucleophile of *E. coli* MraY¹³⁰. The NCBI's sequence alignment program revealed 48 % identities and 66 % similarities in and *E. coli* and *Aquifex aeolicus* MraY sequences and Asp-115, Asp-116 and Asp-267 residues correspond to Asp-117, Asp-118 and Asp-265 of *Aquifex aeolicus* MraY respectively. Figure 1-43 shows the proposed catalytic mechanism by Lloyd *et al.* and the corresponding conserved aspartate residues of *Aquifex aeolicus* MraY. The distances between Mg^{2+} and the three aspartate residues were measured as 5.8 Å, 4.9 Å and 2.2 Å for Asp-117, Asp-118 and Asp-265 respectively. Chung *et al.* performed anomalous scattering studies with Mn^{2+} and concluded that the divalent metal ions interacted with the Asp-265 residue and this residue was suggested to interact with Mg^{2+} as well¹³⁷.

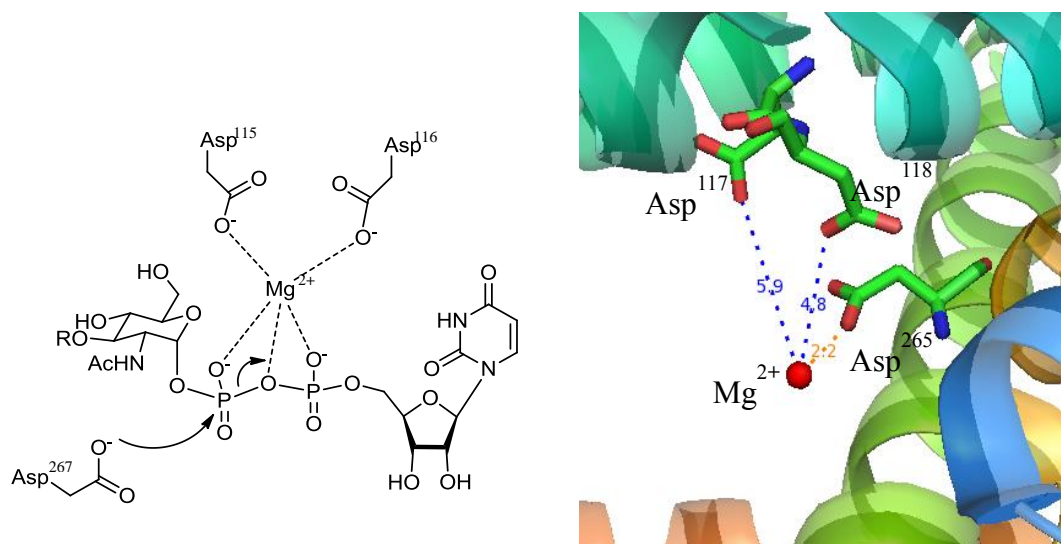


Figure 1-43: MraY active site, suggested active site mechanism by Lloyd *et al.* for *E. coli* MraY (left) and distance between Mg^{2+} and the conserved active site residues Asp¹¹⁷, Asp¹¹⁸ and Asp²⁶⁵ of *Aquifex aeolicus* MraY (right); figure on the right was prepared using PyMOL molecular graphics software

However, it should be noted that 100 mM $MgCl_2$ was needed to obtain these crystals, so these results are perhaps not conclusive, further studies and an MraY-substrate complex structure could help elucidate the catalytic residues and their role in the mechanism of action of MraY.

Amer and Valvano reported the presence of an HHH motif in MraY sequences, His-326, His 327 and His-328 in *E. coli* MraY. A similar HXH motif is found in WecA sequences, His-279 and His-281 in *E. coli* WecA. This motif is completely absent in the eukaryotic enzymes and a role was proposed in the specificity of nucleotide substrate binding^{130, 138}. Figure 1-44 shows the conserved HHH motif of loop E (fifth cytoplasmic loop) of *Aquifex aeolicus* MraY (His-324, His-325 and His-326), but only the mutation of His-324 resulted in significant loss of MraY activity for Chung *et al.*¹³⁷.

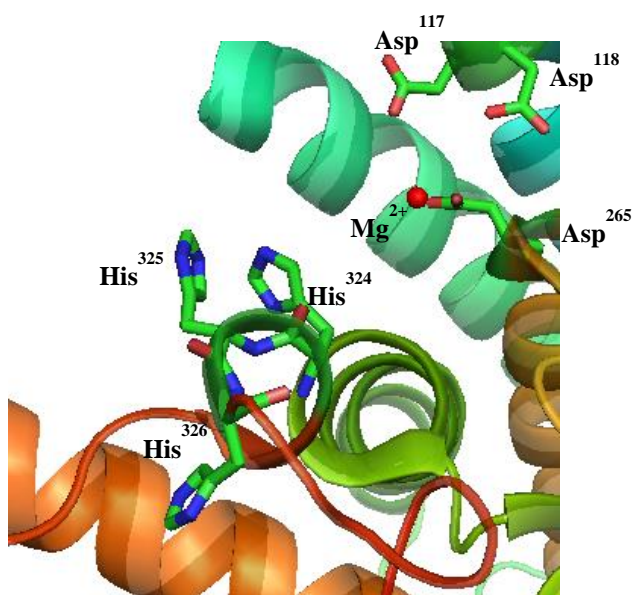


Figure 1-44: HHH motif on loop E and the conserved aspartate residues as sticks, red spheres are Mg^{2+} ; figure was prepared using PyMOL molecular graphics software

In Figure 1-45 the amphipathic helix 9b with highly conserved polar amino acid residues together with the HHH motif containing loop E point towards the region of the active site cleft with the Mg^{2+} and the highly conserved aspartate residues¹³⁷.

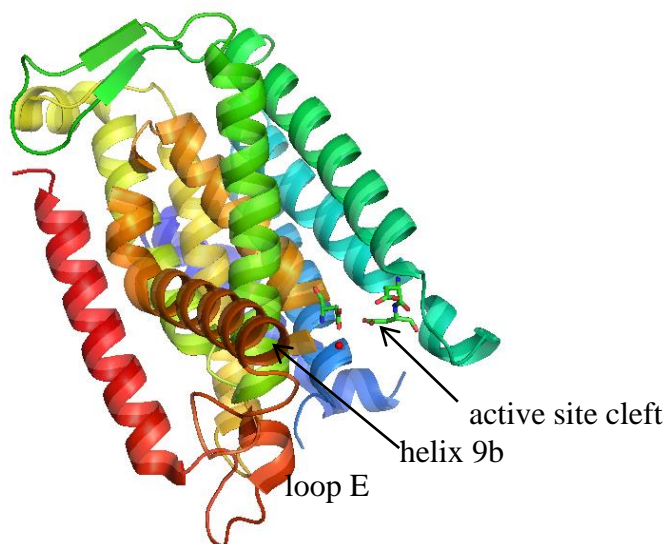


Figure 1-45: transmembrane helix 9b, loop E and the active site of MraY with the three conserved aspartate residues as sticks, red sphere Mg^{2+} ; figure was prepared using PyMOL molecular graphics software

The surface representation of the enzyme revealed an inverted-U-shaped hydrophobic groove surrounding transmembrane (TM) helix 9b and extending towards the active site encompassing the aspartate residues and Mg^{2+} suggesting a possible undecaprenyl phosphate binding site (Figure 1-46)¹³⁷.

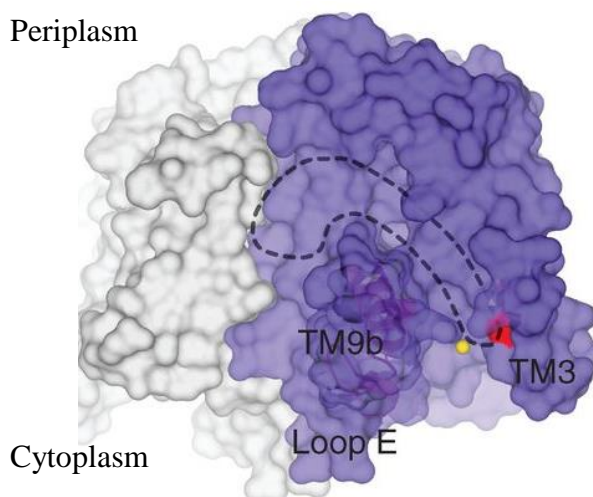


Figure 1-46: Representation of the hydrophobic groove by dashed lines (right), yellow sphere: Mg^{2+} , Asp-117 in red, transmembrane (TM) helices 3 and 9b are also shown¹³⁷

1.2.5 Solubilisation, expression and purification of MraY

The preparation of a pure, stable, soluble and active form of the low-abundance integral membrane protein MraY is the first step in order to investigate its biochemical properties^{9, 10}. A series of detergents have been tried for the solubilisation of the protein from the membranes over the years such as Triton X-100 or CHAPS^{13, 128} and n-dodecyl- β -D-maltoside and N-lauroyl-sarcosine were claimed to be the most effective¹³³. Attempts to purify detergent solubilized MraY often failed and resulted in significant loss of activity and SDS-PAGE showed many protein bands¹³. Only partially purified enzymes were used for enzymatic assays in the presence of phosphatidylglycerol which enhanced the activity of

solubilized *S. aureus*¹³⁵ and *E. coli*¹³ MraY. Several attempts have been made to express *E. coli* MraY as a fusion protein. No active enzyme was obtained using N-terminal (His)₆-MraY, or C-terminally labelled MBP-MraY. C-terminal (His)₆-MraY could be overexpressed and visualised by Western blotting¹³⁰, but attempts to purify this protein to homogeneity were unsuccessful, and the activity of the (C-His)₆-MraY was significantly lower than that of the wild type MraY^{13, 130}.

Bouhss *et al.* described the high-level overexpression of N-terminal (His)₆-*B. subtilis* MraY and its purification by affinity chromatography to homogeneity in milligram quantities for the first time. Interestingly, SDS-PAGE and Western blot indicated a lower mass (31 kDa) than expected (36 kDa) for *B. subtilis* MraY but the purity and homogeneity of the protein was confirmed by MALDI-TOF mass spectrometry analysis¹³³.

Due to difficulties in the production of large integral membrane proteins in conventional cellular expression systems, cell-free expression technologies have been optimised in recent times in the presence of detergents. Expression of these membrane proteins in a cell-free environment has several advantages over *in vivo* systems, such as minimizing toxic effects, high hydrophobicity, inefficient translocation and degradation. The preparative scale cell-free production of *Escherichia coli* and *Bacillus subtilis* MraY with a C-terminal poly-(His)₁₀ tag has been reported. The two MraY enzymes have similar topology with 47 % sequence identity and 64 % similarity (Table 2-1), and the *E. coli* enzyme has a slightly higher molecular mass than the *B. subtilis* enzyme, 40 and 36 kDa respectively. The two MraY proteins showed different characteristics upon applying different cell-free expression systems. While the *B. subtilis* protein seemed to be highly

stable and functionally folded, the *E. coli* protein was unstable and required the presence of preformed liposomes during expression for stability¹³⁹.

1.2.6 MraY assays

MraY catalyses the first step in the membrane cycle of events which utilises undecaprenyl phosphate as the lipid carrier. Alternative substrates as lipid carriers such as heptaprenyl and dodecaprenyl phosphate were shown to be accepted *in vitro* by *E. coli* MraY¹³.

The MraY activity could be determined by means of radiochemical assays¹⁰. One of the options is the transfer assay (Figure 1-47) which consists of the incubation of radiolabelled (most commonly ¹⁴C) UDPMurNAc-pentapeptide with the lipid acceptor and MraY and the reaction is monitored by extraction of the radiolabelled lipid product into an organic solvent, 1-butanol or chloroform/methanol (1:1)¹⁴⁰.

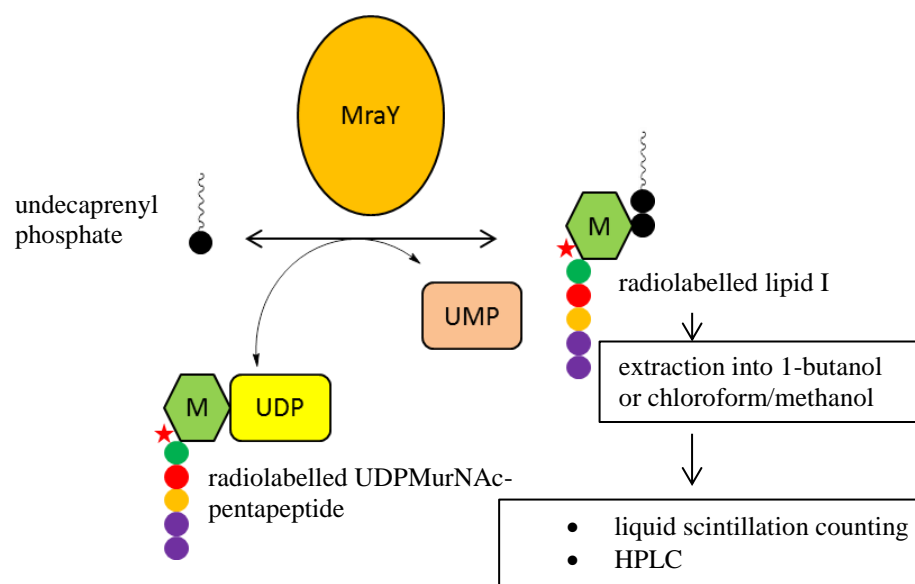


Figure 1-47: The “transfer” radiochemical MraY assay

The other possibility, the exchange assay (Figure 1-48) involves the incubation of radiolabelled (^3H) UMP with unlabelled UDPMurNAc-pentapeptide and the lipid acceptor, undecaprenyl phosphate. The assay relies on the reversible nature of the reaction since the reverse reaction results in the incorporation of the radiolabel into UDPMurNAc-pentapeptide which is then separated from radiolabelled UMP by thin layer chromatography and counted¹⁴⁰. Unfortunately, these stopped assays are not suitable for kinetic studies or high-throughput screening¹⁰.

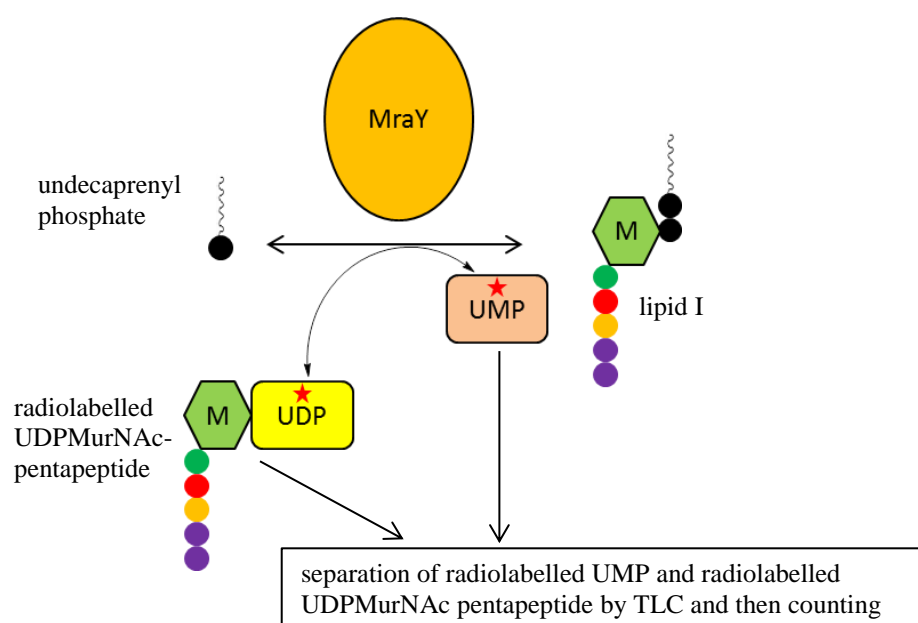


Figure 1-48: The “exchange” radiochemical MraY assay

Weppner and Neuhaus used a dansyl fluorophore attached to the ϵ -amino group of the amino acid at the third position of UDPMurNAc-pentapeptide (Figure 1-50) which was an accepted substrate for MraY. The reaction resulted in a 30 nm blue shift in the fluorescence emission spectrum and a 6-fold increase in quantum yield indicating that the dansyl moiety was transferred from a hydrophilic environment of the cytoplasm to a more hydrophobic environment of the membranes and/or detergent micelles¹⁴¹ (Figure 1-49).

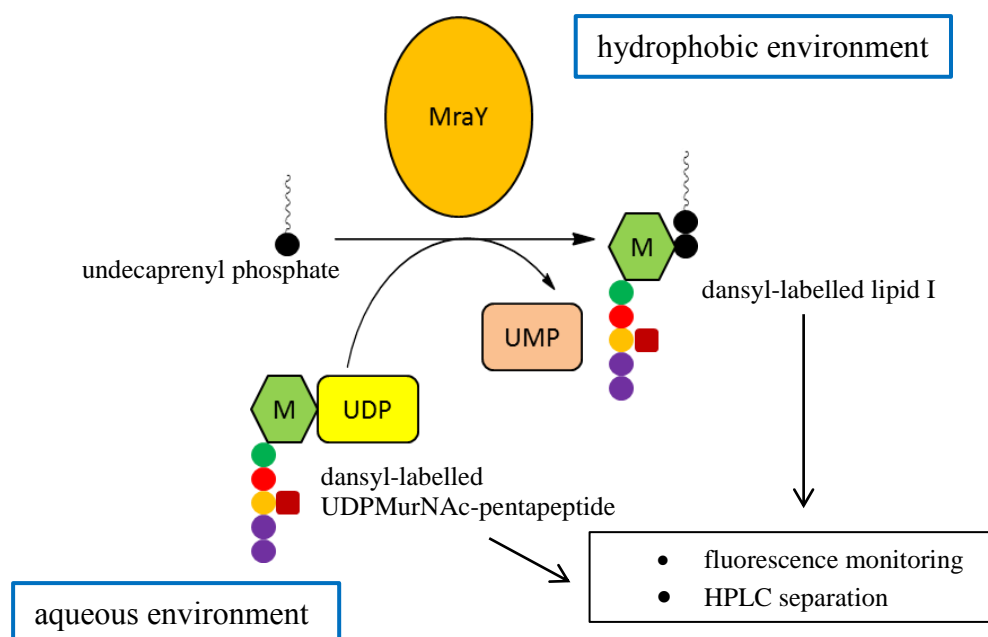


Figure 1-49: Fluorescence MraY assays

The effectiveness of the dansylated substrate in the transfer reaction proved to be higher than the unlabelled UDPMurNAc-pentapeptide either at low or high concentrations but this is not the case for the exchange reaction indicating the dansyl group's preference for the hydrophobic environment. However, in the biosynthesis of peptidoglycan the dansylated substrate cannot form peptidoglycan since it is blocked at position 3, and hence cannot cross-link. In conclusion, the dansylated substrate can be used to assess the activity of MraY but it is a poor substrate for the full synthesis of nascent peptidoglycan¹⁴¹.

P. Brandish developed further the fluorescence MraY assay into a continuous fluorescence assay also using the dansyl fluorophore¹³ which he used to study the slow-binding inhibition of mureidomycin A¹⁴² and liposidomycin B¹⁴³. Stachyra *et al.* adapted this method to 96- and 384-well plates and also developed an HPLC assay to separate the fluorescent labelled UDPMurNAc-pentapeptide and fluorescent labelled lipid I¹⁴⁴.

In addition, N-fluorescamine-labelled and N-o-phthalaldehyde-labelled derivatives (Figure 1-50) were prepared by labelling the amino acid residue at position 3¹⁴⁵, or D-cysteine was incorporated into UDPMurNAc-pentapeptide by MurF at position 4 or 5. D-Ala-D-Cys or D-Cys-D-Ala was either enzymatically or chemically synthesised. The D-Cys-containing UDPMurNAc-pentapeptides were labelled with pyrene maleimide (Figure 1-50) and gave 1.5-150-fold changes in fluorescence upon transformation to lipid I by *M. flavus* membranes¹⁴⁶.

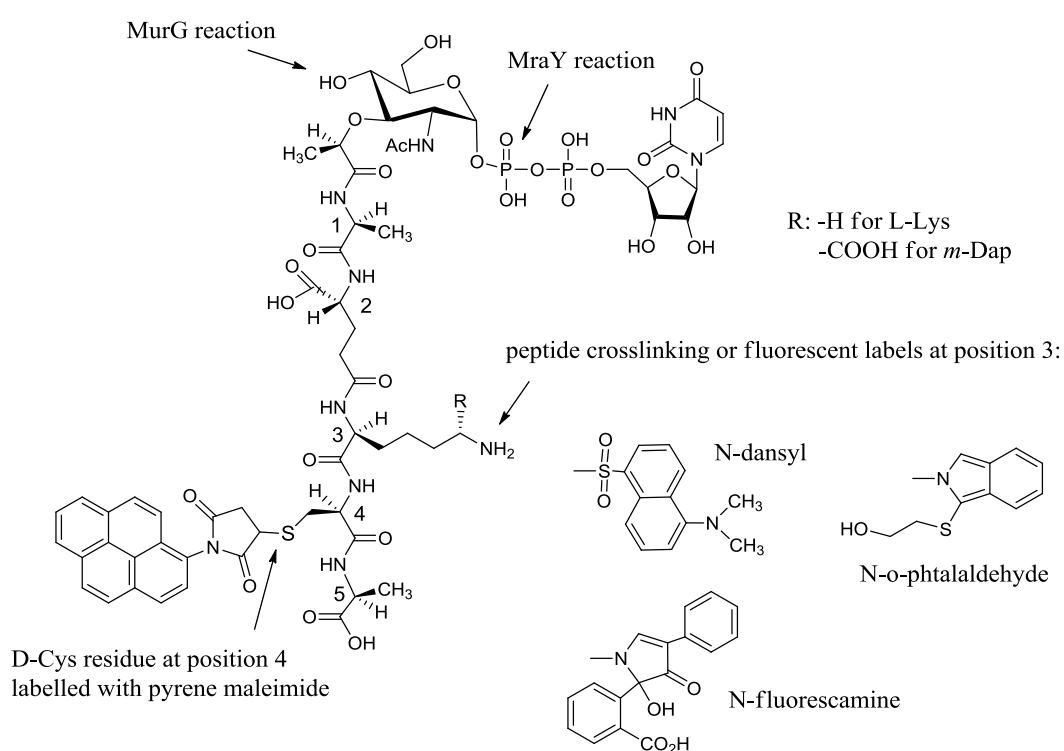


Figure 1-50: Fluorescent labels introduced into UDPMurNAc-pentapeptide

Solapure *et al.* developed a scintillation proximity MraY assay for high throughput screening of large compound libraries. Wild type *E. coli* membranes were incubated with UDP-MurNAc-(³H-propionate) pentapeptide and lipid I was captured by the addition of wheat germ agglutinin coated beads. The radiolabelled lipid I molecules trigger the bead to emit light which can be then detected. Lipid I

formation was confirmed by specific inhibitors of MraY such as tunicamycin and vancomycin¹⁴⁷.

There have been several coupled MraY-MurG assays (Figure 1-51) reported where radiolabelled UDPGlcNAc is added to membranes in which lipid I was pre-formed by incubation with UDPMurNAc-pentapeptide and undecaprenyl phosphate. The lipid product is either extracted into an organic solvent^{85, 130} or separated by solid-phase extraction such as streptavidin-coated beads¹⁴⁸ or wheat germ agglutinin coated beads^{69, 149}

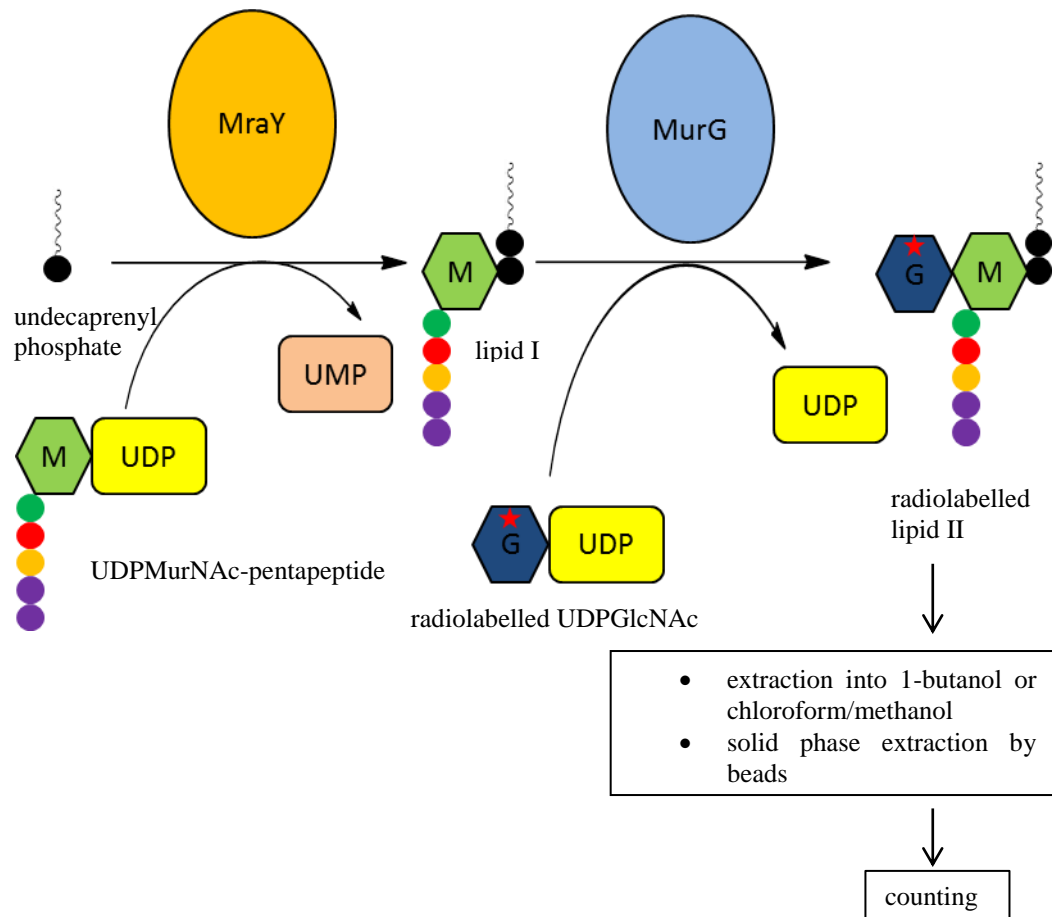


Figure 1-51: Schematic representation of the coupled radiochemical MraY-MurG assays

1.3 Known inhibitors of MraY

1.3.1 Uridyl-peptide inhibitors of MraY

There are five classes of uridine-containing nucleoside natural antibiotic products that target MraY, tunicamycins, mureidomycins, liposidomycins, muraymycins and capuramycins, and they were suggested to target the active site of MraY at the cytoplasmic face of the membrane. Some of them have been the target of detailed structure-activity relationship, kinetic or mechanistic studies⁹ but none of them has been progressed to a clinical drug so far, mainly due to very small available quantities. Drug candidates also need to have good pharmacokinetic properties, low toxicity, and progress through clinical trials successfully. One of the caprazamycin analogues from the family of uridyl-peptide MraY inhibitors, CPZEN-45 is a candidate today for clinical trials for the treatment of tuberculosis in Japan (Section 1.3.1.3).

1.3.1.1 Tunicamycins

The tunicamycins are a family of nucleoside disaccharides containing a unique 11-carbon core and varying fatty acid side chains (Figure 1-52) that were first isolated from *Streptomyces lysosuperficus* in 1971 and showed antibacterial activity against *B. subtilis* with MIC values ranging between 0.1-20 µg/ml¹⁵⁰. They were also reported to have antiviral¹⁵¹ and antitumor activities¹⁵².

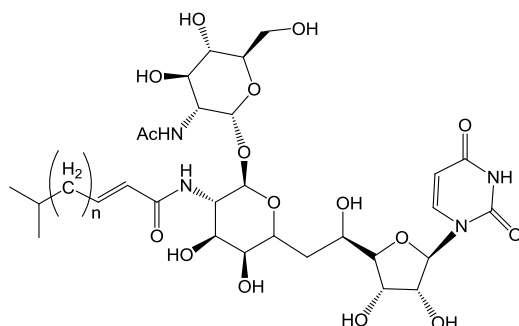


Figure 1-52: Chemical structure of tunicamycins, n: 7-11

They inhibit prokaryotic enzymes from the polyisoprenyl-phosphate *N*-acetylhexosamine-1-phosphate transferase family including *MraY* and the eukaryotic paralogue *GlcNAc-1-phosphate transferase* involved in the first step of mammalian *N*-linked glycoprotein biosynthesis¹⁵³. Consequently the tunicamycins are toxic to humans (Figure 1-53).

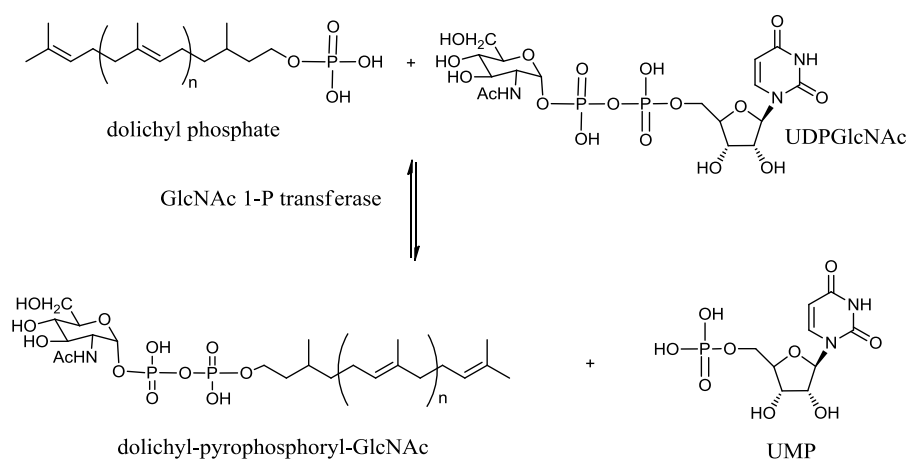


Figure 1-53: Biosynthesis of dolichyl-pyrophosphoryl-GlcNAc in mammalian *N*-linked glycoprotein biosynthesis

Tunicamycins were the first antibiotics reported to inhibit *MraY* and their inhibition kinetics were studied in detail by means of a continuous fluorescence assay showing that tunicamycin was a reversible inhibitor of *MraY* with a

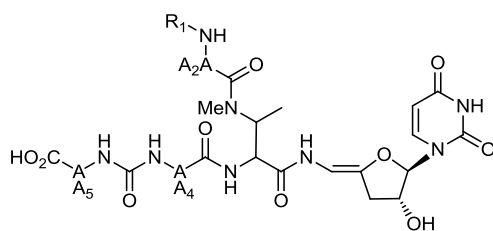
K_i value of $0.6 \mu\text{M}$ ¹⁴³. IC_{50} values were determined against MraYs from various organisms in Section 5.1.4.

Since the tunicamycins are isolated as mixtures, separation of which is tedious, it was important to develop their chemical synthesis in order to enable the study of the biological activities of the individual structures¹⁵⁴. Efforts are being made to date in order to elucidate the biosynthetic pathway of tunicamycins, which could perhaps be used to prepare more selective and clinically useful drugs¹⁵⁵.

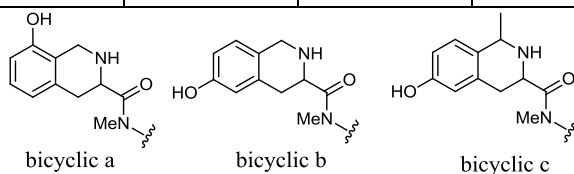
1.3.1.2 Mureidomycins, pacidamycins, napsamycins and sansanmycins

The mureidomycins, pacidamycins, napsamycins and sansanmycins (Table 1-1) are peptidyl nucleoside natural products sharing a common structural skeleton containing a 3'-deoxyuridine nucleoside attached via an enamide linkage to an N-methyl 2,3-diaminobutyric acid (DABA) residue. To the α -amino group of DABA amino acid 4 (AA_4) is attached (either Met or Ala) and it is linked to the C-terminal amino acid 5 (AA_5) via a urea linkage. This amino acid has an aromatic side-chain. The β -amino group of DABA is linked to amino acid 2 (A_2A) which is most commonly *m*-Tyr, Ala or a bicyclic amino acid¹⁵⁶.

Table 1-1: Chemical structure of mureidomycins, pacidamycins, napsamycins and sansanmycins



Name	R	A ₂ A	AA ₄	AA ₅	Other
mureidomycin A	H	m-Tyr	Met	m-Tyr	
mureidomycin B	H	m-Tyr	Met	m-Tyr	dihydrouracil
sansanmycin A	H	m-Tyr	Met	Trp	
sansanmycin C	H	m-Tyr	MetSO	Trp	
pacidamycin 4	H	m-Tyr	Ala	Trp	
pacidamycin 5	H	m-Tyr	Ala	Trp	
pacidamycin 5T	H	m-Tyr	Ala	m-Tyr	
sansanmycin B	H	m-Tyr	Leu	Trp	
pacidamycin D	H	Ala	Ala	Trp	
pacidamycin 1	Ala	m-Tyr	Ala	Trp	
pacidamycin 2	Ala	m-Tyr	Ala	Phe	
pacidamycin 3	Ala	m-Tyr	Ala	m-Tyr	
mureidomycin C	Gly	m-Tyr	Met	m-Tyr	
mureidomycin D	Gly	m-Tyr	Met	m-Tyr	dihydrouracil
pacidamycin 6	Gly	m-Tyr	Ala	Trp	
pacidamycin 7	Gly	m-Tyr	Ala	Phe	
mureidomycin E	H	bicyclic a	Met	m-Tyr	
napsamycins A, mureidomycin F	H	bicyclic b	Met	m-Tyr	
napsamycins B	H	bicyclic c	Met	m-Tyr	
napsamycins C	H	bicyclic b	Met	m-Tyr	
napsamycins D	H	bicyclic c	Met	m-Tyr	dihydrouracil
pacidamycin 4N	H	bicyclic a	Ala	Trp	dihydrouracil



The mureidomycins were discovered in 1989 when mureidomycins A-D were isolated from *Streptomyces flavidovirens* SANK 60486 and showed antimicrobial

activity against *Pseudomonas* species with MIC values ranging between 1.5-12.5 µg/ml and mureidomycin A had an ED₅₀ value of 69 mg/kg for protecting mice against *Pseudomonas aeruginosa* infections¹⁵⁷⁻¹⁵⁹. Mureidomycin A was shown to selectively inhibit *MraY* over teichoic acid biosynthesis and mammalian N-linked glycoprotein biosynthesis^{160, 161} and was found to be a slow-binding inhibitor of *E. coli* *MraY* with K_i^* : 2.2 nM, competitive versus both substrates (UDPMurNAc-pentapeptide and polyprenyl phosphate lipid) which was determined by a continuous fluorescence enhancement assay¹⁴². Further analogues were discovered in 1993 from the same *Streptomyces flavidovirens* SANK 60486, mureidomycin E and F¹⁶².

Pacidamycins 1-7 were isolated from *S. coeruleorubidus* strain AB 1183-64 in 1989 as well¹⁶³⁻¹⁶⁵ and pacidamycin D, 4N and 5T were isolated later from strain NRRL 18730¹⁶⁶. They showed antibacterial activity against *Pseudomonas species* with MIC values ranging from 4-125 µg/ml^{165, 166}. It was possible to reduce the 4'-exoenamidofuranosyl moiety of pacidamycin D by hydrogenation and the resulting dihydropacidamycin analogues retained activity¹⁶⁷. The configuration of all naturally occurring amino acids in the pacidamycins has been elucidated to be (*S*) configuration, and the DABA residue is of (*S,S*) configuration¹⁶⁸. Structure-activity relationship studies were carried out on the dihydropacidamycins and it was shown that the lack of the ribose sugar or uracil base caused complete loss of activity while amino acids at position 2, 4 and 5 could be replaced without significant loss of antibacterial activity (Figure 1-54)^{156, 168}.

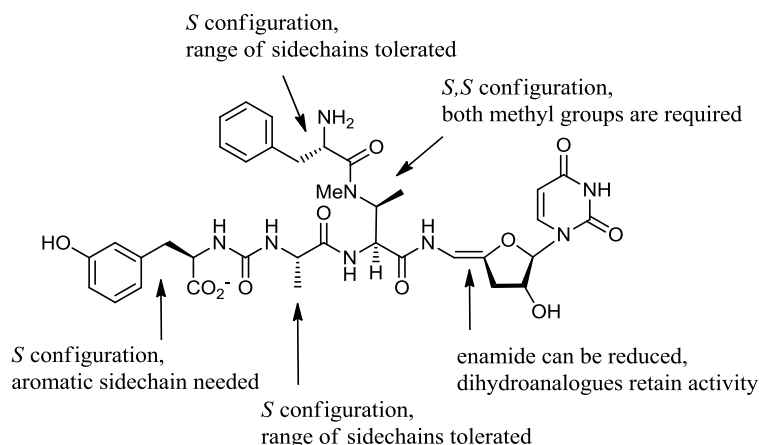


Figure 1-54: Structure-activity relationship studies on pacidamycins

The pacidamycin gene cluster was identified which facilitates the identification of their biosynthetic pathway¹⁶⁹. The inhibitory potential of pacidamycin 1,2 and pacidamycin D against *E. coli* and *P. aeruginosa* MraY was investigated by the means of a continuous fluorescence assay and described in Section 5.1.3.

The napsamycins A-D containing N-terminal bicyclic amino acids were isolated from *Streptomyces* sp. HIL Y-82 in 1994¹⁷⁰ and the sansanmycins were isolated from *Streptomyces* sp. SS in 2007¹⁷¹, both showing similar anti-pseudomonal activity as the mureidomycins and the pacidamycins¹⁵⁶. In addition, sansanmycin B was also found to be active against *Mycobacterium tuberculosis* with MIC values of 8-20 µg/ml¹⁷².

1.3.1.3 Liposidomycins, caprazamycins

The liposidomycins and caprazamycins are structurally related liponucleoside natural products and their structure is derived from 5'-(β-*O*-aminoribosyl)-glycyluridine with a unique N,N'-dimethyldiazepanone ring. The liposidomycins contain a sulphate group at the 2''-position of the aminoribose while the caprazamycins possess a permethylated L-rhamnose^{173, 174}. The name of the

liposidomycin and caprazamycin analogues (A – G) comes from the attached β -hydroxy-fatty acids of different chain length¹⁷³ (Figure 1-55).

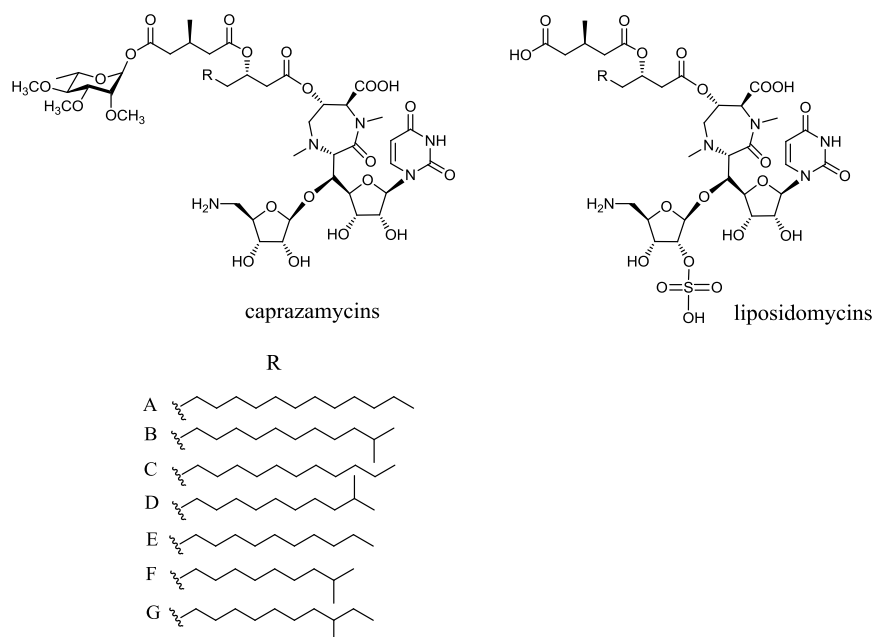


Figure 1-55: Chemical structure of the caprazamycins and the liposidomycins

The liposidomycins were first isolated from *Streptomyces griseosporus* in 1985 with growth inhibitory activity against *Mycobacterium* sp.¹⁷⁵ and were shown to inhibit Mray selectively, more precisely only affected glycoprotein and teichoic acid biosynthesis at very high concentrations¹⁷⁶. Liposidomycin B is a slow-binding inhibitor of solubilised *E. coli* Mray with K_i^* : 80 nM, non-competitive versus UDPMurNAc-pentapeptide and competitive versus the polyprenyl phosphate lipid, which was determined by a continuous fluorescence enhancement assay¹⁴³.

The caprazamycins, potent liponucleoside inhibitors of Mray were isolated from *Streptomyces* sp. MK730-62F2. They have potent antibacterial activity against mycobacteria and do not exhibit significant toxicity in mice¹⁷⁷⁻¹⁸⁰. Hirano *et al* synthesized a palmitoylcaprazol analogue which had antimicrobial activity against

MRSA with an MIC value of 6.25 µg/ml and against VRE with an MIC of 12.5 µg/ml¹⁸⁰.

Caprazamycins A-G have some antibacterial activity against a whole range of Gram-positive bacteria and they were modified by acid hydrolysis to increase and optimise their activity against *Mycobacteria* and target tuberculosis. CPZEN-45, a 4-butylanilide derivative of the caprazene core structure (Figure 1-56), was chosen as the most promising derivative^{181, 182} possessing a narrower antibacterial spectrum towards *Mycobacteria* with MIC values ranging between 0.2-1.56 µg/ml. CPZEN-45 inhibited *B. subtilis* MraY with an IC₅₀ value of 400 ng/ml and was also found to inhibit the first step of teichoic acid biosynthesis in *B. subtilis* catalysed by TagO (IC₅₀: 50 ng/ml) and its ortholog, WecA in *M. tuberculosis* (4.4 ng/ml)¹⁸¹. Today, CPZEN-45 is going through preclinical studies in Japan and no mutagenicity or cytotoxicity has been reported so far^{181, 183-185}.

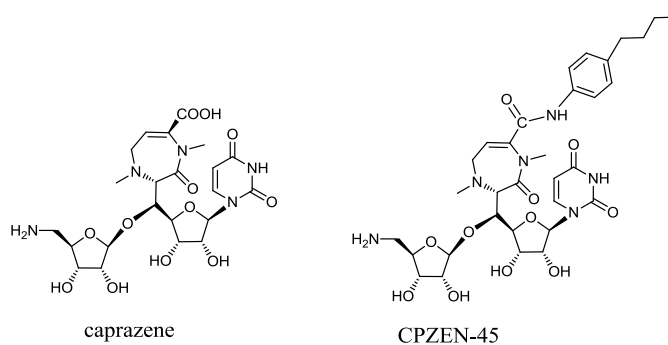


Figure 1-56: Chemical structure of the caprazene core structure (no antibacterial activity) and the antibacterial drug candidate CPZEN-45, a 4-butylanilide derivative of caprazene

A series of new caprazamycin analogues were tested against *E. coli* MraY by a continuous fluorescence enhancement assay and the results are shown in Section 5.1.2.

1.3.1.4 Muraymycins

The core structure of the muraymycin nucleoside antibiotics consists of a peptide-appended glycosylated uronic acid and different analogues have different fatty acid chains (R)¹⁵⁶ (Figure 1-57).

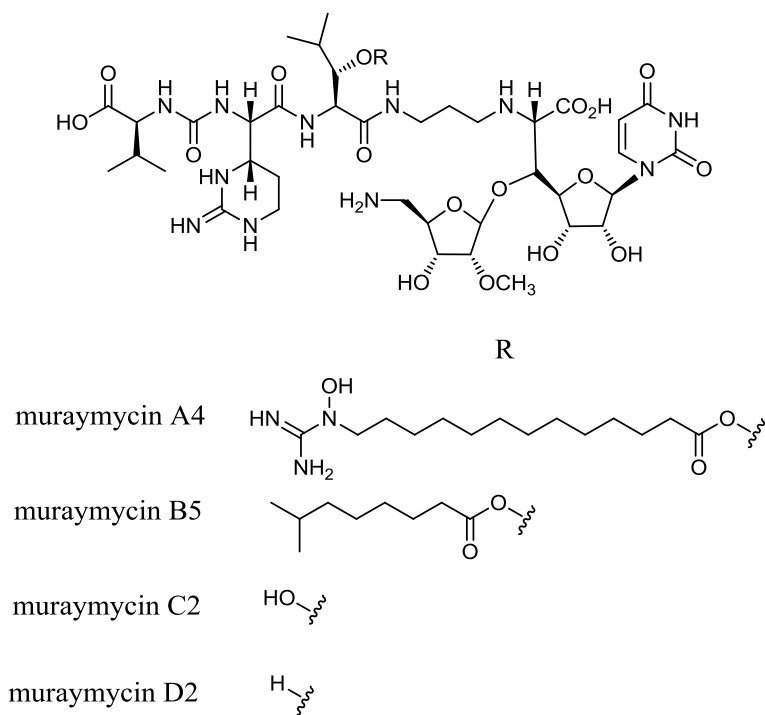


Figure 1-57: Chemical structure of the muraymycins

The muraymycins were first isolated from *Streptomyces sp.* and the analogues with a lipophilic side-chain showed antimicrobial activity against Gram-positive bacteria such as *Staphylococcus aureus* with MICs ranging between 2-16 $\mu\text{g/ml}$ and *Enterococcus* strains with the lowest MIC measured as 16 $\mu\text{g/ml}$ which makes them attractive candidates for drug development¹⁸⁶. Structure-activity relationship studies showed that the lipophilic side-chain plays a key role in antibacterial activity but not essential for Mray activity, simplification of the urea-peptide moiety seemed possible and the aminoribosyluridine group was proposed to

interact with the active site of *MraY*¹⁸⁷. A new synthetic muraymycin analogue lacking the 5'-aminoribose was assayed against *MraY*s from various organisms by a continuous fluorescence enhancement assay and the results are shown in Section 5.1.1.

1.3.1.5 Capuramycins

Capuramycins are uracil nucleoside antibiotics containing a caprolactam substituent (Figure 1-58).

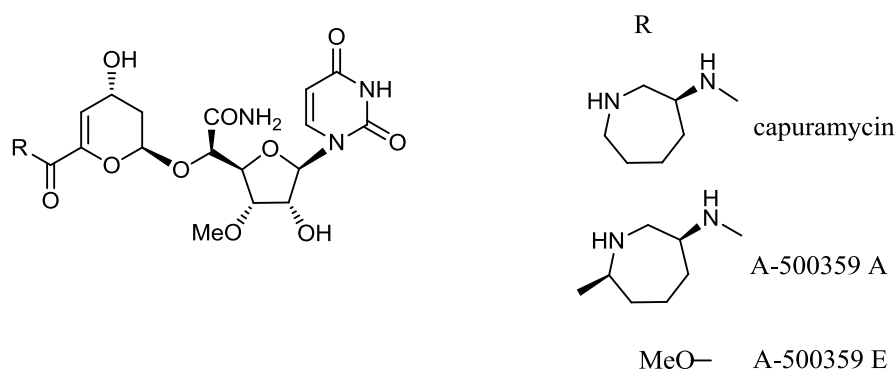


Figure 1-58: Chemical structure of the capuramycins

A compound named capuramycin was isolated from *S. griseus* 446-S3 in 1985¹⁸⁸,¹⁸⁹ with antibacterial activity against *S. pneumoniae* with and *Mycobacterium smegmatis* with MIC values of 12.5 µg/ml and 3.13 µg/ml respectively^{188, 190}. Further analogues were isolated from the same *Streptomyces* strain, A-500359 A and E with MIC values of 6.25 µg/ml and >100 µg/ml respectively against *Mycobacterium smegmatis*¹⁹¹. Capuramycin, A-500359 A and E were assayed against *MraY* with IC₅₀ values of 18 nM, 17 nM and 27 ng/ml respectively^{192, 193}. Therefore, it was obvious that the replacement of the caprolactam moiety to a methoxy group reduced activity against *MraY* and antibacterial activity was not even detected¹⁹¹. Methylated and acylated derivatives also showed very potent

antibacterial activity against *Mycobacteria* with the most potent MIC value of 0.06 µg/ml¹⁹⁴. The inhibitory potential of two known capuramycin analogues was investigated against *E. coli* and *B. subtilis* MraY by a continuous fluorescence enhancement assay and it is described in Section 5.1.5.

1.3.2 Inhibition of MraY by E lysis protein from phage ϕX174

Double stranded DNA phages cause cell lysis by producing a soluble, muralytic enzyme known as endolysin that requires a small membrane protein called holin to get access to the cell wall for bacteriolytic action¹⁹⁵. However, the single-stranded DNA phage ϕ174 uses a single lysis gene, *E*, to cause lysis of the host cell^{195, 196}. *E* encodes a 91-amino-acid membrane protein that was shown to inhibit *E. coli* MraY^{197, 198}. SlyD, an FKBP-type peptidyl-prolyl *cis-trans* isomerase, was reported to play an essential role in stabilizing E protein and allowing it to accumulate to the necessary levels for causing host cell lysis but its precise role is uncertain¹⁹⁹.

Mutation of Phe-288 to lysine in *E. coli* MraY resulted in resistance to E protein¹⁹⁷. This phenylalanine residue *E. coli* MraY is located at the periplasmic face of the membranes next to a conserved glutamate residue (Glu-287)¹²⁹ while the proposed catalytic active site of MraY is at the cytoplasmic face of the membranes¹³⁰.

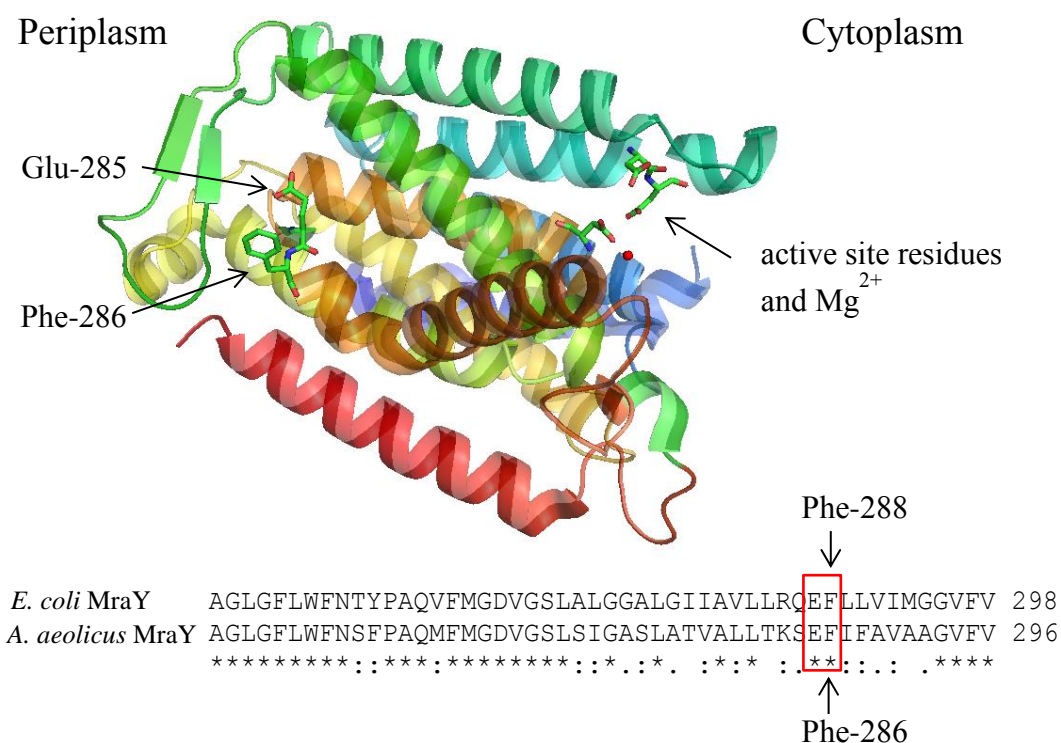


Figure 1-59: Position of the phenylalanine residue of helix 9 of *Aquifex aeolicus* MraY, essential for E protein inhibition of MraY at the periplasmic phase of the membranes, proposed catalytic active site with three conserved aspartate residues, Asp-117, Asp-118 and Asp-265, red sphere Mg^{2+} ; figure was prepared using PyMOL molecular graphics software

Very recently the crystal structure of MraY from *Aquifex aeolicus* was solved¹³⁷ and NCBI sequence alignment of *E. coli* and *A. aeolicus* MraY revealed that the *A. aeolicus* MraY has a phenylalanine residue (Phe-286 in *A. aeolicus* sequence) at the same position as Phe-288 in *E. coli* MraY.

Figure 1-59 shows the position of the Phe-286 residue of the unusually bent helix 9 of *Aquifex aeolicus* MraY at the periplasmic face of the membranes in relation to the proposed catalytic active site of MraY at the cytoplasmic face of the membranes.

A 37-amino-acid synthetic peptide containing the N-terminal transmembrane domain of E protein was reported to inhibit particulate *E. coli* MraY but not the solubilized enzyme, and it was proposed that it blocks a protein-protein interaction involving MraY²⁰⁰. This seems quite possible given the location of Phe-288 in the MraY structure, on the outside of the protein dimer.

The inhibitory activity of E peptide was investigated against MraY from various organisms in Section 5.3.1.

1.3.3 Inhibition of MraY by cyclic peptides and small molecules

Amphomycin (Figure 1-60) and tsushimycin are known inhibitors of MraY where 20 µg/ml amphomycin caused 45 % inhibition in a radiochemical assay by forming a complex with undecaprenyl phosphate^{201, 202}. The eukaryotic enzyme responsible for mannosylphosphoryldolichol synthesis was also inhibited by amphomycin forming a 1:1 complex with dolichylmonophosphate in the presence of Ca²⁺²⁰³. Further amphomycin analogues were identified such as friulimicin and glycinocins and their cyclic structure was confirmed by spectroscopic and chemical degradation studies²⁰⁴.

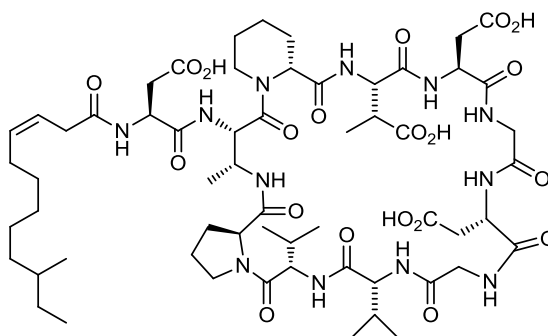


Figure 1-60: Chemical structure of amphomycin

The glycopeptide vancomycin also inhibits MraY by complexing the D-Ala-D-Ala termini of UDPMurNAc-pentapeptide, however its inhibitory potency strongly depends on the quantity of the substrates and the enzyme used for the assay¹⁴⁷. Vancomycin was tested against MraY in Section 5.2 using a radiochemical assay.

Heydanek *et al* observed in the course of testing various surfactants to be used for biochemical studies on MraY that dodecylamine was an effective inhibitor of *S. aureus* MraY with K_i value of 0.65 mM¹³¹. In addition, Porcion Yellow HE-3G dye was reported to bind to solubilised *E. coli* MraY and inhibit the enzyme with an IC_{50} value of 1 mg/ml¹³⁰.

1.4 Aims and objectives of the project

This research project focuses on the first lipid-linked step of peptidoglycan biosynthesis catalysed by phospho-MurNAc-pentapeptide translocase MraY. To date, there is no drug in clinical use that would target this enzyme and previous screening efforts concentrated mainly on the cytoplasmic steps of the pathway. The aim of the project was to screen for structurally new inhibitors of MraY.

The U.S. National Cancer Institute's (NCI) Development Therapeutics Program maintains a large screening collection of over 140,000 compounds. These have been evaluated as potential anticancer and anti-HIV agents and among them are synthetic compounds and natural products representing unique structural diversity. The NCI also has a small library of around 2,000 compounds ideal for beginning a screening process. Many hospitalised cancer patients treated with anticancer agents develop life-threatening bacterial infections so the National Cancer Institute will send their diversity set to academic groups able to demonstrate a microtitre-based assay for an antibacterial target enzyme. Following a request from Professor T. D. H. Bugg, the NCI generously provided the diversity set of 1,717 compounds in 2012.

First of all, assay methods needed to be optimised for MraY screening since the fluorescence and radiochemical assays for MraY had not been used in our laboratory for several years. A continuous fluorescence MraY assay was to be developed and optimised and then to be adapted to a high-throughput assay in 96-well microtitre plate format to screen the NCI diversity set against *E. coli* MraY. During the project it became apparent that we also needed a second independent assay method (many compounds interfered with fluorescence) to test possible hits,

so radiochemical and HPLC MraY assays were also investigated, even though these methods are not suitable for high-throughput screening.

In addition, we aimed to assay new natural or synthetic analogues of the known MraY inhibitor families of nucleoside antibiotics such as the pacidamycins, muraymycins and the caprazamycins against *E. coli* MraY and against MraY from their antibacterial target organisms whenever it was possible, supplied by research groups working on uridyl-peptide analogue natural product biosynthesis and total synthesis.

We also planned to investigate the inhibitory activity of the known *E. coli* MraY inhibitor, the bacteriolytic E peptide against *S. aureus*, *B. subtilis*, *P. aeruginosa* and *M. flavus* MraYs. Furthermore, we wished to assay more antibacterial peptides against MraY that were available to us, amongst them another lytic peptide, P1.

Finally, we aimed to test halogenated fluorescein analogues against MraY and MurG since similar structures were published by Zawadzke *et al.* as potential MraY or MurG inhibitors (Figure 1-61) based on a combined MraY-MurG microtitre plate scintillation proximity-based assay⁶⁹.

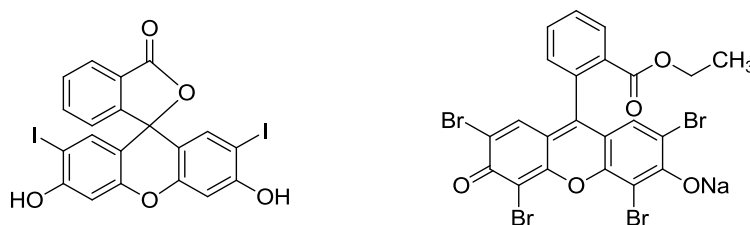


Figure 1-61: Halogenated fluorescein analogues from the combined MraY-MurG screen of Zawadzke *et al.* (2003)

2 Development of assay methods for screening

MraY

The major goal of the project is to screen for structurally novel inhibitors against the bacterial peptidoglycan enzyme MraY. One of the options is to use a radiochemical MraY assay that was used by P. Brandish¹³. This assay can give accurate measurements of the lipid I product over a time-course assay (20-30 minutes) by measuring the incorporation of a ¹⁴C label from UDPMurNAc-pentapeptide into the butanol extractable product lipid I (Figure 2-1).

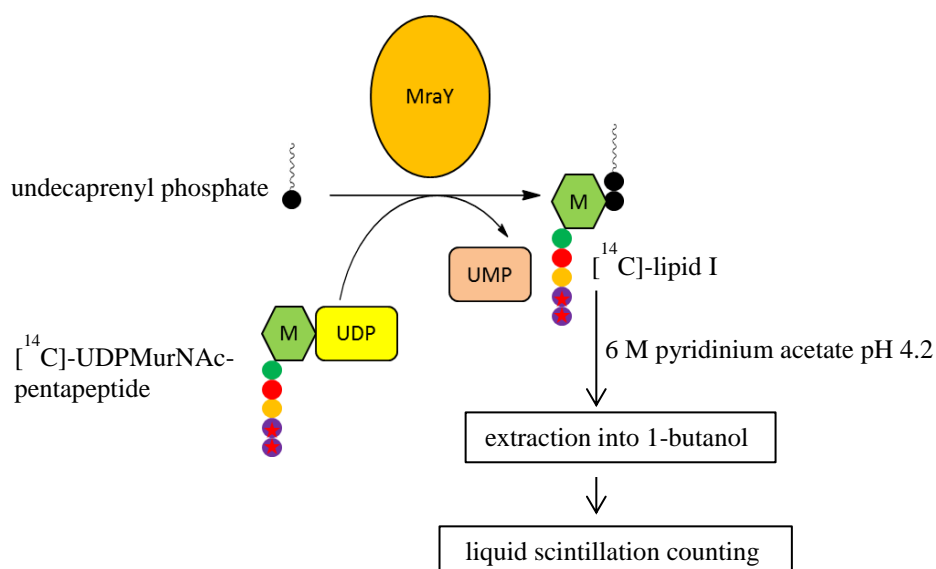


Figure 2-1: Schematic representation of the radiochemical MraY assay

However, this stopped assay is very difficult to use for enzyme kinetics, especially when the time-course of the reaction is non-linear or the inhibition is time-dependent¹³. Moreover, this assay is not suitable to screen a large number of compounds for potential inhibition. P. Brandish developed a continuous fluorescence assay⁹ as well (Figure 2-2), using a dansyl fluorophore on UDPMurNAc-pentapeptide, which was further developed by S. Bagga into a high-throughput assay in micro-titre plate format¹⁴⁵.

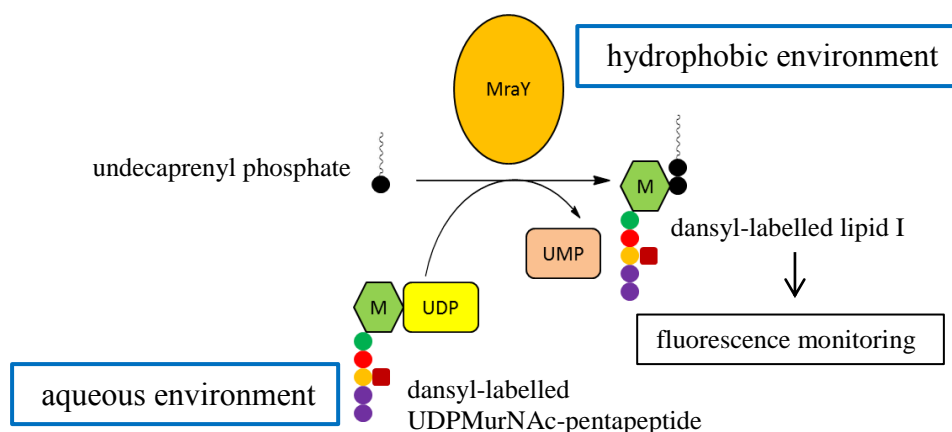


Figure 2-2: Schematic representation of the fluorescence MraY assay

The basis of the fluorescence assay relies on the fact that the dansyl fluorophore experiences a change in environment upon incorporation into the hydrophobic environment of the membranes and/or detergent micelles from an aqueous environment of the cytoplasm, and this phenomenon results in a 50 % enhancement in fluorescence¹⁴¹.

The first step of the project was to optimise the fluorescence MraY assay so that it could be used for screening 2,000 compounds from the diversity set of the National Cancer Institute under the present conditions at the Chemical Biology Laboratory at the University of Warwick.

2.1 MraY enzymes from various organisms

Membrane proteins are low abundance proteins and generally extremely difficult to over-express, due to their toxic nature resulting from their disturbing the integrity and the content of the membrane. MraY has both the N and the C termini located in the periplasmic space¹²⁹, therefore a high level overexpression of the protein is even more challenging, since N- or C-terminal fusion tags would need to be translocated across the cytoplasmic membrane^{10, 205}. Previous efforts in our group for overexpressing MraY resulted in modest (28-fold) overproduction of

enzyme activity with specific activities varying between 1-2 nmol min⁻¹ mg⁻¹ protein by a radiochemical assay and 2-3 FAU min⁻¹ mg⁻¹ by a fluorescence assay with the *E. coli* MraY solubilised in 1 % Triton X-100, however SDS-PAGE showed many protein bands¹³.

Several attempts have been made to express *E. coli* MraY as a fusion protein. No active enzyme was obtained using N-terminal (His)₆-MraY, or C-terminally labelled MBP-MraY or GFP-MraY. C-terminal (His)₆-MraY could be overexpressed and visualised by Western blotting¹³⁰, but attempts to purify this protein to homogeneity were unsuccessful, and the activity of the (C-His)₆-MraY was significantly lower than that of the wild type MraY^{13, 130}.

Due to the above mentioned problems related to the purification of the enzyme, P. Brandish and S. Bagga used *E. coli* MraY for their experiments by overexpressing the enzyme in *E. coli* membranes. While P. Brandish used detergent (Triton X-100) solubilised enzyme^{13, 142, 143}, S. Bagga used the overexpressed MraY membranes directly in the assays, avoiding having to prepare the solubilised enzyme every day because of its time-dependent loss of activity^{139, 145}.

As a general procedure, the overexpressed *E. coli* strain is grown in LB media containing the resistance marker antibiotic (ampicillin or kanamycin) up to OD₆₀₀ 0.4-1.3 and induced by the addition of 1 mM IPTG. Membranes are isolated by ultracentrifugation (> 100,000 x g), re-suspended and diluted in membrane buffer (50 mM Tris pH 7.5, 1 mM MgCl₂, 2 mM β-mercaptoethanol) to achieve an optimal protein concentration for the assays. The total protein concentration of the membranes is estimated by a Bradford assay using albumin standards. In order to prepare the solubilised enzyme, the membranes are treated

with a detergent containing buffer (1 % Triton X-100 or 0.1 % CHAPS) and an extra ultracentrifugation step is introduced to eliminate the insolubilized material. These enzyme preparations are not as stable as the membranes which can be kept at -80 °C for several months without manifesting significant loss of activity¹³.

For this work, MraY membranes were used for the assays. At present, we are able to study the inhibition against *Escherichia coli* (360 amino acids), *Pseudomonas aeruginosa* (360 amino acids), *Staphylococcus aureus* (321 amino acids), *Bacillus subtilis* (324 amino acids) and *Micrococcus flavus* MraYs (375 amino acids). The variety of enzymes enables us to test specificity of inhibition. The overexpression of the membranes with MraY leads to 6-10 and 6-13 fold increase in specific activity for the radiochemical and the fluorescence MraY assays respectively (see Sections 2.2.4 and 2.4.2.6). The MraY enzymes used for this project:

- The *E. coli mraY* construct (pJFY3c) was provided by D. Boyle (Edinburgh University). The pJFY3c plasmid is under the control of a *tac* promoter regulated by the lacI^q repressor¹³⁰. The MraY enzyme was expressed in C43 (DE3) with ampicillin as described in Section 7.1.
- The *P. aeruginosa mraY* construct was a gift from R. C. Lévesque (Laval University). This *mraY* gene was cloned into pET30c vector and it was called pMON2320. The production of MraY protein is possible from HMS174 (λDE3) strain with a V-D-K-L-A-A-A-L-E-(His)₆ tag at C-terminus end using kanamycin as an antibiotic resistance marker, see Section 7.3.
- The *S. aureus* and *B. subtilis* MraYs were overexpressed as an N-terminal Strep-tag fusion protein in vector pET52b. They were cloned by A. O'Reilly

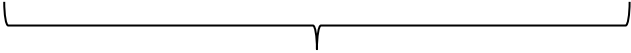
during her MOAC mini-project in 2012 at the Chemistry and the Life Sciences Departments of the University of Warwick. The constructs were transformed into C43 (DE3). The resistant antibiotic marker is ampicillin.

- Moreover, it is possible to use *M. flavus* (formerly known as *M. luteus*) membranes for the MraY assays as these membranes naturally contain a high level of expression of MraY and MurG^{59, 89}. For the preparation of *M. flavus* membranes, see Section 7.4.

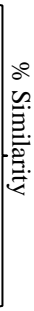
The five MraY protein sequences were aligned by the ClustalW2 multiple sequence alignment program (Figure 2-3). The identity and similarity of their sequences in pairs were determined by the NCBI's sequence alignment program with identities ranging from 37-66 % and similarities from 54-80 %. The *E. coli* and *P. aeruginosa* MraYs are the two most closely related enzymes with 66 % sequence identity and 80 % similarity. It is also notable that the *S. aureus* and *B. subtilis* MraYs have 57 % identity and 76 % similarity in their sequences (Table 2-1).

Table 2-1: MraY enzymes aligned in pairs, sequence identity and similarity (%)

	<i>E. coli</i>	<i>P. aeruginosa</i>	<i>S. aureus</i>	<i>B. subtilis</i>	<i>M. flavus</i>
<i>E. coli</i>	x	80	61	64	59
<i>P. aeruginosa</i>	66	x	63	63	56
<i>S. aureus</i>	42	43	x	76	54
<i>B. subtilis</i>	47	41	57	x	58
<i>M. flavus</i>	40	39	37	38	x



 % Identity



 % Similarity

<i>E. coli</i> Mray	MLVWLA EH LVKYYSGFNVFSYLT F RAIVSLLTALFI SL WMG PR MI HL LQK	50
<i>P. aeruginosa</i> Mray	MLLLLA YL QQFY K GF GV FQY L TL R GILSVLTALSL SL WL G PWMIR TL QI	50
<i>S. aureus</i> Mray	-----MIFVYALLALVITFVLVPVLIPTLKR	26
<i>B. subtilis</i> Mray	-----ML E QVILFTILMGFLISVLLSPILIPFLRR	30
<i>M. flavus</i> Mray	-----MI G LLIG GV LGLVLSAAGT PL FIR FL VK	28
	: . : . : : * : *	
<i>E. coli</i> Mray	LSFGQVVRNDGPESHFSKRGTPTMGGIMILTAIVIS-----VLLWAY	92
<i>P. aeruginosa</i> Mray	RQIGQAVRNDGPQSHLSKKGTPTMGGALILTAIAIS-----TL L WAD	92
<i>S. aureus</i> Mray	M K FGQSI R EEGPQSHMKKTGTPTMGGLTFLLSIVITSLV-----AIIFVD	71
<i>B. subtilis</i> Mray	L K FGQSI R EEGP K SHQ K SGTPTMGGMILSIIIVTTIV-----MTQ K FS	75
<i>M. flavus</i> Mray	RGY G QFVRDDGPTTHKT K RGTPTMGGA VI IGSLVLA YL I TH GL L AVL GV D	78
	* * : * : * : * . * * * * : : : :	
<i>E. coli</i> Mray	PSNPY--VWCVLVVLVGYGVIGFVDDYRKVVRKDTKGLIARWKYFWMSVI	140
<i>P. aeruginosa</i> Mray	LSNRY--VWVVLVVTLFGAIGWVDDYRK VI E K NSRGLPSRWKYFWQSVF	140
<i>S. aureus</i> Mray	QANP---IILLLFVTIGFGLIGFIDDIIVVKNNQGLTSKQKFLAQIGI	118
<i>B. subtilis</i> Mray	EISPE--MVL LL FVTLGYLLGLDDYIKVVMKRN L GLTSKQKLIGQII	123
<i>M. flavus</i> Mray	FGGPTASGLILLLLTVGMAFVG FV DDFT K IT K Q R SLGLTPRGKIIILQALI	128
	. : * . : : . : * : * : : : . * . : * : :	
<i>E. coli</i> Mray	ALGVAFALY-----LAGK D TPATQLVVPFFKDVMPQ L G-LFYILL	179
<i>P. aeruginosa</i> Mray	GIGAAVFLY-----MTA E TPIETTLIVPMLKS VE IQLG-IF F VVL	179
<i>S. aureus</i> Mray	AIIFVLSN-----VFHLVNFSTS I HIP-FTNVA I PLS-FAY VI F	156
<i>B. subtilis</i> Mray	AIVFYA-----VYHYNFAT D IRVP-GT D LS F DLG-WAY F IL	158
<i>M. flavus</i> Mray	GTAFAVLALNFP DE RGLTPASTAIS F ARDIPWLDLAFAGPAIGVILFVIW	178
	. : : : : : : : : :	
<i>E. coli</i> Mray	AYFVIVGTGNAVNLTDGLDGLAIMP TV FVAGGFALVAWATGNMNFAS Y --	227
<i>P. aeruginosa</i> Mray	TYFVIVGSSNAVNLTDGLDGLAIMP TV MVAGALGIFCYLSGN V KFA Y --	227
<i>S. aureus</i> Mray	IVFWQVGF S NAVNLTDGLDGLATGL SI IGFTMYAIM S FVLG-----	197
<i>B. subtilis</i> Mray	VLFMLVGGSNAVNLTDGLDGLSGTAAIA F GA FI LAW NS -----	199
<i>M. flavus</i> Mray	SNLITTA T NAVNLTDGLDGLATGATAMI T GA Y VLI S LFQSSQ S CALEGT	228
	: . . * * * * * : : : . . .	
<i>E. coli</i> Mray	LHIPY L RHAGELVIVCTAIVGAGLGFLWFNTYPAQVFMGDV G SLALGGAL	277
<i>P. aeruginosa</i> Mray	LLIPNVPGAGELIVFCAALVGAGLGFLWFNTYPAQVFMGDV G ALALGAAL	277
<i>S. aureus</i> Mray	-----E T AI G IFCIIMLFALLGFLPY NI PAKVFMGDT G SLALGGIF	239
<i>B. subtilis</i> Mray	-----QYD VA IFSVAVVGAVLGFLVFNA H PAKVFMGDT G SLALGGAI	241
<i>M. flavus</i> Mray	RGCY EV RDPMDLALLAAILTGSLLGFLWNT S PA K IFMGDT G SLGLGGAL	278
	: : . . : : * * * : * * * : * * * . * * . :	
<i>E. coli</i> Mray	GI I AVLL R QEFLVIMGGVFV ET LSVILQVGS F KL R G-Q R IFRMAPI HH	326
<i>P. aeruginosa</i> Mray	GT I AVIV R QEIVLFIMGGVF ME TL S VMIQV S FKL T G- R R V FRMAPI HH	326
<i>S. aureus</i> Mray	ATISIMLNQ E LSLIFIGLVF VI ETLSV M LQV S FKL T G- K RIFK M SPI HH	288
<i>B. subtilis</i> Mray	VTIAIL T KLEILLVIGGV VI ETLSVILQ VI S F K T TG- K RIFK M SPL HH	290
<i>M. flavus</i> Mray	AGFA I FT R TEILVAVLAGLMVAITLSV II QV G W F KVSGG K R V FLMAPI QH	328
	: : : . * : : . . : * * * * : * * * * : * * * : *	
<i>E. coli</i> Mray	HYEL K GW PE PRVIVRFWII S LMVLIGLAT L K VR -----	360
<i>P. aeruginosa</i> Mray	HFEL K GW PE PRVIVRFWII T VI L VIGLAT L K LR -----	360
<i>S. aureus</i> Mray	HFEL I GW SE WKVVTFWAVGLISGLIGLWIG VH -----	321
<i>B. subtilis</i> Mray	HYEL V GW SE WRVVTFWTAGLLAVLG IY IE V WL-----	324
<i>M. flavus</i> Mray	HFEL K GW AE VTVVVRFWLL S MCVTVGLAIF Y GDWL IR QGGLAG VT P	375

Figure 2-3: From top to bottom: *E. coli*, *P. aeruginosa*, *S. aureus*, *B. subtilis* and *M. flavus* Mray sequence alignment, colour of the amino acids: small and hydrophobic: AVFPMILW, acidic: DE, basic: RK, hydroxyl + sulfhydryl + amine + G: STYHCNGQ

2.2 Development of the fluorescence assay for MraY

2.2.1 Preparation of UDP-N-acetylmuramyl-L-Ala- γ -D-Glu-m-

Dap -D-Ala-D-Ala (UDPMurNAc-pentapeptide)

The UDPMurNAc-pentapeptide was purchased on a number of occasions from the BaCWAN facility of the University of Warwick where it was made enzymatically using enzymes MurA-F. On one occasion, it was isolated from antibiotic-treated cells of *B. subtilis* in mg quantities based on procedures used by P. Brandish and S. Bagga^{13, 145}. Based on its cell wall structure, *B. subtilis* belongs to the family of Gram-positive bacteria, however it unusually uses diaminopimelic acid and not lysine at the third amino acid position of the UDPMurNAc-pentapeptide as a peptidoglycan precursor¹².

B. subtilis was provided by Dr. Christophe Corre and cells were grown at 37 °C into mid-logarithmic phase in a rich medium. Pellets were collected by centrifugation and kept cool on ice bath. Then the cells were re-suspended in a warm CWSM medium (cell wall synthesis medium) which contained 12.5 mg/ml vancomycin, 50 mg/ml chloramphenicol, and 50 mg/ml ampicillin. Vancomycin inhibits the formation of glycosidic bonds between the sugars by the transglycosidase enzymes and the formation of the peptide cross-links by the transpeptidase enzymes by complexing D-Ala-D-Ala of the pentapeptide unit of lipid II¹⁰⁷, therefore helps accumulating UDPMurNAc-pentapeptide. Chloramphenicol has a detrimental effect on bacterial protein synthesis²⁰⁶ while ampicillin seemed to have improved the yield for P. Brandish¹³. The addition of uracil and amino acids, Ala, Glu and diaminopimelic acid helps to increase the yield of the product. Cells were grown for 45 minutes in Cell Wall Synthesis

Medium (CWSM). The cultures were chilled on ice again and cells collected by centrifugation, re-suspended in ice-cold 5 % (w/v) trichloroacetic acid (TCA) at 5 ml/g cells. The pellet was extracted two more times with half volumes of ice-cold TCA. The supernatants (60 ml) were pooled and extracted three times with an equal volume of ice-cold ether (3 x 60 ml) in order to remove the TCA. The aqueous phase was neutralised with 3 M NaOH. The traces of ether were evaporated by rotary evaporation and the sample was lyophilised overnight. The sample was clarified by microcentrifugation and subjected to gel filtration (Sephadex G25 3 x 80 cm) eluting with water. The highest molecular weight fractions with absorbance at 260 nm were pooled and lyophilised. UDPMurNAc-pentapeptide was identified by a run on Agilent 1200 HPLC with a Bruker HCT Ultra Mass Spectrometer, m/z $[M-H]^-$: 1192.3359 calculated for $C_{41}H_{65}N_9O_{28}P_2$ 1192.3341. The correct isotopic pattern was confirmed by high resolution LC-MS (HR LC-MS) by a run on a Dionex Ultramate3000 uHPLC with the Bruker MaXis (Figure 2-4). The yield was 15 mg from a 2 l culture. All the LC-MS from this project was run on the above mentioned two instruments; the high resolution analysis was performed by Philip Aston and Lijiang Song from the Mass Spectrometry Facility of the Chemistry Department of the University of Warwick. The procedure and the LC-MS conditions are detailed in Sections 7.5, 7.6 and 7.7. Figure 2-4 shows the isotopic pattern of the doubly and negatively charged ion for the UDPMurNAc-pentapeptide.

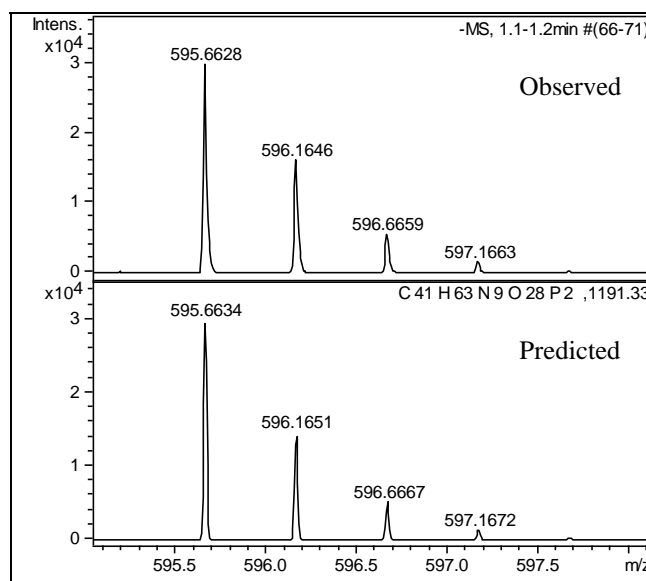


Figure 2-4: Isotopic pattern for the doubly and negatively charged ion of the UDPMurNAc-pentapeptide

2.2.2 Preparation of UDP-N-acetylmuramyl-L-Ala- γ -D-Glu-(N^ε-dansyl)-*m*-Dap-D-Ala-D-Ala (dansyl-labelled UDPMurNAc-pentapeptide)

One of the substrates of the fluorescence MraY assay is the dansylated UDPMurNAc-pentapeptide. The procedure for the preparation of this derivative is based on the procedures of Weppner and Neuhaus¹⁴¹ and P. Brandish¹³.

The procedure starts with the reaction between 1 equivalent UDPMurNAc-pentapeptide and 96 equivalent dansyl chloride in a 50 % acetone NaHCO₃ buffer at pH 9 (see 1. in Figure 2-5)

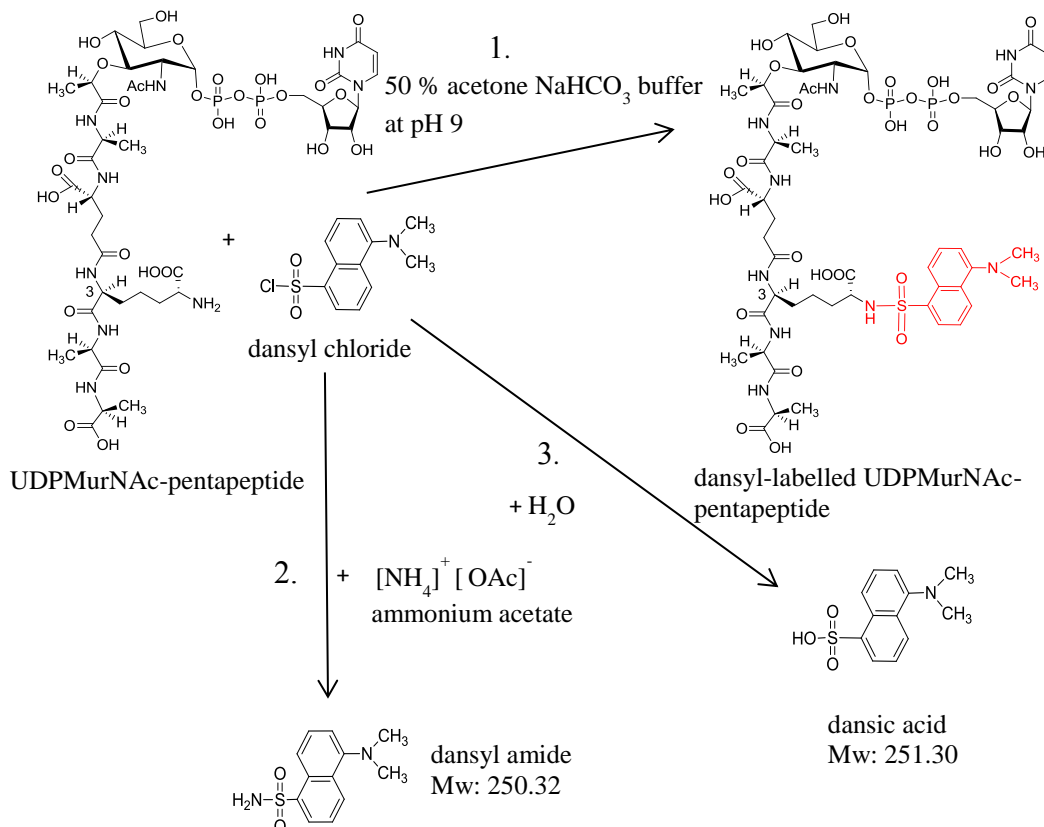


Figure 2-5: Dansylation of the UDPMurNAc pentapeptide, 1.: formation of the dansyl-labelled UDPMurNAc-pentapeptide, 2.: formation of dansyl amide with ammonium acetate, 3.: formation of the by-product, dansic acid with water

Even though it is a relatively simple procedure, it proved to be very challenging. After a number of failed reactions, we identified that the UDPMurNAc-pentapeptide that we purchased from the BaCWAN facility of the University of Warwick contained unexpected amounts of ammonium acetate (coming from the buffer used for purification by anion exchange) which led to the formation of dansyl amide with the dansyl chloride, instead of the desired dansyl UDPMurNAc-pentapeptide (see 2. in Figure 2-5). This mystery, together with problems in overexpression of MraY, delayed progress 12-18 months. Hence the UDPMurNAc-pentapeptide was purified from ammonium acetate by gel filtration (Sephadex G25 80 x 3 cm), after which the dansylation method worked well.

The procedure that we followed is described in Section 7.8. The most challenging part of the procedure is the separation of the labelled UDPMurNAc-pentapeptide from the by-product dansic acid (see 3. in Figure 2-5). The separation was carried out by using gel filtration (Sephadex G25 80 x 3 cm). The column was washed with water, and 5 ml fractions were collected. All fractions were monitored on a PerkinElmer UV/Vis spectrophotometer and a PerkinElmer fluorimeter. The absorbance spectrum of the dansyl-labelled UDPMurNAc-pentapeptide has two characteristic peaks, at 250 nm and 330 nm (Figure 2-6), while the fluorescence emission spectrum has a maximum at 530 nm with excitation at 340 nm (Figure 2-7). These properties enabled the isolation of the fractions of interest. The fractions of interest were pooled and lyophilised overnight.

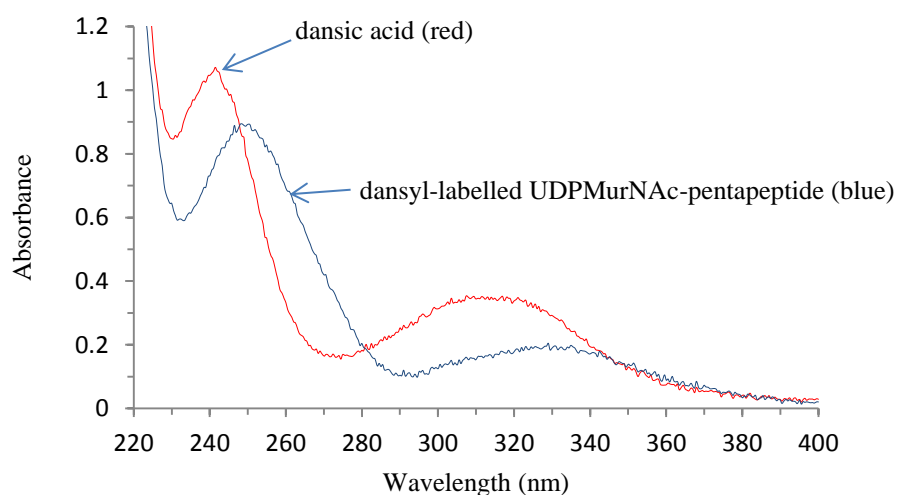


Figure 2-6: UV-Vis absorbance spectrum of the dansyl-labelled UDPMurNAc-pentapeptide (in blue) and dansic acid (in red)

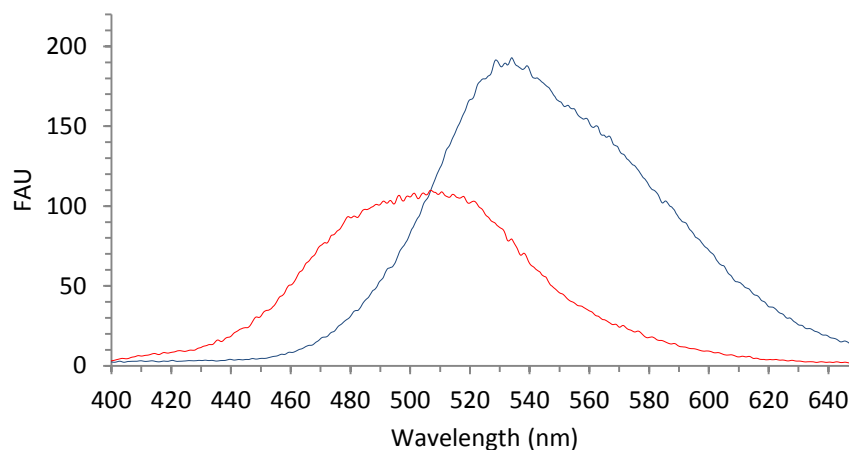


Figure 2-7: Fluorescence emission spectrum of the dansyl-labelled UDPMurNAc-pentapeptide (in blue) and dansic acid (in red), excitation: 340 nm

A sample of the material was analysed by HR LC-MS (Figure 2-8). For LC a linear gradient of methanol/water was used, with the percentage of methanol running up from 1 to 100 % starting at 5 minutes to 25 minutes at a flow rate of 0.2 ml/min. The largest peak, the main compound of the spectrum is the dansyl-labelled UDPMurNAc-pentapeptide (m/z $[M-2H]^{2-}$: 712.1884) at 1.1-1.2 min retention time. There is evidence for the presence of an insignificant amount of dansic acid (m/z $[M-H]^-$: 250.0530 see in Figure A 1 in Appendix 1) at ~10.8-10.9 min (possibly formed during the MS analysis) and also for the formation of a small amount of a didansyl-labelled UDPMurNAc-pentapeptide (m/z $[M-2H]^{2-}$: 828.7073) at 12.5-12.7 minutes. The presence of the starting material, the UDPMurNAc-pentapeptide, was not detected in the sample.

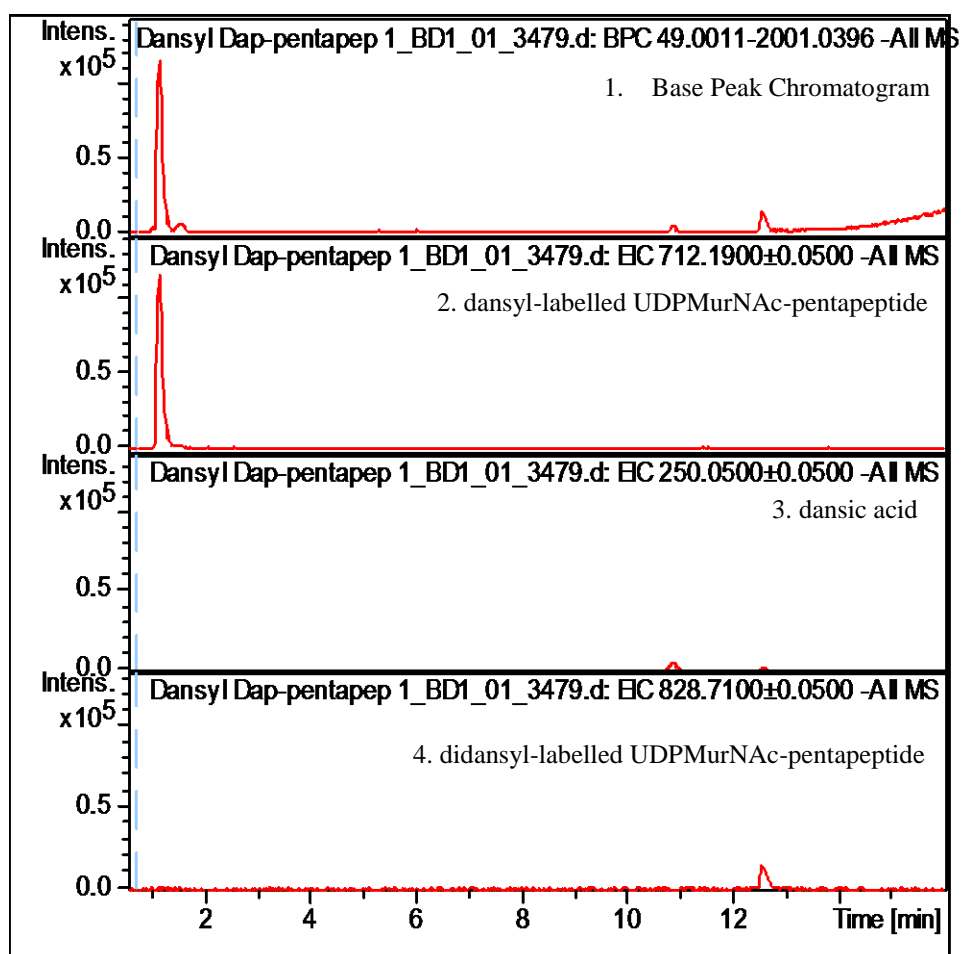


Figure 2-8: HR LC-MS results, 1: Base Peak Chromatogram 2: Extracted Ion Chromatogram for the negatively and doubly charged dansyl-labelled UDPMurNAc-pentapeptide (m/z : 712.19), 2: Extracted Ion Chromatogram for dansic acid (m/z : 250.06) and 3: Extracted Ion Chromatogram for the negatively and doubly charged didansyl-labelled UDPMurNAc-pentapeptide (m/z : 828.71)

Negative MS showed the correct isotopic pattern for the doubly charged ion of the dansyl-labelled UDPMurNAc-pentapeptide (Figure 2-9).

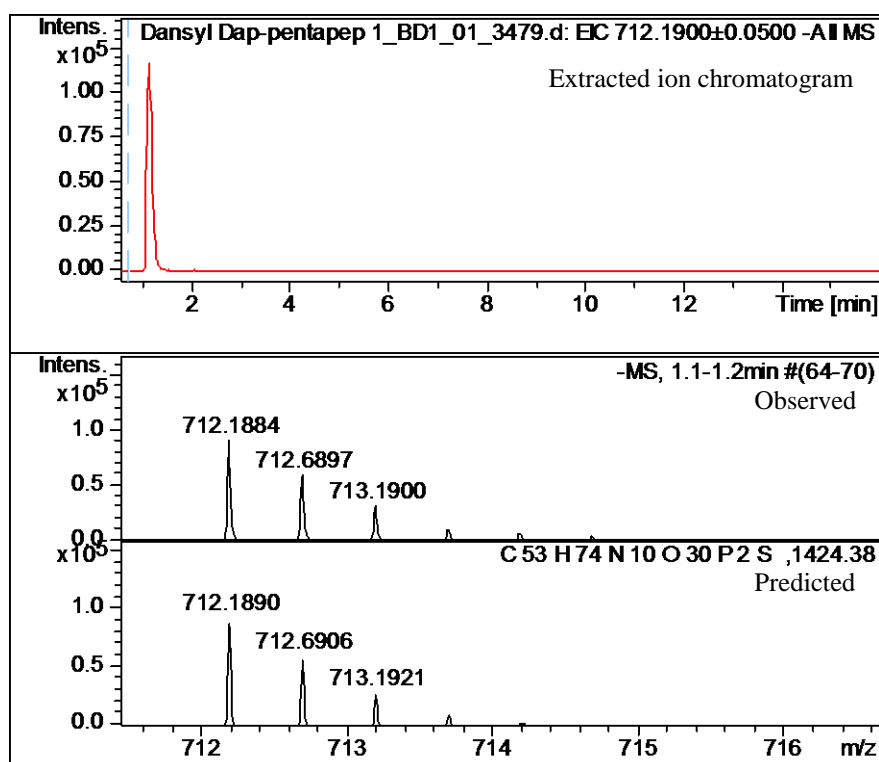


Figure 2-9: The extracted ion chromatogram and the doubly and negatively charged ion for the dansyl-labelled UDPMurNac-pentapeptide

The chemical composition of the didansyl-labelled UDPMurNac-pentapeptide was confirmed by HR LC-MS (Figure 2-10). However, the exact position of the second label would need to be confirmed by further tests.

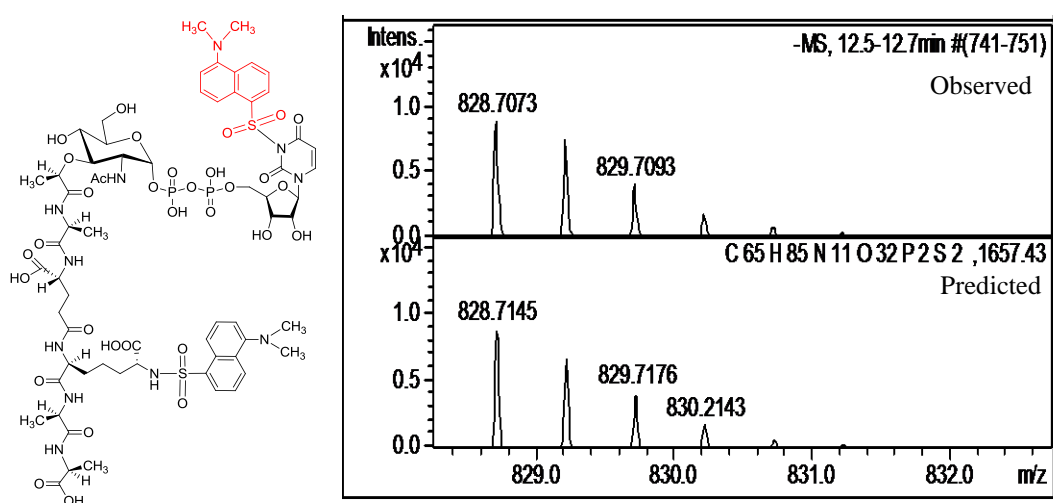


Figure 2-10: Suggested chemical structure (second label in red), the isotopic pattern for the negatively and doubly charged ion of the didansyl-labelled UDPMurNac pentapeptide

The pale yellow powder of the identified dansyl pentapeptide, the fluorescence substrate for the assays, was then dissolved in water and stored as a stock solution (3.75 mg/ml) at -20 °C. Every preparation of the dansyl-labelled UDPMurNAc-pentapeptide was routinely identified by a run on an Agilent 1200 HPLC coupled with the Bruker HCT-Ultra (LC-MS), see Figures in Appendix 1: Figures A 2 and A 3.

2.2.3 Optimisation of the continuous fluorescence assay

2.2.3.1 Changes in the fluorescence emission spectrum during the

MraY reaction

Weppner and Neuhaus experienced a 30 nm blue shift in the fluorescence emission spectrum and a 6-fold increase in the quantum yield during the MraY reaction, and they associated the changes with the formation of the dansyl derivative of lipid I¹⁴¹. However, P. Brandish only saw an 11 nm shift upon formation of the dansyl-labelled lipid I¹³.

The first experiment we did in order to investigate the reliability of the assay was to incubate in a total volume of 400 µl 100 µM dansyl-labelled UDPMurNAc-pentapeptide with 80 µg/ml undecaprenyl phosphate in 100 mM Tris pH 7.5, 25 mM MgCl₂ 6 % glycerol, 0.15 % Triton X-100 and 240 µg *E. coli* MraY membranes as described in Section 7.9. We prepared two samples; one of them for the MraY reaction (Figure 2-11A) and the other one also contained 83 µg/ml tunicamycin (Figure 2-11B), a known inhibitor of MraY. The fluorescence emission spectrum was recorded a few minutes after sample preparation (excitation at 340 nm). The measurement was repeated after 30 minutes, then

0.1 mM UMP was added to both samples. UMP is one of the products of the *MraY* reaction, and addition of this was expected to favour the reverse reaction¹⁰. The spectrum of the sample with tunicamycin had a lower maximum in fluorescence intensity (FAU: Fluorescence Arbitrary Units) right from the start (FAU: 425). In Figure 2-11A the fluorescence maximum increased from 610 to 660 FAU in 30 minutes; however, there was no change in fluorescence intensity after 30 minutes (FAU: 425) in the sample with inhibition (Figure 2-11B). When 0.1 mM UMP was added to the samples, a significant decrease in fluorescence was observed for both samples. The fluorescence maximum decreased from 660 to 375 FAU (Figure 2-11) and from 425 to 315 FAU for the tunicamycin-inhibited sample (Figure 2-11B).

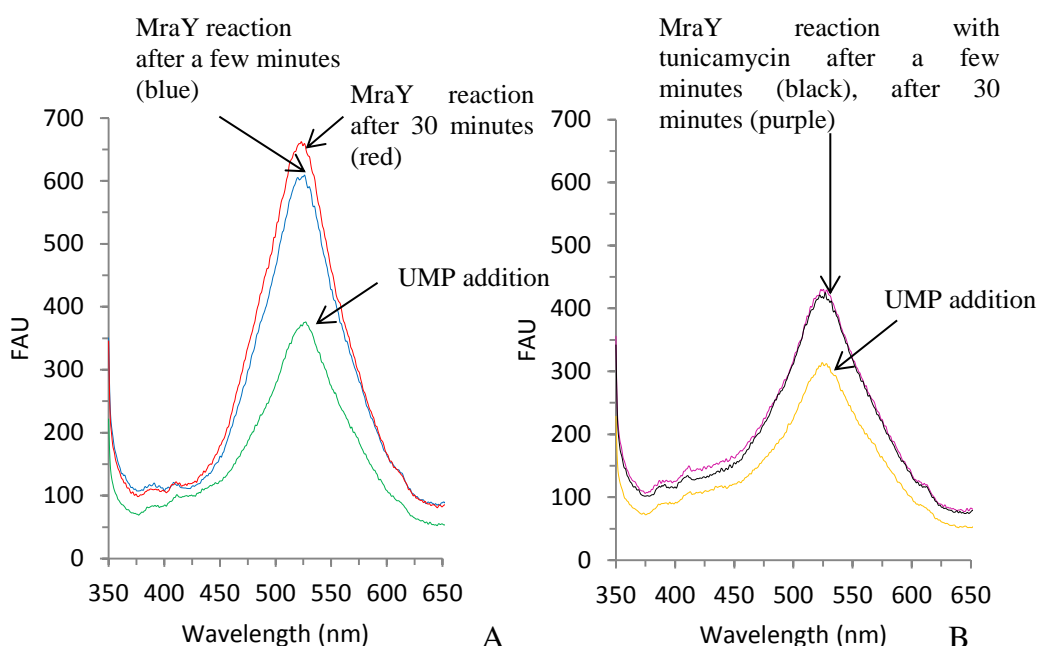


Figure 2-11: Emission spectrum of the dansyl-labelled UDPMurNAc pentapeptide incubated with *E. coli* *MraY* membranes recorded twice over 30 minutes and the effect of UMP addition, A: sample without inhibitor, B: sample with 83 µg/ml tunicamycin, λ_{ex} : 340 nm

A small blue shift in the fluorescence emission spectrum could be observed during the MraY reaction leading to the formation of lipid I. However, this shift is very small between the lowest maximum (UMP treated sample) and the highest maximum (lipid I formation) in the fluorescence emission spectrum, around 5 nm (the difference between 522 nm and 527 nm) which is even smaller than the 11 nm observed by Brandish (Figure 2-12). However, this experiment did not determine the exact location of the maximum of the fluorescence emission spectrum of the MraY reaction at 0 minutes accurately.

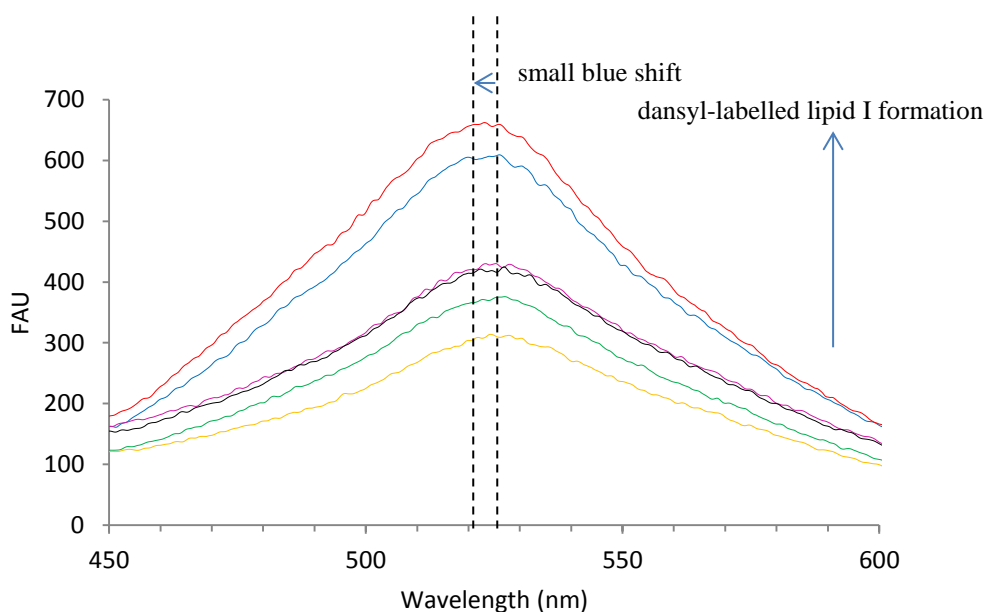


Figure 2-12: Observed small blue shift in the fluorescence emission spectrum associated with dansyl-labelled lipid I formation, same experiment as in Figure 2-11, (the two graphs are combined in one graph), λ_{ex} : 340 nm

2.2.3.2 Time-course of the *E. coli* MraY reaction

The time-course behaviour of the reaction was investigated by the following experiment (Section 7.10.1). A master mix containing 26 μM dansyl-labelled UDPMurNAc-pentapeptide, 30 $\mu\text{g/ml}$ undecaprenyl phosphate at final concentrations was prepared in the assay buffer (83 mM Tris pH 7.5, 21 mM

MgCl₂) as described in Section 7.10. Note that the continuous fluorescence MraY assays always contains 6 % glycerol and 0.15 % Triton X-100 from the buffer that the undecaprenyl or heptaprenyl phosphate solution was made. The presence of detergent is essential for the MraY assay. The reaction was started with the addition of 90 µg protein containing overexpressed *E. coli* MraY membranes in a total volume of 180 µl. The reaction was monitored by a PerkinElmer fluorimeter over 15 minutes. A gradual increase was observed in fluorescence intensity, indicating the formation of dansyl-labelled lipid I. As each membrane preparation can contain a different level of MraY expression, it is important to find the optimal dilution for the membranes in order to see a gradual increase in fluorescence over 5-15 minutes so that the reaction kinetics can be studied, which meant ~6 mg total protein/ml stock solution for ~90 µg protein containing membranes for an assay of 180 µl total volume for this experiment. The repeated reaction containing 83 µg/ml tunicamycin did not result in a significant increase in fluorescence, showing that the reaction was inhibited (Figure 2-13).

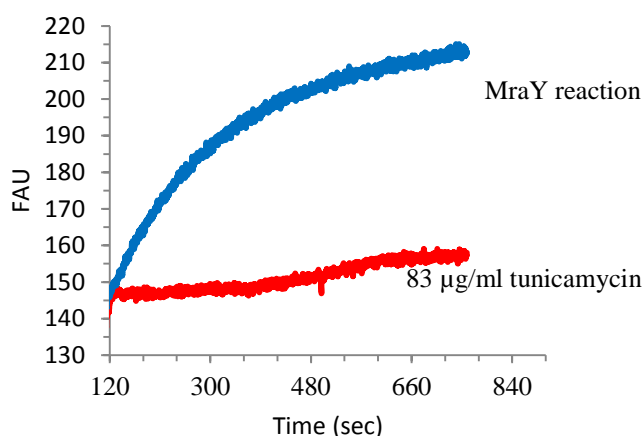


Figure 2-13: Gradual increase in fluorescence associated with the formation of dansyl-labelled lipid I following addition of 90 µg *E. coli* MraY membranes and 83 µg/ml tunicamycin inhibition, λ_{ex} : 340nm, λ_{em} : 530 nm

2.2.3.3 Experiment with inactivated *MraY* membranes

Another experiment was carried out in a 180 μ l total volume containing 20 μ M dansyl-labelled UDPMurNAc-pentapeptide, 30 μ g/ml undecaprenyl phosphate in the assay buffer (83 mM Tris pH 7.5, 21 mM MgCl_2) and started with the addition of 90 μ g protein (membranes) as described in Section 7.10.2. Under the same conditions previously boiled *E. coli* *MraY* membranes (C43) were added (90 μ g), and no increase in fluorescence intensity was observed over time (Figure 2-14), indicating the lack of *MraY* activity and dansyl-labelled lipid I product formation.

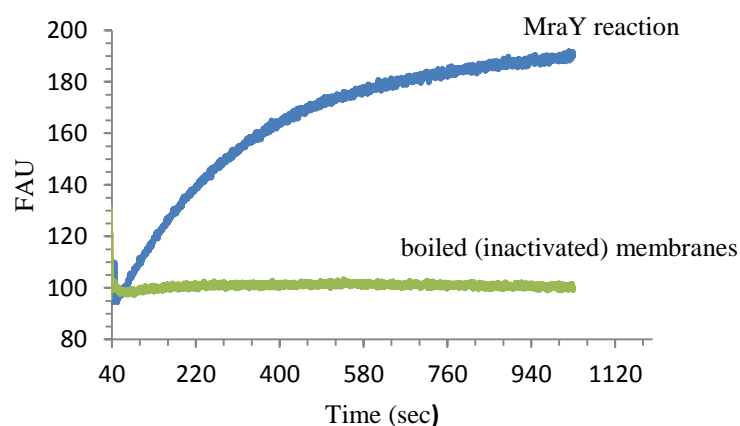


Figure 2-14: No fluorescence changes were observed with 90 μ g inactivated *MraY* enzyme, λ_{ex} : 340nm, λ_{em} : 530 nm

2.2.3.4 Reverse *MraY* reaction with UMP addition

The *MraY* reaction is reversible (Figure 2-15), thus the addition of 0.1 mM UMP, one of the products, to a solution of dansyl labelled lipid I should result in a decrease in fluorescence intensity (Figure 2-16)¹⁰.

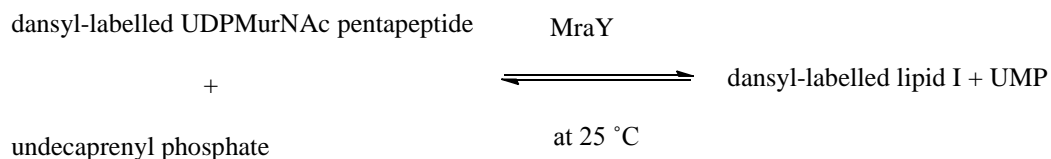


Figure 2-15: Schematic representation of the reversible fluorescence MraY assay

180 μl total volume containing 20 μM dansyl-labelled UDPMurNAc-pentapeptide, 30 $\mu\text{g/ml}$ undecaprenyl phosphate in the assay buffer (83 mM Tris pH 7.5, 21 mM MgCl_2) was started with the addition of 90 μg protein containing membranes. After 13 minutes reaction time, 0.1 mM UMP was added, which induced a decrease in fluorescence intensity (Figure 2-16) indicating the formation of the dansyl-labelled UDPMurNAc-pentapeptide from dansyl-labelled lipid I (Section 7.10.3).

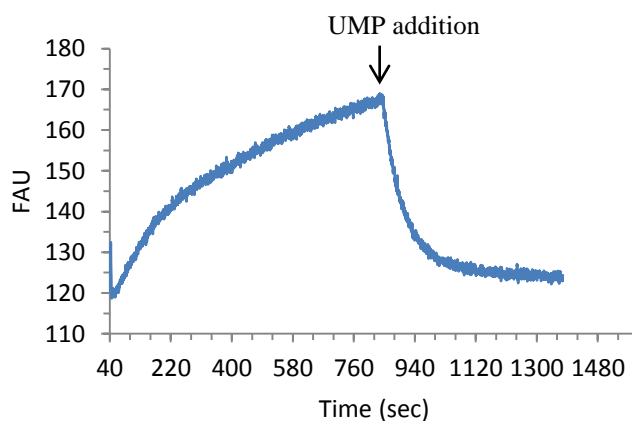


Figure 2-16: Decrease in fluorescence following 0.1 mM UMP addition to the *E. coli* MraY reaction, λ_{ex} : 340nm, λ_{em} : 530 nm

2.2.3.5 Effect of added heptaprenyl phosphate to the fluorescence substrate incubated with MraY membranes

The MraY enzyme has two substrates, UDPMurNAc-pentapeptide and undecaprenyl phosphate (C₅₅-P). Brandish showed that heptaprenyl phosphate (C₃₅-P) is a good substrate for the *E. coli* MraY enzyme, and he successfully used it for his fluorescence and radiochemical assays, with similar kinetic properties to those of undecaprenyl phosphate¹³. The following experiments show that the lack of heptaprenyl phosphate does not result in significant increase in fluorescence intensity upon the reaction of the dansyl-labelled UDPMurNAc-pentapeptide with the MraY membranes. (The presence of some endogenous undecaprenyl phosphate in the membranes could lead to the formation of lipid I and some increase in the fluorescence intensity.) The master mix for the following experiment contained 20 µM dansyl-labelled UDPMurNAc-pentapeptide but no heptaprenyl phosphate, 83 mM Tris pH 7.5, 21 mM MgCl₂, 6 % glycerol and 0.15 % Triton X-100. 90 µg *E. coli* MraY membranes (C43) were added and no increase in fluorescence was observed over 10-minute reaction time. 8 µg/ml (final concentration) heptaprenyl phosphate induced the fluorescence changes, indicating the formation of the dansyl-labelled lipid I product (Figure 2-17 and Section 7.10.4).

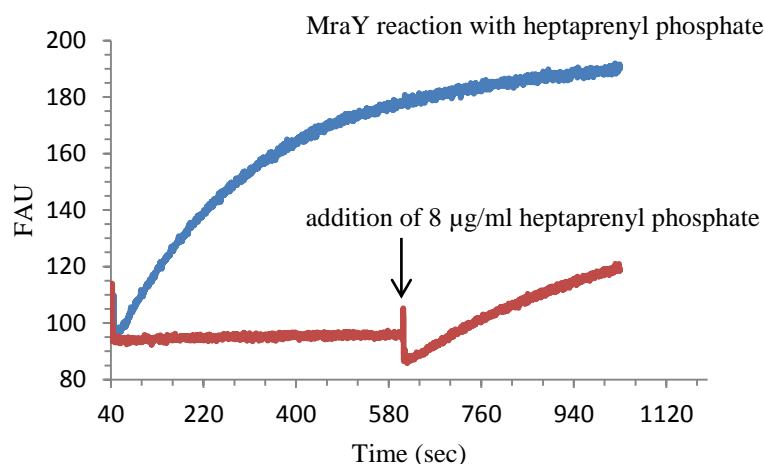


Figure 2-17: Effect of heptaprenyl phosphate on the MraY reaction, λ_{ex} : 340nm, λ_{em} : 530 nm

2.2.3.6 Evidence for the dansyl-labelled lipid I by high resolution LC-MS (HR LC-MS)

In order to identify the forming lipid I product, the dansyl-labelled lipid I, HR LC-MS analysis was performed. Two samples were prepared, both containing ~80 μM dansyl-labelled UDPMurNAc-pentapeptide, one with added 20 $\mu\text{g/ml}$ undecaprenyl phosphate, the other with 20 $\mu\text{g/ml}$ heptaprenyl phosphate. The reaction was started by the addition of 240 μg *E. coli* MraY membranes and incubated for 30 minutes at 37 °C. Then 6 M pyridinium acetate was added in order to stop the reaction. The formed lipid products were extracted into 1-butanol. HR LC-MS analysis that was performed in the conditions written in Section 7.13, showed the evidence for the existence of the dansyl-labelled lipid I in the sample (Figure 2-18).

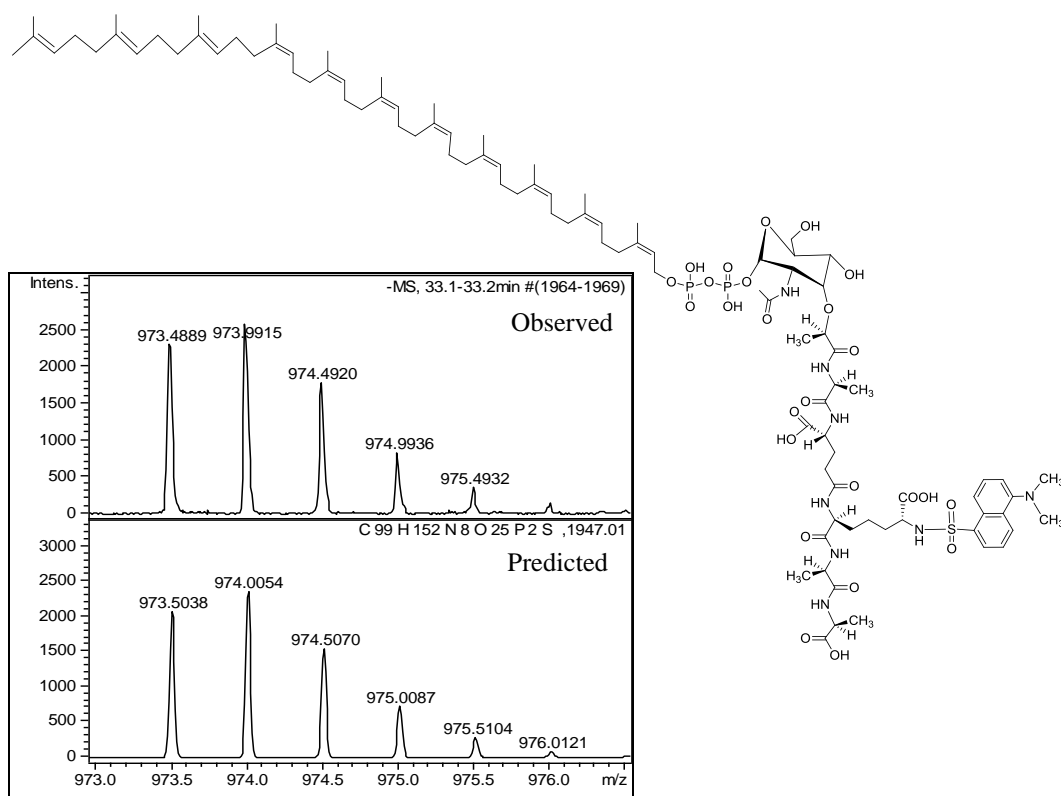


Figure 2-18: Isotopic pattern of the negatively and doubly charged ion for the dansyl-labelled C₅₅ lipid I and the chemical structure

Evidence was also found for the existence of the chemical composition of the dansyl-labelled C₃₅ lipid I (formed with heptaprenyl phosphate) by HR LC-MS (Figure 2-19).

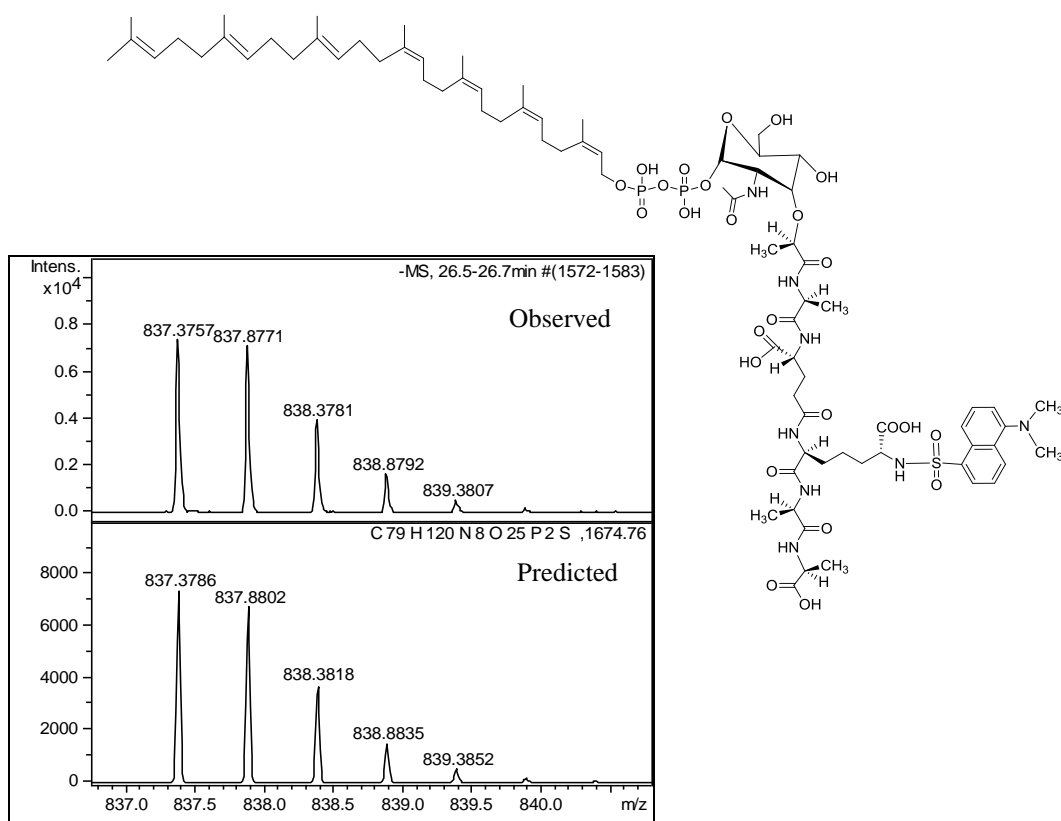


Figure 2-19: Isotopic pattern for the negatively and doubly charged ion for the dansyl-labelled C₃₅ lipid I and the chemical structure

Interestingly, from this sample where the dansyl-labelled UDPMurNAc-pentapeptide reacted with heptaprenyl phosphate, evidence was found that the dansyl-labelled lipid I also formed with endogenous undecaprenyl phosphate of the *E. coli* MraY membranes (Figure 2-20). However, the intensity of the peaks is very low, implying a very low concentration of the compound.

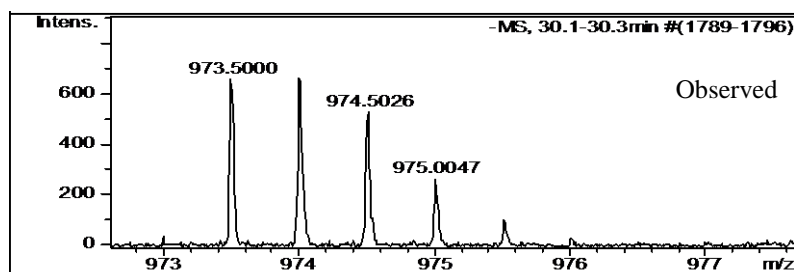


Figure 2-20: Isotopic pattern for the negatively and doubly charged ion for the dansyl-labelled C₅₅ lipid I formed with endogenous undecaprenyl phosphate

2.2.4 Continuous fluorescence assays with MraY enzymes from bacteria other than *E. coli*

In this section, examples are shown for the continuous fluorescence assay with the wild type *E. coli*, *P. aeruginosa*, *S. aureus*, *B. subtilis* and *M. flavus* MraYs.

2.2.4.1 Background MraY activity in the wild type *E. coli* membranes

When wild type *E. coli* (C43) membranes were used for the MraY reaction in a total volume of 180 μ l assay containing 20 μ M dansyl-labelled UDPMurNAc-pentapeptide, 35 μ g/ml heptaprenyl phosphate, 83 mM Tris pH 7.5, 21 mM MgCl₂ and 60 μ g protein membranes where the enzyme was not overexpressed, the increase in fluorescence intensity was less than 10 FAU over a 15 minutes reaction time. These changes in fluorescence are too small to determine the level of inhibition or perform kinetic studies (Figure 2-21).

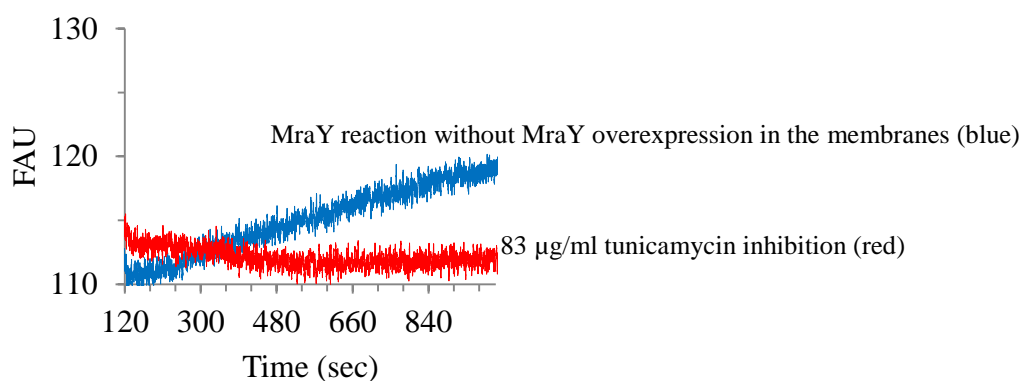


Figure 2-21: Fluorescence MraY assay with wild type 90 μ g *E. coli* membranes (MraY is not overexpressed) λ_{ex} : 340 nm, λ_{em} : 530 nm

This observation highlights the necessity of overexpressing the MraY enzyme in the membranes.

2.2.4.2 *P. aeruginosa* MraY reaction and inhibition by a known inhibitor, pacidamycin D

The *P. aeruginosa* MraY was overexpressed in *E. coli* C43 membranes as well. One example for the assay is the well-known inhibitor of MraY, pacidamycin D. The compound was a gift from Antoine Abou Fayad (University of St Andrews) and was tested against *P. aeruginosa* MraY, (see Section 5.1.3) in a total volume of 180 µl containing 30 µM dansyl-labelled UDPMurNAc-pentapeptide, 35 µg/ml heptaprenyl phosphate in buffer 83 mM Tris pH 7.5, 21 mM MgCl₂ and 90 µg protein membranes. Figure 2-22 shows the MraY assay from the time point of the addition of 90 µg protein with only one curve for each concentration of Pacidamycin D.

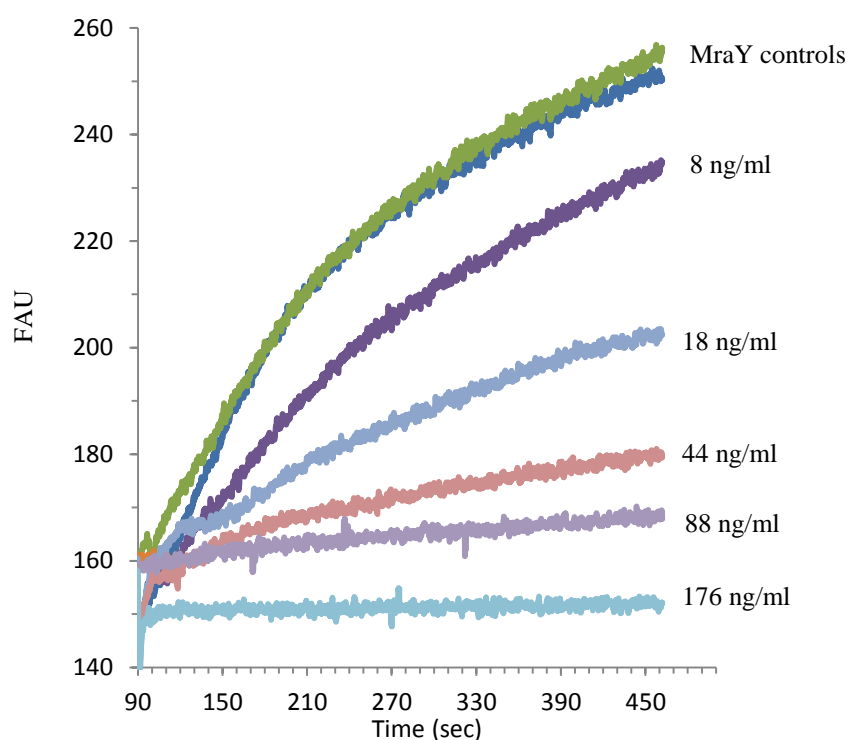


Figure 2-22: *P. aeruginosa* Mray assay, pacidamycin D concentration 0-180 ng/ml, 90 μ g protein, λ_{ex} : 340 nm, λ_{em} : 530 nm

2.2.4.3 *S. aureus* Mray reaction and inhibition by a synthetic muraymycin analogue

S. aureus was overexpressed in *E. coli* C43 membranes. A synthetic muraymycin analogue was tested against *S. aureus* Mray (see Section 5.1.1). A total volume of 180 μ l contained 20 μ M dansyl-labelled UDPMurNAc-pentapeptide, 83 mM Tris pH 7.5, 21 mM MgCl_2 and 90 μ g protein membranes. Figure 2-23 shows the Mray assay with only one curve for each concentration of the muraymycin analogue, starting from the membrane addition.

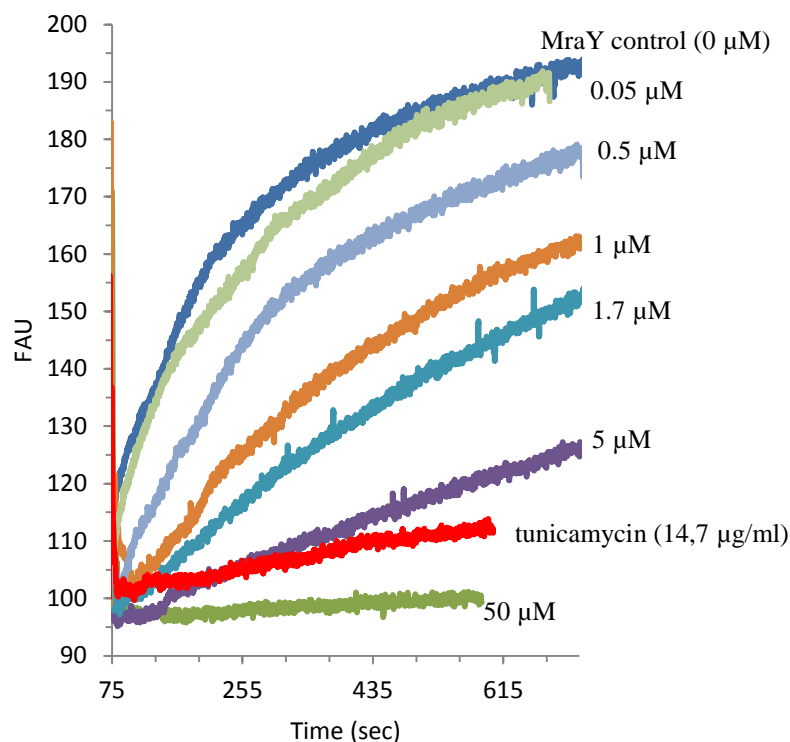


Figure 2-23: *S. aureus* Mray assay, testing a muraymycin analogue between 0-80 μM, 90 μg protein, λ_{ex} : 340nm, λ_{em} : 530 nm

2.2.4.4 *B. subtilis* Mray reaction and inhibition by a known inhibitor, A-503083 B

B. subtilis Mray was expressed in *E. coli* (C43) membranes. The capuramycin analogue, A-503083 B, was tested against *B. subtilis* Mray in order to test inhibition (see Section 5.1.5) in a total volume of 180 μl containing 30 μM dansyl-labelled UDPMurNAc-pentapeptide, 35 μg/ml heptaprenyl phosphate in a buffer 83 mM Tris pH 7.5, 21 mM MgCl₂ and 60 μg protein (overexpressed *B. subtilis* Mray containing *E. coli* membranes). The concentration of the inhibitor varied in the range of 0 to 2.5 μg/ml (see Figure 2-24).

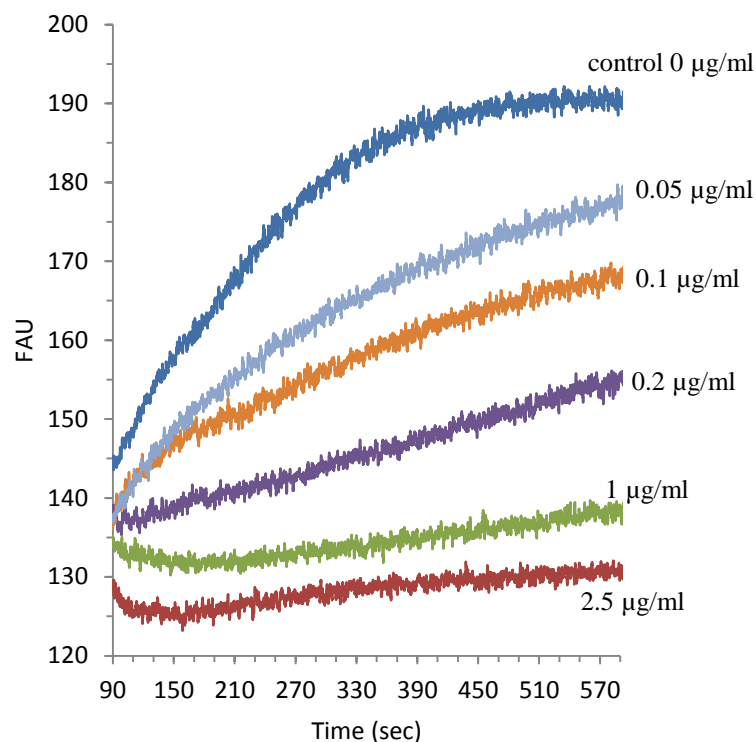


Figure 2-24: Inhibition of a capuramycin analogue, A-503083 B, against *B. subtilis* MraY, concentrations of the inhibitor ranging from 0-2.5 µg/ml, 60 µg protein, λ_{ex} : 340nm, λ_{em} : 530 nm

2.2.4.5 *M. flavus* MraY reaction and inhibition by a known inhibitor, tunicamycin

Micrococcus flavus membranes which naturally contain high level of the MraY enzyme, were assayed in a total volume of 180 µl containing 23 µM dansyl-labelled UDPMurNAc-pentapeptide in 83 mM Tris pH 7.5, 21 mM MgCl₂ and 100 µg protein membranes gave only 25 FAU changes over 15 minutes. These small changes are enough to detect inhibition but not ideal to perform detailed kinetic studies on the *M. flavus* MraY (Figure 2-25).

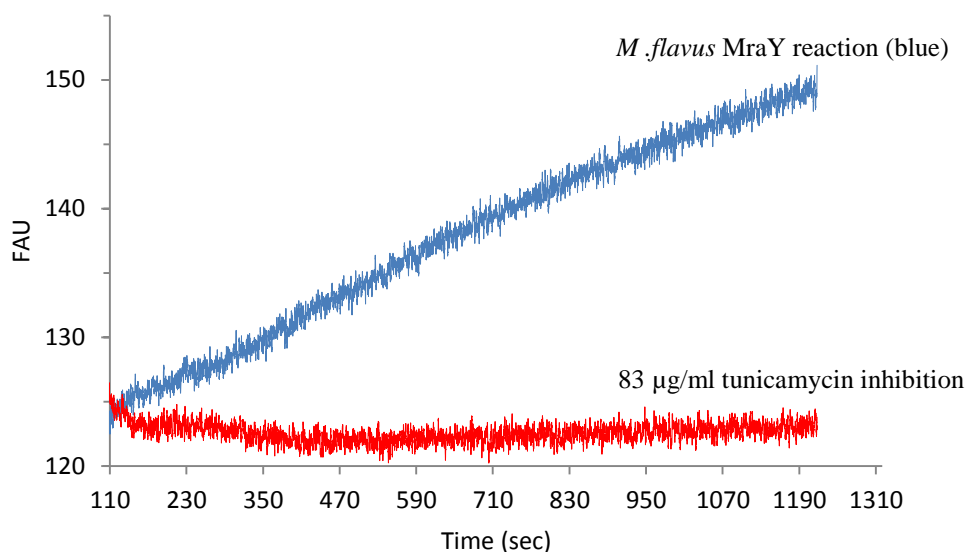


Figure 2-25: *M. flavus* Mray reaction and 83 µg/ml tunicamycin inhibition, 90 µg protein containing membranes, λ_{ex} : 340nm, λ_{em} : 530 nm

2.2.5 Specific activity of recombinant Mray enzymes in the fluorescence assay

An experiment was carried out in order to estimate the specific activity in the fluorescence Mray assay of the membrane preparations containing Mrays from the 5 organisms in a total volume of 180 µl containing 20 µM dansyl-labelled UDPMurNAc-pentapeptide, 30 µg/ml heptaprenyl phosphate in 83 mM Tris pH 7.5, 21 mM MgCl₂ and 15 µl wild type *E. coli* membranes (50 µg) or overexpressed *E. coli* membranes containing Mray from either *E. coli* (50 µg), or *P. aeruginosa* (45 µg) or *S. aureus* (50 µg) or *B. subtilis* (65 µg) or 15 µl *M. flavus* (75 µg) membranes. The initial rate of the reaction was calculated from the slope of the curves between 50 and 110 second reaction time (avoiding mixing effects after the addition of the membranes). The specific activity of the enzymes was calculated as fluorescence unit changes (ΔFAU) minute⁻¹ mg protein⁻¹ (see Table 2-2 and Section 7.10).

Table 2-2: Increase in specific activity by the fluorescence MraY assay in the membranes by overexpressing MraY

overexpressed MraY	total protein/assay (mg)	fluorescence changes (FAU) over 1 minutes (initial rate of the reaction)	specific enzyme activity (FAU min ⁻¹ mg protein ⁻¹)	overproduction of enzyme activity (FAU min ⁻¹ mg protein ⁻¹) compared to the wild type <i>E. coli</i> C43
wild type <i>E. coli</i> C43	0.050	0.0186	0.372	-
<i>E. coli</i>	0.060	0.136	2.27	6 fold
<i>P. aeruginosa</i>	0.045	0.221	4.91	13 fold
<i>S. aureus</i>	0.050	0.149	2.98	8 fold
<i>B. subtilis</i>	0.065	0.176	2.71	7 fold
wild type <i>M. flavus</i>	0.075	0.053	0.707	2 fold

P. Brandish calculated a specific activity of 2.66 FAU min⁻¹ mg protein⁻¹ for the fluorescence MraY assay using a dansyl-labelled UDPMurNAc-pentapeptide and solubilised *E. coli* MraY¹³. Our estimated specific activity for the *E. coli* MraY is within the same range with 2.3 FAU min⁻¹ mg protein⁻¹. In conclusion, the overexpression of the MraY enzymes resulted in 6-13 fold increase in enzyme activity in the fluorescence MraY assay. The specific fluorescence activity of the wild type *M. flavus* MraY was 2 fold higher than that of the wild type *E. coli* MraY.

2.2.6 Determination of IC₅₀ values of potential MraY inhibitors

The half maximal inhibitory concentrations of the known or novel MraY inhibitors were determined by the means of the continuous fluorescence MraY assay on a number of occasions. Examples for the known MraY inhibitors are the pacidamycins (1.3). A sample of a mixture of pacidamycin 1 and 2 (Mw: 874.3 and 835.3 respectively) was provided by Antoine Abou Fayad (University of St Andrews). The MraY reaction was started by the addition of 60 µg protein containing *E. coli* MraY membranes (C43) as described in the experimental chapter (Section 7.11). The inhibitor concentration in the assays varied between 0 and 9 µg/ml. Figure 2-26 shows the inhibition of *E. coli* MraY by the fluorescence assay with only one example for each inhibitor concentration.

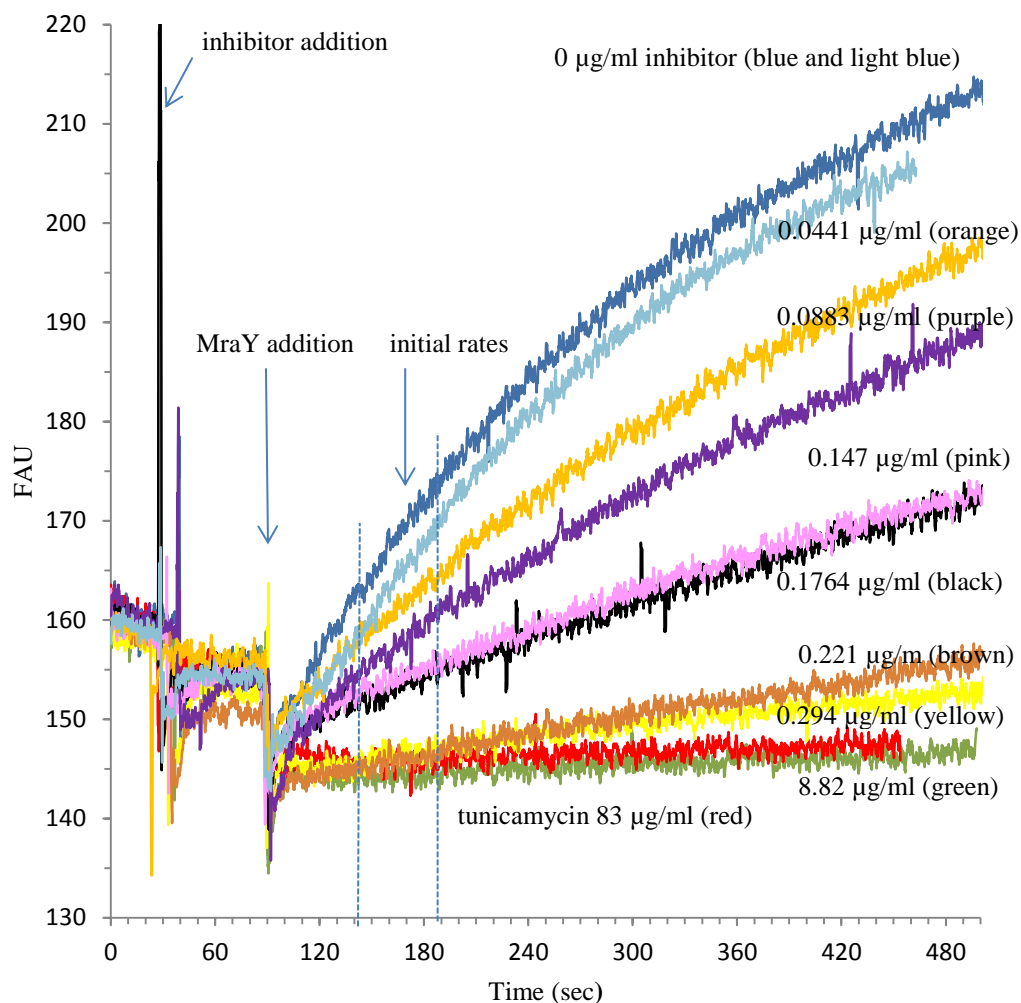


Figure 2-26: Example for the fluorescence Mray assay: Pacidamycin 1,2 inhibition against *E. coli* Mray, 60 µg protein, showing only one curve for each inhibitor concentration, λ_{ex} : 340 nm, λ_{em} : 530 nm

In Figure 2-26 a regression line was fitted to the data from a run of an individual inhibitor concentration between 140-190 seconds (50 seconds after membrane addition in order to avoid mixing effects) using GenStat. That provided an estimate for the slopes, e.g. the initial rates of the Mray reactions. The means of the slopes of the repetitions related to inhibitor concentrations were then used to calculate % activity, the control lacking inhibitor taken as 100 % activity (Table 2-3).

Table 2-3 : Calculation of % activity versus inhibitor concentration

Pacidamycin 1,2 concentration (µg/ml)	Means of the slopes (FAU/sec)	Standard deviation	Activity (%)	Error related to activity (%)
0	0.243	0.009	100	3.70
0.0441	0.141	0.012	58.5	5.06
0.0882	0.132	0.017	54.2	6.99
0.1470	0.064	0.007	26.2	2.68
0.1764	0.073	0.009	30.3	3.91
0.2210	0.029	0.002	11.8	0.86
0.2940	0.024	0.003	10.0	1.19
8.8200	0.0055	0.0009	2.3	0.38

A further non-linear regression was used to fit the activity against concentration:

$$\% \text{ activity} = A * e^{-B * \text{concentration}}$$

Where:

A: 100% activity

B: constant related to the gradient (slope)

The calculation for 50 % activity with the standard error was estimated using a curve fitting program in GenStat (Figure 2-27).

$$\text{Concentration at 50 \% activity} = -\frac{\ln(0.5)}{B}$$

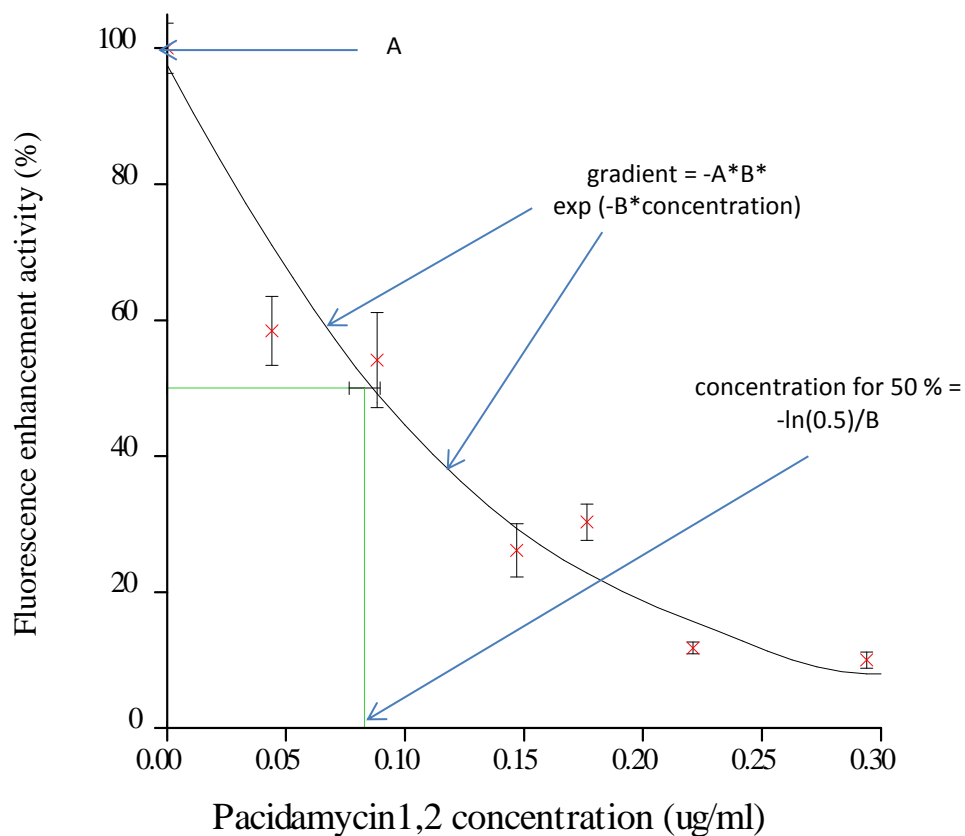


Figure 2-27: IC₅₀ for pacidamycin 1,2 inhibition of MraY

The calculation of the value for the IC₅₀ of the pacidamycin 1,2 sample resulted in 83 ± 7 ng/ml (8 % error).

The standard errors for the IC₅₀s calculated by the program were typically in the range of 5-15 %. The curve fitting program is the work of Dr. Julie Jones from the Quantitative Biology Centre (QuiBic) of the University of Warwick.

2.2.7 K_M determination for the dansyl-labelled UDPMurNAc-pentapeptide in the fluorescence MraY assay

The K_M parameter is known as the Michaelis constant for the enzyme, the concentration of the substrate at which half-maximal rate is observed. If the substrate bound tightly by the enzyme the K_M is small. On the other hand, a weakly bound substrate has a large K_M . K_M can be determined by measuring the rate of the enzymatic reaction at a range of different substrate concentrations²⁰⁷.

P. Brandish determined the K_M for the dansyl-labelled UDPMurNAc-pentapeptide for the *E. coli* MraY enzyme as 19 μM ¹⁴³. For both Gram-negative and Gram-positive MraYs, the reported values for K_M for the UDPMurNAc-pentapeptide vary from 5 to 30 μM ¹⁰. However, a K_M value of 1 mM was reported for a purified *B. subtilis* enzyme with a N-terminal (His)₆ fusion tag which was determined by a radiochemical transfer assay^{10, 133}. In order to investigate whether the K_M for the dansyl-labelled UDPMurNAc-pentapeptide with *P. aeruginosa* MraY enzyme (there is a C-terminal tag on the protein, see Section 2.1) is within the usual range, a series of assays were performed using various concentrations of the dansyl-labelled UDPMurNAc-pentapeptide between 0-180 μM (Section 7.12). It was not possible to increase further the concentration of the fluorescence substrate because it would have been out of the measurement range of the fluorimeter. The concentration of the heptaprenyl phosphate (20 $\mu\text{g/ml}$), the membranes and the buffer was kept constant over the experiments. The steady state approximation of the Michaelis Menten kinetics was assumed for the experiment.

In order to determine K_M the concentrations of the dansyl-labelled UDPMurNAc-pentapeptide [s], a non-linear regression was used to fit the initial rates (v) against concentration [s]:

$$v = A * e^{-B * [s]}$$

Where:

A : maximum rate (v_{\max})

B : constant related to the gradient (slope)

Figure 2-28 shows the graph in GenStat plotted with the help of a curve fitting program made by Dr. Julie Jones.

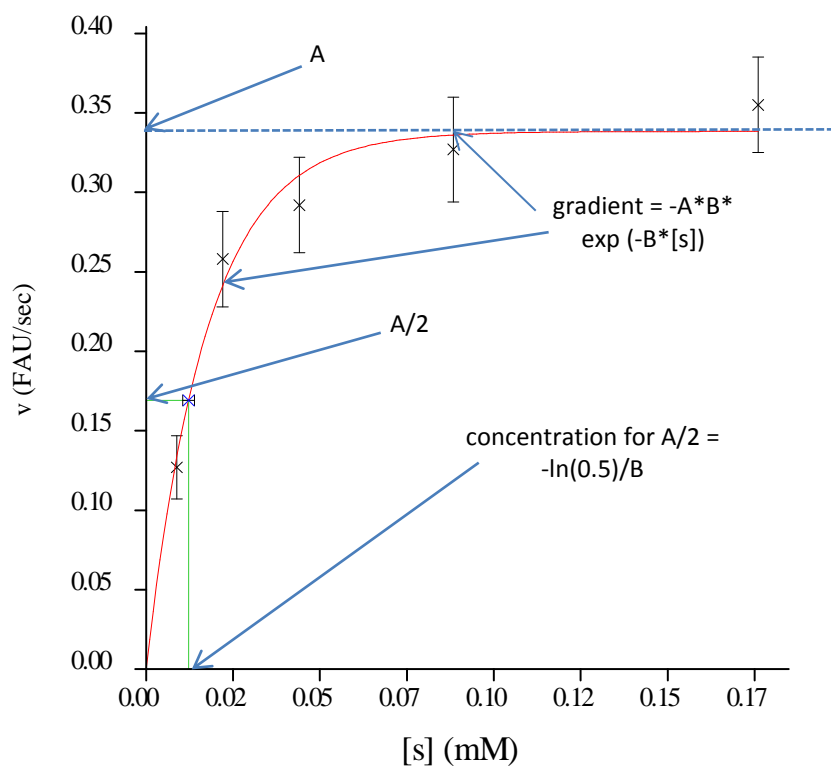


Figure 2-28: dansyl-labelled UDPMurNAc-pentapeptide concentrations [s] versus initial rates (v)

At higher concentrations, a maximum rate of the reaction is observed (v_{\max}), when the enzyme is fully saturated with the substrate. In this case the estimated maximum rate by the curve fitting program is 0.338 FAU/sec. Therefore half v_{\max} (A/2) is 0.169 FAU/sec.

The curve fitting program in GenStat calculated the concentration at A/2 with the standard error as:

$$[s] \text{ at } A/2 = -\frac{\ln(0.5)}{B}$$

The K_M , the concentration of the dansyl-labelled UDPMurNAc-pentapeptide at half maximum rate of the reaction with the standard error was estimated as $12.2 \pm 1.7 \mu\text{M}$ in GenStat.

For the Eadie-Hofstee graphical K_M determination method $v/[s]$ and v were calculated and a linear curve was fitted in Excel (Figure 2-29).

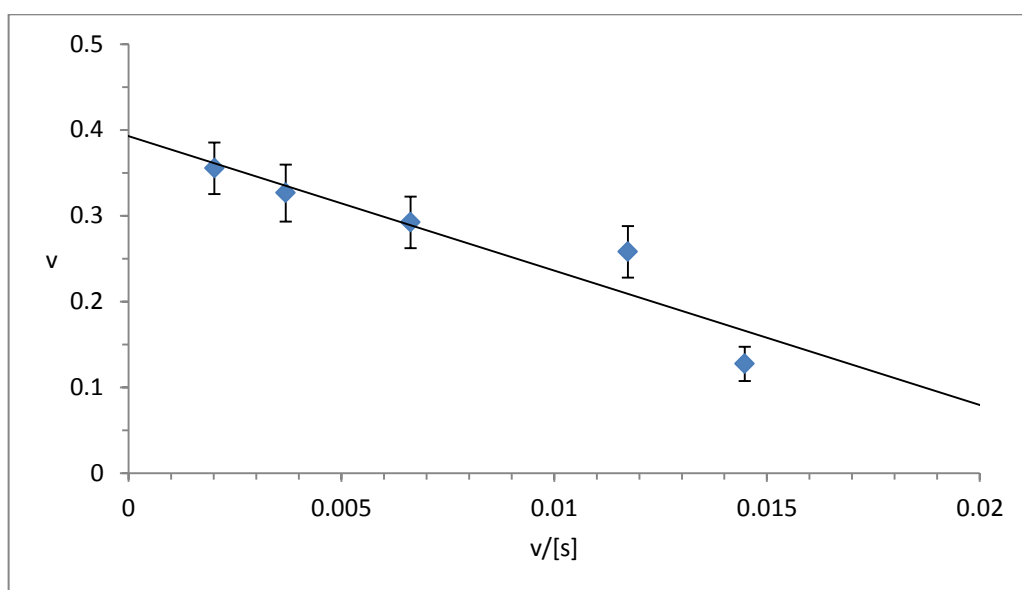


Figure 2-29: Eadie-Hofstee plot for K_M of the dansyl-labelled UDPMurNAc-pentapeptide in the *P. aeruginosa* MraY assay

The slope of this linear curve represents $-K_M$ for the dansyl-labelled UDPMurNAc-pentapeptide:

$$v = -15.7 * v/[s] + 0.39$$

The standard error on the slope of the fitted linear curve was determined in GenStat resulting in $15.7 \pm 3.5 \mu\text{M}$.

$1/v$ and $1/[s]$ were plotted for the Lineweaver-Burk plot (Figure 2-30):

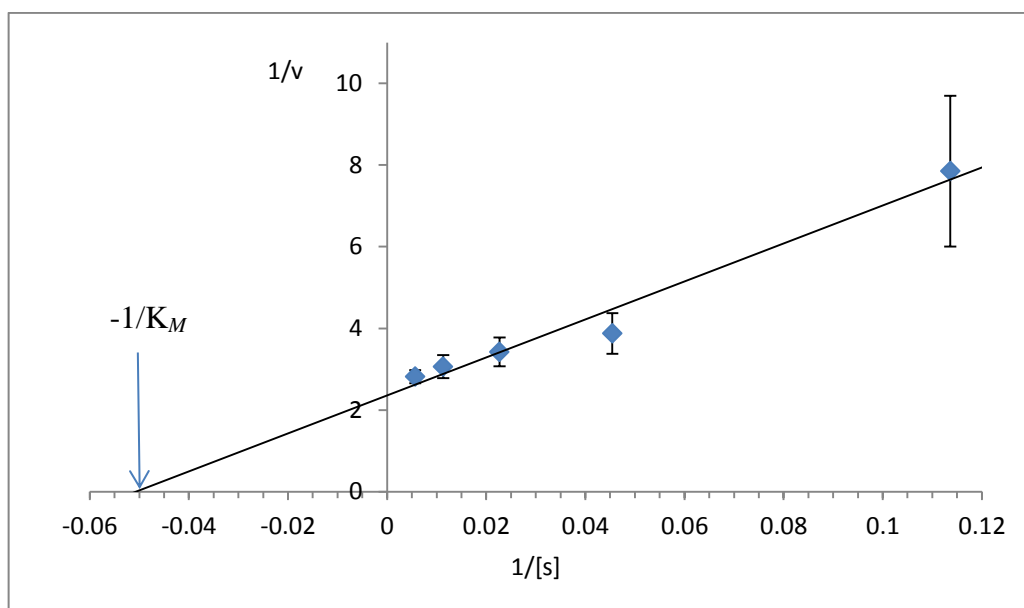


Figure 2-30: Lineweaver-Burk plot for K_M of the dansyl-labelled UDPMurNAc-pentapeptide for *P. aeruginosa* MraY

The intercept with the horizontal axis means $-1/K_M = -0.051$. Therefore, $K_M = 19.6 \pm 4 \mu\text{M}$. The error was calculated from the standard error of the gradient of the linear regression line.

Figure 2-31 shows the Hanes-Woolf graphical method, where $[s]/v$ is plotted versus $[s]$.

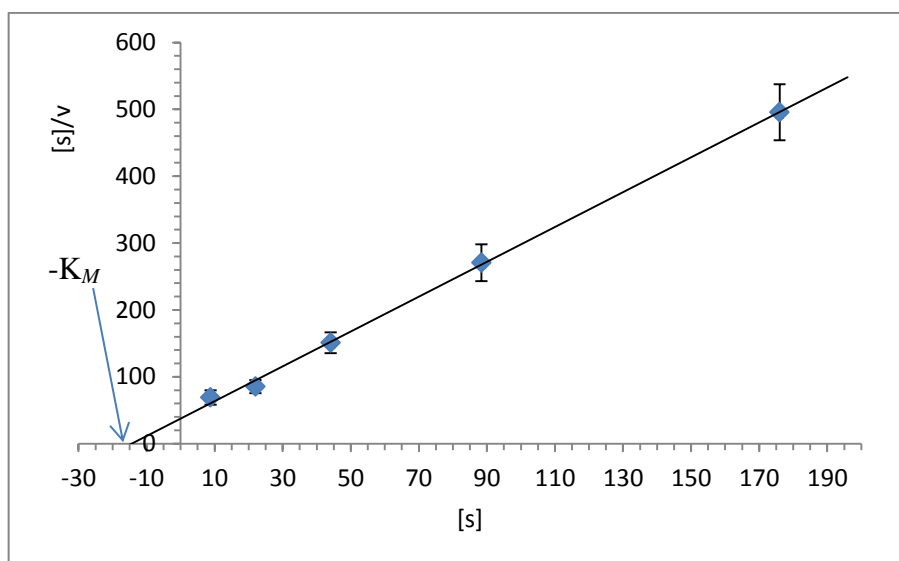


Figure 2-31: Hanes-Woolf method for the dansyl-labelled UDPMurNAc-pentapeptide K_M determination for *P. aeruginosa* MraY

For the Hanes-Woolf method, the intercept with the horizontal axis is $-K_M$. $K_M = 15.0 \pm 3 \mu\text{M}$. The error is based on the standard error of the linear curve. Table 2-4 shows the results from the graphical methods used for calculating K_M for the dansyl-labelled UDPMurNAc-pentapeptide.

Table 2-4: K_M determination for the dansyl-labelled UDPMurNAc-pentapeptide with *P. aeruginosa* MraY by graphical methods

Graphical method	K_M (μM)
v versus $[s]$	12.2 ± 1.7
Eddie-Hofstee	15.7 ± 3.5
Lineweaver-Burk	19.6 ± 4
Hanes-Woolf	15.0 ± 3

A. O'Reilly performed fluorescence assays in 2012 during her MOAC mini-project and measured K_M values for the *S. aureus* and *B. subtilis* MraYs of 20 and 15 μM respectively.

These results fit in the typical range for K_M values previously determined by researchers (5-30 μM). It shows that there is no significant difference in the kinetic behaviour of the four MraY enzymes (*E. coli*, *S. aureus*, *B. subtilis* and *P. aeruginosa*) with respect to their K_M for the dansyl-labelled UDPMurNAc-pentapeptide.

2.3 Attempted HPLC-based MraY assay

During the screening of the NCI Diversity Set (Chapter 3) with the fluorescence enhancement MraY assay, it became evident that many compounds interfere with fluorescence and an independent method was needed in order to test these compounds. Lipid I and II are very difficult to detect using HPLC because of their weak absorbance properties, but S. Sandhu developed an HPLC method where he was able to detect 2,4-dinitrophenyl-labelled (DNP-labelled) lipid II where he used Sanger's reagent (1-fluoro-2,4-dinitro-benzene) for labelling⁵⁹. We therefore attempted to develop an HPLC MraY assay to detect the formation of labelled lipid I derivatives by making a more UV active derivative.

2.3.1 Preparation of N-labelled UDPMurNAc-pentapeptides

We prepared N-labelled UDPMurNAc-pentapeptides at the third position amino acid with DNP, fluorescamine and dansyl labels in order to make UV active derivatives (structures are shown in Figure 2-32 and Figure 2-33). DNP- and fluorescamine-labelled pentapeptides were prepared in NaHCO_3 buffer at pH 9

and 50 % acetone as described in the experimental chapter (Sections 7.14 and 7.15), based on the method for the dansylation of the UDPMurNAc-pentapeptide. The acetone was evaporated and the samples were purified on a Sephadex G25 gel filtration column, eluting with water. The fractions with the absorbance maxima at ~250 nm (uridine) and 360 nm (DNP-label) were collected and lyophilised overnight to obtain the DNP-labelled UDPMurNAc-pentapeptide (Figure 2-32). In the case of the fluorescamine-labelled UDPMurNAc-pentapeptide fractions with absorbance maxima at 250 nm (uridine) and 390 nm were collected and lyophilised (Figure 2-33).

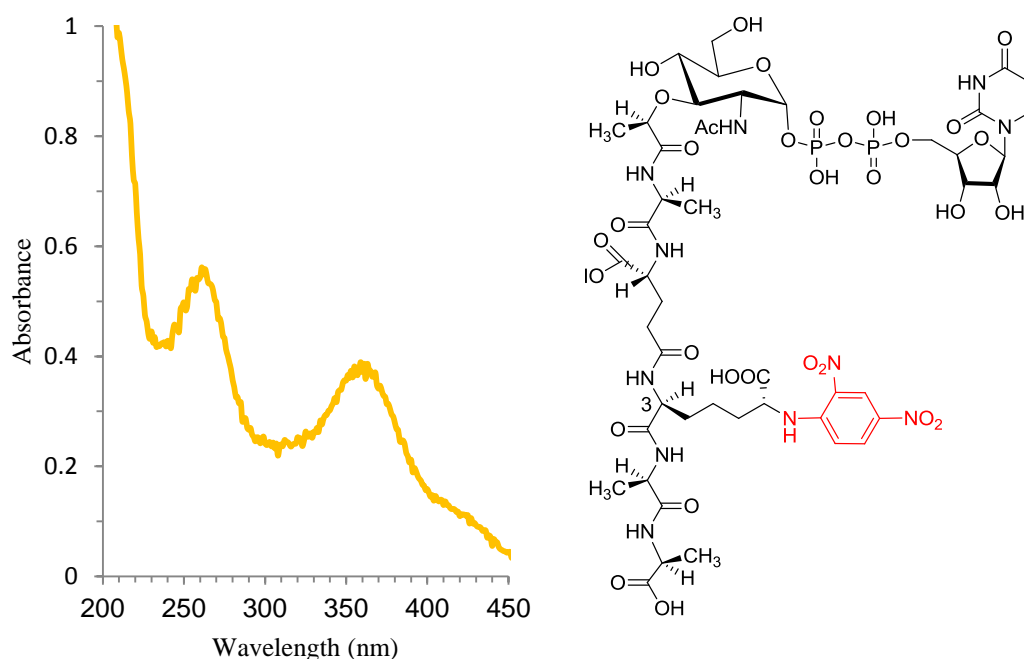


Figure 2-32: UV-Vis absorbance spectrum of the DNP-labelled UDPMurNAc-pentapeptide

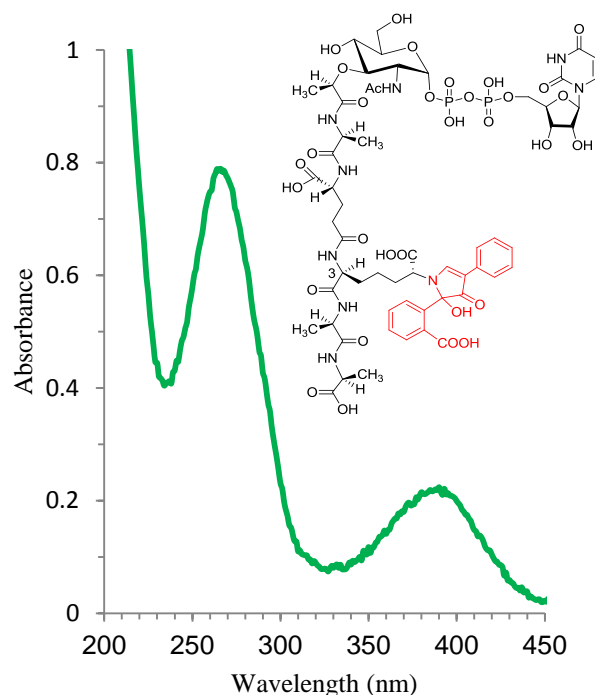


Figure 2-33: UV-Vis absorbance spectrum of the fluorescamine-labelled UDPMurNAc-pentapeptide

The compounds were analysed using HR LC-MS (see Section 7.6). For LC a linear gradient of methanol/water was used, with the percentage of methanol running up from 1 to 100 % starting at 5 minutes to 25 minutes at a flow rate of 0.2 ml/min. Evidence was found for the presence of the DNP-labelled UDPMurNAc-pentapeptide substrate (m/z $[M-H]^-$: 1358.3045 predicted 1358.3429). The sample also contained a trace of the pentapeptide with two DNP labels (m/z $[M-H]^-$: 1524.3011 predicted 1524.3443), three DNP labels (m/z $[M-H]^-$: 1690.2986 predicted 1690.3458) and a fragment lacking UDP that possibly formed during analysis (m/z $[M-H]^-$: 972.3213 predicted 972.3512 in Figure 2-34), all of these compounds eluted with the same retention time (1.2-1.3 minutes).

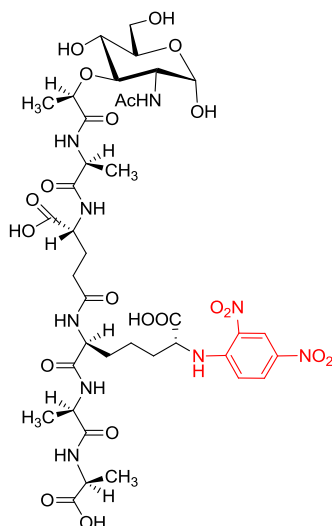


Figure 2-34: Possible DNP-labelled UDPMurNAc-pentapeptide fragment (m/z $[M-H]^-$: 972.3213 corresponding to predicted 972.3512)

The sample containing the DNP-labelled UDPMurNAc-pentapeptide was not purified further. The isotopic patterns for the DNP-labelled compounds are shown in Appendix 2, A 4 - A 7.

The fluorescamine-labelled UDPMurNAc-pentapeptide was detected at 2.4 minutes (m/z $[M-2H]^{2-}$: 734.6912 predicted 734.6924). The isotopic pattern for the fluorescamine labelled UDPMurNAc-pentapeptide is shown in Figure A 8 in Appendix 2. There was no sign of any remaining unlabelled UDPMurNAc-pentapeptide in either of the samples (m/z $[M-2H]^{2-}$ predicted: 595.6634).

2.3.2 HPLC assay methods

The *MraY* reaction containing 300 $\mu\text{g/ml}$ UDPMurNAc-pentapeptide or one of the N-labelled pentapeptides, 20 $\mu\text{g/ml}$ heptaprenyl phosphate in Tris buffer at pH 7.5 was started with the addition of 200 μg protein containing *MraY* membranes in 200 μl total volumes. The mixture was incubated at 37 $^{\circ}\text{C}$ for 30 minutes. Then 200 μl 6 M pyridinium acetate at pH 4.2 was added in order to

acidify and stop the reaction (see Section 7.16). The formed lipid products were then extracted into 400 μ l 1-butanol. LC-MS analysis was performed using a C18 reverse-phase HPLC column (4.6 x 150 mm) with 0.1 % ammonium water/methanol gradient at 0.8 ml/min, coupled with the Bruker HCT Ultra Mass Spectrometer. The conditions are written in Section 7.7.

Table 2-5 shows the masses for the various lipid I products and their specific absorbance wavelengths.

Table 2-5: Lipid I derivatives of the MraY reaction

UDPMurNAc-pentapeptide	LC-MS C₃₅ lipid I <i>m/z</i> [M-H]⁻	Characteristic wavelengths (nm)	Retention time (min) based on EIC
unlabelled	1442.71	-	18.5
dansyl-labelled	1675.76	330	19
fluorescamine-labelled	1702.76 (-H ₂ O) 1720.77	390	17
DNP-labelled	1608.71	360	18

We already saw the evidence for the dansyl-labelled lipid I (C₃₅ and C₅₅) formation during the MraY reaction by HR LC-MS in Section 2.2.3.6. Further evidence was found by LC-MS which revealed that it is possible to produce the fluorescamine- and the DNP-labelled derivatives of lipid I with MraY (see Appendix 2). The lipid I derivatives also formed with MraYs from *P. aeruginosa*, *S. aureus* and *B. subtilis*, however they were expressed in *E. coli* membranes, therefore the lipid I derivatives could have been produced by the catalytic activity

of the background *E. coli* MraY. The lipid I derivatives formed with *M. flavus* membranes as well.

The DNP-labelled lipid I (C₃₅) typically eluted at 18 minutes from the C18 column (for the correct isotopic pattern see Figure A 9 and for the chemical structure see Figure A 10 in Appendix 2). However, surprisingly, no peak was observed by absorbance at 360 nm or any other wavelength on the HPLC chromatograms for the chemical composition of the DNP-labelled lipid I in Figure 2-35.

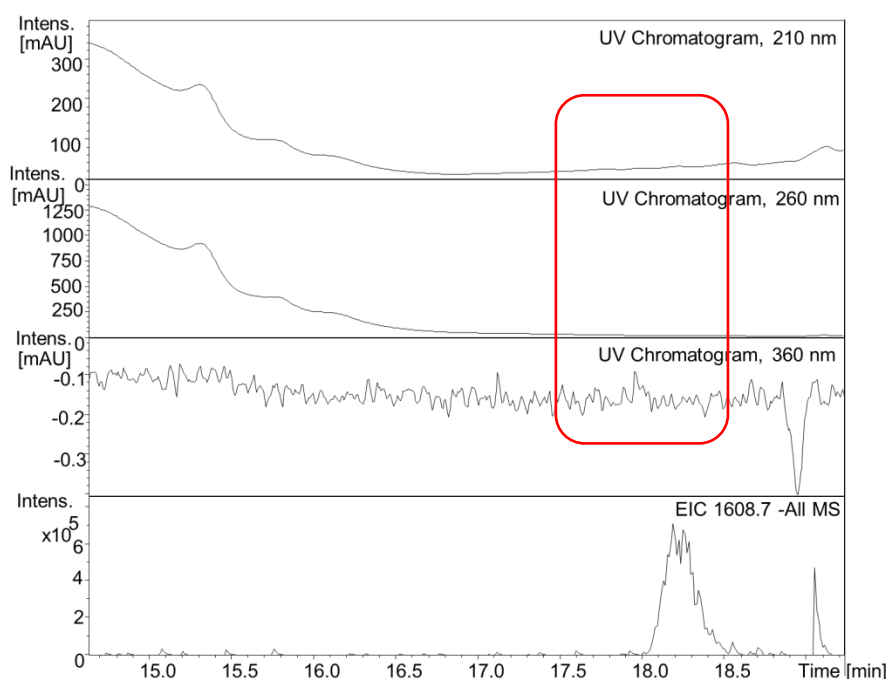


Figure 2-35: No peak detected for the DNP-labelled C₃₅ lipid I at 210, 260 and 360 nm, EIC: 1608.7

The doubly and negatively charged fluorescamine-labelled lipid I formed by *E. coli* MraY was detected by LC-MS and the correct isotopic pattern was confirmed by HR LC-MS (Appendix 2, Figures A 11 and A 12 for the isotopic pattern and A 13 for the chemical structure). Only a small peak was observed at

390 and 210 nm that could be associated with the fluorescamine-labelled lipid I eluting at 17 minutes, and no peak was observed at 260 nm (Figure 2-36).

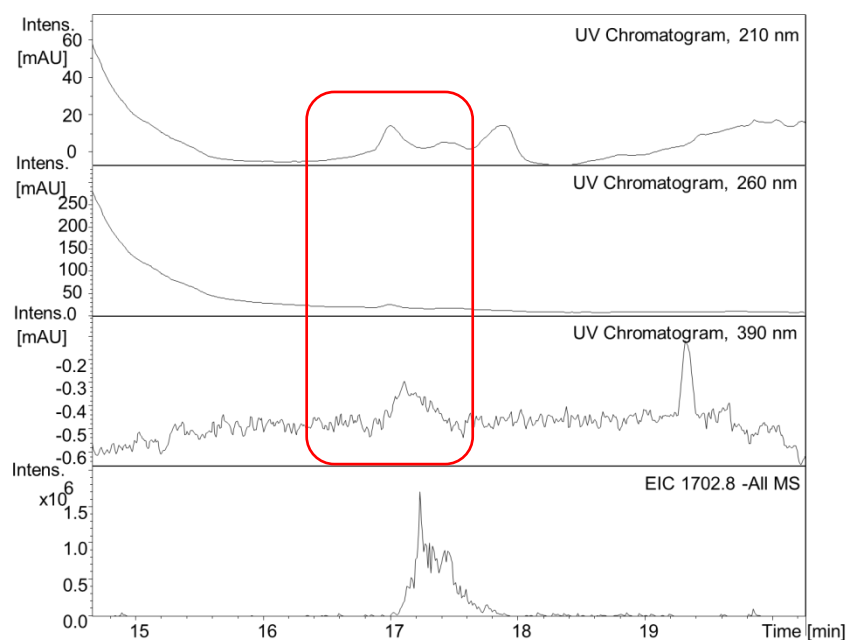


Figure 2-36: Absorbance at 210, 260 and 390 nm for the fluorescamine-labelled lipid I (C35)-H₂O EIC: 1702.8

The dansyl-labelled lipid I (Figure 2-37) that formed with endogenous undecaprenyl phosphate (m/z [M-H]⁻: 1948.01, Figure A 14 in Appendix 2), typically eluted from the column 2-3 minutes later than the C₃₅ analogue (Figure A 15 in Appendix 2).

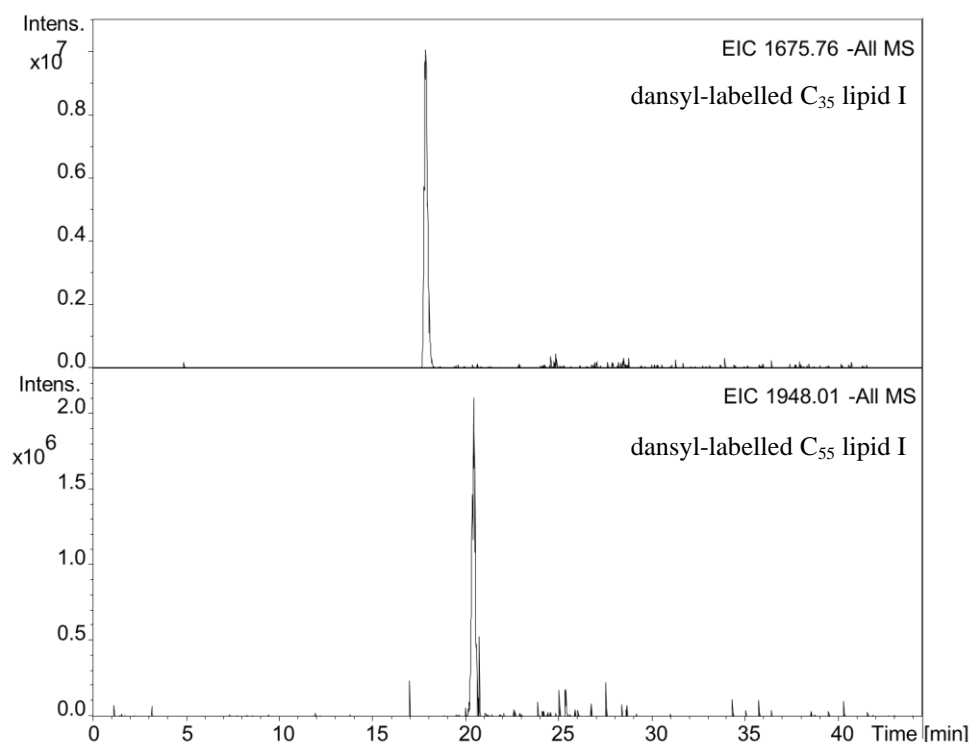


Figure 2-37: Extracted ion chromatograms of the dansyl-labelled lipid Is, the C₅₅ analogue eluting from the C18 column 2-3 minutes later than the C₃₅ analogue formed by overexpressed *S. aureus* MraY membranes (*E. coli*)

Interestingly, in the sample with the unlabelled UDPMurNAc-pentapeptide, not only the predicted mass for the chemical composition of C₃₅ lipid I (m/z [M-H]⁻: 1442.71, Figure A 16 in Appendix 2) was observed but we saw evidence for formation of C₃₅ lipid II (m/z [M-H]⁻: 1645.79, Figure A 17 in Appendix 2), even though no UDPGlcNAc was added to the reaction. Lipid I and II eluted with the same retention time (18.5 minutes). The membranes could contain MurG (extrinsic membrane protein), but the source of UDPGlcNAc for lipid II formation is not clear. Figure 2-38 shows the example of lipid I and II with *M. flavus* membranes.

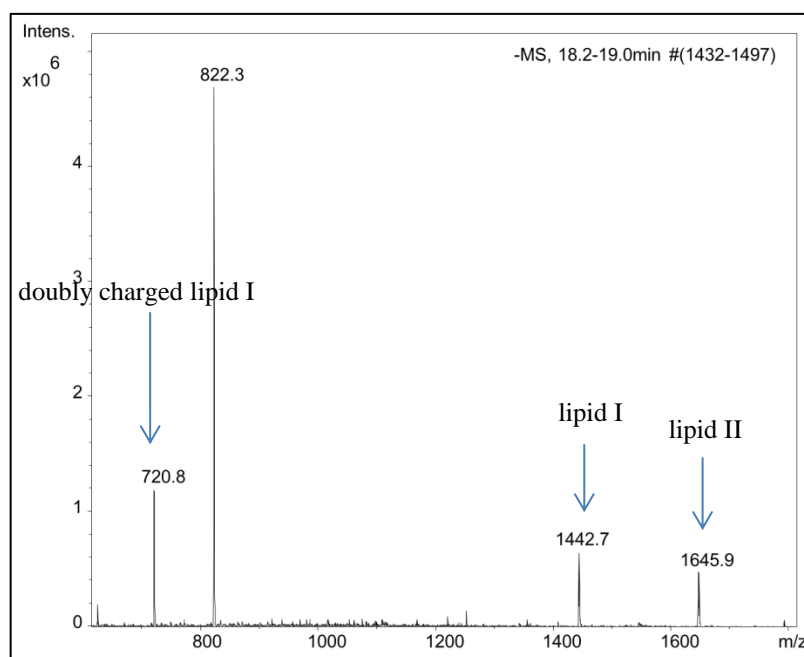


Figure 2-38: Lipid I and lipid II (C₃₅) with *M. flavus* membranes

Sodium adducts were often observed in the samples (Figure 2-39).

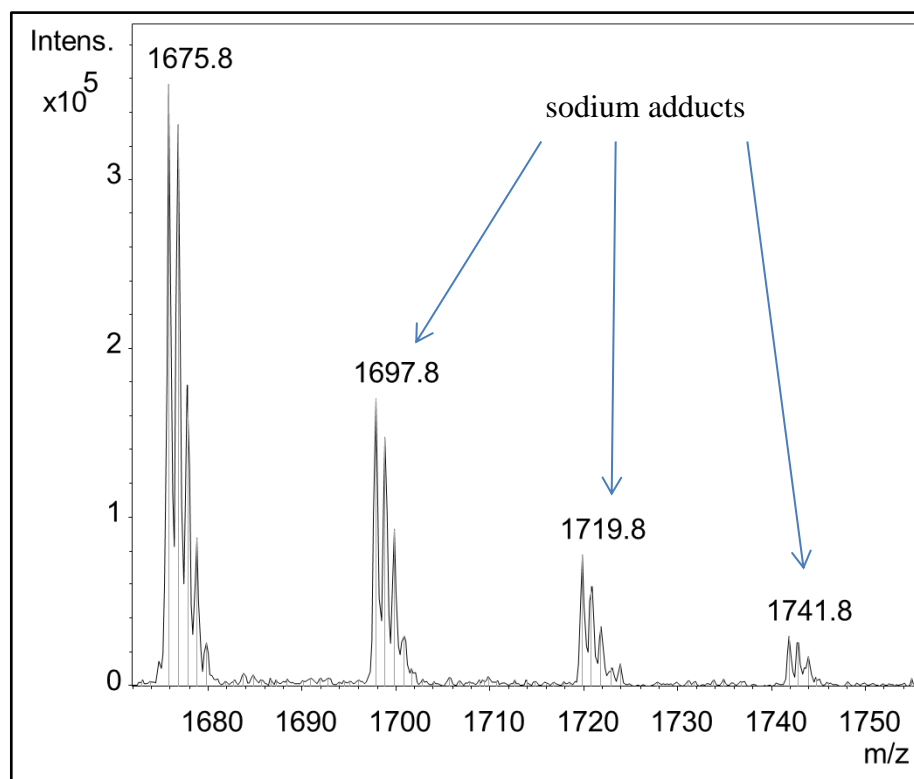


Figure 2-39: An example for sodium adducts, C₃₅ lipid I formed with *E. coli* MraY

In order to be able to develop an HPLC assay, an HPLC peak associated with the expected masses for lipid I products should have been seen with satisfactory intensity, preferably at selective wavelengths. The peak with the highest intensity was observed for the dansyl C₃₅ lipid I at 210 nm. However, only very low intensity peaks were observed, which were too small to be used for assays (Figure 2-40).

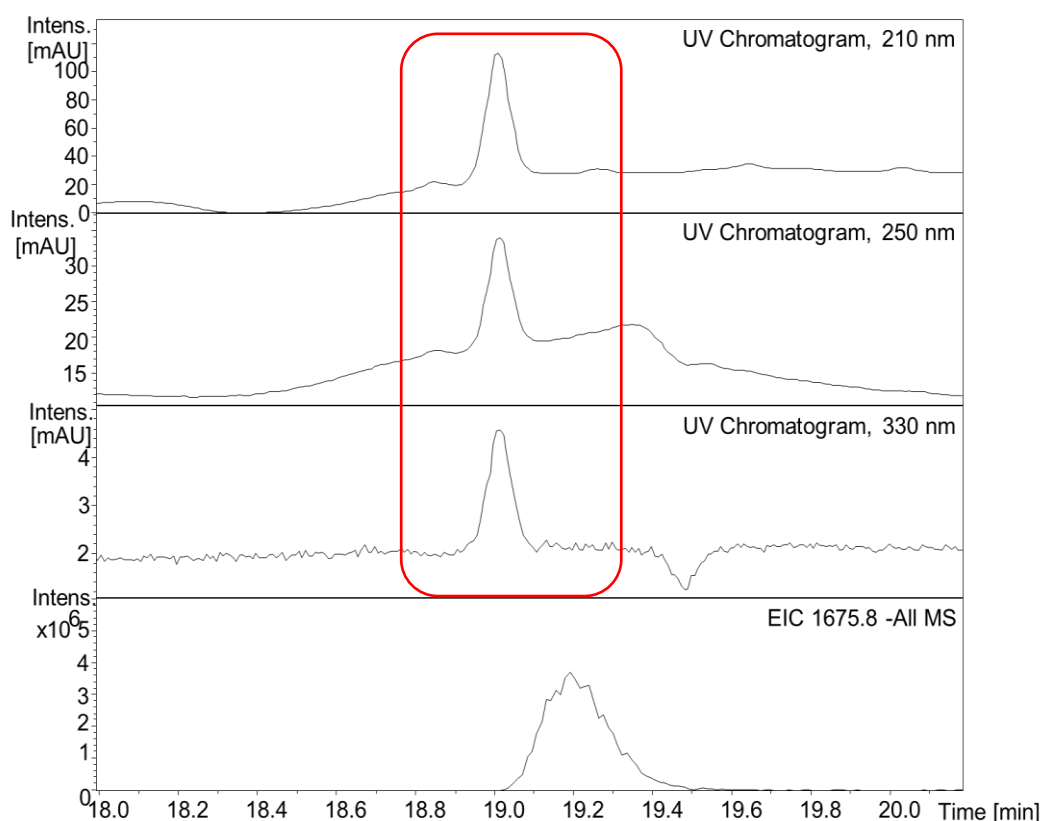


Figure 2-40: Absorbance at 210, 250 and 330 nm of the dansyl-labelled lipid I (C₃₅), EIC: 1675.8

The LC-MS analysis showed that the DNP- and the fluorescamine-labelled UDPMurNAc-pentapeptides are all accepted substrates for the MraY enzyme just like the dansyl-labelled UDPMurNAc-pentapeptide. However, it is not possible to quantify the production of these compounds using mass spectrometry. In the control samples that lacked UDPMurNAc-pentapeptide and the N-labelled

derivatives, there was no sign of the presence of any of the lipid I derivatives (Table 2-5) or lipid II. The controls are shown in Figure A 18 in Appendix 2.

The HPLC detection of the lipid products did not seem to be reproducible and sensitive enough to be used for an MraY assay under the above mentioned conditions. Increasing the concentrations of the substrates in the samples could improve HPLC detection; however it did not seem to be practical. We decided to develop a radiochemical MraY assay which was shown to be a more sensitive assay^{13, 130}. It is not clear why the UV absorbance of lipid I derivatives were so small; perhaps the lipid environment reduced the extinction coefficient for UV/Vis spectroscopy.

2.4 Development of the radiochemical MraY assay

The radiochemical MraY assay follows the incorporation of ^{14}C radiolabel from UDPMurNAc-pentapeptide into the butanol-extractable product, lipid I which is then measured by liquid scintillation counting. The first step is a radiochemical synthesis of the [^{14}C]-UDPMurNAc-pentapeptide¹³.

2.4.1 Radiochemical synthesis of [^{14}C]-UDPMurNAc-pentapeptide

The synthesis of the radiolabelled substrate uses UDPMurNAc-tripeptide and ^{14}C -L-alanine. The reaction needs to be catalysed by three enzymes, alanine racemase, DdlB and MurF (Figure 2-41). Alanine racemase requires pyridoxal phosphate whereas DdlB and MurF are ATP dependant ligases. The procedure is based on a method used by P. Brandish at Smith Kline Beecham Pharmaceuticals in 1991,

and the method of Tanaka, where an *E. coli* extract contained the three enzymes¹³,

201

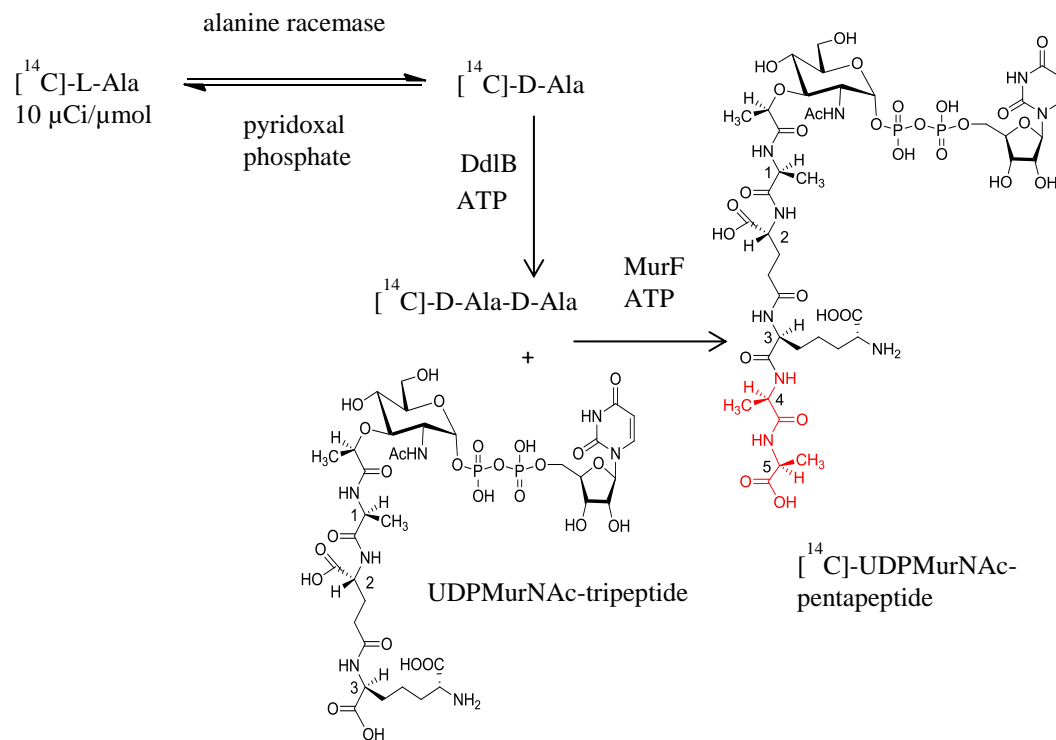


Figure 2-41: Steps of the radiochemical synthesis of the $[^{14}\text{C}]$ -UDPMurNAc-pentapeptide, the product is ^{14}C -labelled at the D-Ala residues at position 4 and 5 (in red)

The enzymatic synthesis was first optimised by a non-radiolabelled version. The method described by P. Brandish used a 1 eq. to 2 eq. ratio of UDPMurNAc-tripeptide to ^{14}C -L-alanine and an *E. coli* extract (see Section 7.17). This procedure was attempted using unlabelled substrates but did not seem to result in a satisfactory conversion because the presence of the UDPMurNAc tripeptide was also detected in the sample by LC-MS (m/z $[\text{M}-\text{H}]^-$: 1050.2, predicted: 1050.26 see Figure 2-42). The correct isotopic patterns for the two compounds are shown in Appendix 3, Figures A 19 and A 20.

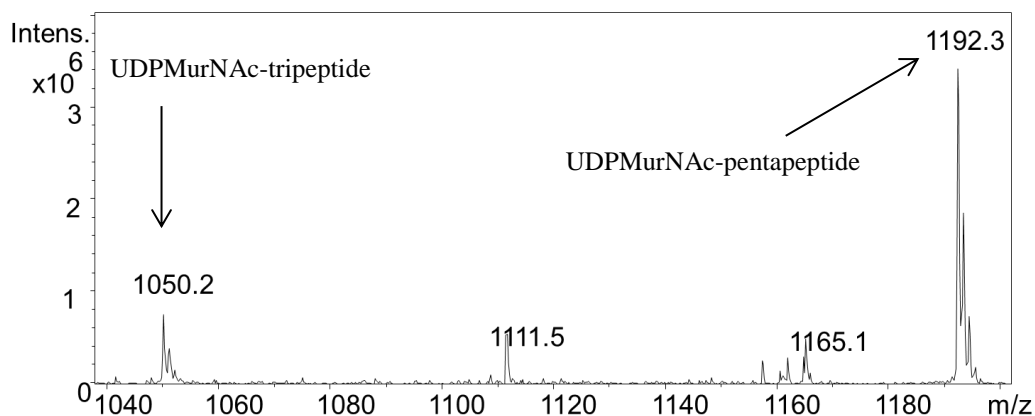


Figure 2-42: UDPMurNAc tripeptide and pentapeptide by LC-MS at 2 minute retention time

Therefore, the ratio of UDPMurNAc tripeptide and L-alanine was changed to 1:3 in order to use the L-alanine in excess and help the conversion. In addition, the *E. coli* extract was replaced by the three purified enzymes, *E. coli* alanine racemase and DdlB and *P. aeruginosa* MurF. The enzymes were a gift from Dr. David Roper.

The enzymatic synthesis consists of a single overnight incubation at 37 °C of 1 μ mol UDP-MurNAc tripeptide with 3 μ mol L-alanine, 20 μ l alanine racemase (9.7 mg/ml), 20 μ l DdlB (3.5 mg/ml), 10 μ l MurF (24 mg/ml), 100 μ l ATP (200 mM) and 50 μ l pyridoxal phosphate (8 mM) in 250 mM Tris pH 8.4 (total volume: 450 μ l). The enzymes were removed by ultrafiltration with a Centricon membrane (cut off 10,000 Da). The filtrate was purified by gel filtration (Sephadex G25) where the high molecular weight fractions showing absorbance maxima at 210 nm and 260 nm were collected and lyophilised overnight. HR LC-MS showed m/z $[M-H]^-$: 1192.3359 for the negatively and singly charged UDPMurNAc-pentapeptide see Appendix 3 Figure A 21. The presence of the UDPMurNAc-tripeptide was not detected in the sample.

The radiochemical synthesis was carried out under the same conditions using 10 $\mu\text{Ci}/\mu\text{mol}$ [^{14}C]-L-Ala. After gel filtration the high molecular weight fractions with absorbance maxima at 210 nm and 260 nm were collected and counted by a liquid scintillation counter. The two fractions with higher radioactivity (24,575 and 9,575 dpm/10 μl) were collected to be used as a substrate for the radiochemical MraY assays. The obtained [^{14}C]-UDPMurNAc-pentapeptide is labelled at the D-Ala residues at position 4 and 5. The procedure is described in detail in Section 7.18. The radiolabelled product gave a peak for the negatively doubly charged ion of the UDPMurNAc-pentapeptide (m/z $[\text{M}-2\text{H}]^{2-}$: 595.70 predicted 595.66) by electrospray mass spectrometry. The MS analysis of the radiolabelled UDPMurNAc-pentapeptide was performed by Susan Slade at the Life Sciences Department of the University of Warwick (Appendix 3, Figure A 22).

2.4.2 Radiochemical MraY assay development

The specific activity of the radiochemical and the fluorescence MraY assays was calculated by P. Brandish with 1.28 $\text{nmol min}^{-1} \text{mg}^{-1}$ and 2.66 $\text{FAU min}^{-1} \text{mg}^{-1}$ respectively. It was concluded that the sensitivity of the two assays were within the same range and both assays could detect the same concentrations of enzyme activity¹³.

2.4.2.1 General procedure for the radiochemical MraY assays

The radiochemical MraY assay follows the transfer of phospho-MurNAc-L-Ala- γ -D-Glu-*m*-Dap-[^{14}C]-D-Ala-[^{14}C]-D-Ala from UDPMurNAc-L-Ala- γ -D-Glu-*m*-Dap-[^{14}C]-D-Ala-[^{14}C]-D-Ala to undecaprenyl or heptaprenyl phosphate catalysed by MraY to form [^{14}C]-lipid I (Figure 2-43).

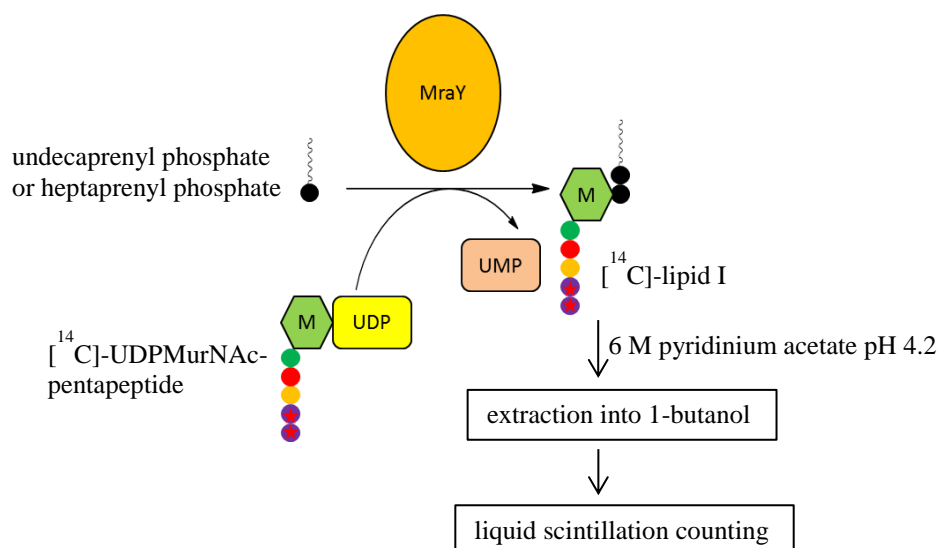


Figure 2-43: Schematic representation of the radiochemical MraY assay

100 μ l total volume contained 1-4 nCi/sample of UDPMurNAc-L-Ala- γ -D-Glu-*m*-Dap-[¹⁴C]-D-Ala-[¹⁴C]-D-Ala, 23.3 μ g/ml undecaprenyl phosphate or heptaprenyl phosphate, 90 mM Tris pH 7.5, 23 mM MgCl₂, 4.0 % (vol/vol) glycerol, 2.3 % (vol/vol) DMSO, 0.1 % Triton X-100 to which was added 20-50 μ g *E. coli* (C43) membranes containing overexpressed MraY or *M. flavus* membranes. Mixtures were incubated for 30 minutes at 35 °C. Reactions were stopped by the addition of 100 μ l 6 M pyridinium acetate at pH 4.2. Lipid products were extracted into 200 μ l 1-butanol and quantified by liquid scintillation counting (see Section 7.19).

2.4.2.2 MraY activity and inhibition in the wild type *E. coli* membranes

Figure 2-44 shows an example for the radiochemical MraY assay where inhibition with known inhibitors such as tunicamycin (125 μ g/ml), E peptide (100 μ g/ml), pacidamycin D (3 μ g/ml) and a capuramycin analogue, A-503083 B (1.2 μ g/ml) can be observed.

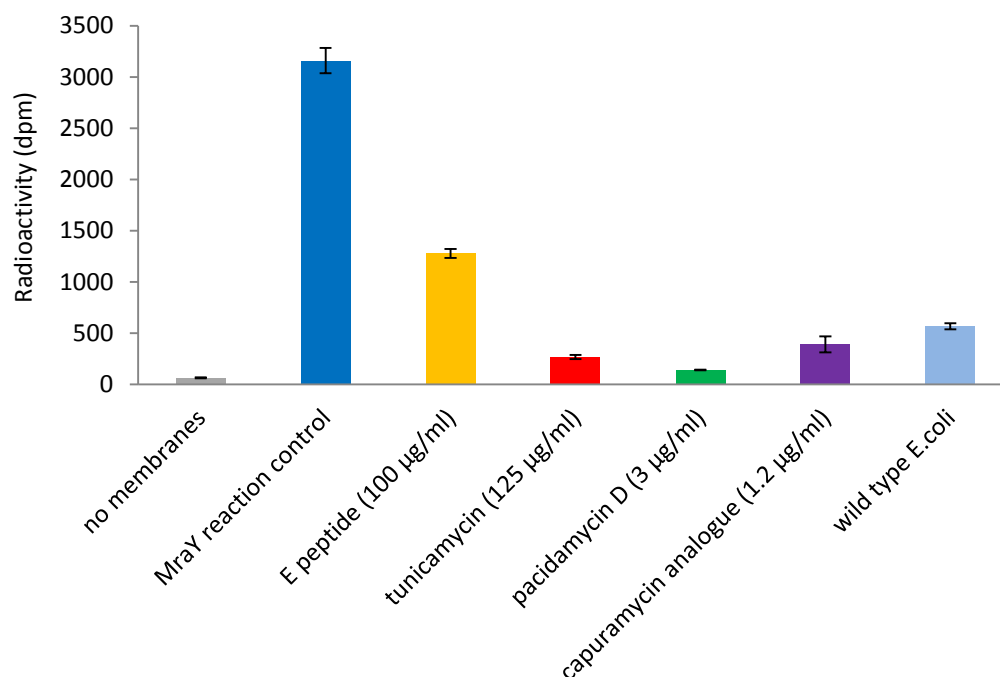


Figure 2-44: Inhibition of MraY and activity in the wild type *E. coli* membranes with the radiochemical MraY assay

The total volume of 100 µl sample contained 1.7 µM ^{14}C -labelled UDPMurNAc-pentapeptide (3.38 nCi, 7,500 dpm), 27 µg/ml heptaprenyl phosphate and 40 µg protein containing overexpressed *E. coli* C43 membranes in 90 mM Tris pH 7.5, 23 mM MgCl_2 , 4.0 % (vol/vol) glycerol, 2.3 % (vol/vol) DMSO, 0.1 % Triton X-100. The radioactivity was counted (dpm) after 30 minutes reaction time in a volume of 200 µl from the butanol layer. The volume of the whole butanol layer was normally ~250 µl. The measured radioactivity in the samples should always be corrected with the measured radioactivity from the sample lacking the MraY enzyme “no membranes“, before the product is quantified or % activity is calculated because we have to exclude the radioactivity from the measurement originating from the amount of ^{14}C -labelled UDPMurNAc-pentapeptide that

extracted into butanol. The sample that lacked membranes (“no membranes”) had slightly higher radioactivity (63 dpm) than the background (45 dpm) where 200 µl butanol was pipetted into scintillation liquid and counted. This value for background radioactivity (63 dpm) was used for the corrections.

From 7,500 dpm total radioactivity in one sample, 3,159 dpm was counted in 200 µl butanol for the control *MraY* reaction without inhibitor. This number was corrected with the background (63 dpm) and the radioactivity was calculated to 250 µl organic phase:

$$(3159-63) \text{ dpm} \times 1.25 = 3870 \text{ dpm.}$$

The conversion was around 52 %, 1.74 nCi containing lipid product got extracted into 250 µl butanol phase. (Conversions into the butanol phase were typically observed in the range of 50-75 %.) Since the specific activity of the L-alanine is 10 µCi/µmol, and two molar eq. D-alanine are incorporated into one molar eq. ¹⁴C-labelled lipid I product, the yield was calculated as:

$$1.74 \times 10^{-3} \text{ µCi} / (2 \times 10 \text{ µCi/µmol}) = 8.7 \times 10^{-5} \text{ µmol } ^{14}\text{C-labelled lipid I product.}$$

The lipid I product contains a mixture of C₃₅-lipid I from the added heptaprenyl phosphate and C₅₅-lipid I from the endogenous undecaprenyl phosphate (both ¹⁴C-labelled and unlabelled).

Table 2-6 shows the calculated % inhibition for the known inhibitors of *MraY*, the negative control (no inhibitor) taken as 100 % activity (or 0 % inhibition). E peptide showed 61 %, tunicamycin 93 %, pacidamycin D 98 % and the capuramycin analogue 89 % inhibition against *MraY* in the radiochemical assay.

Table 2-6: % inhibition of known inhibitors against MraY by the radiochemical assay

	E peptide (100 µg/ml)	tunicamycin (100 µg/ml)	pacidamycin D (3 µg/ml)	Capuramycin analogue: A-503083 B (1.2 µg/ml)
% inhibition	60.8 ± 2	93.4 ± 8	97.5 ± 2	89.4 ± 5

The wild type *E. coli* showed 16.1 ± 2 % of the activity of the overexpressed *E. coli* MraY membranes, therefore the wild type *E. coli* generated 1.4×10^{-5} µmol ^{14}C -labelled and unlabelled lipid I product that was extracted into a volume of 250 µl butanol. Thus, the overexpression of *E. coli* MraY resulted in a 6 fold increase in lipid I production over 30 minutes.

2.4.2.3 Investigation of D, D-carboxypeptidase activity

D,D-carboxypeptidase activity from the membranes could release free [^{14}C]-D-Ala from the labelled substrate and interfere with the measurement. The following experiment aimed to investigate the presence of D,D-carboxypeptidase activity. Each sample contained 1,800 dpm in total, 27 µg/ml heptaprenyl phosphate and 40 µg protein containing overexpressed *E. coli* C43 membranes in 90 mM Tris pH 7.5, 23 mM MgCl_2 , 4.0 % (vol/vol) glycerol, 2.3 % (vol/vol) DMSO, 0.1 % Triton X-100. The first two columns in Figure 2-45 following the “no membranes” control contained 100 µg/ml ampicillin in order to stop D,D-carboxypeptidase activity. The third and the fourth columns did not contain ampicillin. Based on the nearly identical amount of radioactivity that got extracted into 1-butanol from the ampicillin treated and the control samples, it was concluded that there is no significant D,D-carboxypeptidase activity in the membranes that would interfere with the MraY assay.

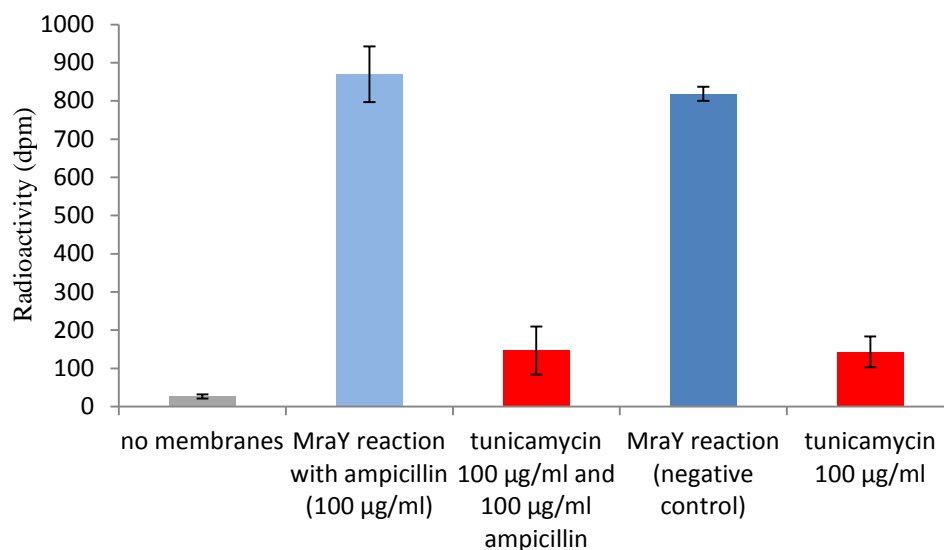


Figure 2-45: No significant D,D-carboxypeptidase activity in the membranes

2.4.2.4 Background activity from the endogenous undecaprenyl phosphate in *E. coli* C43 membranes

Another experiment was carried out to investigate the background activity of the endogenous undecaprenyl phosphate in *E. coli* C43 membranes (see Figure 2-46). 2.4 nCi (5,275 dpm) was the total radioactivity in each sample with no heptaprenyl phosphate in 90 mM Tris pH 7.5, 23 mM MgCl₂, 4.0 % (vol/vol) glycerol, 2.3 % (vol/vol) DMSO, 0.1 % Triton X-100 . The Mray reaction was started with the addition of 40 µg protein containing *E. coli* (C43) membranes.

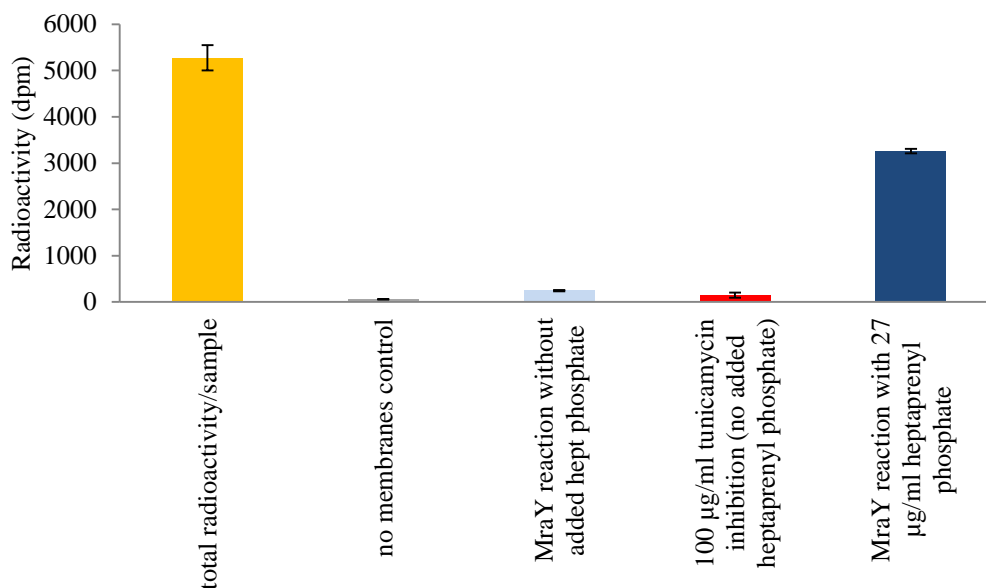


Figure 2-46: low background activity from endogenous undecaprenyl phosphate from *E. coli* C43 Mray membranes

Only 4.5 % conversion was achieved in the butanol extract [$189 \text{ (dpm)} \times 100 \times 1.25 / 5,275 \text{ (dpm)}$] meaning the low abundance of the endogenous undecaprenyl phosphate in the membranes. The control experiment containing 27 µg/ml heptaprenyl phosphate resulted in 75 % conversion. This means that for every 1 molar eq. C₅₅ lipid I, there was 15.7 molar eq. C₃₅ lipid I product in the butanol extracted sample.

2.4.2.5 The time-course of the Mray reaction by the radiochemical assay

In order to investigate the time-course of the Mray reaction, the reaction was stopped at 1, 5 10 and 15 minutes after the membrane addition. Lipid products were extracted each time into butanol as described in Section 2.4.2.1 and radioactivity was measured by liquid scintillation counting. The membranes were

diluted to a concentration where it was possible to see the time-course of the reaction.

100 μ l total volume contained 1.7 μ M 14 C-labelled UDPMurNAc-pentapeptide (3.4 nCi), 27 μ g/ml heptaprenyl phosphate and 40 μ g protein containing overexpressed *E. coli* (C43) membranes in 90 mM Tris pH 7.5, 23 mM MgCl₂, 4.0 % (vol/vol) glycerol, 2.3 % (vol/vol) DMSO, 0.1 % Triton X-100. The experiment was repeated with the addition of 40 μ g protein overexpressed *B. subtilis*, 35 μ g protein overexpressed *S. aureus*, 20 μ g protein overexpressed *P. aeruginosa* in *E. coli* (C43) membranes and 40 μ g *M. flavus* membranes.

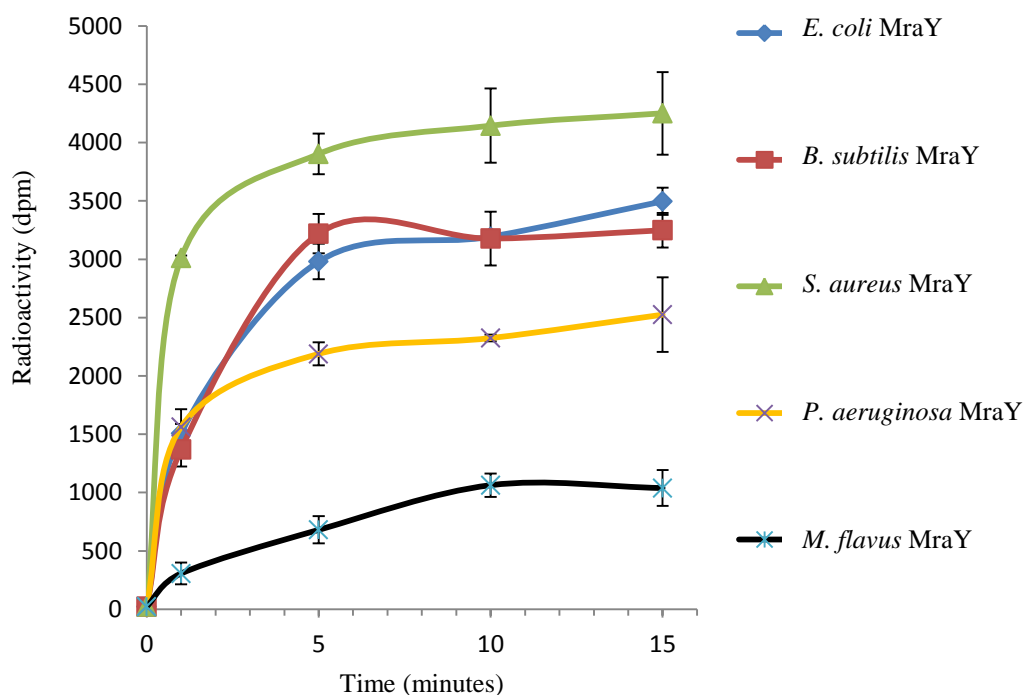


Figure 2-47: Time-course profile of the MraY reaction by the radiochemical assay, 40 μ g protein overexpressed *E. coli* and *B. subtilis*, 35 μ g protein overexpressed *S. aureus* and 20 μ g protein overexpressed *P. aeruginosa* in *E. coli* (C43) membranes and 40 μ g *M. flavus* membranes

After 10-15 minutes of the membrane addition the reactions seemed to reach equilibrium in the case of the five *MraY*s, (*E. coli*, *S. aureus*, *B. subtilis*, *P. aeruginosa* and *M. flavus*) and there was no significant increase in product formation after 5 minutes apart from the *M. flavus* *MraY*.

2.4.2.6 Overproduction of enzyme activity in the overexpressed *E. coli* *MraY* membranes and comparison with the wild type *M. flavus*

In order to investigate the overproduction of the radiolabelled lipid I product during the *MraY* reaction, we quantified the forming radiolabelled lipid product after 30 minutes reaction time using overexpressed *MraY* *E. coli* and *M. flavus* membranes. Lipid products were extracted each time into butanol as described in Section 2.4.2.1 and radioactivity of 200 μ l butanol was measured by liquid scintillation counting. 100 μ l total volume contained 1.7 μ M 14 C-labelled UDPMurNAc-pentapeptide (3.4 nCi), 27 μ g/ml heptaprenyl phosphate and 40 μ g protein containing overexpressed *E. coli* (C43) membranes in 90 mM Tris pH 7.5, 23 mM MgCl_2 , 4.0 % (vol/vol) glycerol, 2.3 % (vol/vol) DMSO, 0.1 % Triton X-100. The experiment was repeated with the addition of 40 μ g protein overexpressed *B. subtilis*, 35 μ g protein overexpressed *S. aureus*, 20 μ g protein overexpressed *P. aeruginosa* in *E. coli* (C43) membranes and 40 μ g *M. flavus* membranes (Table 2-7).

Table 2-7: Comparison of the level of radiolabelled lipid I production for 1 mg protein containing *E. coli* membranes overexpressed with *MraY* from *E. coli*, *S. aureus*, *B. subtilis* and *P. aeruginosa* with the wild type *E. coli* membranes and radiolabelled lipid I production for *M. flavus* membranes over 30 minutes reaction time by the radiochemical assay

over-expressed <i>MraY</i>	mg protein (total)	dpm in 200 μ l butanol	nCi in 200 μ l butanol	nmol lipid I product in 200 μ l butanol	nmol lipid I product/mg protein	over-production of lipid I
wild type <i>E. coli</i> C43	0.040	502	0.226	1.13×10^{-2}	0.282	-
<i>E. coli</i>	0.040	3096	1.39	6.85×10^{-2}	1.71	6 fold
<i>S. aureus</i>	0.035	3437	1.55	7.75×10^{-2}	2.21	8 fold
<i>B. subtilis</i>	0.040	3182	1.43	7.15×10^{-2}	1.79	6 fold
<i>P. aeruginosa</i>	0.020	2525	1.14	5.70×10^{-2}	2.85	10 fold
<i>M. flavus</i>	0.040	1088	0.490	2.45×10^{-2}	0.613	2 fold

Table 2-7 shows the amount of radioactivity measured in 200 μ l organic phase, and the converted number in nCi. Knowing the specific activity for the radiolabelled lipid I product (20 μ Ci/ μ mol), it was possible to calculate the yield in nmol for 200 μ l butanol. (The total yield would have to be multiplied with 1.25 for the total volume of 250 μ l butanol.) Then, the production of lipid I was calculated for 1 mg total protein. These calculations resulted in 6-10 fold overproduction of the radiolabelled lipid I by the overexpressed *MraY* membranes compared to the wild type *E. coli* membranes. The *M. flavus* membranes produced double the amount of lipid I than the wild type *E. coli*.

2.4.2.7 Determination of IC₅₀s by means of the radiochemical Mray assay for compounds that interfere with fluorescence

IC₅₀s were determined by the means of the radiochemical Mray assay for compounds that interfere with fluorescence (see Sections 3.3.1.1, 5.2, 5.3.2 and 5.4). Activity which is directly related to the amount of product, was plotted versus inhibitor concentrations, taking the measured radioactivity (dpm) (corrected with the background) of the control Mray reaction as 100 % activity. The same curve fitting program was used in GenStat to determine inhibitor concentrations at 50 % inhibition as for the continuous fluorescence assay in Section 2.2.6.

3 Screening of the Diversity Set of the National Cancer Institute

The Development Therapeutics Program at the U.S National Cancer Institute maintains a large screening collection of over 140,000 compounds that have been evaluated as potential anticancer and anti-HIV agents. Among these compounds there are synthetic compounds and natural products representing unique structural diversity. The National Cancer Institute also possesses a small library of around 2,000 compounds, ideal for beginning a screening process. Since many hospitalised cancer patients treated with anticancer agents develop life-threatening bacterial infections, the National Cancer Institute will send their diversity set to academic groups who can demonstrate a microtitre-based assay for an antibacterial target enzyme. Following a request from Professor T. D. H. Bugg, the NCI sent the diversity set of 1,717 compounds in 2012.

We were sent the diversity set III (20 plates) and the natural products set II (2 plates) as a starting package by A. Martinkosky from the NCI Chemotherapeutic Agents Repository. Plates were stored at -20 °C.

The diversity set III plates held 20 μ L of a 10 mM DMSO solution in 96 well polypropylene microtitre plates with 80 compounds per plate.

The natural products set II consist of 120 compounds which were selected from the open repository of 140,000 natural products of the National Cancer Institute. This set was created in order to help drug discovery research groups intending to study a variety of scaffold structures having multiple functional groups. These compounds were selected by purity (> 90 % by ELSD, major peak has correct

mass ion), structural diversity and availability. These natural products were also stored in 96 well polypropylene microtitre plates with 60 compounds per plate. Each well contained 0.2 μ moles compound and 1 μ l glycerol. By the addition of 19 μ l of DMSO we obtained a 10 mM solution in 20 μ l volume. The information about the diversity set was provided by A. Martinkosky.

Our aim was to test these compounds at 100 μ M concentrations against *E. coli* MraY by the fluorescence enhancement assay (Figure 2-2) in 96-well plates. We hoped to find potential MraY inhibitors by this rapid screening method which would have been tested further by the continuous fluorescence assay to study the reaction kinetics. We also planned to test promising MraY inhibitors with MraY enzymes from *P. aeruginosa*, *S. aureus*, *B. subtilis* and *M. flavus*.

3.1 Initial screening data for the diversity set of the National Cancer Institute

In our research group, the fluorescence enhancement MraY assay was first used in a 96-well microtitre format by S. Bagga in 2004¹⁴⁵.

The assays were carried out in a 100 μ l total volume, containing 85 μ l master mix (containing 11.2 μ M dansyl-labelled UDPMurNAc-pentapeptide, 17 μ g/ml heptaprenyl phosphate in a buffer 85 mM Tris, 21.25 mM $MgCl_2$), 5 μ l test compound solution at 100 μ M concentration and 10 μ l 40 μ g total protein containing *E. coli* MraY membranes. Note that the assay always contains 3.4 % glycerol and 0.1 % Triton X-100 from the buffer that the heptaprenyl phosphate solution was made. The presence of detergent is essential for the MraY assay. The 10 mM compound solutions from the diversity set were diluted to 2 mM in the

assay buffer (200 mM Tris at pH 7.5, 50 mM MgCl₂) and 5 µl of these solutions was added to the assay at 100 µM final concentration. 25 µg/ml tunicamycin was used as a positive control, the negative control (no inhibitor) contained 5 µl 20 % (v/v) DMSO and the control “no membranes” contained 10 µl “membrane buffer” (50 mM Tris pH 7.5, 2 mM β-mercaptoethanol, 1 mM MgCl₂) instead of the membranes. The samples for the test compounds were carried out in duplicates, the first and the last column was used for the controls (16 wells). The conditions of the screening are described in Section 7.20. The arrangement in a 96-well microtitre plate for testing 40 compounds from the diversity set is shown in Figure 3-1.

	1	2	3	4	5	6	7	8	9	10	11	12
A	No inhibitor	A2	A2	A3	A3	A4	A4	A5	A5	A6	A6	No membranes
B	No inhibitor	B2	B2	B3	B3	B4	B4	B5	B5	B6	B6	No membranes
C	No inhibitor	C2	C2	C3	C3	C4	C4	C5	C5	C6	C6	tunicamycin
D	No inhibitor	D2	D2	D3	D3	D4	D4	D5	D5	D6	D6	tunicamycin
E	tunicamycin	E2	E2	E3	E3	E4	E4	E5	E5	E6	E6	No inhibitor
F	tunicamycin	F2	F2	F3	F3	F4	F4	F5	F5	F6	F6	No inhibitor
G	tunicamycin	G2	G2	G3	G3	G4	G4	G5	G5	G6	G6	No inhibitor
H	tunicamycin	H2	H2	H3	H3	H4	H4	H5	H5	H6	H6	No inhibitor



Test compounds at 100 µM concentrations

Figure 3-1: Arrangements of the test compounds (wells A2-H6 from a diversity set plate) and controls (no inhibitor, 100 µg/ml tunicamycin and no membranes) in 96-well plate format

Before the reaction was started by the addition of 10 µl *E. coli* MraY membranes the plate was tested for high fluorescence compounds by a fluorescence

measurement with excitation at 340 nm and emission at 353 nm. These high fluorescence compounds make it impossible to monitor relatively small fluorescence changes during the MraY reaction due to the fact that the instrument calculates arbitrary fluorescence units based on relative fluorescence in the wells. Figure 3-2 shows an example of 40 compounds that were tested at the same time in 96-well plate format from the diversity set III, plate: 4737067/4737.

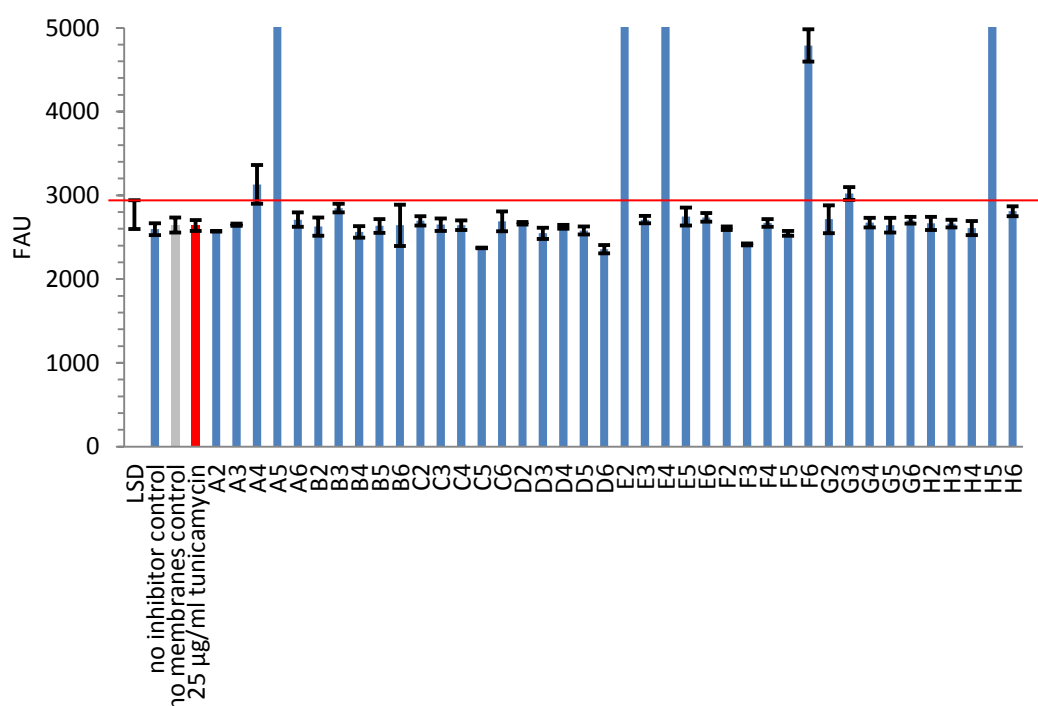


Figure 3-2: Eliminating compounds with high fluorescence from the wells before the MraY reaction, compounds A4 (3130 FAU), A5 (6,445 FAU), E2 (44,153), E4 (6,844), F6 (4,789 FAU), G3 (3,023) and H5 (13,007) with higher fluorescence had to be removed from the assay λ_{ex} : 340 nm, λ_{em} : 535 nm

By eliminating the compounds with obvious high fluorescence first (A5, E2, E4, F6 and H5) and repeating the measurement, we got to the conclusion that compounds A4 (3,130 FAU), A5 (6,445 FAU), E2 (44,153), E4 (6,844), F6 (4,789 FAU), G3 (3,023) and H5 (13,007) had significantly higher

fluorescence than the controls and had to be removed from the assay before we started the reaction.

Another way of establishing which compounds will interfere with our measurement is to do an analysis of variance for the set of samples and calculate the “Least Significant Difference” (LSD) between the highest and the lowest means. The LSD was calculated for this particular set of data in GenStat at 5 % level between the highest (44,153 FAU, measured for E2) and the lowest means (2358 FAU measured for D6) and gave a value of 344.4 FAU. Therefore every compound with higher fluorescence than the controls plus the LSD (2971 FAU) had to be eliminated from the experiment above red line in Figure 3-2, which lead to the removal of the very same compounds that we found by repeated measurements.

It is possible to measure the fluorescence at several time-points during the MraY reaction. We chose to measure the fluorescence every 5 minutes up to 20 minutes reaction time e.g. 0, 5, 10, 15 and 20 minutes after the addition of the membranes with excitation at 340 nm and emission at 350 nm. Figure 3-3 shows the time-course assay of 7 selected compounds and the controls from the diversity set III, plate: 4737067/47**37**.

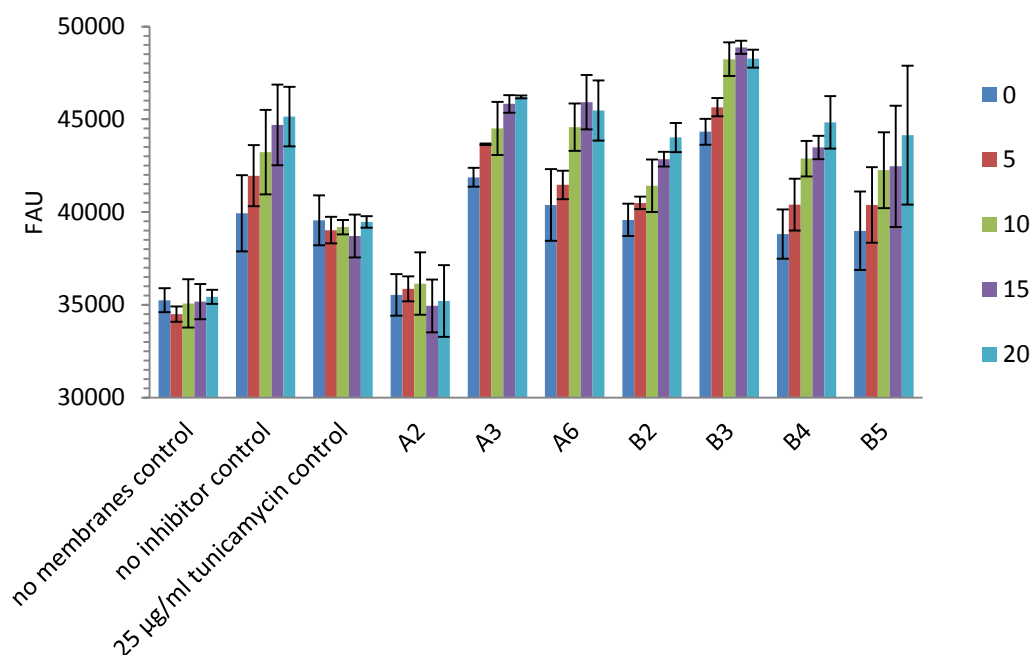


Figure 3-3: Time-course of the fluorescence MraY assay in microtitre plate format (0, 5, 10, 15 and 20 minutes)

After 30 minutes reaction time, we took a final measurement (λ_{ex} : 340 nm, λ_{em} : 535 nm) to screen compounds with lower fluorescence enhancement activity than 80 %. Figure 3-4 shows the measured fluorescence values and the compounds with less than 80 % fluorescence enhancement activity, which were chosen for further testing (under the red line).

The LSD was calculated for the final set of data (30 minutes) from the fluorescence microtitre plate assay in GenStat at 5 % level between the highest (45,176 FAU, measured for B2) and the lowest means (31,157 FAU, measured for the “no membranes” control) and gave a value of 2054.1 FAU. These calculations were in agreement with the limit that we set for 80 % for this set of data.

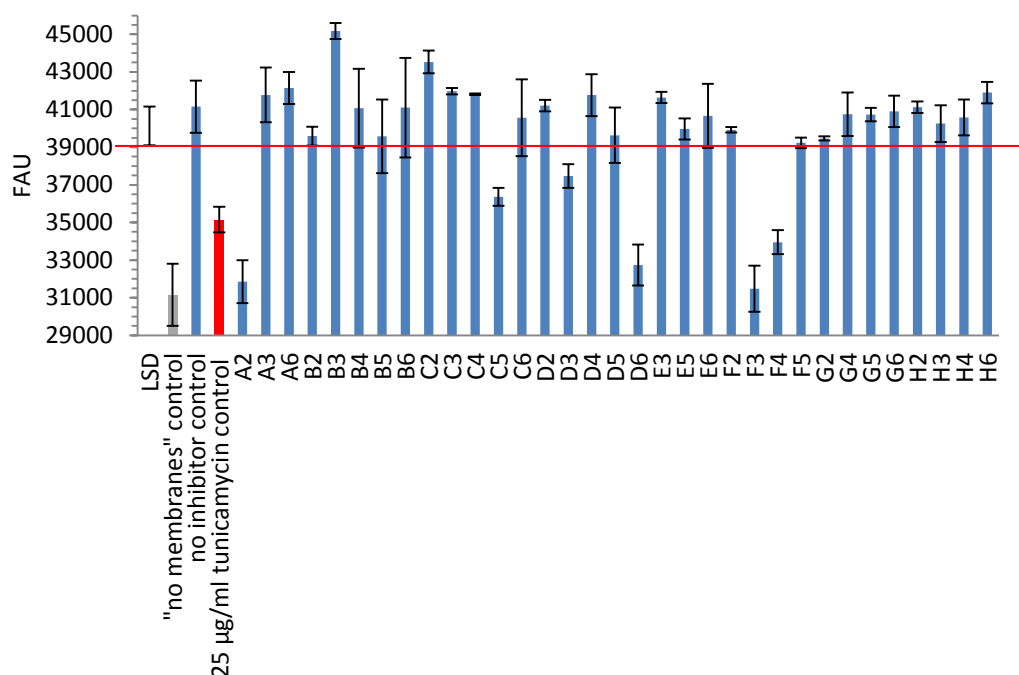


Figure 3-4: Screening compounds with lower fluorescence enhancement activity than 80 %

Compounds A2, C5, D3, D6, F3 and F4 from the diversity set III, plate: 4737067/4737, were chosen for further testing by the continuous fluorescence *MraY* assay. From the original 1,717 compounds, 134 compounds (8 %) showed low fluorescence in the initial microtitre plate screen, and were then analysed by the continuous fluorescence assay.

The low fluorescence compounds were tested at 60 µM concentration in a total volume of 170 µl containing 15 µM dansyl-labelled UDPMurNAc-pentapeptide 35 µg/ml heptaprenyl phosphate, 83 mM Tris pH 7.5, 21 mM MgCl₂, 6 % glycerol and 0.15 % Triton X-100. The reaction was started by the addition of 60 µg *E. coli* *MraY* membranes. Figure 3-5 shows that all of the compounds in this group interfered with fluorescence, because as soon as they were added to the cuvette, a significant decrease in fluorescence was observed.

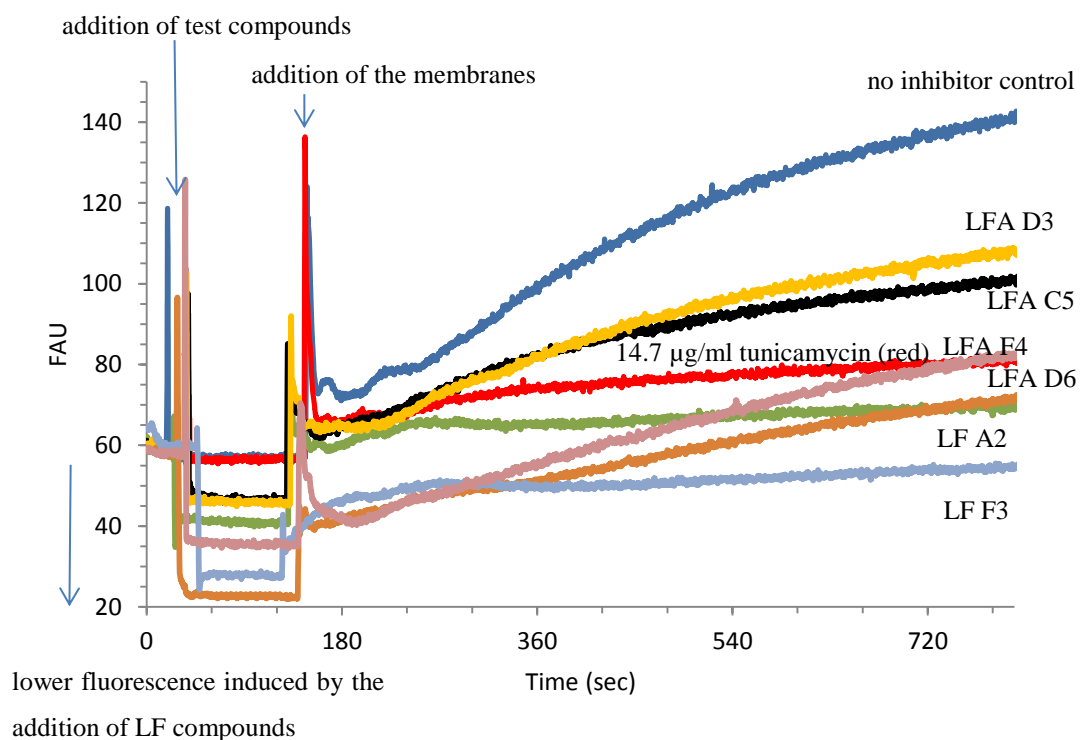


Figure 3-5: The hits tested at 60 µM from the initial screen of the diversity set interfered with fluorescence: low fluorescence (LF) compounds and low fluorescence compounds with fluorescence enhancement activity (LFA), 15 µM dansyl pentapeptide, 35 µg/ml heptaprenyl phosphate, 60 µg protein, λ_{ex} : 340 nm, λ_{em} : 530 nm

In this set, the test compounds A2 and F3 were classified as low fluorescence (LF) compounds, since after the initial mixing effect; they showed no fluorescence enhancement activity in the MraY assay. On the other hand, compounds C5, D3, D6 and F4 showed some fluorescence enhancement activity, therefore, they were classified as low fluorescence with activity (LFA) compounds.

Unfortunately, all of our 134 apparent hits from the initial screen were found to interfere with fluorescence. However, it is said to be a very common phenomenon while screening by fluorescence-based assays²⁰⁸. There are various reasons for a test compound to interfere with the fluorescence measurement, it could be due to

intrinsic fluorescence, fluorescence quenching or the compound absorbs light at the excitation or the emission wavelength²⁰⁸.

The compounds that interfered with fluorescence from our screen fell into three categories:

1. compounds with high fluorescence (HF) that were impossible to test in the fluorescence plate reader MraY assay (Figure 3-2),
2. compounds with low fluorescence (LF) that were tested by the continuous fluorescence MraY assay (Figure 3-5),
3. and low fluorescence compounds with fluorescence enhancement activity (LFA) that we also tested by the continuous fluorescence MraY assay (Figure 3-5).

Table 3-1 shows the results from our initial screen of the NCI diversity set. Out of 1,717 compounds 1,340 did not show inhibition at 100 μ M concentrations in the fluorescence MraY assay (78 %). However, 22 % of the test compounds interfered with fluorescence and it was impossible to exclude the possibility of inhibition for these compounds. An independent assay was needed in order to examine the possibility of MraY inhibition by these compounds.

Table 3-1: Categories of test compounds from the NCI diversity set

High fluorescence (HF)	243	14 %
Low fluorescence with activity (LFA)	83	5 %
Low fluorescence (LF)	51	3 %
No inhibition	1,340	78 %
Total number of compounds	1,717	100 %

The detailed results for each plate from the NCI diversity set are shown in Appendix 4.

3.2 Testing of Low Fluorescence compounds with the radiochemical assay

The radiochemical MraY assay (Figure 2-43) was our chosen method for testing the compounds that interfered with the fluorescence MraY assay. The radiochemical MraY assay (Section 2.4) is not a high-throughput assay; therefore we had to target a smaller group of compounds than the 417 compounds that interfered with fluorescence. Our first choice were the low fluorescence compounds (LF) because they did not show fluorescence enhancement activity in the fluorescence assay and also because it was a smaller group of compounds (51 compounds). These were tested in four groups of 10 and one group of 11 compounds at five occasions by the radiochemical MraY assay at 100 μ M concentrations in a total volume of 100 μ l which contained 1.2 μ M 14 C-labelled UDPMurNAc-pentapeptide (2.4 nCi), 27 μ g/ml heptaprenyl phosphate in 90 mM Tris pH 7.5, 23 mM MgCl_2 , 4.0 % (vol/vol) glycerol, 2.3 % (vol/vol) DMSO, 0.1 % Triton X-100. The reaction was started by the addition of 40 μ g protein containing overexpressed *E. coli* C43 membranes (see Section 7.22).

Figure 3-6 shows an example of seven low fluorescence compounds tested against *E. coli* MraY by the radiochemical assay at 100 μ M concentrations. The limit was set at 20 % inhibition.

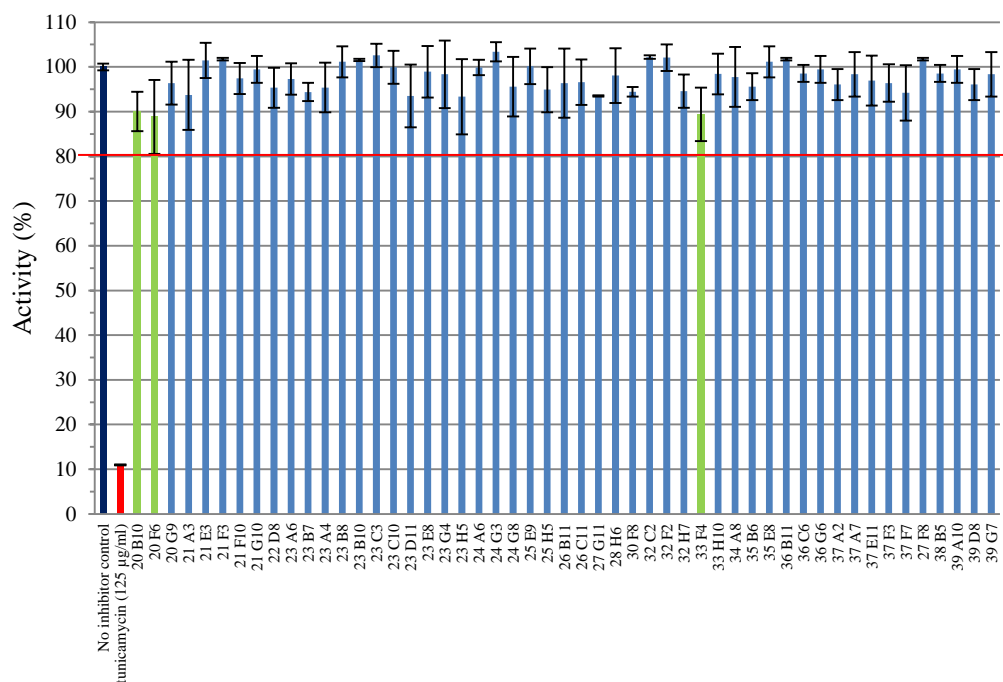


Figure 3-6: Testing low fluorescence compounds (LF) by the radiochemical MraY assay

However, there was no inhibition greater than 20 % observed for the LF compounds by the radiochemical MraY assay at 100 µM concentrations. Three of the low fluorescence compounds where inhibition seemed $\geq 10\%$ (green in Figure 3-6), were tested again at 500 µM concentration, however, no inhibition over 10 % was observed at 500 µM so no hits were obtained from this group of compounds.

3.3 Testing of high fluorescence (HF) and low fluorescence with activity (LFA) natural products with the radiochemical assay

Since the chemical structures of the natural products set appeared structurally more diverse than the diversity set III, a decision was made to concentrate our attention to the natural products set II which contained only 120 compounds. There were no LF compounds on these natural products plates, 13091250 and 13091251 each holding 60 compounds. However, there were 11 LFA compounds and 21 HF compounds that we tested at 500 μ M concentrations by the radiochemical MraY assay. The conditions for the assay were the same as for the LF compounds (see Section 3.2). Figure 3-7 shows the LFA and HF compounds from the NCI diversity set plate 13091251 that were tested by the radiochemical MraY assay.

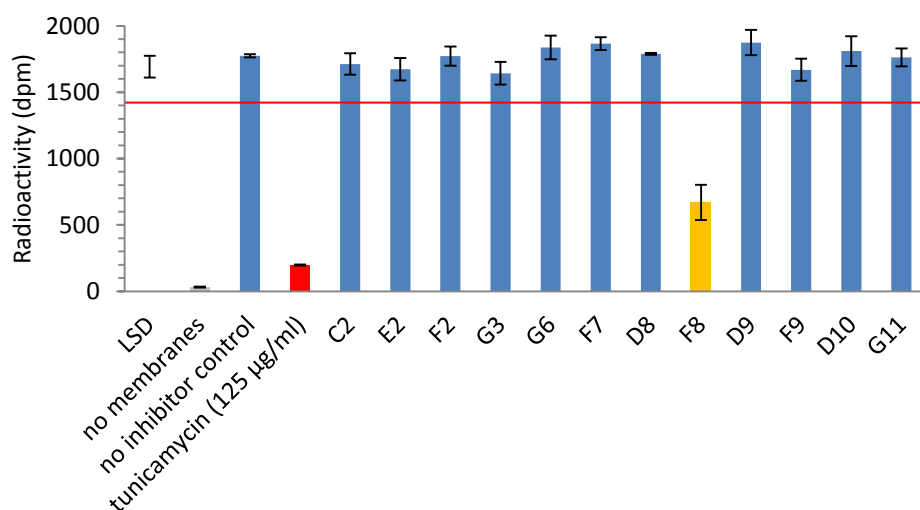


Figure 3-7: Testing high fluorescence and LFA compounds from the NCI diversity set plate 13091251, LSD calculated in GenStat: 162.5 dpm for the highest and lowest means at 5 % level, compound F8 in yellow, tunicamycin in red

Only one compound, F8 from the NCI diversity set plate 13091251, showed more than 20 % inhibition against *E. coli* MraY by the radiochemical assay at 500 μ M concentrations. None of the other compounds showed more than the set limit, 20 % inhibition in the assay from the two natural products plates. The compound that showed 60 % inhibition at 500 μ M was identified by its NSC number (661755) as an alkaloid, michellamine B. This was one of the high fluorescence compounds.

3.3.1 Testing michellamine B against MraY

The michellamines are naturally occurring dimeric naphthylisoquinoline alkaloids, isolated from a West African plant called *Ancistrocladus abbreviatus* (*Ancistrocladaceae*). Michellamine B is well-known antiviral agent with high cytotoxic activity against the human immunodeficiency virus (HIV1 and HIV-2)^{209, 210, 211}. Michellamine B was also found to inhibit protein kinase C (PKC)²¹² and human lipoxygenases (12-hLO and 15-hLO-1)²¹³ which makes it an interesting agent for anti-cancer research (see Section 3.3.2). The chemical structure of the michellamine B di-acetate salt is shown in Figure 3-8.

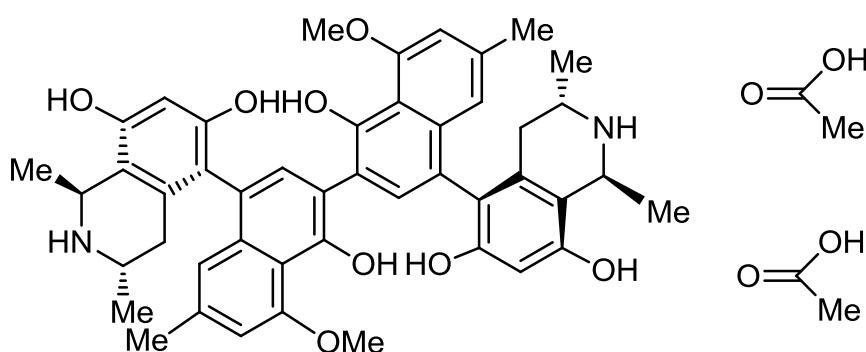


Figure 3-8: Chemical structure of Michellamine B as defined by the National Cancer Institute, Exact mass: 876.38

3.3.1.1 Inhibition of michellamine B against the MraY enzyme by the radiochemical assay

A second sample of michellamine B from the National Cancer Institute was tested again by the radiochemical MraY assay (Figure 2-43) against *E. coli* MraY as described in Section 7.23. 100 μl assay contained 3.2 nCi (7,094 dpm) [^{14}C]-UDPMurNAc-pentapeptide, 27 $\mu\text{g/ml}$ heptaprenyl phosphate in 90 mM Tris pH 7.5, 23 mM MgCl_2 , 4.0 % (vol/vol) glycerol, 2.3 % (vol/vol) DMSO, 0.1 % Triton X-100. Michellamine B was tested at 125, 250 and 500 $\mu\text{g/ml}$ final concentrations, the reaction was started by the addition of 40 μg protein containing overexpressed *E. coli* MraY membranes. IC_{50} was determined with the standard error by a plot of % activity versus michellamine B concentrations with the help of a curve fitting program in GenStat (see Section 2.2.6) with a value of 400 ± 50 $\mu\text{g/ml}$ as seen in Figure 3-9. A repeat experiment gave a value of 402 ± 60 $\mu\text{g/ml}$ for IC_{50} .

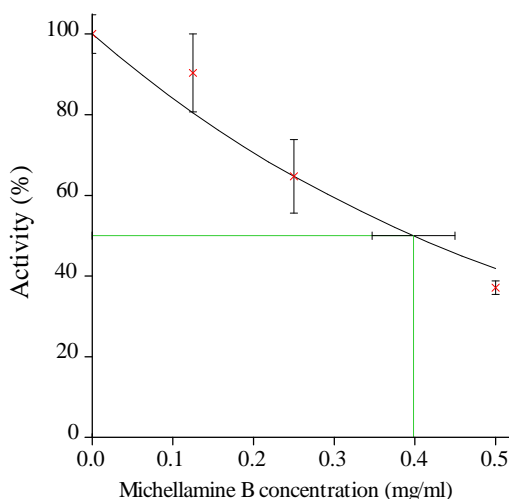


Figure 3-9: IC_{50} for Michellamine B against MraY: 400 ± 50 $\mu\text{g/ml}$

This IC₅₀ value (458 μ M) is significantly higher than we aimed for the screening (100 μ M). However, it is the only compound that we were able to screen and showed some inhibition from the NCI set.

This compound was then tested in duplicate against *S. aureus*, *P. aeruginosa*, *B. subtilis* and *M. flavus* MraYs at 500 μ g/ml concentration (Table 3-2).

Table 3-2: Michellamine B inhibition against *S. aureus*, *P. aeruginosa*, *B. subtilis* and *M. flavus* MraYs at 500 μ g/ml concentration and comparison with two known inhibitors of MraY, tested by the radiochemical MraY assay

MraY from various organisms	% inhibition of michellamine B	% inhibition of pacidamycin D (3 μ g/ml)	% inhibition of tunicamycin (125 μ g/ml)
<i>S. aureus</i>	no inhibition	98.4 \pm 2	93.7 \pm 4
<i>P. aeruginosa</i>	37.6 \pm 1	99.5 \pm 3	72.3 \pm 8
<i>B. subtilis</i>	75.7 \pm 11,	93.9 \pm 3	96.8 \pm 3
<i>M. flavus</i>	14.2 \pm 2	77.3 \pm 7	86.3 \pm 10
<i>E. coli</i>	62.8 \pm 7	97.5 \pm 2	93.4 \pm 8

Michellamine B did not inhibit *S. aureus* MraY despite repeated experiments but showed inhibition against *P. aeruginosa* (38 %), *B. subtilis* (76 %) and *M. flavus* (14 %) MraYs, tested at 500 μ g/ml concentration. *M. flavus* was not significantly inhibited by michellamine B, but interestingly the two known inhibitors, pacidamycin D and tunicamycin were less effective as well compared to the inhibition of MraYs from other organisms with 77 % and 86 % inhibition respectively. It is notable, that tunicamycin only showed 72 % inhibition against *P. aeruginosa* MraY at 125 μ g/ml concentrations.

The IC₅₀ of michellamine B (Figure 3-10) was estimated for the *B. subtilis* MraY under the same conditions as for the *E. coli* MraY (Section 7.23). The reaction started with 40 µg overexpressed *B. subtilis* MraY membranes.

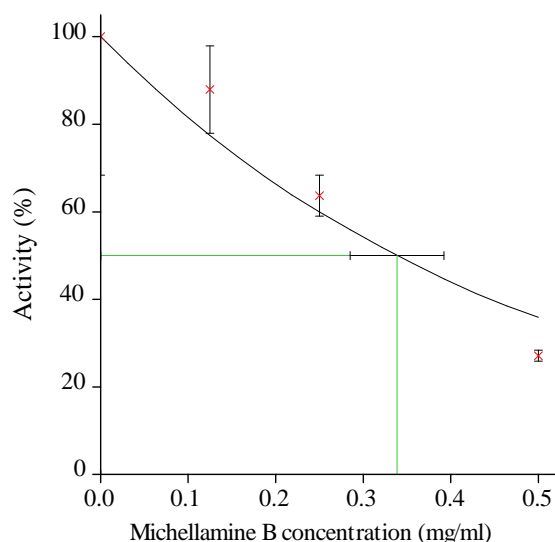


Figure 3-10: Michellamine B inhibition against *B. subtilis* MraY, IC₅₀: 338 ± 54 µg/ml

Michellamine B inhibited *B. subtilis* MraY with an IC₅₀ value of 338 ± 54 µg/ml.

3.3.1.2 Testing Michellamine B for antibacterial activity

Michellamine B was tested for antibacterial activity against *E. coli*, *B. subtilis* and *P. putida*. 3 x 10 ml LB medium was inoculated by a single colony of one of the three strains picked from an LB agar plate and incubated and shaken overnight at 37 °C. 10 µl of the overnight culture was used to inoculate 10 ml LB which was incubated at 37 °C and shaken at 180 rpm until OD₆₀₀ was 0.6. This culture was diluted 100 fold. 95 µl of the diluted culture was placed in 96-well plates and to each well 5 µl antibiotic solution was added up to a total volume 100 µl. A two-fold serial dilution of michellamine B was prepared at 125, 62.5, 31.3, 15.6, 7.81, 3.91 and 1.95 µg/ml final concentrations. The samples were prepared in

triplicates. 6 wells contained 100 μ l LB for checking bacterial contamination. 5 μ l water or 5 μ l DMSO containing solutions were added for the negative control and 5 μ l kanamycin solutions between 0.391 and 50 μ g/ml final concentrations for the positive control. The plates were incubated and shaken at 37 °C and bacterial growth was monitored by the naked eye^{59, 214}.

Michellamine B had no effect on the growth of *E. coli* and *P. putida* at 125 μ g/ml final concentration, but it inhibited the growth of *B. subtilis*. The lowest concentration of michellamine B at which there was no visible growth of *B. subtilis* gave an MIC value of 15.6 μ g/ml (3 repeats). The inhibition was confirmed by an agar plate filter disc assay²¹⁴, where a small zone of inhibition was observed at 50 μ g/ml concentration against *B. subtilis* (see Section 7.24).

Figure 3-11 shows the inhibition zone on *B. subtilis* agar plate caused by michellamine B.

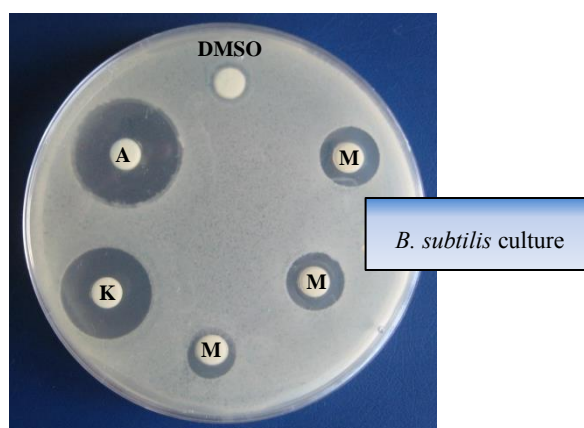


Figure 3-11: Picture of michellamine B inhibition of *B. subtilis*, from the top clockwise: 25 μ l DMSO, 25 μ l of 2.5, 1,25 and 0.05 mg/ml stock solutions of michellamine B (M), 25 μ l of 2 mg/ml kanamycin and 25 μ l 1 mg/ml ampicillin

3.3.2 Michellamine family of natural products

This section describes what is known about the biological activities of the alkaloid michellamine B and its mechanism of action on known target enzymes.

3.3.2.1 Isolation and structure of michellamines

The National Cancer Institute carried out a search for novel drug development candidates for anti-HIV agents and reported two new antiviral compounds from their *in vitro* screen in 1991, the atropisomeric pair alkaloids michellamine A and B²¹⁰.

Boyd *et al* reported the isolation and the absolute configuration of michellamine A, B and C in 1994. They were isolated from a newly discovered plant that they named *Ancistrocladus korupensis* using methods such as solvent-solvent partitioning, centrifugal partition chromatography, size exclusion chromatography, and HPLC²¹⁵. The stereo-structures of the michellamines were determined by ¹H and ¹³C NMR and CD spectroscopy^{215, 216}.

The michellamines have a unique dimeric naphthylisoquinoline alkaloid structure; their three phenolic OH and the one secondary amino group in each monomer give them high polarity. They also have some rare C-5/C-8' coupling between the naphthalene and the isoquinoline ring systems, which means they possess six elements of chirality in total (Figure 3-12)²¹⁵.

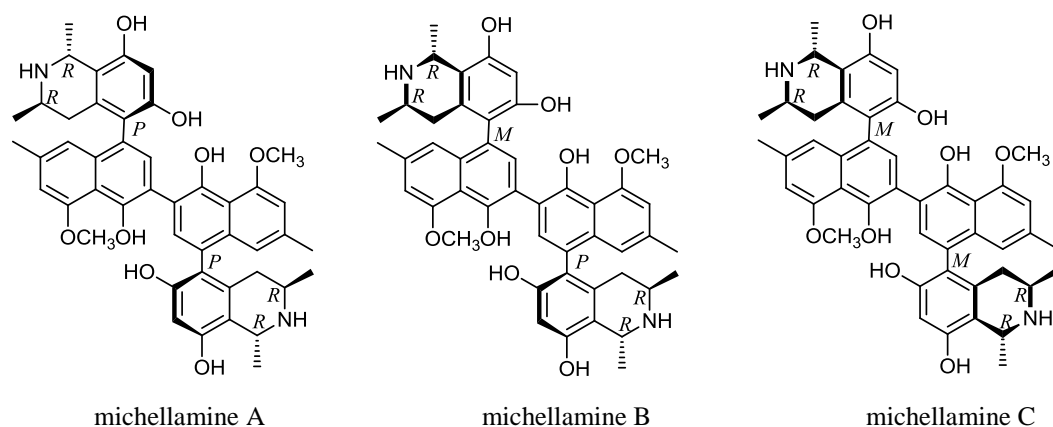


Figure 3-12: Chemical structures of michellamines A, B and C, six elements of chirality

The biosynthetic precursors of the michellamines are presumed to be the korupensamines (Figure 3-13). Korupensamine A and B exhibit good antimalarial activities *in vitro* and *in vivo*. They were isolated from the same plant *Ancistrocladus korupensis* and they structurally also possess axial chirality between the naphthalene and the tetrahydroisoquinoline rings, three elements of chirality in total²¹⁷.

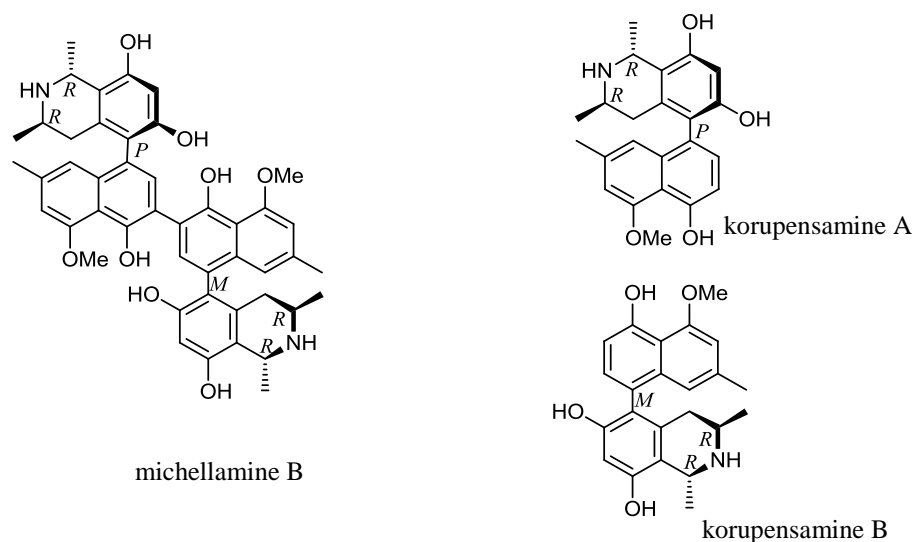


Figure 3-13: Chemical structure of michellamine B and korupensamine A and B

Examples for other monomeric naphthylisoquinoline alkaloids are the dioncophyllines²¹⁸, the ancistrobrevines, the ancistrocladines and the hamatines²¹⁹ shown in Figure 3-14.

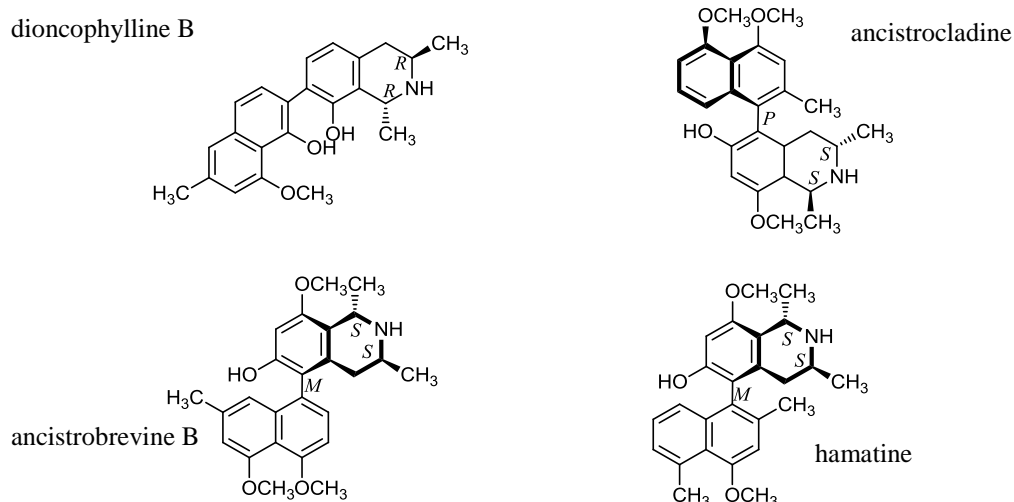


Figure 3-14: Chemical structure of monomeric naphthylisoquinoline alkaloids, three elements of chirality in the monomer units

The isolation of further anti-HIV michellamine isomers (D, E and F) and the anti-malarial korupensamine E from *A. korupensis* have also been reported²¹⁶ and several approaches were developed for the total synthesis of the michellamines^{220, 221}.

3.3.2.2 Biological activities of michellamine B

A. Antiviral activity against the human immunodeficiency virus

Michellamines A, B, and C have shown antiviral activity against HIV-1 and HIV-2 in cell culture and michellamine B, the most prevalent in *A. korupensis* extracts, was found to be the most active with an EC₅₀ value of 1-18 μ M for various HIV strains²¹⁵. The fact that michellamine B has activity against HIV-2 is rare amongst anti-HIV agents and has stimulated further studies²²⁰. The investigations suggested that michellamine B did not block the initial binding of HIV to target cells but inhibited reverse transcriptases from both HIV-1 and HIV-2 noncompetitively with respect to deoxynucleoside triphosphates²²². Michellamine B also inhibited dipyrindodiazepinone-resistant HIV-1 reverse

transcriptase mutants²²² suggesting a different site of interaction for the alkaloid than the previously described hydrophobic pocket for the dipyridodiazepinone drug Nevirapine²²³. Michellamine B also demonstrated a potent dose-dependent inhibition of cellular fusion and syncytium formation with an IC₅₀ value of 20 µM²²².

The di-acetate salt of michellamine B was suggested for pre-clinical development but the NCI discontinued further studies because it was concluded from infusion studies in dogs²²⁴ that the alkaloid had unacceptable levels of neurotoxicity and a narrow therapeutic index²²⁵. The narrow therapeutic index could be partially explained by michellamine B's inhibitory activity against cellular DNA polymerases^{222, 225}.

B. Michellamines acting as antioxidants

The michellamines were also reported to be potent antioxidants by inhibiting the azo-induced oxidation of β-phycoerythrin with IC₅₀ values ranging from 0.5 to 0.8 µM which means they were as active as trolox, a vitamin E analogue²²⁶. Moreover, it was shown that rat liver mitochondria was protected against lipid peroxidation by michellamine B²²⁶.

C. Inhibition of protein kinase C

The michellamines (A, B and C) were investigated for protein kinase C (PKC) inhibition because of their structural similarity to other PKC inhibitors (perylenequinones²²⁷)²¹².

PKC isoforms are a family of enzymes that play an important role in signal transduction pathways, therefore in a wide range of cellular processes such as cell proliferation. These enzymes can also act as a receptor for the tumour-promoting

phorbol esters which makes them an interesting target for inhibitor development in cancer research²¹². They transfer the γ -phosphate of ATP or GTP to an alcohol phenol group of proteins. They have a phospholipid-dependent regulatory domain that can be activated by diacylglycerol or Ca^{2+} , and an ATP and peptide substrate binding catalytic domain which is relatively conserved in the enzyme family^{212, 228}.

The michellamines (A, B and C) showed inhibition against rat brain PKC with IC_{50} values ranging from 15-35 μM . The most potent inhibitor, michellamine B inhibited the kinase domain of PKC in a non-competitive manner with respect to ATP (K_i value of 20 μM) and mixed-type inhibition was assumed for the peptide substrate (K_i' value of 3 μM). Michellamine B inhibited the kinase domain both in the presence or absence of phospholipid and Ca^{2+} . The authors developed a model where the michellamines bind to the active site cleft of the kinase domain not to the regulatory domain of PKC and block both the ATP and the peptide substrate binding sites²¹².

D. Inhibition of human lipoxygenases

Human lipoxygenases are a family of iron-containing enzymes catalysing the incorporation of oxygen into polyunsaturated fatty acids to form hydroperoxy acids while their metal cofactor changes its oxidation state (Fe^{2+} to Fe^{3+})²¹³. They are involved in various diseases such as inflammatory responses, cancers, and kidney diseases, however different isoenzymes have different biological activities, therefore their inhibitors should be selective²²⁹.

Deschamps *et al* developed a high-throughput 384-well plate xylenol orange assay in order to screen libraries from the NCI diversity set and the UC Santa Cruz

marine library against platelet type 12-hLO that is largely implied in cancer regulation (pancreatic, breast and prostate cancer). They also tested the hits against 15-hLO-1 and 2. 15-hLO-1 is also associated with colorectal and prostate cancer. On the other hand 15-hLO-2 was suggested to play an anti-tumorigenic role in prostate cancer. One of their hits from the NCI diversity set was michellamine B, which was found to inhibit 12-hLO and 15-hLO-1 with IC₅₀ values of 4.9 µM and 7.6 µM and did not inhibit 15-hLO-2. This discovery also made michellamine B a potentially interesting anti-tumour agent²¹³.

3.4 Summary of screening the NCI diversity set

Table 3-3 summarises the process of screening the diversity set of the National Cancer Institute against *E. coli* MraY.

Table 3-3: Summary of screen

Total of 1,717 compounds in diversity set III and natural products set II		
Assay method	diversity set III, 1,597 compounds	natural products set II, 120 compounds
	↓	↓
Fluorescence microtitre plate assay, compounds tested at 100 µM	1,252 compounds with no inhibition, 222 HF compounds 123 low fluorescence compounds	88 compounds with no inhibition, 21 HF compounds 11 LFA compounds
	↓	↓
Continuous fluorescence assay, compounds tested at 60 µM	72 LFA compounds 51 LF compounds	11 LFA compounds
	↓	↓
Radiochemical assay, compounds tested at 100 and/or 500 µM	51 LF compounds tested at 100 µM, 0 hits, 3 out of 51 LF compounds also checked at 500 µM, 0 hits	21 HF and 11 LFA compounds tested at 500 µM, 0 hits from LFA compounds, 1 hit from HF compounds, michellamine B

We tested 1, 597 compounds from the diversity set III and 120 compounds from the natural products set II plates against *E. coli* MraY by the microtitre plate fluorescence assay at 100 µM concentrations. 1,252 plus 88 compounds showed

less than 20 % inhibition in the assay and therefore were excluded from further tests (no inhibition). 222 compounds plus 21 natural products showed high fluorescence and could not be tested by the fluorescence method (λ_{ex} : 340 nm, λ_{em} : 535 nm). A total of number of 134 compounds was tested by the continuous fluorescence assay against *E. coli* MraY, where 51 was classified as low fluorescence compounds and 83 as low fluorescence compounds with fluorescence enhancement activity. The 51 low fluorescence compounds were tested by a radiochemical MraY assay against *E. coli* MraY at 100 μM and their activity was above the 80 % limit that we set. However, three of them with 10 % apparent inhibition were tested at 500 μM as well but the results showed that there was no inhibition at higher concentrations.

Finally, we tested 11 LFA and the 21 HF compounds by the radiochemical MraY assay from the natural products set II, and found 1 hit with 60 % inhibition. The compound is called michellamine B. IC_{50}s were determined for michellamine B against *E. coli* and *B. subtilis* MraYs, 400 ± 50 and 338 ± 54 $\mu\text{g/ml}$ respectively. Interestingly, the compound showed antibacterial activity (MIC: ~ 15.6 $\mu\text{g/ml}$) against *B. subtilis*, the bacteria against which the MraY inhibition was the strongest.

3.5 Future work in the field of naphthylisoquinoline alkaloids

Professor Gerhard Bringmann's research group (University of Würzburg) works in the field of natural products isolated from tropical plants for the search for novel bioactive agents against infectious diseases such as malaria and African sleeping sickness.

For future work, in collaboration with Professor Gerhard Bringmann's group, it would be interesting to test some of the monomeric naphthylisoquinoline analogues (Figure 3-14) against Mray. Perhaps, it would be even more interesting to test the structurally related novel naphthylisoquinoline dimers (Figure 3-15) isolated from *Congolese Ancistrocladus* species that possess a rotationally hindered biaryl axis between the two monomer units, an additional seventh element of chirality (in red in Figure 3-15) compared to the michellamines with six elements of chirality.

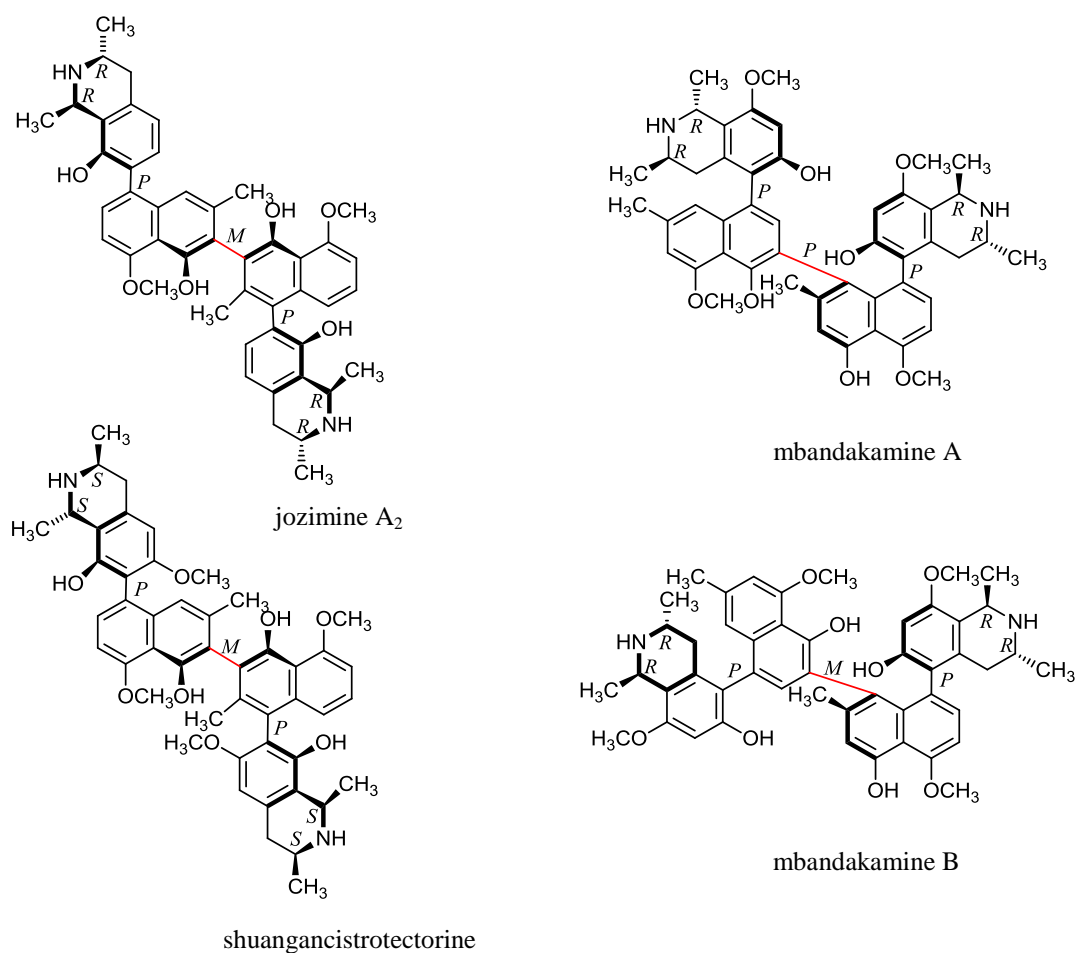


Figure 3-15: Chemical structure of jozimine A₂, the structurally related shuangancistrotectorine and mbandakamine A and B, the seventh element of chirality is the rotationally hindered biaryl axis between the two monomer units (in red)

One of the options for testing naphthylisoquinoline dimers against Mray would be jozimine A₂ with excellent antiplasmodial activity, the first dioncophyllaceae-type naphthylisoquinoline alkaloid²¹⁹ and shuangancistrotoectone a structurally closely related natural alkaloid²¹⁹. Another interesting option would be the anti-malarial mbandakamine A and mbandakamine B²³⁰. These molecules too have an exceptionally high steric hindrance in the bi-naphthalene core, thus they also possess seven elements of chirality²³⁰.

The testing of further naphthylisoquinoline analogues could make it possible to perform some structure-activity relationship studies which would help to elucidate the mechanism of action of michellamine B inhibition and perhaps locate a novel site of interaction with Mray.

4 Screening for new natural product inhibitors

Streptomyces belong to the group of soil-dwelling, filamentous Gram-positive bacteria with high guanine-cytosine containing genome, called *Antinomycetes*^{231, 232}. Antinomycetes produce over two-thirds of the clinically useful antimicrobial agents of microbial origin as well as anti-tumour agents and immunosuppressants. In the soil they play a crucial role in carbon recycling by degrading insoluble remains of other organisms, such as lignocellulose and chitin²³³. Most of them develop a mycelial habit at some stage in their complex life-cycle such as *Streptomyces coelicolor* that differentiates by forming specialized, spore-bearing hair-like aerial mycelia on the colony surface that grow into the air. On the other hand, mutant colonies have a smooth, undifferentiated appearance which gave the name 'bld' (bald) to the genes required for the initiation of aerial mycelium formation²³⁴. The complete genome of *Streptomyces coelicolor* A(3)2 as a model organism for pathogenic bacteria from the same taxonomic order such as *Mycobacterium tuberculosis*, *M. leprae* and *Corynebacterium diphtheria*, has been sequenced by Bentley *et al* (2001)²³³.

The antibiotic production (Figure 4-1) of *Streptomyces* is growth phase-dependent. In liquid culture, antibiotic production begins in stationary phase, while in solid media it starts with morphological differentiation. The antibiotics are secondary metabolites of biosynthetic pathways where around 20-30 genes are responsible for the production of one compound²³⁵. The onset of antibiotic synthesis is regulated by several factors such as growth rate, γ -butyrolactone signalling molecules²³⁶, imbalances in metabolism²³⁷ and physiological stresses²³⁵.



Figure 4-1: Antibiotic droplet from a *Streptomyces* colony (Higher Education and Research Opportunities, the John Innes Centre)

Table 4-1 shows examples for antibacterial drugs currently used in medicine produced by *Antinomycetes*²³⁵.

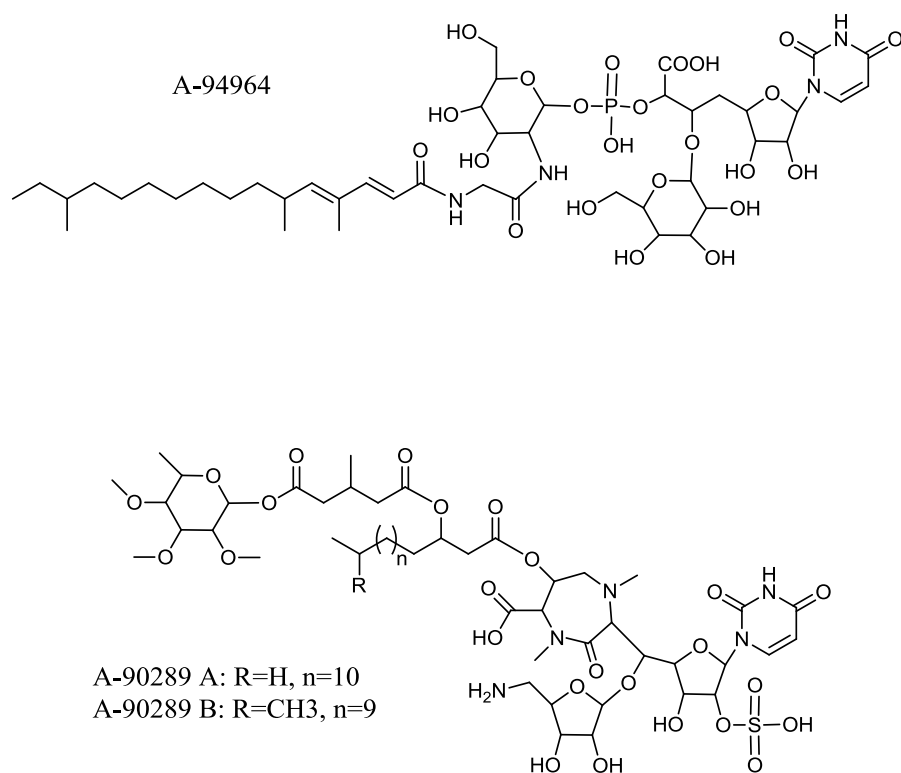


Figure 4-2: Chemical structures of A-94964 and A-90289 A and B

Table 4-1: Examples for antibacterial agents produced by *Antinomycetes*²³⁵

Antibiotic	Producer	Chemical class	Target
Chloramphenicol	<i>S. venezuelae</i>	N-dichloroacyl phenylpropanoid	“ribosome inhibitor”
Chlortetracycline	<i>S. aureofaciens</i>	Tetracycline polyketide	“ribosome inhibitor”
Clavulanic acid	<i>S. clavuligerus</i>	β -lactam	β -lactamase inhibitor
Cycloserine	<i>S. orchidaceus</i>	Substituted cyclic peptide	peptidoglycan biosynthesis
Daptomycin	<i>S. roseosporus</i>	Lipopeptide	lipoteichoic acid biosynthesis
Erythromycin	<i>Sac. erythraea</i>	Macrolide polyketide	“ribosome inhibitor”
Fortimicin	<i>Micromonospora olivoasterospora</i>	Aminoglycoside	“ribosome inhibitor”
Fosfomycin	<i>S. spp.</i>	Phosphoric acid	peptidoglycan biosynthesis
Gentamicin	<i>Micromonospora spp.</i>	Aminoglycoside	“ribosome inhibitor”
Kanamycin	<i>S. kanamyceticus</i>	Aminoglycoside	“ribosome inhibitor”
Lincomycin	<i>S. lincolnensis</i>	Sugar-amide	“ribosome inhibitor”
Neomycin	<i>S. fradiae</i>	Aminoglycoside	“ribosome inhibitor”
Nocardicin	<i>Nocardia uniformis</i>	β -lactam	peptidoglycan biosynthesis
Novobiocin	<i>S. niveus</i>	Coumerin glycoside	DNA gyrase
Oleandomycin	<i>S. antibioticus</i>	Macrolide polyketide	“ribosome inhibitor”
Oxytetracycline	<i>S. rimosus</i>	Tetracycline polyketide	“ribosome inhibitor”
Rifamycin	<i>Amycolatopsis mediterranei</i>	Ansamycin polyketide	RNA polymerase
Ristocetin	<i>Nocardia lurida</i>	Glycopeptide	peptidoglycan biosynthesis
Spectinomycin	<i>S. spectabilis</i>	Aminocyclitol	“ribosome inhibitor”
Spiramycin	<i>S. ambofaciens</i>	Macrolide polyketide	“ribosome inhibitor”
Streptogramins	<i>S. graminofaciens</i>	Macrocyclic lactones	“ribosome inhibitor”
Streptomycin	<i>S. griseus</i>	Aminoglycoside	“ribosome inhibitor”
Teichoplanin	<i>Actinoplanes teichomyceticus</i>	Glycopeptide	peptidoglycan biosynthesis
Tetracycline	<i>S. aureofaciens</i>	Tetracycline polyketide	“ribosome inhibitor”
Thienamycin	<i>S. cattleya</i>	β -lactam	peptidoglycan biosynthesis
Tobramycin	<i>S. tenebrarius</i>	Aminoglycoside	“ribosome inhibitor”
Vancomycin	<i>Amycolatopsis orientalis</i>	Glycopeptide	peptidoglycan biosynthesis

The nucleoside natural product inhibitors of the *MraY* enzyme are all secondary metabolites of various *Streptomyces* strains such as the pacidamycins, produced by *S. coeruleorubidus* (Section 5.1.3).

Researchers have used microtitre plate fluorescence-based assays to screen for *MraY* inhibitors, and successfully identified a novel nucleoside antibiotic,

A-94964 (IC₅₀: 1.1 µg/ml) from culture broth *Streptomyces* sp. SANK 60404 with a unique structure, partially resembling to tunicamycin²³⁸ (Figure 4-2). In addition, two liposidomycin related compounds, A-90289 A and B (Figure 4-2), were identified from SANK 60405 with IC₅₀ values of 36.5 and 33.8 ng/ml respectively²³⁹.

Since three other research groups in the Chemical Biology Cluster work with *Streptomyces* natural product producers, the aim of this chapter was to investigate the possibility of detecting inhibition directly from *Streptomyces* culture supernatants and cell extracts of the known pacidamycin producer, *S. coeruleorubidus* by the fluorescence or the radiochemical *MraY* assays. We were to use these methods in order to identify potentially new natural product inhibitors of *MraY* from a range of *Streptomyces* strains.

4.1 Assay of culture supernatants

We first wanted to test a strain which is known to produce an *MraY* inhibitor, as a positive control. *S. coeruleorubidus* grown on 20 % (w/v) mannitol and soya containing agar plates (MS agar) was a gift from Dr. Rebecca Goss (University of St Andrews). 10 ml of a rich medium (ISP2) containing 4 g yeast extract, 10 g malt extract, 4 g glucose / litre, was inoculated with 10 µl spore stock solution of *S. coeruleorubidus* and incubated at 30 °C for 2 days at 30 °C. Then, 50 µl of the culture were used to inoculate 10 ml ISP2 and 1 % lactose containing minimal medium (Lac-MM), and the cultures were incubated for 8 days at 30 °C. The cultures were centrifuged for 2 minutes at 5,000 x g and 10 µl of the supernatants were tested against *MraY* by the continuous and microtitre plate fluorescence *MraY* assays against *E. coli* *MraY*. *B. subtilis* was used as a control strain, as not

known to produce *MraY* inhibitors, as well as ISP2 and Lac-MM medium was used as negative controls.

The continuous fluorescence assay (Figure 2-2) was carried out as described in Section 7.10. A total volume of 180 μ l contained 30 μ M dansyl-labelled UDPMurNAc-pentapeptide, 35 μ g/ml heptaprenyl phosphate in 83 mM Tris pH 7.5, 21 mM $MgCl_2$ and the reaction was started by the addition of 60 μ g overexpressed *E. coli* *MraY* membranes (Figure 4-3).

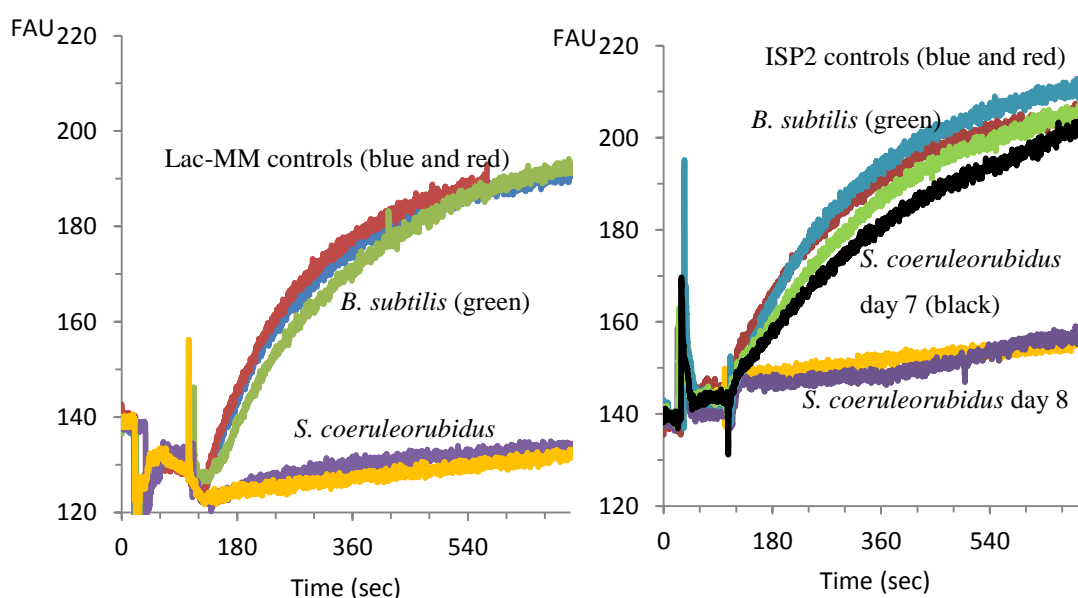


Figure 4-3: *S. coeruleorubidus* grown in Lac-MM (left) and ISP2 media (right) and tested by the continuous fluorescence *MraY* assay after 8 days incubation at 30 °C, λ_{ex} : 340 nm, λ_{em} : 530 nm

The *S. coeruleorubidus* culture supernatants tested in 8 % assay volume (15 μ l in 180 μ l) from both Lac-MM and ISP2 media showed over 93 % and 91 % inhibition respectively in the continuous fluorescence *MraY* assay after 8 days of incubation at 30 °C. However, it was not possible to detect the presence of any of the known pacidamycins in the sample by LC-MS due to the low abundance of the compounds.

4.1.1 Screening *Streptomyces* culture supernatants

S. venezuelae, *S. fungicidicus*, *S. longispororubres*, *S. ambofacient*, *S. albus*, *S. avermitilis* DSM 41443, *S. coelicolor* A3(2) and eight *S. coelicolor* mutants were also grown in Lac-MM and ISP2 media and tested against *E. coli* MraY by the continuous and the microtitre plate-reader fluorescence MraY assay (see Section 7.25.1.1). Figure 4-3 shows the example for the culture supernatants from Lac-MM media.

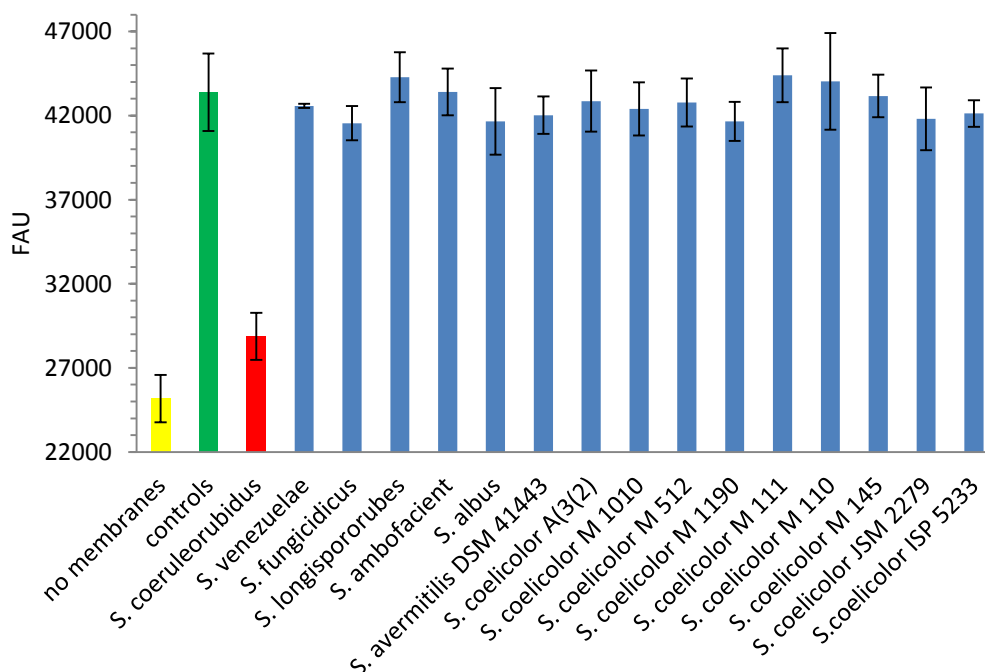


Figure 4-4: *Streptomyces* strains grown in Lac-MM media, tested in the fluorescence MraY assay, λ_{ex} : 340 nm, λ_{em} : 535 nm

No inhibition was found in the culture supernatants from ISP2 or Lac-MM media.

4.2 Assay of *Streptomyces* cell extracts from John Sidda

John Sidda works in the field of natural products in Dr. Christophe Corre's research group at the University of Warwick. They recently published the

inactivation of *gbnR*, a pathway specific transcriptional repressor gene, in *S. venezuelae* which induced the production of a novel group of compounds, the gaburedins (γ -aminobutyrate ureas, see Figure 4-5)²⁴⁰ and which may induce the production of other natural products. The deletion of *gbnB* in the *gbnR* mutant abolished gaburedin production which was consistent with the hypothesis of *gbnA* and *gbnB* genes being responsible for their production²⁴⁰.

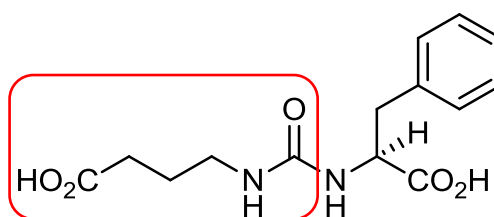


Figure 4-5: Chemical structure of gaburedin A, the conserved GABA fragment is shown in the red box

John Sidda generously provided us with some of his cell extracts from *S. venezuelae* *gbnR* mutants and the wild type. These strains were grown by John Sidda on a supplemented minimal agar medium (SMMS) for three days, the acidified agar medium was extracted with ethyl acetate and dried and re-suspended in 50 % methanol/water²⁴⁰:

- JDS349 *S. venezuelae* wild type culture extract
- JDS369 *S. venezuelae* *gbnR* mutant, which produces novel compounds that are not characterized yet
- JDS374 *S. venezuelae* *gbnB/gbnR* mutant, which only produces some of the novel compounds that have not been fully characterized yet, but does not produce gaburedins
- JDS198 *S. venezuelae* *gbnR* mutant, which overproduces gaburedin-Val

- JDS352 *S. venezuelae* *gbnR* mutant, which overproduces gaburedin-GABA
- JDS316 *S. venezuelae* *gbnR* mutant, which overproduces gaburedin-Pro

These cell extracts were tested by the microtitre plate fluorescence assay and the most active samples were also tested by the radiochemical MraY assay (Figure 2-43) against recombinant *E. coli* MraY.

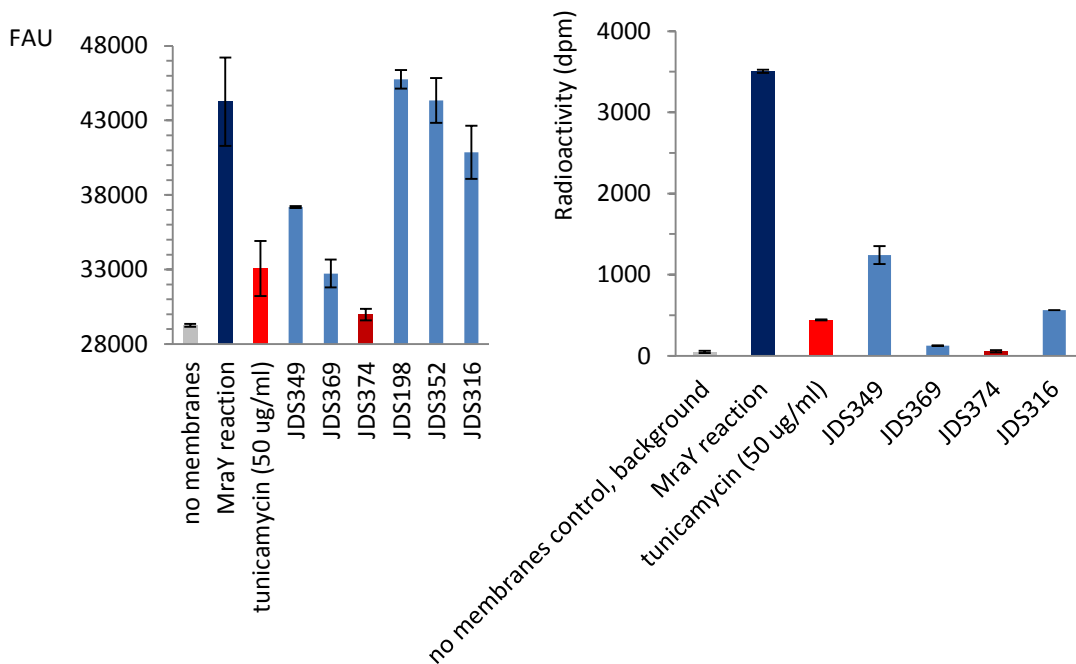


Figure 4-6: John's Sidda's cell extracts tested by the microtitre plate fluorescence assay (left) and the radiochemical assay (right) against *E. coli* MraY

The cell extract JDS374, the *S. venezuelae* *gbnB/gbnR* mutant, was found to be the most active against *E. coli* MraY with 95 % inhibition in the fluorescence assay and 99 % inhibition by the radiochemical assay. Even the wild type *S. venezuelae* (JDS349) showed 50 % and 65 % inhibition in the fluorescence and the radiochemical assay respectively (Figure 4-6). The apparent weaker inhibition of the samples in the fluorescence assay can be explained by the fact that some of the cell extracts showed high fluorescence, such as JDS 316 with the highest fluorescence, which was confirmed by the continuous fluorescence assay.

The cell extract JDS374 was fractionated by John Sidda by preparative HPLC using a linear gradient of methanol/water from 5 % up to 100 % methanol over 35 minutes. John Sidda took a sample of 7 ml for 30 seconds every 2 minutes (from 5 to 31 minutes). The fractions were tested again by the fluorescence microtitre plate *MraY* assay but no inhibition was found (Figure 4-7). The methanol was then evaporated and the samples were assayed again but no inhibition was found.

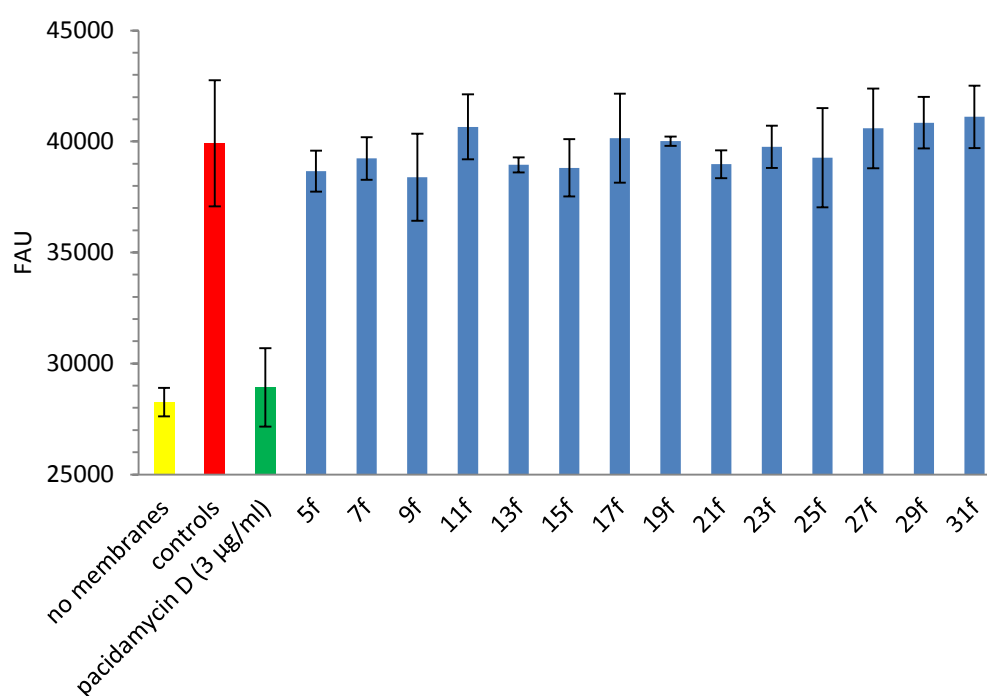


Figure 4-7: Testing the fractionated JDS374 cell extract by the microtitre plate fluorescence assay, fractions collected from 5 to 31 minutes (5f-31f)

Possibly, the compound was missed during the HPLC separation. John Sidda also provided us with his low resolution LC-MS data on the JDS374 cell extract sample. We analysed his data and at 29 minutes retention time a peak was observed at m/z $[M+H]^+$: 879.5 corresponding to a compound of molecular weight 878.5 Da. This is similar to the molecular weight range for the

pacidamycin/mureidomycin family of uridyl-peptide natural products (Mw: 765-899), but this mass and the isotopic pattern for the positively and singly charged ion do not match any of the known compounds. It could in theory be a novel member of this family, but it could be completely unrelated, and we do not know whether the observed *MraY* inhibition is due to this compound.

4.3 Screening *Streptomyces* cell extracts from solid media

John Sidda's cell extract preparation procedure for *Streptomyces* strains grown on supplemented minimal agar media²⁴⁰ was used to prepare more cell extracts for screening against *E. coli* *MraY*. We wished to test the wild type *S. venezuelae* and various *Streptomyces* strains and mutants in solid media as well, despite the fact that they did not inhibit in liquid culture (Section 4.1).

10 µl of stock spore collections was spread on MS agar plates and incubated for 10 days (only *S. venezuelae* and *S. coeruleorubidus*) or SMMS plates and incubated for 3 days at 30 °C. Secondary metabolites were extracted by ethyl acetate in equal volume to the volume of culture media used. The ethyl acetate layer was removed by filtration and evaporated under reduced pressure. The remaining residue was re-dissolved in 500 µl 50:50 HPLC grade methanol/water. Because some of the cell extracts interfered with fluorescence, all the samples were tested by the radiochemical *MraY* assay.

The total volume of 100 µl sample contained 1.7 µM ¹⁴C-labelled UDPMurNAc-pentapeptide (3.38 nCi, 7,500 dpm), 27 µg/ml heptaprenyl phosphate and 40 µg protein containing overexpressed *E. coli* C43 membranes in 90 mM Tris pH 7.5,

23 mM MgCl₂, 4.0 % (vol/vol) glycerol, 2.3 % (vol/vol) DMSO, 0.1 % Triton X-100. The assays were carried out as in Section 7.19.

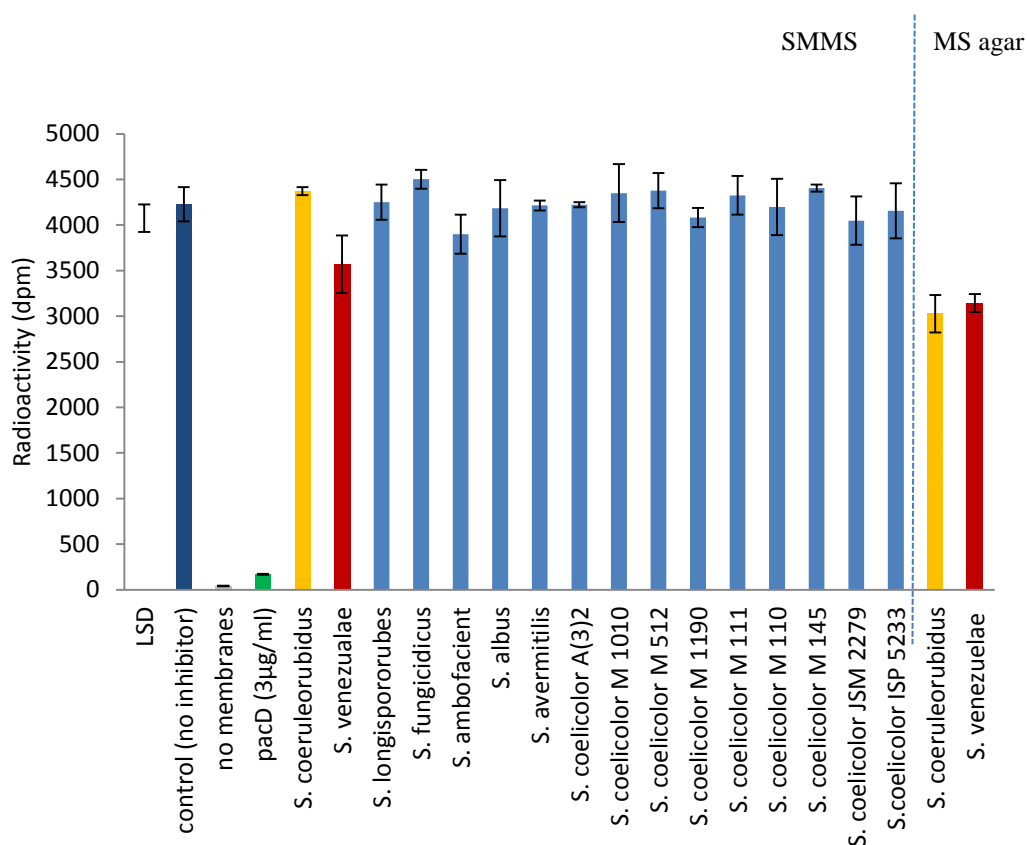


Figure 4-8: Streptomyces cell extracts from solid media tested by the radiochemical assay against *E. coli* MraY, all the strains were grown for 3 days on SMMS media and *S. coeruleorubidus* and *S. venezuelae* were grown on MS agar plates as well, the control contains 10 % methanol/water (1:1)

Interestingly, from the pacidamycin producer *S. coeruleorubidus* cell extract, no inhibition was detected from SMMS media, suggesting that on that media it will not produce the pacidamycin analogues in detectable quantity. However, grown on MS agar plate, the cell extract showed 29 % inhibition, which is still significantly lower than the 93 % and 91 % inhibition that we detected from 10 µl liquid culture.

The *S. venezuelae* cell extract that was extracted from SMMS media showed only 16 % inhibition compared to John Sidda's wild type cell extract with 65 % inhibition in the radiochemical *MraY* assay. A further attempt was made to grow the wild type *S. venezuelae* for longer (incubation time 10 days) but this time no inhibition at all was detected in the sample. When *S. venezuelae* was grown on MS agar, the cell extract showed 26 % inhibition. One important difference compared to John Sidda's procedure is that he acidified the solid media using hydrochloric acid during the extraction protocol which could lead to the decomposition of metabolites in the cell extract.

None of the other *Streptomyces* cell extracts showed inhibition against *E. coli* *MraY* (Figure 4-8).

Nevertheless, we have identified from John Sidda's cell extracts that *S. venezuelae* appears to produce a natural product *MraY* inhibitor, which is not one of the already identified gaburedins, because the *gbnB* gene was deleted in the most active *gbnR* mutant. However, the production of this compound must require very specific conditions. It is quite possible that this is a known uridyl-peptide inhibitor, but it would require additional work to confirm this.

5 Assay of novel and known MraY inhibitors

5.1 Inhibition of translocase MraY by uridyl-peptide natural products and their synthetic analogues

The uridyl-peptide natural products were suggested to target the active site of MraY at the cytoplasmic face of the membrane (see Section 1.3.1). Previously uridyl-peptide natural products were tested by P. Brandish against translocase MraY by the means of the continuous fluorescence enhancement assay (1992-95). Availability of other MraY enzymes allows us to compare specificity of inhibition for five MraY enzymes; also new synthetic uridyl-peptide analogues have become available to us during the project.

The general procedure applies for the continuous fluorescence assays (Figure 2-2), unless otherwise specified (see Section 7.10). The graphs showing % activity vs. inhibitor concentration for IC₅₀ determination, if not featuring in this chapter, are shown in Appendix 5.

5.1.1 Inhibition by a synthetic muraymycin derivative

The muraymycins nucleoside-lipopeptide antibiotics were first isolated from *Streptomyces sp.* They show antimicrobial activity against Gram-positive bacteria such as *Staphylococcus aureus* and *Enterococcus* strains which makes them attractive candidates for drug development because of the emergence of MRSA and VRE strains¹⁸⁶.

A new synthetic muraymycin analogue, the 5'-deoxy muraymycin as the bis-TFA salt (Figure 5-1), was sent by Professor Christian Ducho (Paderborn University)

whose group developed a modular tripartite synthetic approach towards synthesising this group of nucleoside peptide *MraY* inhibitor²⁴¹. We wished to test this compound against *E. coli* and *S. aureus* *MraY* because the muraymycins have antibacterial activity against *S. aureus* *MraY*.

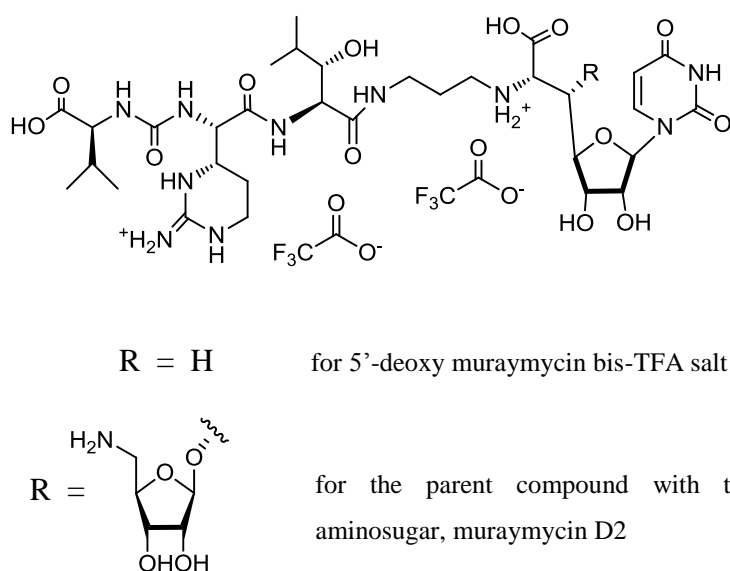


Figure 5-1: Chemical structure of the synthetic muraymycin analogue, Mw: 1012.5973 and the parent compound with the aminosugar (muraymycin D2)

The inhibitory activity of the compound was investigated against *MraY* by the means of the continuous fluorescence assay in a total volume of 170 μ l containing 23 μ M dansyl-labelled UDPMurNAc-pentapeptide, 29 μ g/ml heptaprenyl phosphate in buffer 83 mM Tris pH 7.5, 21 mM $MgCl_2$, and the reaction was started by the addition of 90 μ g protein containing recombinant *E. coli* or *S. aureus* *MraY* membranes (Figure 2-23, Figure 5-2, A 23 and A 24 in Appendix 5a).

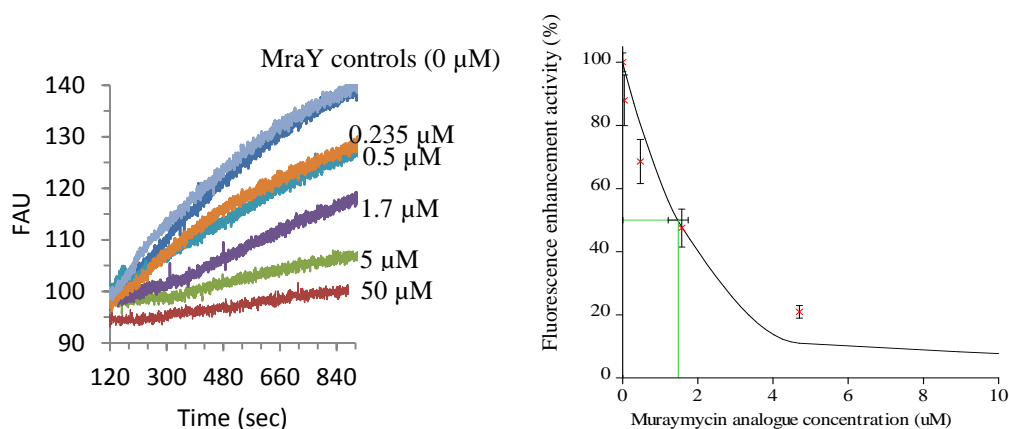


Figure 5-2: Muraymycin analogue inhibition against *E. coli* MraY, λ_{ex} : 340 nm, λ_{em} : 530 nm, 90 μg protein (left), IC_{50} : $1.6 \pm 0.3 \mu\text{M}$ (right)

The muraymycin derivative inhibited recombinant MraY from *E. coli* and *S. aureus* in the low μM range (IC_{50} : $1.6 \pm 0.3 \mu\text{M}$ for *E. coli* and $1.6 \pm 0.2 \mu\text{M}$ for *S. aureus* MraY). This inhibitory potency is very similar to the one for tunicamycin (IC_{50} : $1.9 \mu\text{M}$ ¹⁴³). However, the parent compound with the 5'-aminoribose unit had been reported to be significantly more active (IC_{50} : $0.01 \mu\text{M}$ ¹⁸⁷) indicating the importance of this sugar unit in MraY binding. The IC_{50} for the parent compound was determined by a radiochemical TLC assay against purified *B. subtilis* MraY and the compound showed no antibacterial activity which was explained by the lack of a lipophilic side chain¹⁸⁷.

In addition, the muraymycin analogue also showed inhibition against *P. aeruginosa*, *B. subtilis* and *M. flavus* MraY at 50 μM concentrations with estimated 98 %, 89 % and 85 % inhibition (Figure 5-3).

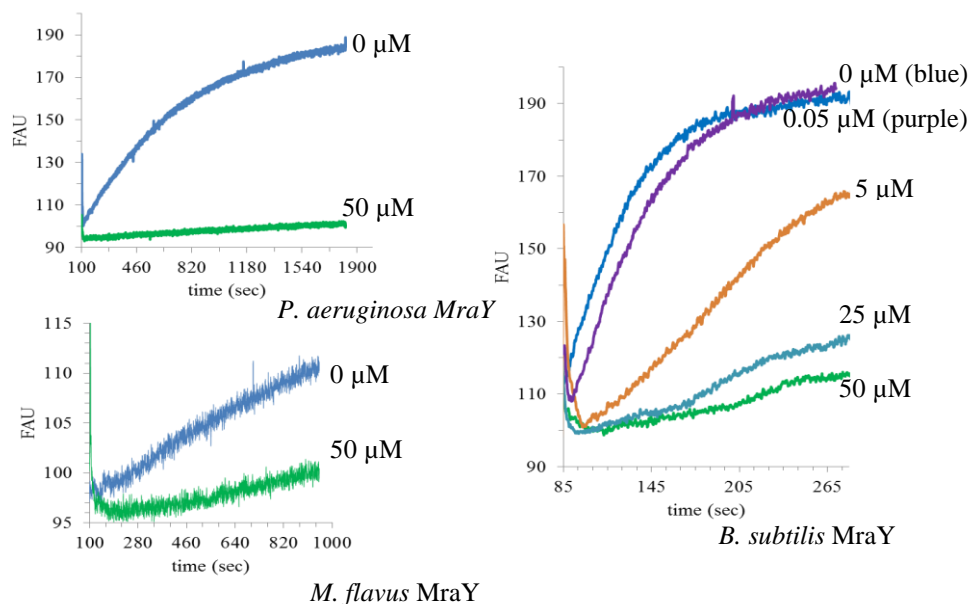


Figure 5-3: Muraymycin analogue inhibition against *P. aeruginosa*, *B. subtilis* and *M. flavus* Mray, 40-90 μ g protein, λ_{ex} : 340 nm, λ_{em} : 530 nm

The uridyl-peptide antibiotics interact with Mray at the catalytic binding site on the cytoplasmic phase of the membranes where the suggested catalytic residues are conserved for all five organisms. Therefore, it is not surprising to see inhibition of Mray from all five organisms.

The aminosugar of the liposidomycin and the caprazamycin uridyl-peptide antibiotics were shown to be important for activity¹⁵⁶, so it is interesting that the 5'-deoxy muraymycin analogue retains inhibitory activity. The results suggest that the peptide chain is involved in binding to the active site of Mray.

5.1.2 Inhibition by caprazamycin derivatives

The caprazamycins, potent liponucleoside inhibitors of MraY were isolated from *Streptomyces* sp. MK730-62F2. They have potent antibacterial activity against mycobacteria and do not exhibit significant toxicity in mice¹⁷⁷⁻¹⁸⁰. Hirano *et al* synthesized a palmitoylcaprazol analogue which had antimicrobial activity against MRSA (MIC: 6.25 µg/ml) and VRE (MIC: 12.5 µg/ml)¹⁸⁰.

The caprazamycins are structurally related to liposydomycons and their structure is derived from 5'-(β -O-aminoribosyl)-glycyluridine with a unique N,N'-dimethyldiazepanone ring. The name of the caprazamycin analogues (A–G) comes from the attached β -hydroxy-fatty acids of different chain length. The absence of a sulphate group at the 2''-position of the aminoribose and the presence of a permethylated L-rhamnose makes them different to liposidomycons^{173, 174}. Figure 5-4 shows the chemical structure for caprazamycin A and E.

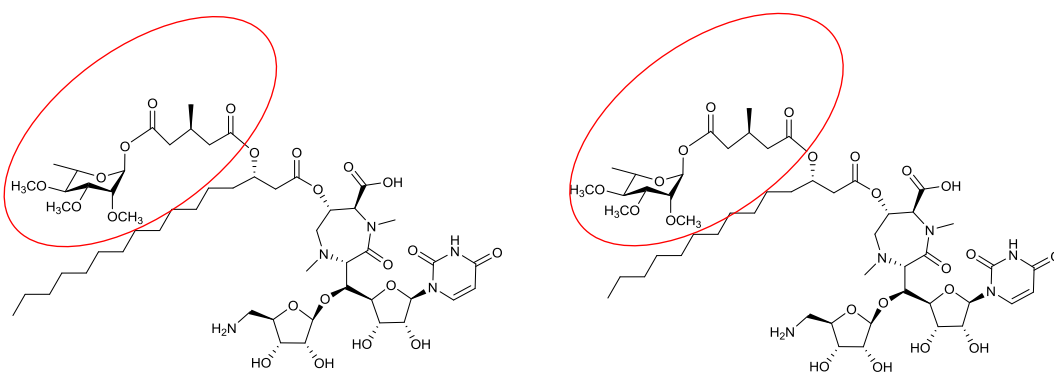


Figure 5-4: Chemical structure of caprazamycin A on the left (Exact mass: 1145.58) and caprazamycin E on the right (Exact mass: 1117.55), the additional unit compared to hydroxyacyl-caprazol A and E are circled in red

In order to develop clinically useful drugs the permeability of caprazamycin analogues into bacterial cells should be improved by optimizing the lipophilic side chain. In addition, work needs to be done on simplifying the hydrophilic core structures, and reducing the size of the molecules¹⁸⁰.

The biosynthetic gene clusters of the caprazamycins and the liposidomycins were compared, and the set of genes responsible for the sulphating of the liposidomycins were identified as well as similar genes were found adjacent to the caprazamycin gene cluster leading to the identification of new sulphated caprazamycin derivatives^{177, 242}. Sulphating considerably alters the compounds solubility, charge and size²⁴² which are important features in drug design.

Professor Bertolt Gust's research group at the University of Tübingen works in the field of liponucleoside and uridyl-peptide *MraY* inhibitors and sent us new caprazamycin analogues to test their inhibitory potential against *E. coli* *MraY* in order to establish some structure-activity relationship. The following samples were sent to be analysed: hydroxyacyl-caprazol A and E, compounds generated enzymatically from hydroxyacyl-caprazol E (hydroxyacyl-caprazol E-acetate and hydroxyacyl-caprazol E-butyrate) and sulphated caprazamycin aglicon A and E. All of the samples lack the permethylated L-rhamnose unit from their structure. The sulphated caprazamycin aglycons have exactly the same chemical structure as members of the liposidomycins. Figure 5-5 shows the chemical structure of the samples, the units that make them different from the hydroxyacyl caprazol core structure are circled in red.

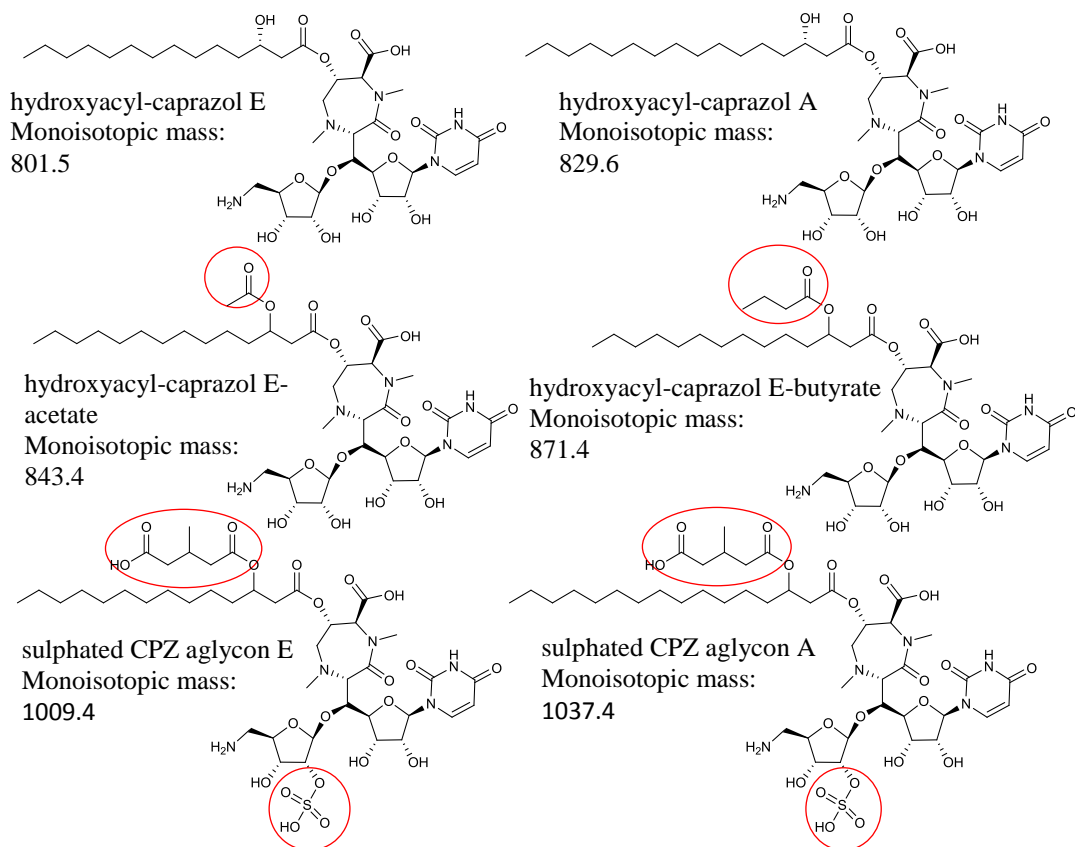


Figure 5-5: Chemical structure of caprazamycin analogues, the additional groups compared to hydroxyacyl-caprazol E and A are circled in red

The caprazamycin analogues were tested by the continuous fluorescence assay against recombinant *E. coli* MraY in a total volume of 180 μ l containing 30 μ M dansyl-labelled UDPMurNAc-pentapeptide, 35 μ g/ml heptaprenyl phosphate in buffer 83 mM Tris pH 7.5, 21 mM MgCl_2 and the reaction was started by the addition of 90 μ g protein containing recombinant *E. coli* MraY membranes.

Figure 5-6 shows the example for one of the interesting new compounds, hydroxyacyl-caprazol E-acetate, which proved to be less active by the fluorescence assay against *E. coli* MraY than hydroxyacyl-caprazol E.

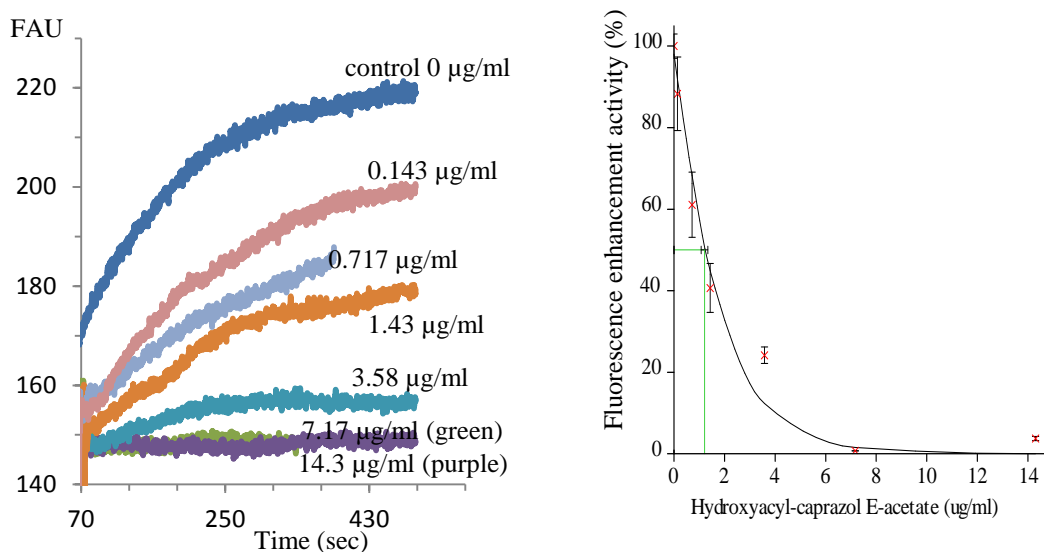


Figure 5-6: Hydroxyacyl-caprazol E-acetate inhibition against *E. coli* MraY, IC₅₀: 1.21 ± 0.13 µg/ml

Table 5-1 summarizes the results for the measured IC₅₀s for all of the caprazamycin analogues (Figures A 25 - A 30 in Appendix 5b).

Table 5-1: IC₅₀s of caprazamycin analogues against *E. coli* MraY

Caprazamycin analogue	IC ₅₀ against <i>E. coli</i> MraY
hydroxyacyl-caprazol A	0.339 ± 0.035 µg/ml, 0.41 µM
hydroxyacyl-caprazol E	0.602 ± 0.019 µg/ml, 0.75 µM
hydroxyacyl-caprazol E-acetate	1.21 ± 0.13 µg/ml, 1.4 µM
hydroxyacyl-caprazol E-butyrate	5.78 ± 0.41 µg/ml, 6.6 µM
sulphated CPZ aglycon E	0.314 ± 0.042 µg/ml, 0.31 µM
sulphated CPZ aglycon A	0.250 ± 0.035 µg/ml, 0.24 µM

The A analogues with the 2-unit longer lipophilic chain seem to be slightly more active than E. The most active compound in the fluorescence assay against *E. coli*

MraY is the sulphated caprazamycin aglycon A with an IC_{50} value of 0.24 μ M. The presence of the sulphate group makes the structure identical to the liposidomycins. The sulphated caprazamycin aglycon E has very similar inhibitory activity with 0.31 μ M, perhaps it is a marginally less active compound. The IC_{50} values of the butyrate and acetate derivatives of hydroxyacyl-caprazol E increased nine and two fold respectively which means that the less polar esters are significantly less active than hydroxyacyl-caprazol E or the sulphated caprazamycin aglycons.

5.1.3 Inhibition by pacidamycin derivatives

The pacidamycins are uridyl tetra/pentapeptide antibiotics structurally related to the mureidomycins and the napsamycins¹⁰. Pacidamycins 1-7 were isolated from *S. coeruleorubidus* strain AB 1183-64¹⁶³⁻¹⁶⁵ and pacidamycin D, 4N and 5T were isolated from strain NRRL 18730¹⁶⁶. They show antibacterial activity against *Pseudomonas species*¹⁶⁵, and pacidamycin D was found to be active against *P. aeruginosa* as well¹⁶⁶. Figure 5-7 shows the chemical structure for pacidamycin 1, 2 and D.

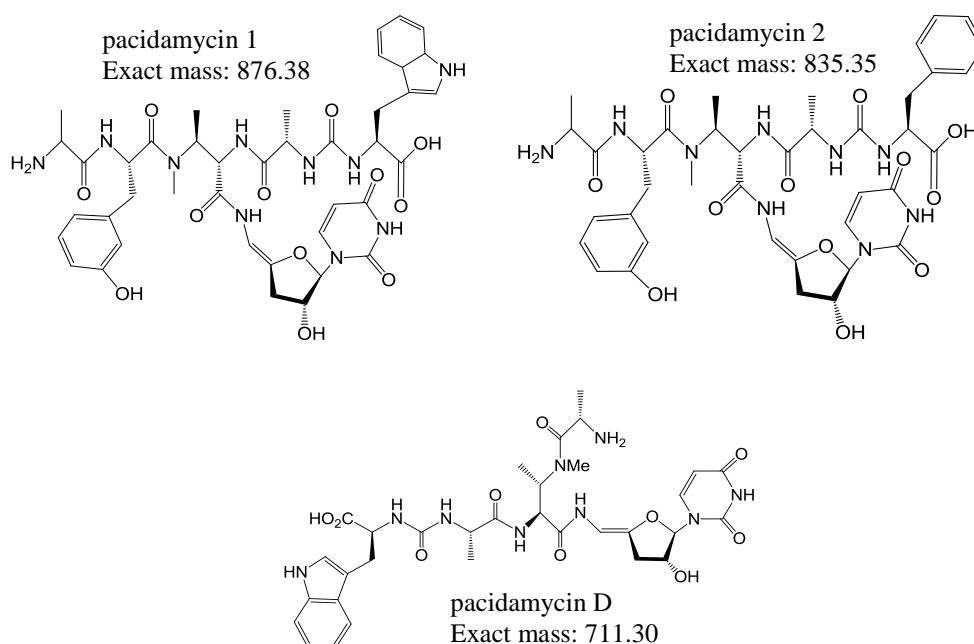


Figure 5-7: Chemical structure for pacidamycin 1, 2 and D

The pacidamycin 1,2 and D samples were provided by Antoine Abou Fayad (University of St Andrews) and tested in a total volume of 180 μ l containing 30 μ M dansyl-labelled UDPMurNAc-pentapeptide, 35 μ g/ml heptaprenyl phosphate in buffer containing 83 mM Tris pH 7.5, 21 mM MgCl_2 against *E. coli* and *P. aeruginosa* MraY (90 μ g protein). Since the pacidamycins show

antibacterial activity against *P. aeruginosa*, it was of interest to test the compounds against *P. aeruginosa* MraY.

Figure 2-22 and Figure 5-8 show the graphs for the fluorescence measurements.

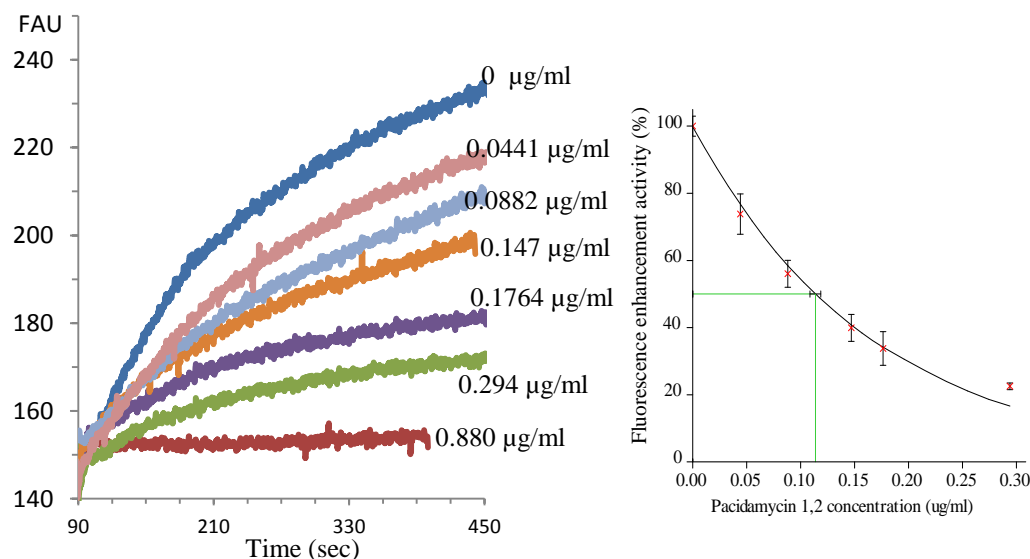


Figure 5-8: Pacidamycin 1,2 inhibition against *P. aeruginosa* MraY tested between 0-0.88 µg/ml, 90 µg protein, , λ_{ex} : 340 nm, λ_{em} : 530 nm, IC₅₀: 114 ± 5 ng/ml

Table 5-2 shows the IC₅₀s that were measured by the continuous fluorescence assay against *E. coli* and *P. aeruginosa* MraY. The remaining graphs for % activity vs. inhibitor concentration are shown in Figures A 31 - A 34 in Appendix 5c.

Table 5-2: Pacidamycin 1,2 and D inhibition against *E. coli* and *P. aeruginosa* MraYs, IC₅₀s

Pacidamycin analogue	<i>E. coli</i> MraY IC ₅₀	<i>P. aeruginosa</i> MraY IC ₅₀
Pacidamycin 1, 2	83 ± 7 ng/ml, 97 nM	114 ± 5 ng/ml, 130 nM
Pacidamycin D	46 ± 7 ng/ml, 65 nM	27 ± 4 ng/ml, 38 nM

Pacidamycin D was a more active compound than the pacidamycin 1,2 sample, and showed two-fold higher activity against *P. aeruginosa* MraY whereas pacidamycin 1,2 was slightly less active against *P. aeruginosa*.

5.1.4 Inhibition by tunicamycin

The tunicamycins are well known reversible¹⁴³ nucleoside disaccharide inhibitors of *MraY* and commercially available (Sigma), therefore it was used as a positive control during assay development. They were first isolated from *S. lysosuperficus* and have antibacterial activity against Gram-positive bacteria¹⁵⁰. Unfortunately, tunicamycin can not be used as an antibacterial agent because it inhibits GlcNAc-1-phosphate transferase in mammalian N-linked glycoprotein biosynthesis¹⁵³:

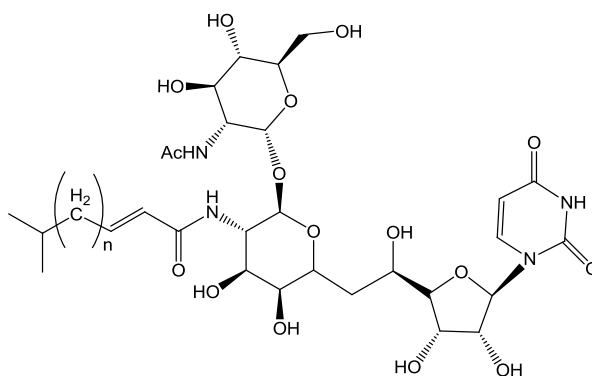
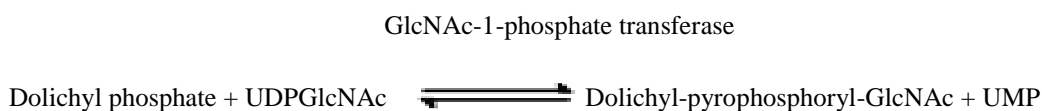


Figure 5-9: Chemical structure of tunicamycins, n: 7-11, and the reaction they inhibit in mammalian N-linked glycoprotein biosynthesis

Tunicamycin was tested in our research group by the continuous fluorescence *MraY* assay, and the determined IC_{50} s are shown in Table 5-3 for *MraY* from *E. coli*, *P. aeruginosa*, *S. aureus* and *B. subtilis* with values ranging between 0.6-4.4 μ g/ml.

Table 5-3: Tunicamycin inhibition by a fluorescence assay against MraYs from *E. coli*, *P. aeruginosa*, *S. aureus*, *B. subtilis* and *M. flavus*, a: determined by P. Brandish¹⁴³, b: determined by A. O'Reilly

MraY	Tunicamycin IC₅₀ (µg/ml)
<i>E. coli</i> MraY	1.0 ^a
<i>P. aeruginosa</i> MraY	4.44 ± 1.38
<i>S. aureus</i> MraY	1.4 ^b
<i>B. subtilis</i> MraY	0.6 ^b
<i>M. flavus</i> MraY	95 % inhibition at 83 µg/ml

Tunicamycin was tested against *P. aeruginosa* in a total volume of 180 µl contained 30 µM dansyl-labelled UDPMurNAc-pentapeptide, 35 µg/ml heptaprenyl phosphate in 83 mM Tris pH 7.5, 21 mM MgCl₂ and the reaction was started by the addition of 45 µg recombinant *P. aeruginosa* MraY membranes (see general procedure in Section 7.10). IC₅₀ was determined as 4.44 ± 1.38 µg/ml (data in Appendix 5d, Figure A 35) which is 4 fold higher than the IC₅₀ for *E. coli*, *S. aureus* and *B. subtilis* MraYs. In addition, evidence from the radiochemical assays shows (Table 3-2) that tunicamycin is less active against *P. aeruginosa* MraY (72 % inhibition) than against *E. coli*, *S. aureus* and *B. subtilis* MraY (93-97 % inhibition) at high concentrations (125 µg/ml).

5.1.5 Inhibition by capuramycin derivatives

Samples of well-known capuramycin analogues, A-503083 F and A-503083 B, were sent by Steven Van Lanen (University of Kentucky). The reason for testing these compounds against *E. coli* MraY was to assay them against two MraY

mutants (F288L and E287A) as well and compare the IC₅₀ values in order to investigate a potential second binding site on Mray. However, this work was carried out for Maria T. Rodolis's project and the results have not been published yet. For this thesis, one of the compounds, A-503083 B was chosen to demonstrate uridyl-peptide inhibition against *B. subtilis* Mray as an example.

Capuramycins are nucleoside antibiotics first isolated from *S. griseus*¹⁸⁸. They have antibacterial activity against *mycobacteria*¹⁹⁰.

A-503083 F and A-503083 B (Figure 5-10) were isolated from *Streptomyces species* SANK 62799 broth cultures and they are 2'-*O*-carbamoyl derivatives of A-500359 F and B¹⁹⁰. A-500359 F (2.4 μ M) was found to be significantly less active against *E. coli* Mray than B (18 nM), due to the lack of the aminocaprolactam ring¹⁹².

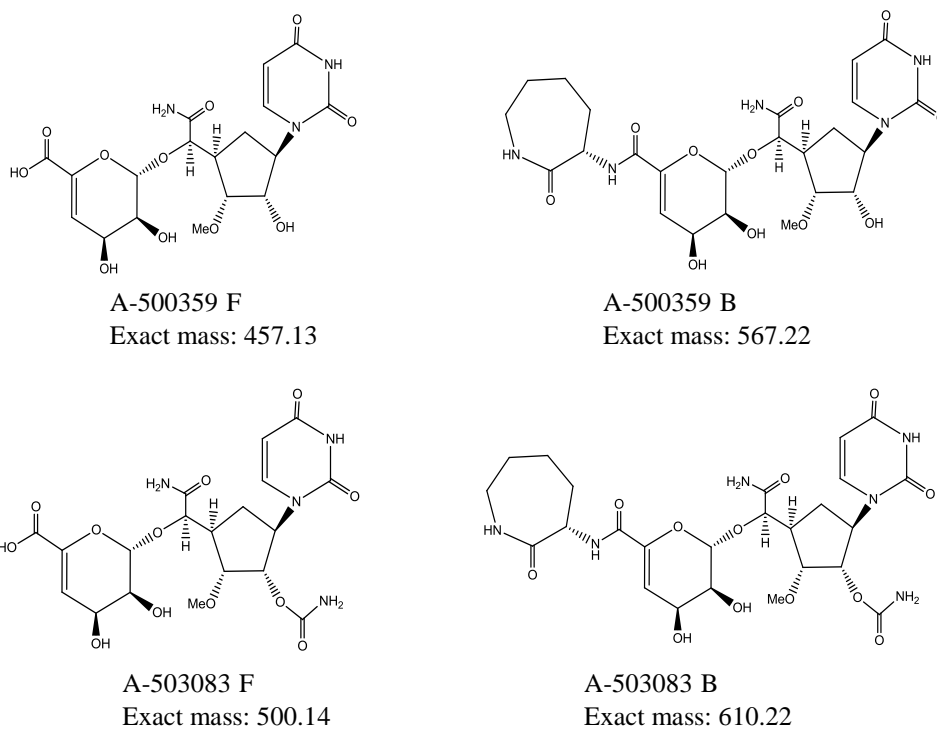


Figure 5-10: Chemical structures of the capuramycin analogues, A-500359 F and B, and A-503083 F and B

A-503083 F has no antibacterial activity while A-503083 B was found to be active against *Streptococcus pneumoniae*, *Streptococcus pyogenes*, *Mycobacterium smegmatis* and *Moraxella catarrhalis*. The IC₅₀s for *E. coli* MraY inhibition were determined by a fluorescence assay with 17.9 µM and 38 nM respectively by Muramatsu *et al*¹⁹⁰. These values meant that the presence of the 2'-*O*-carbamoyl unit reduced the activity 8 and 2 fold respectively. Moreover, A-503083 F was less active than B which highlighted once more the important role of the aminocaprolactam ring in MraY inhibition¹⁹⁰.

The two samples of capuramycin analogues (A-503083 F and A-503083 B) were tested against *E. coli* MraY by the continuous fluorescence MraY assay in a total volume of 180 µl containing 30 µM dansyl-labelled UDPMurNAc-pentapeptide, 35 µg/ml heptaprenyl phosphate in buffer 83 mM Tris pH 7.5, 21 mM MgCl₂ against *E. coli* MraY (60 µg protein). Table 5-4 shows the results (Figures A 36 and A 37 in Appendix 5e).

Table 5-4: Inhibition and IC₅₀s of capuramycin analogues against *E. coli* and *B. subtilis* MraYs

Capuramycin analogue	<i>E. coli</i> MraY	<i>B. subtilis</i> MraY
A-503083 F	4.8 ± 0.6 µg/ml	not tested
A-503083 B	0.139 ± 0.016 µg/ml	0.062 ± 0.006 µg/ml

The IC₅₀ for A-503083 F was half the value determined by Mutamatsu *et al* and we saw a 6-fold increase in the IC₅₀ for A-503083 B compared to the published value which could be explained by the differences in the assay conditions, such as

concentration of the substrates, detergent, Mg^{2+} or other salts present²⁰⁸.

Therefore, in order to compare IC_{50} s, it is important to keep these factors constant.

The more active compound, A-503083 B, was tested against *B. subtilis* MraY under the same conditions where the reaction was started with 60 μg protein containing recombinant *B. subtilis* MraY membranes (Figure 2-24). The measured IC_{50} value was estimated as $62 \pm 6 \text{ ng/ml}$ (Figure 5-11) against *B. subtilis* MraY. It is half of the IC_{50} for the *E. coli* MraY which means that the inhibitory potency of this compound against *B. subtilis* MraY is slightly higher.

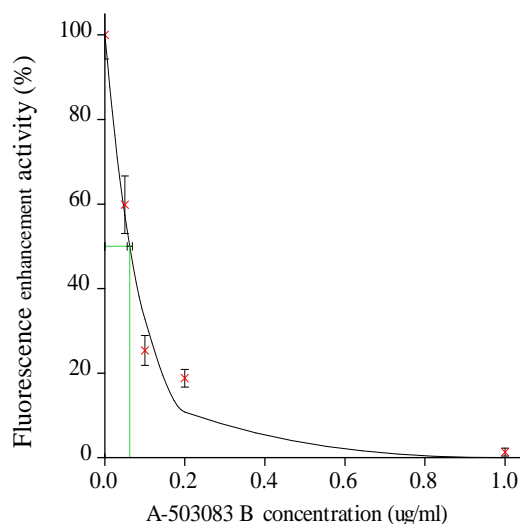


Figure 5-11: A-503083 inhibition against *B. subtilis* MraY, IC_{50} : $62 \pm 6 \text{ ng/ml}$

5.2 Inhibition of MraY by vancomycin

During the search for a natural product producing bacterial strain as a positive control for testing *Streptomyces* cell extracts against *E. coli* MraY, the inhibitory potential of vancomycin was tested against MraY.

The glycopeptide antibiotic vancomycin that was isolated from *Amycolatopsis orientalis* (formerly known as *S. orientalis*)¹¹² is the last line of defence against life-threatening Gram-positive infections, such as the ones caused by MRSA²⁴³. Vancomycin is not thought to penetrate the cell membrane therefore unable to inhibit enzymes from the cytoplasmic phase of the membranes^{9, 244}, or interact with proteins in the bacterial cell but was reported to inhibit bacterial peptidoglycan biosynthesis by binding to the D-alanine-D-alanine termini of lipid II which leads to sterically preventing their transglycosylation (Section 1.1.3.1) and transpeptidation steps and eventually weakens the forming peptidoglycan cell wall^{112, 243, 245, 246}.

Vancomycin could complex the D-Ala-D-Ala unit of UDPMurNAc-pentapeptide, lipid I and lipid II¹¹², however it has very rarely been reported as an MraY inhibitor. At one occasion, this natural product was used by Solapure *et al.* as a positive control for their development of a scintillation proximity assay for MraY where they measured an IC₅₀ value of 20 µM for vancomycin inhibition. Their assay contained 5 µM UDPMurNAc-pentapeptide and 12.5 µg protein from wild type *E. coli* membranes^{147, 247}. It was suggested that higher concentration of membrane protein could affect the inhibitory potency of vancomycin because it can bind to pre-existing peptidoglycan fragments on the membranes¹⁴⁷. Ravishankar *et al.* showed that vancomycin inhibits MurG but the IC₅₀ of

vancomycin largely depended on the quantity of lipid I (~9 μM), because it binds to vancomycin neutralizing its inhibitory effect¹⁴⁹. In addition, the use of large quantity of enzyme was found unfavourable for vancomycin inhibition once again¹⁴⁹.

The hydrogen bond formation between vancomycin and the D-Ala-D-Ala terminus of peptidoglycan precursors is shown in Figure 5-12. Vancomycin resistant bacteria learned to synthesise and use e.g. D-Ala-D-Lac instead of D-Ala-D-Ala for building its precursors and polymerising the peptidoglycan chain and the mutation from amide to ester disrupts the hydrogen bonding network with vancomycin²⁴⁵.

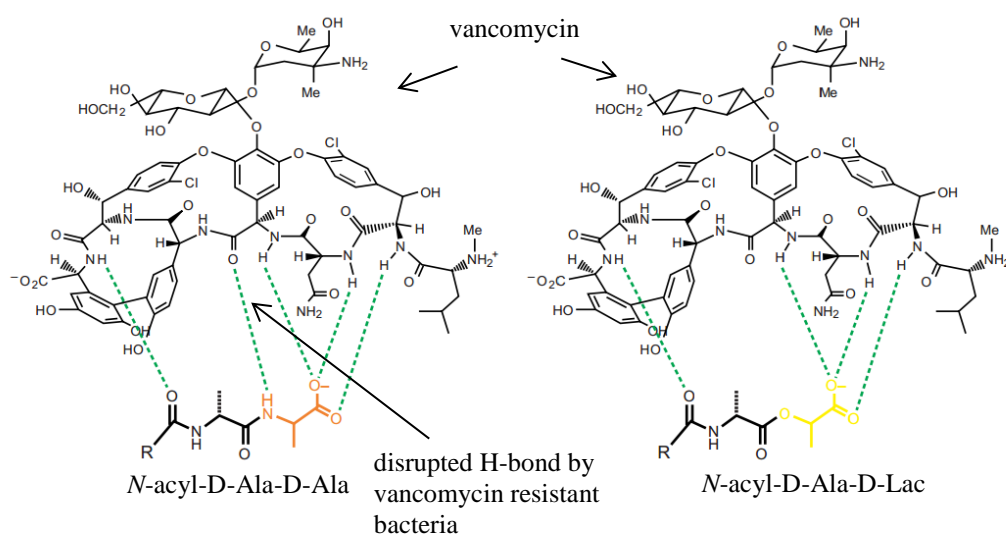


Figure 5-12: Representation of the vancomycin : *N*-acyl-D-Ala-D-Ala complex (left), and vancomycin : *N*-acyl-D-Ala-D-Lac complex in vancomycin resistant bacteria (right), dashed lines represent H-bonds²⁴⁵

Vancomycin interfered with fluorescence in our assay (λ_{ex} : 340 nm λ_{em} : 530 nm) and was tested by the radiochemical *MraY* assay (Figure 2-43). 100 μl assay contained 1.1 μM (2.12 nCi)/assay) [^{14}C]-UDPMurNAc-pentapeptide, 23.3 $\mu\text{g/ml}$ heptaprenyl phosphate, 70 mM Tris pH 7.5, 17.5 mM MgCl_2 , 4.0 % (vol/vol) glycerol, 2.3 % (vol/vol) DMSO, 0.1 % Triton X-100, and the reaction was started

by the addition of recombinant *E. coli*, or *S. aureus* or *P. aeruginosa* MraY membranes, containing 40, 35 and 20 µg protein (see general procedure in Section 7-19). The % activity versus vancomycin concentration graph for *E. coli* MraY inhibition is shown in Figure 5-13.

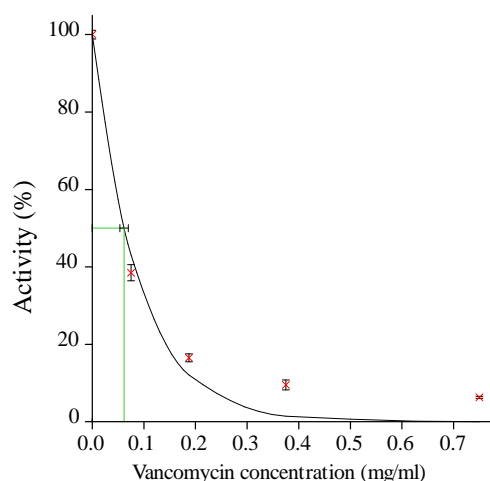


Figure 5-13: Vancomycin inhibition against *E. coli* MraY

IC₅₀ values were estimated and are shown in Table 5-5. The data for IC₅₀ determination for *S. aureus* and *P. aeruginosa* are shown in Figures A 39 and A 40 in Appendix 6.

Table 5-5: Vancomycin inhibition against *E. coli*, *S. aureus* and *P. aeruginosa* MraYs

Vancomycin inhibition against MraY	IC ₅₀
<i>E. coli</i>	61.6 ± 8 µg/ml, 43 µM
<i>S. aureus</i>	130 ± 12 µg/ml, 90 µM
<i>P. aeruginosa</i>	288 ± 44 µg/ml, 199 µM

The strongest inhibition was observed against *E. coli* MraY (IC₅₀: 43 µM for 1.1 µM [¹⁴C]-UDPMurNAc-pentapeptide), where a 43 fold molar excess was needed to complex UDPMurNAc-pentapeptide for the half maximal inhibitory concentration. The inhibitory potential of vancomycin did not seem to be strong enough (IC₅₀ > 10 µM) to use this natural product as a positive control for testing cell extracts.

5.3 Inhibition by E peptide, antimicrobial peptides and P1 peptide

E protein (see Section 1.3.2) is known to inhibit *E. coli* MraY^{197, 198}. In this section its inhibition against MraY from other organisms was investigated. Moreover, we tested some antimicrobial peptides, which have a similar motif to E protein in their sequences against *E. coli* MraY, and the cell wall synthesis targeting P1 peptide was tested against MraY and MurG.

5.3.1 Testing E peptide against *E. coli*, *S. aureus*, *P. aeruginosa*, *B. subtilis* and *M. flavus* MraYs

Bacteriophage ϕ 174 uses a single lysis gene, *E*, to cause lysis of the host cell and the encoded 91-amino-acid membrane protein¹⁹⁶ was shown to inhibit *E. coli* MraY^{197, 198}. Only the 29 amino-terminal amino acids of the transmembrane domain of E protein were found to be essential for lytic function²⁴⁸⁻²⁵⁰. A 100 % α -helical 37-amino-acid synthetic peptide (MALDI-TOF *m/z* (M+H)⁺: 4334.7) containing the N-terminal transmembrane domain of E protein was shown to be effective against membrane-bound *E. coli* MraY by a microtitre plate fluorescence enhancement assay (IC₅₀: 0.8 μ M)²⁰⁰. The amino acid sequence of the synthetic E peptide is the following²⁰⁰:



A sample of the above mentioned 37-amino-acid peptide was tested by the continuous fluorescence MraY assay (Figure 2-2) against *E. coli*, *S. aureus*, *P. aeruginosa*, *B. subtilis* and *M. flavus* MraYs in a total volume of 180 μ l containing 30 μ M dansyl-labelled UDPMurNAc-pentapeptide, 35 μ g/ml

heptaprenyl phosphate in a buffer 83 mM Tris pH 7.5, 21 mM MgCl₂, 6 % glycerol, 0.15 % Triton X-100. The reactions were started by the addition of 40-60 µg protein containing membranes (see Section 7.10). Significant inhibition was only detected against *E. coli* MraY, where IC₅₀ was determined as 17.2 ± 2.11 µg/ml (Figure 5-14).

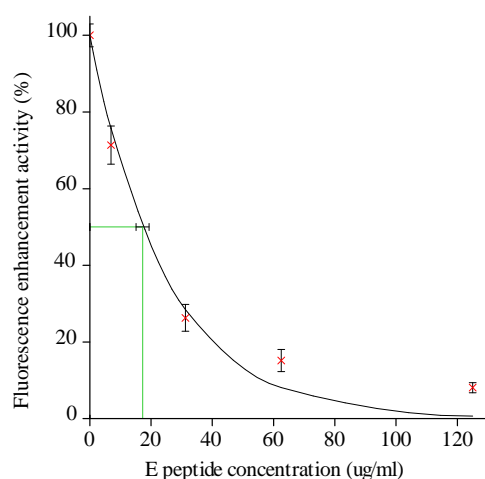


Figure 5-14: E peptide inhibition against *E. coli* MraY, IC₅₀: 17.2 ± 2.11 µg/ml

Phe-288 is known to be an essential residue of *E. coli* MraY for the E protein mediated lysis, mutation of this residue to lysine resulted in resistance to E protein¹⁹⁷. There is no phenyl-alanine residue at the same position for *S. aureus*, *B. subtilis*, *P. aeruginosa* and *M. flavus* MraYs (Figure 5-15).

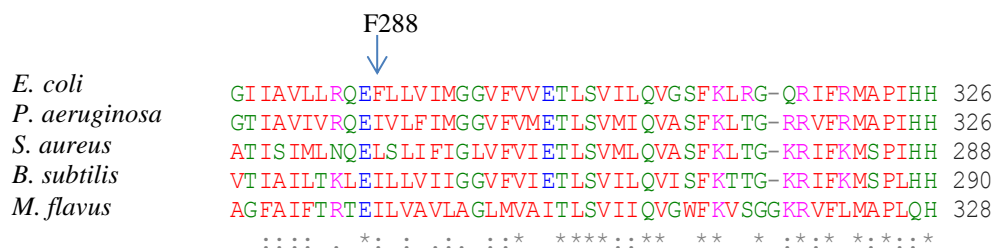


Figure 5-15: Position of F288 of *E. coli* MraY compared to *S. aureus*, *B. subtilis*, *P. aeruginosa* and *M. flavus* MraYs

No inhibition was observed against *S. aureus*, *B. subtilis*, *P. aeruginosa* and *M. flavus* MraYs at 83 µg/ml concentrations by the continuous fluorescence MraY assay (Figure 5-16).

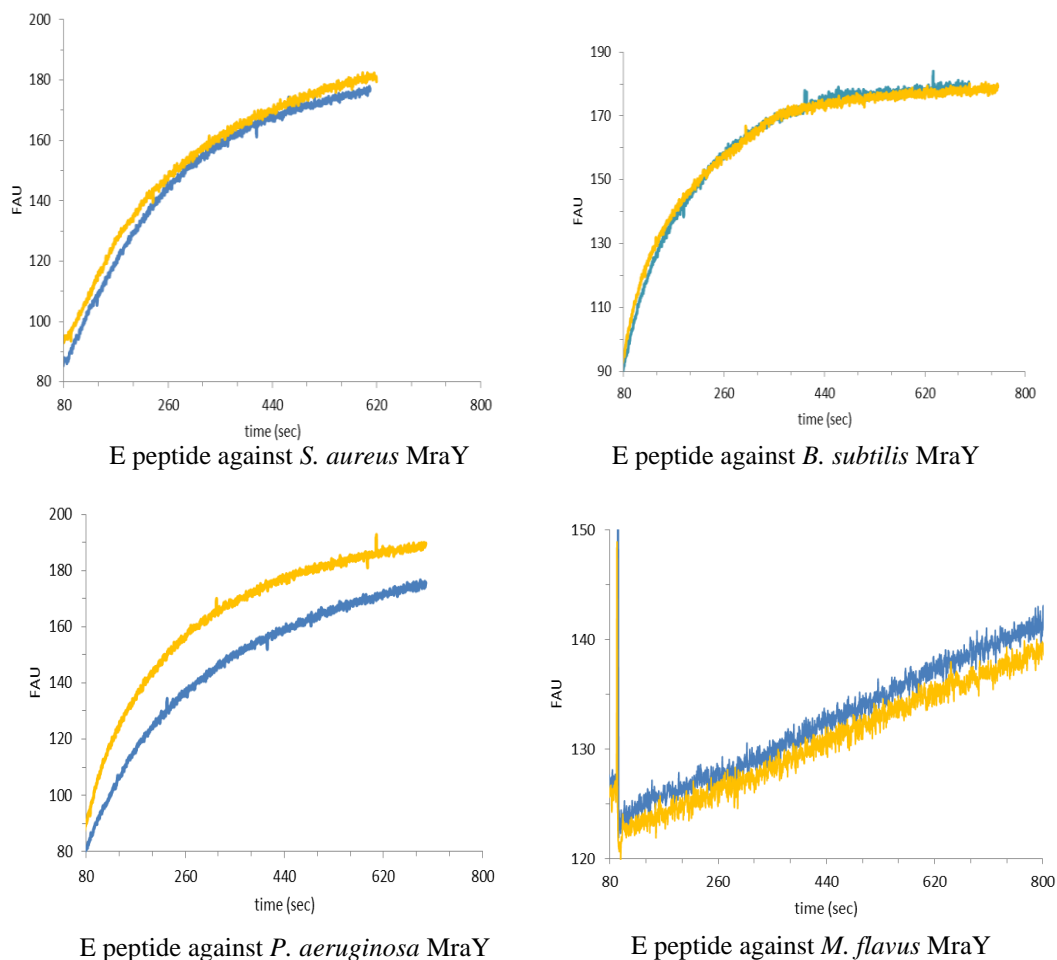


Figure 5-16: E peptide inhibition against *S. aureus*, *B. subtilis*, *P. aeruginosa* and *M. flavus* MraYs, control (no inhibitor) in blue, 125 µg/ml E peptide in orange, 40-90 µg protein, λ_{ex} : 340 nm, λ_{em} : 530 nm

The lack of inhibition was confirmed against *S. aureus*, *P. aeruginosa*, *B. subtilis* and *M. flavus* MraYs when E peptide was tested by the radiochemical MraY assay (see general procedure in Section 7.19) at 150 µg/ml concentrations.

5.3.2 Testing antimicrobial peptides against MraY

Cationic antimicrobial peptides, also named as host defence peptides, are produced by various organisms, such as plants, insects, amphibians, even human beings. These peptides can be directly antimicrobial or can play an important role in the innate immune and inflammatory responses²⁵¹⁻²⁵⁴. The natural cationic peptides are generally 12-50 amino acids in length, have a net positive charge due to an excess of basic lysine and arginine residues over acidic residues, and contain approximately 50 % hydrophobic amino acids²⁵⁵. Four major structural categories are shown in Figure 5-17 based on their amphiphilic conformations forming before or after membrane interaction and insertion²⁵⁶⁻²⁵⁸.

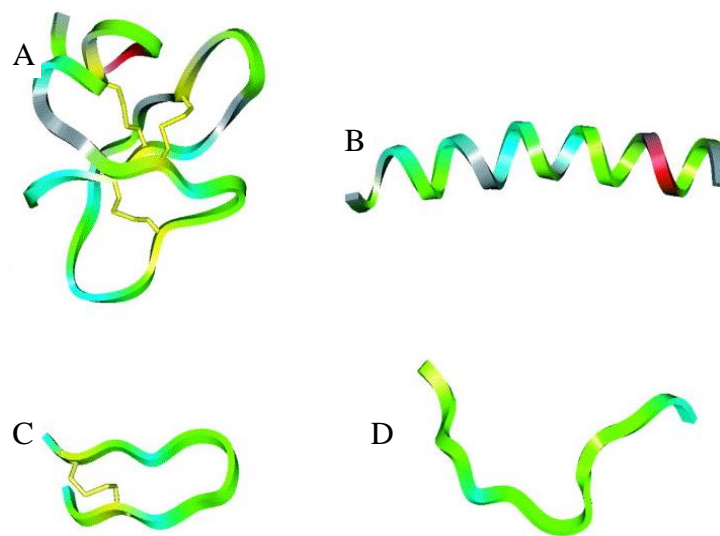


Figure 5-17: Major structural conformations of natural antimicrobial peptides, charged regions in blue and hydrophobic residues in green, A: β -structures with 2-4 β -strands, stabilized by two to four disulphide bridges, B: α -helical peptides, C: loop structures with one disulphide bridge, D: extended structures²⁵⁵.

Cationic antimicrobial peptides interact with bacterial cell membranes by binding to their negatively charged surfaces and then insert through a combination of

electrostatic and hydrophobic interactions. Insertion into eukaryotic cell membranes which have zwitterionic lipids at their surfaces is more difficult²⁵¹.

These peptides have a broad spectrum of activity against Gram-positive and negative bacteria, as well as fungi, viruses and parasites they can kill multidrug resistant bacteria and not highly affected by antibiotic-resistance mechanisms²⁵⁹. They are also capable of neutralizing endotoxemia and sepsis as well as stimulating the innate immune response²⁶⁰. Moreover, several antimicrobial peptides have been reported to have anticancer activity^{261, 262}.

However, there are obstacles in their widespread clinical use resulting from the high cost of preparation, their unknown toxicities and their rapid degradation by proteases in the digestive tract. More structure-activity relation studies need to be done in order to increase their specificity and tolerability²⁶⁰.

Cherkasov *et al* used peptide array technology to create 9-amino-acid peptide libraries and applied quantitative structure-activity approaches based on some physicochemical properties of the peptides, such as polar and hydrophobic characteristics of the constituent amino acids. The best of these 9-amino-acid peptides were effective even against multidrug-resistant “Superbugs”, especially tryptophan- and arginine-rich peptides that also exist in nature but longer and less active²⁵¹. Examples for tryptophan- and arginine-rich peptides are indolicidin, a 13-amino acid cationic antimicrobial peptide isolated from bovine neutrophils with very high tryptophan content²⁶³ and a parent compound MX-226 which has shown to be an effective antimicrobial agent in phase III clinical trials²⁶⁴.

Professor Timothy D. H. Bugg noticed that these antimicrobial peptides contain an arginine-tryptophan motif (N...-R-W-X-X-W-...C) near their N-terminus

similarly to E protein. Since Professor Timothy D. H. Bugg developed a model for the E protein MraY interaction where there are hydrophobic interactions between Trp-4 and Trp-7 of E protein with Phe-288 of *E. coli* MraY and electrostatic interactions between Arg-3 of E protein and Glu-287 of *E. coli* MraY²⁶⁵, these peptides were interesting to test against MraY.

The antimicrobial peptides such as indolicidin, MX-226, Kai-47, Kai-50, 1002 and Sub-6 were provided by Professor Robert E. W. Hancock (University of British Columbia). It was not possible to test them by the fluorescence assay because they showed high fluorescence (λ_{ex} : 340 nm, λ_{em} : 530 nm). They were tested against *E. coli* MraY by the radiochemical MraY assay (see general procedure in Section 7.19 and Figure 2-43) at 100 $\mu\text{g/ml}$ concentrations. E peptide was used as a positive control and gave 87 ± 7 % inhibition at 150 $\mu\text{g/ml}$ concentrations. Table 5-6 shows that the peptides inhibited *E. coli* MraY between 30-61 % by the radiochemical assay.

Table 5-6: Inhibition against *E. coli* MraY by antimicrobial peptides determined by a radiochemical MraY assay²⁶⁵

Antimicrobial peptides	Sequence	Inhibition %
Indolicidin	N-RRWPWWPWKWPLI-C	30 ± 5 %
MX-226	C-KRRWPWWPWRLI-N	55 ± 5 %
Kai-47	N-KRWKWWRFKWKIF-C	52 ± 5 %
Kai-50	N-ILRWKWRWWRR-C	61 ± 3 %
1002	C-KRIRWVILWRQV-N	41 ± 3 %
Sub-6	N-RWWKIWWIRWWR-C	58 ± 4 %

These assays were run for Maria T. Rodolis whose PhD project studied the role of the arginine-tryptophan motif of E protein using synthetic peptides²⁶⁵. Maria T.

Rodolis measured MIC values (8-150 µg/ml) for these peptides against *E. coli*. Inhibition normally leads to an increase in MIC with the presence of more enzyme while the MIC should not change if the compounds are inactive. Maria T. Rodolis also measured the MICs (2-63 µg/ml) for cells overexpressing *E. coli* MraY where there was a 2-4 fold decrease in the MIC values. This observation was explained by the possibility of interaction of these peptides at another site, where the higher level of MraY would assist the insertion of these peptides into the membranes and therefore the MIC values would decrease²⁶⁵.

5.3.3 Testing the P1 lytic peptide from phage AP205 against MraY

The ORF1 in *Acinetobacter* phage 205 (AP205) was proposed to encode a lysis peptide (P1) containing 35 amino acids, MKKRTKALLPYAVFIILSFQLTLLTALFMYHYTF (Mw: 4242.16 Da), and expression of this peptide into *E. coli* was shown to cause cell lysis²⁶⁶. Dr. Roger Levesque's research group at the Laval University is interested in the characterization of the lytic mechanism of P1 by using a combination of *in vitro* and *in vivo* approaches. They found that P1 is a bacterial cell wall inhibitor by enzymatic assays against MurA, MurB and MurE with IC₅₀ values of 30 µM, 210 µM and 33 µM, respectively. P1 was found to compete for the Mg²⁺ binding site in MurE. Gene dosage and cell rescue experiments suggested that MraY and MurG are also possible targets for P1. P1 was suggested to be a competitive inhibitor of these enzymes by binding to their Mg²⁺ binding site. The information about the P1 peptide inhibition of bacterial cell wall synthesis was found on the website of the Laval University.

The 35 amino acid containing P1 lytic peptide and the shortened version of it without the C terminal end were provided by Dr. Roger Levesque. The two samples showed high fluorescence in the fluorescence MraY assay and were tested at 300 µg/ml concentration against *E. coli* MraY by the radiochemical assay (Figure 2-43). 100 µl assay contained 1.1 µM (2.12 nCi)/assay) [¹⁴C]-UDPMurNAc-pentapeptide, 23.3 µg/ml undecaprenyl phosphate, 70 mM Tris pH 7.5, 17.5 mM MgCl₂, 4.0 % (vol/vol) glycerol, 2.3 % (vol/vol) DMSO, 0.1 % Triton X-100, and the reaction was started by the addition of 40 µg protein containing overexpressed *E. coli* MraY membranes. P1 peptide and its shortened version gave 68 ± 5 % and 26 ± 3 % inhibition respectively.

IC₅₀ was determined for the more active compound (P1 peptide) against *E. coli* MraY using a dilution series at 75-300 µg/ml concentrations (Figure 5-18) with a value of 157 ± 9 µg/ml.

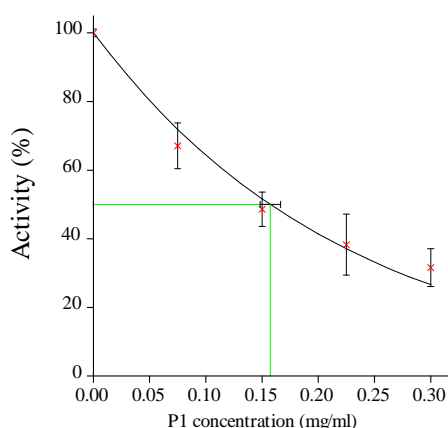


Figure 5-18: P1 peptide inhibition against *E. coli* MraY (radiochemical assay) IC₅₀: 157 ± 9 µg/ml

P1 peptide was also tested at 300 µg/ml concentrations by the radiochemical assay against *P. aeruginosa* and *S. aureus* MraY, but inhibition was not detected. This

enzyme selectivity could suggest that the P1 peptide interacts with *E. coli* MraY at a different site from the site of the uridyl-peptide inhibitors.

5.3.4 Testing the P1 lytic peptide against MurG

P1 peptide was assayed against MurG using a coupled radiochemical assay, as described by Trunkfield *et al.* (2010)^{85, 267}. Lipid I was generated from UDPMurNAc-pentapeptide and undecaprenyl phosphate by recombinant *E. coli* MraY membranes and then converted in the presence of [³H]-UDPGlcNAc and *E. coli* MurG to give radiolabelled lipid II (Figure 5-19).

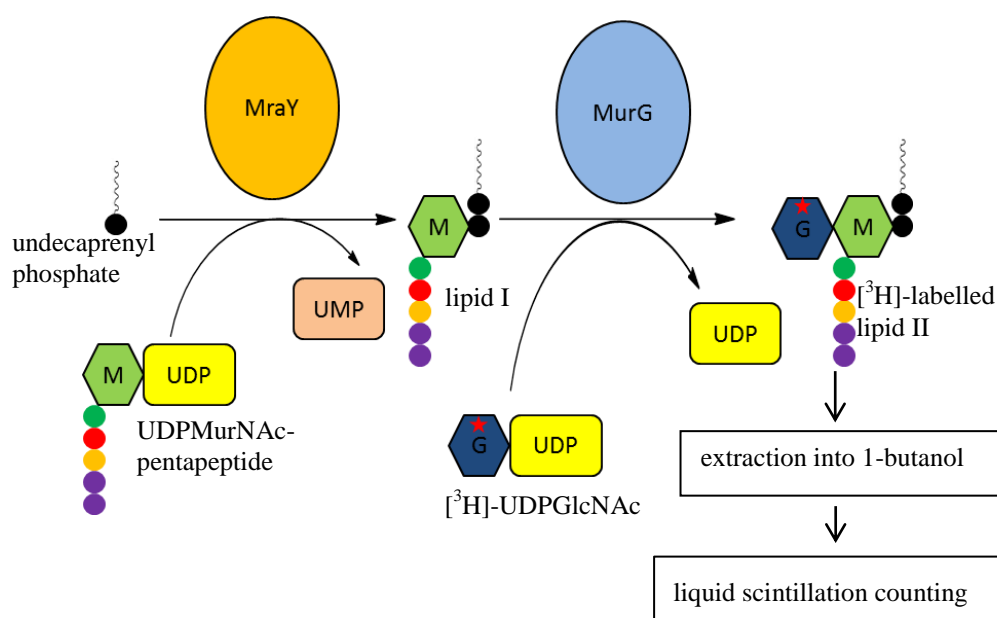


Figure 5-19: Schematic representation of the coupled radiochemical MraY-MurG assay

100 µl total volume contained 100 µM UDPMurNAc-pentapeptide, 23.3 µg/ml undecaprenyl phosphate, 6.6 µM [³H]-UDPGlcNAc (2.53 nCi/assay), 70 mM Tris pH 7.5, 17.5 mM MgCl₂, 4.0 % glycerol (vol/vol), 2.3 % (vol/vol) DMSO, 0.1 % Triton X-100 to which was added 60 µg *E. coli* membranes containing overexpressed *E. coli* MraY, and 60 µg *E. coli* MurG solution. The purified MurG solution was provided by Anita Catherwood from the Life Sciences Department

of the University of Warwick. The mixture was incubated at 35 °C for 20 minutes and reactions were stopped by the addition of 100 µl 6 M pyridinium acetate, pH 4.2. The lipid products were extracted into 200 µl 1-butanol and quantified by liquid scintillation counting. Assays were carried out in duplicates in the presence of inhibitor at concentrations of 18-300 µg/ml, and inhibition by ramoplanin was used as a positive control. Ramoplanin was a gift from Dr. Adrian Lloyd.

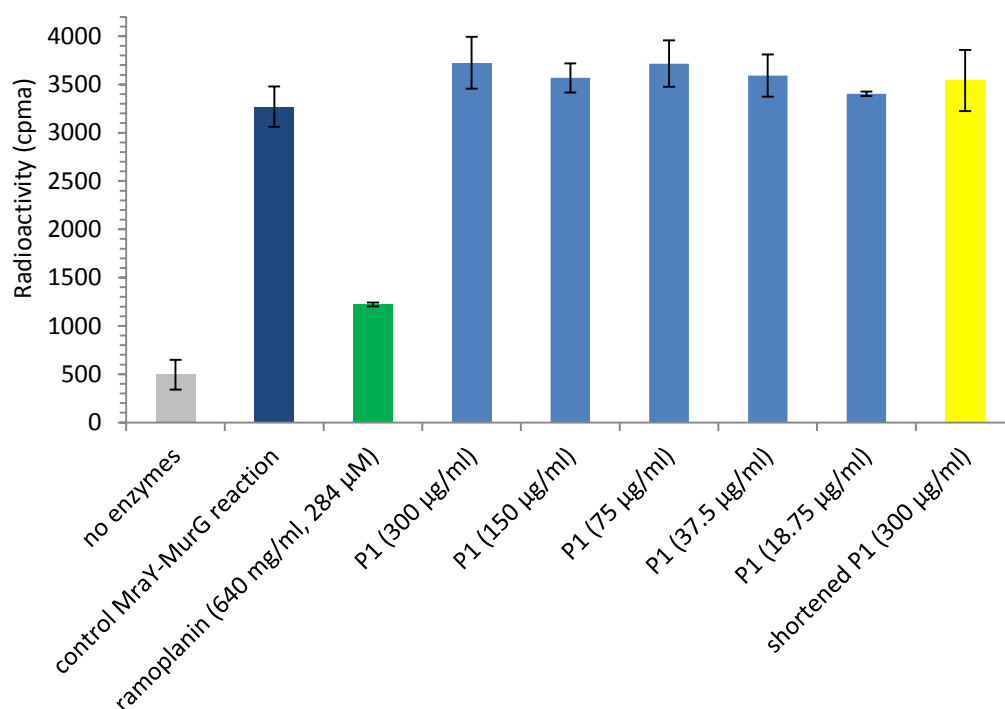


Figure 5-20: P1 against *E. coli* MurG

P1 peptide and its shortened version did not seem to inhibit *E. coli* MurG (Figure 5-20). However, the assay was repeated with *M. flavus* membranes as the unique source of the MraY and MurG enzymes (Section 7.27.2 and Figure 5-21).

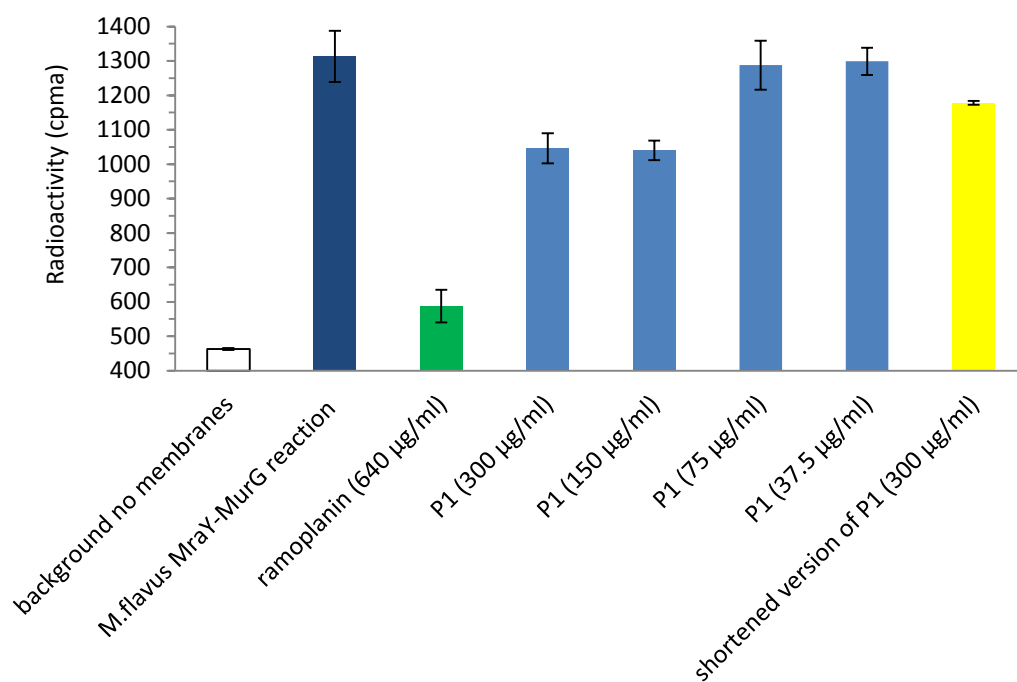


Figure 5-21: P1 against *M. flavus* MurG

Very little inhibition was observed if any, since 300 µg/ml P1 peptide showed 31 ± 2 % inhibition, and the shortened version of P1 showed 16 ± 2 % inhibition against *M. flavus* MurG. The positive control 640 µg/ml ramoplanin showed 85 ± 7 % inhibition.

5.4 Testing of halogenated fluorescein derivatives versus MraY and MurG

Zawadzke *et al* performed a high-throughput screen for MraY-MurG inhibitors by a coupled *E. coli* MraY-MurG scintillation proximity assay⁶⁹. They reported the structures of four hits, which included a di-iodo fluorescein and a tetra-bromo fluorescein analogue (Figure 5-22) with IC₅₀ values of 16.2 and 7.1 μ M respectively. The MIC values against *S. aureus* were determined as >128 and 16 μ g/ml for the two compounds. Further analogues were tested, and it was concluded that the compounds with antimicrobial activity displayed high cytotoxicity which is an undesirable trait for antimicrobial agents. Therefore the inhibition mechanism of the halogenated fluorescein analogues was not investigated any further⁶⁹.

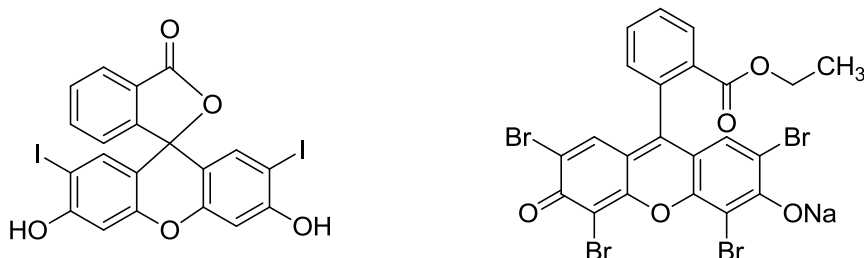


Figure 5-22: Halogenated fluorescein analogues from the hits of the combined MraY-MurG screen of Zawadzke *et al*, di-iodo fluorescein (Mw: 584.10) on the left and tetra-bromo fluorescein analogue (Mw: 697.93) on the right

Fluorescein is known to have some antimicrobial activity against *Streptococcus pneumonia*, *Haemophilus influenzae* and *Moraxella catarrhalis* but not for *S. aureus* or *P. aeruginosa*²⁶⁸. Moreover, halogenated fluoresceins were reported to inhibit *S. aureus* growth²⁶⁹.

An undergraduate chemistry student Justin Slikas synthesised 2,7-dichloro and 2,7-dibromo fluorescein analogues during his summer project in 2011 in Professor Timothy D. H. Bugg's group, the structures are shown in Figure 5-23. Attempts to synthesise the tetrabromo fluorescein were unsuccessful, but he managed to make the mono-bromo-resorcinol as an intermediate which led to the synthesis of the di-bromo fluorescein analogue²⁷⁰. He tested the compounds for antibacterial activity, but they showed no growth inhibition against *E. coli* or *B. subtilis*.

We wished to explore whether these compounds were inhibitors of either MraY or MurG. Since they are highly fluorescent, they could only be assayed by the radiochemical assay which was not working at the time of Justin Slikas's project.

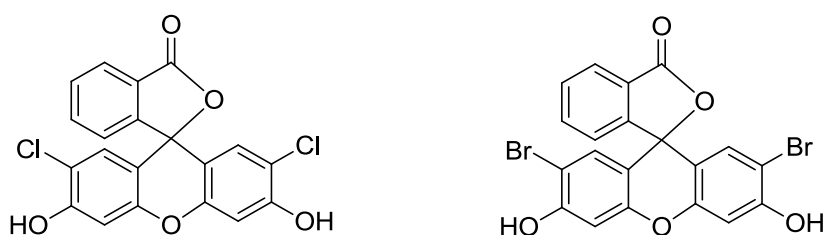


Figure 5-23: 2,7-dichloro fluorescein analogue (Mw: 401.20) and 2,7-dibromo fluorescein analogue (Mw: 490.10) synthesised by Justin Slikas

The compounds were tested by the radiochemical MraY assay (Figure 2-43) in 100 μ l sample containing 1.1 μ M (2.12 nCi/assay) [¹⁴C]-UDPMurNAc-pentapeptide, 23.3 μ g/ml undecaprenyl phosphate, 70 mM Tris pH 7.5, 17.5 mM MgCl₂, 4.0 % (vol/vol) glycerol, 2.3 % (vol/vol) DMSO, 0.1 % Triton X-100, and the reaction was started by the addition of 40 μ g protein containing overexpressed *E. coli* MraY membranes. No inhibition was found against *E. coli* MraY at 165 μ g/ml concentrations for the 2,7-dichloro and 325 μ g/ml concentrations for the 2,7-dibromo fluorescein (Figure 5-24).

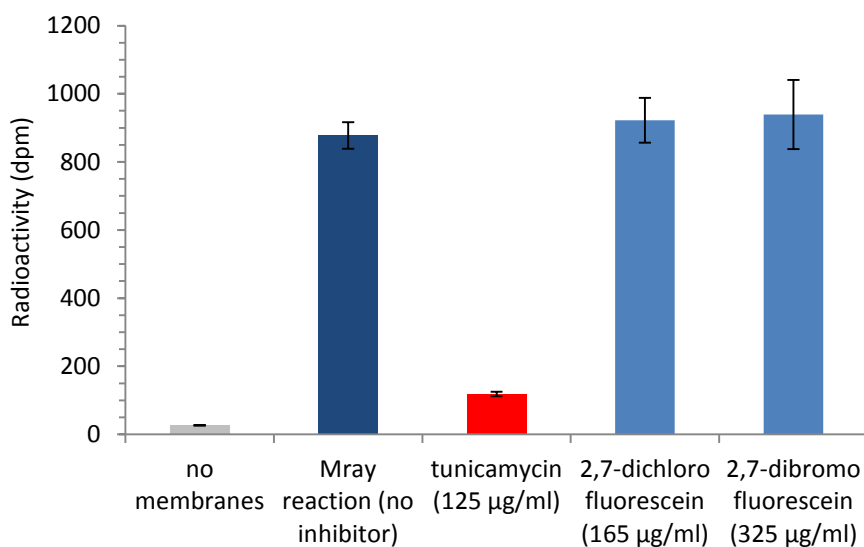


Figure 5-24: Testing halogenated fluorescein analogues against *E. coli* Mray

The 2,7-dichloro and 2,7-dibromo fluorescein analogues were also tested against *E. coli* MurG (Figure 5-19) in a 100 µl total volume that contained 100 µM UDPMurNAc-pentapeptide, 23.3 µg/ml undecaprenyl phosphate, 6.6 µM [³H]-UDPGlcNAc (2.53 nCi/assay), 70 mM Tris pH 7.5, 17.5 mM MgCl₂, 4.0 % glycerol (vol/vol), 2.3 % (vol/vol) DMSO, 0.1 % Triton X-100 to which was added 60 µg *E. coli* membranes containing overexpressed *E. coli* Mray, and 60 µg *E. coli* MurG solution (see Section 7.27.1).

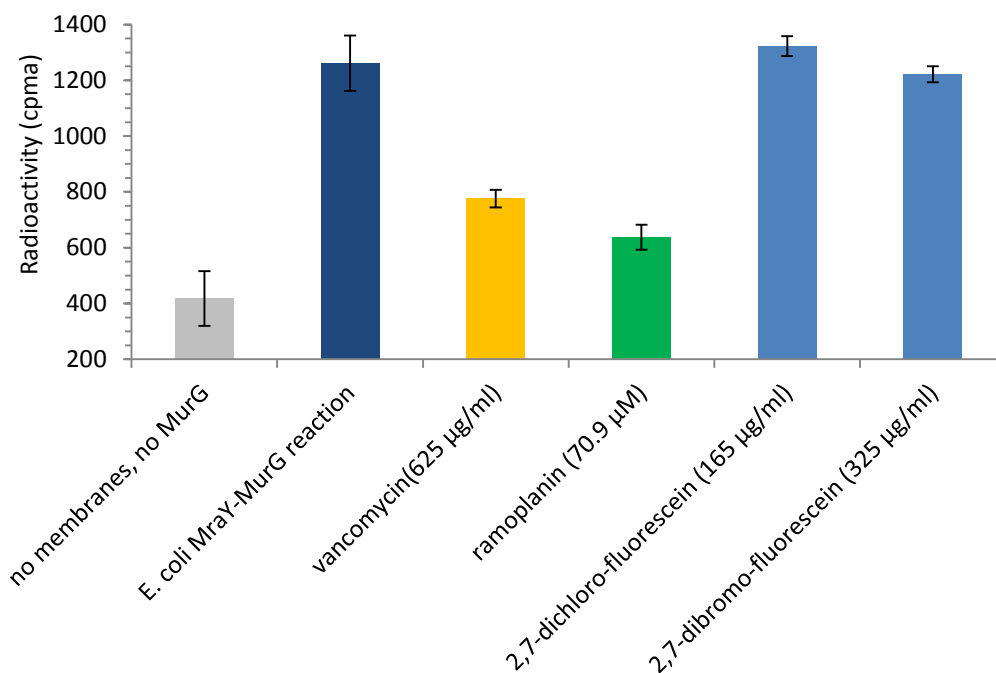


Figure 5-25: Testing halogenated fluorescein analogues against *E. coli* MurG

Figure 5-25 shows that the 2,7-dichloro and the 2,7-dibromo fluorescein did not inhibit *E. coli* MurG at 165 and 325 µg/ml concentrations respectively. It therefore appeared that these compounds do not inhibit MraY or MurG, contrary to the report by Zawadzke *et al.*, although the compounds they reported were di-iodo and tetra-bromo fluorescein analogues. These results suggest that the substitution pattern maybe crucial for inhibition.

It was shown by Rasooly and Weisz that tetra-chlorinated fluorescein analogues significantly inhibit the growth of *S. aureus* and the increase in the number of substituting halogens in the hydroxy-xanthene unit results in an increase in inhibitory activity. Phloxine B, a red dye currently used in cosmetics and as a colour additive in food, was shown to have activity against seven MRSA strains and killed 99 % of mid-log phase *S. aureus* cultures at 100 µg/ml with an MIC of 25 µg/ml²⁶⁹.

The halogenated xanthene dyes are reported insecticides as well because of their photodynamic action. It means that the illumination of the dyes in the presence of oxygen generates singlet oxygen which causes a toxic effect on living cells by reacting with nucleic acids, lipids and proteins²⁷¹. 50 % of *Agrobacterium tumefaciens*, a bacterial pathogen in plants, was shown to be killed by 0.05 μ M phloxine B under continuous illumination²⁷².

Phloxine B's antibacterial activity was investigated further and it was shown that it selectively inhibited the growth of Gram-positive bacteria (*S. aureus*, *B. subtilis*, *B. cereus*, *B. thuringiensis* and *B. mycoides*) in a light-dependent manner. The growth of Gram-negative bacteria (*E. coli*, *Salmonella choleraesuis* and *Shigella flexneri*) was only inhibited in the presence of EDTA by increasing their membrane permeability. The growth inhibition of EDTA-treated Gram-negative organisms was also light-dependent and required longer incubation time²⁷³.

We decided to investigate the potential inhibitory activity of phloxine B, the disodium salt of 2',4',5',7'-tetrabromo-4,5,6,7-tetrachloro fluorescein (Figure 5-26) which is a commercially available dye (Acros), against MraY and MurG.

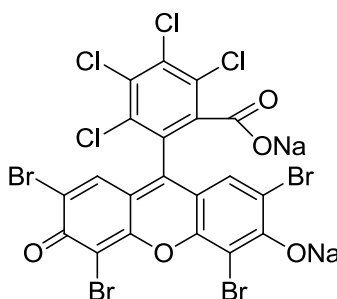


Figure 5-26: Chemical structure of phloxine B, Mw: 829.63

Phloxine B was tested by the radiochemical MraY assay (Section 7.19 and Figure 2-43) at 0-500 μ g/ml in 100 μ l sample containing 3.2 nCi [¹⁴C]-UDPMurNAc-

pentapeptide, 27 µg/ml undecaprenyl phosphate, 70 mM Tris pH 7.5, 17.5 mM MgCl₂, 4.0 % (vol/vol) glycerol, 1 % (vol/vol) DMSO, 0.1 % Triton X-100, and the reaction was started by the addition of 40 µg protein containing overexpressed *E. coli* MraY membranes. 500 µg/ml phloxine B showed 99 ± 9 % inhibition against *E. coli* MraY and an IC₅₀ value of 26.4 ± 1.0 µg/ml was calculated in GenStat (Figure 5-27).

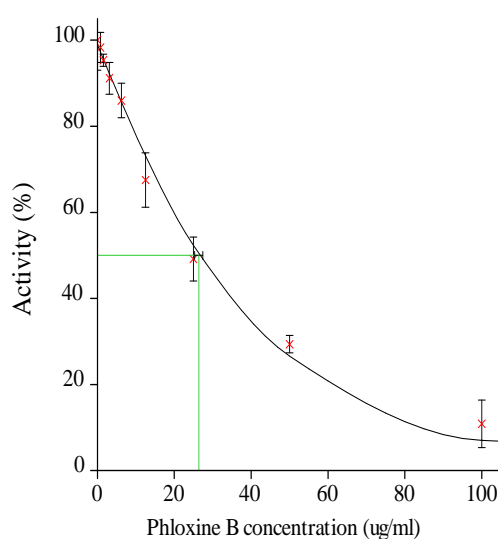


Figure 5-27: Phloxine B inhibition against *E. coli* MraY, IC₅₀: 26.4 ± 1.0

The inhibitory activity of phloxine B was assayed against *S. aureus*, *B. subtilis*, *P. aeruginosa* and *M. flavus* MraY under the same conditions using 35 µg, 40 µg, 20 µg and 40 µg protein containing membranes to start the reactions. Table 5-7 shows the estimated IC₅₀ values (see Figures A 41 - A 45 in Appendix 7).

Table 5-7: Phloxine B inhibition against *S. aureus*, *B. subtilis*, *P. aeruginosa*, *M. flavus* and *E. coli* MraY

MraY from various organisms	IC₅₀ (µg/ml)
<i>S. aureus</i>	211 ± 29
<i>B. subtilis</i>	137 ± 20
<i>P. aeruginosa</i>	106 ± 23
<i>M. flavus</i>	162 ± 25
<i>E. coli</i>	26.4 ± 1.0

The inhibitory activity of phloxine B was the strongest against *E. coli* MraY (IC₅₀: 26.4 ± 1.0 µg/ml, 31.8 µM) and the weakest inhibition was estimated for the *S. aureus* MraY with an estimated IC₅₀ value of 211 ± 29 µg/ml (254 µM). The estimated IC₅₀ values for *P. aeruginosa*, *B. subtilis* and *M. flavus* MraY increased 4, 5 and 6 fold compared to the *E. coli* MraY.

The phloxine B inhibition assay against *E. coli* MraY was repeated in the dark to exclude the possibility of light-activated oxidation of the enzyme as apparent inhibition. An IC₅₀ value of 24.2 ± 1.7 µg/ml was measured (A 46 in Appendix 7) which was almost identical to the previous measurement.

Phloxine B was also tested at 500 µg/ml against *M. flavus* MurG (see Section 7.27.2 and Figure 5-19) in a 100 µl total assay volume that contained 84 µM UDPMurNAc-pentapeptide, 23.3 µg/ml heptaprenyl phosphate, 23.0 µM [³H]-UDPGlcNAc (8.83 nCi/assay), 70 mM Tris pH 7.5, 17.5 mM MgCl₂, 4.0 % glycerol (vol/vol), 2.3 % (vol/vol) DMSO, 0.1 % Triton X-100 to which was added 40 µg protein containing *M. flavus* membranes.

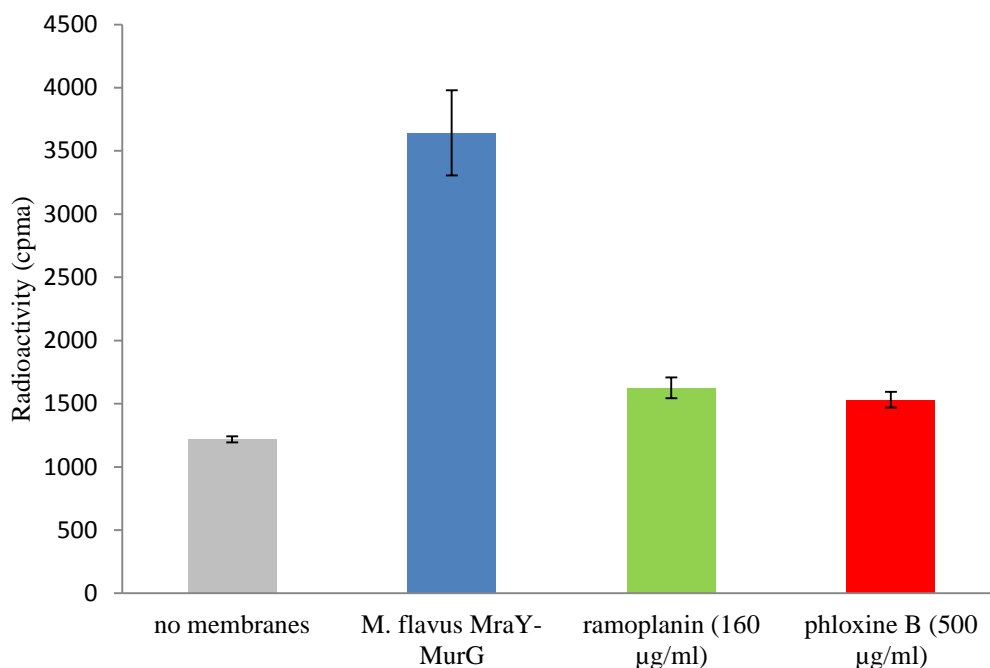


Figure 5-28: Inhibition of phloxine B in the combined *M. flavus* MraY-MurG assay

500 µg/ml phloxine B showed 87.1 ± 3.5 % inhibition in the combined *M. flavus* MraY-MurG assay which is probably due to MraY inhibition (Figure 5-28).

5.4.1 Conclusion

In conclusion, the di-chloro and di-bromo fluorescein analogues did not show inhibition against *E. coli* MraY of MurG at 411 µM and 663 µM respectively. However, when we tested a tetra-bromo fluorescein analogue, phloxine B, a compound structurally more similar to the tetra-bromo fluorescein analogue tested by Zawadzke *et al*, it showed inhibition against *E. coli* MraY with an IC₅₀ value of 31.8 µM. The inhibition we saw in the combined *M. flavus* MraY-MurG assay is probably the result of very potent MraY inhibition at 603 µM concentration of phloxine B. Therefore, phloxine B is definitely an MraY inhibitor. The substitution pattern seems to be important for MraY inhibition for halogenated fluorescein analogues. The increase in the number of substituting bromines in the

hydroxy-xanthene unit from two to four resulted in potent *MraY* inhibition with IC_{50} values of 7.1 μ M for the compound in Zawadzke *et al*⁶⁹ and 31.8 μ M for phloxine B.

Phloxine B is widely used as colour additive in food, drug and cosmetics so it has already met safety specifications^{271, 274}. However, it is worrying that bacteria are constantly exposed to small amounts of phloxine B and therefore they are given the opportunity to develop resistance against it²⁶⁹.

6 Conclusions

Bacterial drug resistance is an increasingly serious problem that threatens public health, and researchers need to develop new drugs. The biosynthetic pathway of the bacterial peptidoglycan is a known and selective target for the development of novel antibacterial agents.

This research project focused on the first lipid-linked step of peptidoglycan biosynthesis. The enzyme required for this step is the integral membrane protein, Phospho-MurNAc-pentapeptide Translocase MraY. The aim of this work was to screen for novel inhibitors of MraY. An existing continuous fluorescence MraY assay was further developed by gathering evidence for the formation of the dansyl-labelled lipid I product of the reaction using LC-MS (Section 2.2). The fluorescence assay was optimised and used to test known and potential MraY inhibitors, such as nucleoside natural products, antimicrobial peptides and structurally new, small molecule potential inhibitors.

The known family of MraY inhibitors, the uridyl-peptide natural products, were suggested to target the active site of MraY at the cytoplasmic face of the membrane. Previously uridyl-peptide natural products were tested by P. Brandish against *E. coli* MraY by means of the continuous fluorescence enhancement assay (1992-95)¹³. The availability of other MraY enzymes allows us to compare the specificity of inhibition for five MraY enzymes; such as *E. coli*, *P. aeruginosa*, *S. aureus*, *B. subtilis* and *M. flavus* (Section 2.1). In addition, new synthetic uridyl-peptide analogues became available during the project. A novel synthetic muraymycin analogue from the University of Paderborn, the 5'-deoxy muraymycin as the bis-TFA salt was tested against *E. coli* MraY and the

antibacterial target *S. aureus* MraY by the continuous fluorescence assay with an IC₅₀ value of 1.6 μ M for each MraY enzyme. The compound also showed 98 %, 89 % and 85 % inhibition against *P. aeruginosa*, *B. subtilis* and *M. flavus* MraYs at 50 μ M (Section 5.1.1). The uridyl-peptide antibiotics interact with MraY at the catalytic binding site on the cytoplasmic phase of the membranes where the suggested catalytic residues are conserved for all five organisms. Therefore, it is not surprising to see inhibition of MraY from all five organisms. In addition, new caprazamycin derivatives from the University of Tübingen were tested against *E. coli* MraY using the continuous fluorescence assay with IC₅₀ values of 1.4 μ M and 6.6 μ M for the hydrocyacyl-caprazol E-acetate and hydrocyacyl-caprazol E-butyrate respectively (Section 5.1.2).

Bacteriophage ϕ 174 uses a single lysis gene, *E*, to cause lysis of the host cell and the encoded 91-amino-acid membrane protein¹⁹⁶ was shown to inhibit *E. coli* MraY^{197, 198}. A 100 % α -helical 37-amino-acid synthetic peptide containing the N-terminal transmembrane domain of E protein was shown to be effective against membrane-bound *E. coli* MraY by a microtitre plate fluorescence enhancement assay (IC₅₀: 0.8 μ M)²⁰⁰. Phe-288 on the periplasmic face of the membrane is known to be an essential residue of *E. coli* MraY for the E protein mediated lysis. Mutation of this residue to lysine resulted in resistance to E protein¹⁹⁷. There is no phenyl-alanine residue at the same position for *S. aureus*, *B. subtilis*, *P. aeruginosa* and *M. flavus* MraYs. No inhibition was observed against *S. aureus*, *B. subtilis*, *P. aeruginosa* and *M. flavus* MraYs at 83 μ g/ml concentrations by the continuous fluorescence MraY assay. The lack of inhibition was later confirmed against *S. aureus*, *P. aeruginosa*, *B. subtilis* and *M. flavus*

MraYs when E peptide was tested by a radiochemical MraY assay at 150 µg/ml concentrations (Section 5.3.1).

The fluorescence assay was adapted to a high-throughput fluorescence assay in microtitre plate format and around 2,000 compounds were screened from the diversity set of the U.S. National Cancer Institute (NCI) against MraY in order to identify novel inhibitors. However, around 22 % of the test compounds from the diversity set interfered with fluorescence and an independent method was needed to complete the testing (Section 3.1).

An attempt was made to develop an HPLC assay that monitors the formation of N-labelled derivatives of lipid I. Consequently; N-labelled UDPMurNAc-pentapeptides at the third position amino acid were prepared with DNP, fluorescamine and dansyl labels in order to make UV-active derivatives. Although, evidence was found for the presence of the labelled lipid I derivatives upon incubation of the UV active UDPMurNAc-pentapeptide derivatives with MraY membranes by LC-MS, the HPLC detection of the lipid I products did not seem to be reproducible and sensitive enough to be used for an MraY assay. Increasing the concentrations of the substrates in the samples could improve HPLC detection but did not seem to be a cost effective solution (Section 2.3).

Therefore, a radiochemical MraY assay was developed using a ¹⁴C-labelled UDPMurNAc-pentapeptide substrate (Figure 2-43), which was enzymatically synthesised, to test compounds that interfered with fluorescence (Section 2.4).

It is important to note of that MraY is an integral membrane protein with ten transmembrane domains (Section 1.2.4). Moreover, one of the substrates of the reaction, the lipid acceptor, undecaprenyl phosphate, or heptaprenyl phosphate

that was also used during the project, needs the use of detergents to be solubilised. Therefore, all *MraY* assays were carried out in the presence of 0.5 % Triton X-100 which would eliminate the danger of protein aggregates appearing as enzyme inhibitors.

We eventually identified one potential *MraY* inhibitor from the NCI diversity set by means of the radiochemical *MraY* assay, the naphthylisoquinoline alkaloid, michellamine B (Figure 6-1), with IC_{50} values of 400 and 340 $\mu\text{g/ml}$ against *E. coli* and *B. subtilis* *MraY* respectively. Interestingly, michellamine B was shown to inhibit reverse transcriptases from both HIV-1 and HIV-2²¹¹, protein kinase C²¹² and human lipoxygenases²¹³. However, we have not been able to establish yet if michellamine B's mechanism of inhibition of these is related to *MraY* inhibition. The compound also showed antibacterial activity against *B. subtilis* with an MIC value of 16 $\mu\text{g/ml}$ (Section 3.3.1). For future work, it would be interesting to synthesise and test some monomeric naphthylisoquinoline analogues against *MraY* for establishing some structure-activity relationship.

The expression of P1 into *E. coli*, a 35-amino acid lysis peptide from the ORF1 in *Acinetobacter* phage 205, was shown to cause cell lysis²⁶⁶. Dr. Roger Levesque's research group at Laval University is interested in the characterization of the lytic mechanism of P1 by using a combination of *in vitro* and *in vivo* approaches. They established that P1 is a bacterial cell wall inhibitor by enzymatic assays against MurA, MurB and MurE with IC_{50} values of 30 μM , 210 μM and 33 μM , respectively. Gene dosage and cell rescue experiments suggested that *MraY* and MurG are also possible targets for P1. P1 was suggested to be a competitive inhibitor of these enzymes by binding to their Mg^{2+} binding site. Therefore, IC_{50}

was determined for the P1 peptide against *E. coli* MraY by means of the radiochemical MraY assay with a value of 157 ± 9 $\mu\text{g/ml}$. P1 peptide was also tested at 300 $\mu\text{g/ml}$ concentrations by the radiochemical assay against *P. aeruginosa* and *S. aureus* MraY, but inhibition was not detected. This enzyme selectivity could suggest that the P1 peptide interacts with *E. coli* MraY at a different site from the site of the uridyl-peptide inhibitors and it may or may not act similarly to E peptide (Section 5.3.3).

It was also established during the project that MraY inhibition from the uridyl-peptide pacidamycin producer, *S. coeruleorubidus*, was detectable directly from culture supernatants by the fluorescence and by the radiochemical MraY assays (Chapter 4). Therefore, we tested culture supernatants and cell extracts from various *Streptomyces* strains. MraY inhibition was observed using cell extracts from *Streptomyces venezuelae*, and higher levels of inhibition were observed from a *gbnB/gbnR* *S. venezuelae* mutant of John Sidda, although it was not possible to identify the active species present. The production of this compound must require very specific conditions. It is quite possible that this is a known uridyl-peptide inhibitor, but it would require additional work to confirm this (Section 4.2).

Following an earlier report of halogenated fluoresceins identified from a combined MraY/MurG screen, we also tested several halogenated fluoresceins (Section 5.4). The di-bromo and di-chloro fluorescein analogues did not inhibit *E. coli* MraY or MurG. However, the antibacterial dye, phloxine B (Figure 6-1), a tetra-bromo fluorescein analogue, was an inhibitor of *E. coli* MraY with an IC_{50} value of 32 μM , and also inhibited MraY from *P. aeruginosa*, *B. subtilis*, *M. flavus* and *S. aureus* with IC_{50} values ranging between 100 and 210 $\mu\text{g/ml}$. The

substitution pattern seems to be important for MraY inhibition for halogenated fluorescein analogues. The increase in the number of substituting bromines in the hydroxy-xanthene unit, from two to four resulted in potent MraY inhibition with IC₅₀ values of 7.1 μ M for the compound in Zawadzke *et al*⁶⁹ and 32 μ M for phloxine B.

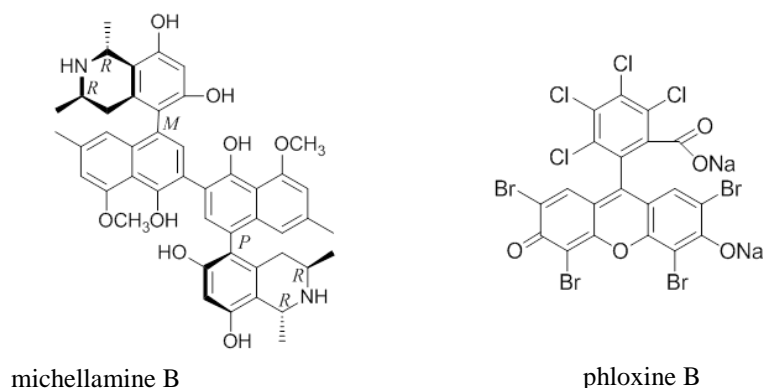


Figure 6-1: Chemical structures of novel MraY inhibitors, michellamine B and phloxine B

For future work, it would be interesting to investigate the sites of interactions of michellamine B, and phloxine B with MraY, the mechanism of action of which may or may not be related. These novel inhibitors of MraY possibly target the previously suggested active site on the cytoplasmic face of the membrane, where three highly conserved aspartate residues, Asp-115, Asp-116 and Asp-267 in *E. coli* MraY, were identified (Section 1.2.3). Alternatively, they target completely different sites on MraY and act by completely different mechanisms of inhibition.

Since, the crystal structure of *Aquifex aeolicus* MraY became available in 2013 (Section 1.2.4); it would be interesting to investigate the binding site of michellamine B and phloxin B with MraY by molecular docking. They could represent new lead compounds for a structure-based design of novel MraY inhibitors.

7 Experimental methods

7.1 Preparation of *E. coli* C43 *MraY* membranes, overexpressed with either *E. coli*, or *S. aureus* or *B. subtilis* *MraY*

Transformation protocol for plasmids carrying the *mraY* gene:

E. coli C43 chemically competent cells were defrosted on ice. A volume of 1-2 μ l plasmid DNA was pipetted into 50 μ l of bacteria and the tube was flicked gently in order to mix. The tube was placed back on ice and incubated for 30 minutes. Then the tubes were placed at 42 °C for 45 seconds. After that the tubes were placed back on ice and 250 μ l of LB media was added. Then the tubes were incubated at 37 °C for 1 hour. 20 μ l and 100 μ l of bacteria were added onto LB agar plates containing the antibiotic resistance marker (100 μ g/ml ampicillin or 50 μ g/ml kanamycin).

An overnight culture derived from a single colony of *E. coli* C43 pJFY3c (LB + 100 μ g/ml ampicillin) was used to inoculate (5 % final concentration) 4 x 1 l of LB/ampicillin in 5 l flasks. The cultures were grown at 37 °C for 4-6 hours with shaking at 180 rpm to an OD_{600nm} \geq 1 (zero on media). IPTG was added to a final concentration of 1 mM and the cultures incubated for a further 3-4 hours before harvesting by centrifugation (4,400 x g, 10 min). Cell pellets were flash frozen in liquid nitrogen and stored overnight at -20 °C. Cells were re-suspended in membrane buffer (50 mM Tris pH 7.5, 2 mM β -mercaptoethanol, 1 mM MgCl₂), 3 ml/g cells at 4 °C. All further steps were carried out at 4 °C or on ice.

Lysozyme 2.5 mg/ml was added and a drop of DNase (Deoxyribonuclease I, bovine pancreas). This suspension was stirred for 1 hour and then cells were broken by passage through a cell disrupter (28 kpsi). Whole cells and debris were removed by centrifugation (24,000 x g, 20 minutes). Membranes were pelleted from the supernatant by ultracentrifugation (150,000 x g, 40,700 rpm, 1 hour). Pellets were re-suspended in ice cold membrane buffer (up to 7 ml). Bradford assay was used to estimate the protein concentration (40-60 mg/ml). The suspension was then flash frozen in liquid nitrogen in 1.5 ml aliquots and stored at -80 °C¹³. The same procedure was used to overexpress *S. aureus* and *B. subtilis* MraYs in C43 *E. coli* membranes.

7.2 Preparation of *E. coli* C43 membranes

An overnight culture derived from a single colony of *E. coli* C43 was used to inoculate (5 % final concentration) 4 x 1 l of LB in 5 l flasks. The cultures were grown at 37 °C shaking at 180 rpm to OD_{600nm}>1 (zero on media), which took 4-6 hours. The cells were harvested by centrifugation (4,400 x g, 10 min). Cell pellets were flash frozen in liquid nitrogen and stored overnight at -80 °C. Cells were re-suspended in membrane buffer (50 mM Tris pH 7.5, 2 mM β-mercaptoethanol, 1 mM MgCl₂), 3 ml/g cells at 4 °C. (All further steps were carried out under 4 °C.) Lysozyme 2.5 mg/ml was added and a drop of DNase (Deoxyribonuclease I, bovine pancreas). This suspension was stirred for 1 hour. Cells were broken through a French Press. Whole cells and debris were removed by centrifugation (24,000 x g, 20 minutes). Membranes were pelleted from the supernatant by ultracentrifugation (150,000 x g, 40,700 rpm, 1 hour). Pellets were re-suspended in ice cold membrane buffer (up to 7 ml max). Bradford assay was carried out to

estimate the protein concentration (15 mg/ml). The suspension was then flash frozen in liquid nitrogen in 1.5 ml aliquots and stored at -80 °C.

7.3 Preparation of *P. aeruginosa* HMS174 pMON2320 membranes (MraY overexpression)

4 x 1 l Terrific media with 50 µg/ml kanamycin was inoculated with 40 ml of an overnight culture of HMS174 carrying the PMON2320 plasmid. Cells were incubated at 37 °C with agitation at 180 rpm until OD_{600nm} ~ 0.4-0.5 was reached. The protein expression was induced with IPTG (1 mM final concentration) for four hours. Cells were harvested by centrifugation (4,400 x g, 10 min). Cell pellets were flash frozen in liquid nitrogen and stored overnight at -80 °C. Cells were re-suspended in membrane buffer (50 mM Tris pH 7.5, 2 mM β-mercaptoethanol, 1 mM MgCl₂), 3 ml/g cells in the cold room. (All further steps were carried out under 4 °C.) Lysozyme 2.5 mg/ml was added and a drop of DNase (Deoxyribonuclease I, bovine pancreas). This suspension was stirred for 30 minutes. Cells were broken using a French Press. Whole cells and debris were removed by centrifugation 2 times (30,000 x g, 16,000 rpm, 20 minutes). Membranes were pelleted from the supernatant by ultracentrifugation (150,000 x g, 40,700 rpm, 1 hour). Pellets were re-suspended in ice cold membrane buffer (up to 7 ml max). Bradford assay was carried out to estimate the protein concentration (12.6 mg/ml). The suspension was then flash frozen in liquid nitrogen in 1.5 ml aliquots. These were stored at -80 °C.

Composition of 1 l Terrific broth media:

12 g Bacto tryptone

24 g yeast extract

9.4 g dipotassium phosphate

2.2 g monopotassium phosphate

4 ml glycerol

7.4 Preparation of *M. flavus* membranes

An overnight culture derived from a single colony of *Micrococcus flavus* was used to inoculate (5 % final concentration) 4 x 1 l of TSB media in 5 l flasks. The cultures were grown at 37 °C shaking at 180 rpm to OD_{600nm} > 1 (zero on media), which took 30 hours. Pellets were harvested by centrifugation (4,400 x g, 10 min). Cell pellets were flash frozen in liquid nitrogen and stored overnight at -80 °C. Cells were re-suspended in membrane buffer (50 mM Tris pH 7.5, 2 mM β-mercaptoethanol, 1 mM MgCl₂), 3 ml/g cells in the cold room. (All further steps were carried out under 4 °C.) Lysozyme 2.5 mg/ml was added and a drop of DNase (Deoxyribonuclease I, bovine pancreas). This suspension was stirred for 30 minutes. Cells were broken by sonication on ice. Whole cells and debris were removed by centrifugation 2 times (~30,000 x g, 16,000 rpm, 20 minutes). Membranes were pelleted from the supernatant by ultracentrifugation (150,000 x g, 40,700 rpm, 1 hour). Pellets were re-suspended in ice cold membrane buffer (up to 4 ml max). Bradford assay was carried out to estimate the protein concentration. And membranes were diluted to achieve 6 mg protein/ml. The suspension was then flash frozen in liquid nitrogen in 1.5 ml aliquots. These were stored at -80 °C.

7.5 Preparation of UDPMurNAc-pentapeptide from *Bacillus subtilis* cells

UDPMurNAc-pentapeptide was isolated from cultures of *Bacillus subtilis* W23. 4 x 500 ml of PYP media was inoculated by an overnight culture of *B. subtilis* at 2 % and grown to $OD_{600} = 1.2$ shaken at 37 °C. The cultures were chilled on ice and cells pelleted by centrifugation at 4,400 x g for 10 minutes at 4 °C. Pellets were re-suspended in 50 ml CWSM. This was added to 500 ml of prewarmed CWSM in a 5 l flask and incubated at 37 °C for 45 minutes. The cultures were chilled on ice again and cells collected by centrifugation at 4,400 x g and at 4 °C for 10 minutes and stored at -20 °C overnight. Thawed cells (~6 g wet weight) were re-suspended in ice-cold 5 % (w/v) TCA (5 ml/g cells). The pellet was extracted two more times with half volumes of ice-cold TCA. The supernatants (60 ml) were pooled and extracted three times with an equal volume of ice-cold diethyl ether (3 x 60ml). The aqueous phase was neutralised with 3 M NaOH, The traces of ether were evaporated by rotary evaporation and the sample was lyophilised overnight. Two ml of the sample was clarified by microcentrifugation and subjected to gel filtration (Sephadex G25, 3 x 80 cm) eluting with water. The highest molecular weight fractions with absorbance at 260 nm were pooled and lyophilised. UDPMurNAc-pentapeptide was identified by LC-MS, m/z [ESI] 1192.30 (M-H)⁻ and HR LC-MS 1192.3359 (M-H)⁻.

PYP medium (pH 7.2) contained bacteriological peptone (20 g/l), yeast extract (1.5 g/l) and K₂HPO₄ (4.5 g/l).

Cell wall synthesis medium (CWSM), (pH 7.4) contained the following ingredients in Table 7-1.

Table 7-1: CWSM medium

Na ₂ HPO ₄	0.26 g/l
NH ₄ Cl	2,0 g/l
KCl	4.0 g/l
MgCl ₂	4.0 g/l
Na ₂ SO ₄	0.15 g/l
FeSO ₄	0.1 g/l
glucose	2.0 g/l
uracil	40 mg/l
L-glutamic acid	120 mg/l
L-lysine	500 mg/l
<i>meso</i> -diaminopimelic acid	120 mg/l
L-alanine	50 mg/l
chloramphenicol	50 mg/l
ampicillin	50 mg/l
vancomycin	12.5 mg/l

PYP and CWSM media were sterilised by autoclaving without FeSO₄ and antibiotics^{13, 145}.

7.6 Conditions for high resolution LC-MS (HR LC-MS)

The high resolution LC-MS analysis was performed by Philip Aston and Dr. Lijiang Song from the Mass Spectrometry Facility of the Chemistry

Department of the University of Warwick by a run on a Dionex Ultramate3000 uHPLC with the Bruker MaXis Mass Spectrometer.

LC parameters and conditions (Table 7-2):

Solvent A: water with 0.1 % ammonium

Solvent B: methanol with 0.1 % ammonium

Flow rate: 0.2 ml/min

Injection volume: 2 μ l

UV: 210 nm

Table 7-2: LC conditions for HR LC-MS

Time (min)	Solvent B (%)
0	1
5	1
25	100
30	100
32	1
40	1

Column: Eclipse plus C18 1.8 μ m 2.1 x 100 mm

7.7 Conditions for LC-MS analysis

LC-MS analysis was performed by a run on an Agilent 1200 HPLC with a Bruker HCT Ultra Mass Spectrometer.

MS conditions:

Mode:

Mass Range Mode: Ultra Scan

Ion Polarity: negative

Ion Source Type: ESI

Alternating Ion Polarity: off

Current Alternating Ion Pol: Negative

Divert Valve: to Waste

Tune SPS:

Target Mass: 1250 m/z

Compound Stability: 100 %

Trap drive Level: 100 %

Optimize: Normal

Smart Parameter Setting: active

Tune Source:

Trap Drive: 94.8

Octopole RF Amplitude: 200.0 Vpp

Lens: 60.0 Volt

Capillary Exit: -184.8 Volt

Dry Temp (Set): 300 °C

Nebulizer (Set): 40.00 psi

Dry Gas (Set): 10.00 l/min

HV Capillary: 4000 V

HV End Plate Offset: -500 V

Trap

Rolling: off

Scan Begin: 50 m/z

Scan End: 3000 m/z

Averages: 5 Spectra

Max. Accu Time: 200,000 μ s

(Smart) ICC Target: 70,000

ICC: on

LC parameters and conditions (Table 7-3 and Table 7-4):

Solvent A: water with 0.1 % ammonium

Solvent B: methanol with 0.1 % ammonium

Flow rate: 0.8 ml/min

Injection volume: 20 µl

Table 7-3: LC conditions for LC-MS analysis of the UDPMurNAc-pentapeptide and the dansyl-labelled UDPMurNAc-pentapeptide

Time (min)	Solvent B (%)
0	5
3	5
8	100
11	100
16	5
21	5

Table 7-4: LC conditions for the LC–MS analysis of lipid products

Time (min)	Solvent B (%)
0	5
5	5
30	100
35	100
40	5
45	5
50	5

Column: Agilent Eclipse XDB-C18 5 µm 4.6 x 150 mm

Detector: Agilent DAD G1315B

7.8 Preparation of UDP-N-acetylmuramyl-L-Ala-γ-D-Glu-(N^ε-dansyl)-*m*-Dap-D-Ala-D-Ala (dansyl-labelled UDPMurNAc-pentapeptide)

UDPMurNAc-pentapeptide (2.5 μmol, 3 mg) was dissolved in 3 ml 0.5 M NaHCO₃ pH 9.0. Dansyl chloride (240 μmol, 64 mg) was dissolved in 3 ml acetone and added to the aqueous solution. The reaction mixture was stirred at room temperature in the dark for 2 hours. After the last addition acetone was removed by rotary evaporation and the yellow solid was removed by microcentrifugation. The dansyl pentapeptide was separated from dansic acid by passage down a gel filtration Sephadex G25 column (80 x 3 cm) eluting with water, collecting 5 ml fractions. All fractions were monitored on a PerkinElmer UV spectrophotometer (absorbance maxima at 250 and 330 nm), and on a PerkinElmer fluorimeter enabling the isolation of the fractions of interest. The fractions of interest were pooled and lyophilised overnight¹⁴¹. The dry powder (yield ~60 %) was dissolved in water to a 1-4 mg/ml stock solution. Negative ion HR LC-MS and LC-MS were performed for analysis of the compound m/z (M-H)⁻ 1425.38.

7.9 Incubation of the dansyl-labelled UDPMurNAc-pentapeptide with MraY membranes

2 x 400 μl of ~100 μM dansyl-labelled UDPMurNAc-pentapeptide (in water), ~80 μg/ml undecaprenyl phosphate (in membrane buffer see Section 7.10) and 240 μg protein containing MraY membranes were incubated in a buffer containing 100 mM Tris pH 7.5, 25 mM MgCl₂, 6 % glycerol and 0.15 %

Triton X-100. One of the samples also contained 83 µg/ml tunicamycin. A total of 150 µl of these mixtures was used to record the fluorescence emission spectrum on a PerkinElmer fluorimeter with excitation at 340 nm at 25 °C a few minutes after sample preparation, 30 minutes later and again straight after 0.1 mM UMP addition.

7.10 General procedure for the continuous fluorescence enhancement MraY assays

The continuous fluorescence assays were performed at 25 °C in a PerkinElmer fluorimeter. The final volume in the cuvette was 180 µl (150 µl master mix, 15 µl test compound and 15 µl membranes) or 170 µl (150 µl master mix, 5 µl test compound and 15 µl membranes.) The MraY reaction was monitored at 340 nm for excitation and at 530 nm for emission.

Preparation of the undecaprenyl or heptaprenyl phosphate solution in a buffer:

A volume of 40 µl undecaprenyl or heptaprenyl phosphate (10 mg/ml stock) that was purchased from Larodan Fine Chemicals was placed in a tube and solvents (chloroform/methanol (2:1) + 3 % (v/v) ammonia) removed with a stream of nitrogen. 4 ml of a buffer containing 50 mM Tris pH 7.5, 2 mM β-mercaptoethanol, 1 mM MgCl₂, 20 % glycerol and 0.5 % TritonX-100 was added, vortexed and sonicated until the solution was clear (0.1 mg/ml).

Preparation of the master mix for the fluorescence enhancement MraY assays:

A typical master mix contains 26 μM dansyl pentapeptide, 35 $\mu\text{g/ml}$ undecaprenyl or heptaprenyl phosphate in a buffer containing ~ 100 mM Tris pH 7.5, ~ 25 mM MgCl_2 (final concentrations). Unless otherwise specified.

An example for the composition of a 20 ml master mix and final concentrations are shown in Table 7-5:

Table 7-5: Composition of the MraY assay mixture for the continuous fluorescence assays

	stock	volume	concentration in the master mix	final concentration in the assay (180 μl)	final concentration in the assay (170 μl)
dansyl-labelled pentapeptide (Mw: 1427.2)	3.75 mg/ml	200 μl	26 μM	22 μM	23 μM
undecaprenyl or heptaprenyl phosphate	0.1 mg/ml	7 ml	35 $\mu\text{g/ml}$	29 $\mu\text{g/ml}$	31 $\mu\text{g/ml}$
buffer	200 mM Tris, 50 mM MgCl_2	10 ml	100 mM Tris, 25 mM MgCl_2	83 mM Tris, 21 mM MgCl_2	88 mM Tris, 22 mM MgCl_2
water		2.8 ml			

Note that the assay always contains 6 % glycerol and 0.15 % Triton X-100 from the buffer that the undecaprenyl or heptaprenyl phosphate solution was made. The presence of detergent is essential for the MraY assay.

A total of 150 μl of the master mix was used for the fluorescence assays in the cuvette. The test compounds were added in 15 or 5 μl volume and for the negative controls the same kind and volume of the solvents was added.

Membranes were diluted in a buffer (membrane buffer) containing a 50 mM Tris pH 7.5, 2 mM β -mercaptoethanol, 1 mM MgCl_2 in order to achieve an ideal stock

concentration. A volume of 15 µl of stock solution of the membranes was added to start the reactions.

7.10.1 Time-course of the MraY reaction

The master mix contained 26 µM dansyl-labelled UDPMurNAc-pentapeptide, 30 µg/ml undecaprenyl phosphate at final concentrations in 83 mM Tris pH 7.5, 21 mM MgCl₂. The reaction was started with the addition of 90 µg protein containing overexpressed MraY membranes in a total volume of 180 µl. The reaction was monitored by a PerkinElmer fluorimeter over 15 minutes. A gradual increase was observed in fluorescence intensity, indicating the formation of dansyl-labelled lipid I. 83 µg/ml tunicamycin was used as a positive control.

7.10.2 Experiment with inactivated MraY membranes

The experiment was carried out in a 180 µl total volume containing 20 µM dansyl-labelled UDPMurNAc-pentapeptide, 30 µg/ml undecaprenyl phosphate in 83 mM Tris pH 7.5, 21 mM MgCl₂ and the reaction was started with the addition of 90 µg protein (membranes) as described in Section 7.10. Under the same conditions previously boiled MraY membranes (C43) were added (90 µg) and no increase in fluorescence intensity was observed over time.

7.10.3 Reverse MraY reaction with UMP addition

180 µl total volume contained 20 µM dansyl-labelled UDPMurNAc-pentapeptide, 30 µg/ml undecaprenyl phosphate in the assay buffer (83 mM Tris pH 7.5, 21 mM MgCl₂) and the reaction was started with the addition of 90 µg protein (membranes) as described in Section 7.10. After 13 minutes reaction time 0.1 mM UMP was added which resulted in a rapid decrease in fluorescence intensity.

7.10.4 Effect of added heptaprenyl phosphate to the fluorescence substrate incubated with *MraY* membranes

The master mix contained 20 μ M dansyl-labelled UDPMurNAc-pentapeptide but no heptaprenyl phosphate, 83 mM Tris pH 7.5, 21 mM $MgCl_2$, 6 % glycerol and 0.1 % Triton X-100. 90 μ g *MraY* membranes (C43) were added and no increase in fluorescence was observed over 10-minute reaction time. 8 μ g/ml (final concentration) heptaprenyl phosphate induced the fluorescence changes.

7.11 IC_{50} determination of pacidamycins by the continuous fluorescence assays

The continuous assays were performed as in Section 7.10. A series of dilutions of pacidamycin 1,2 and pacidamycin D was tested between 0-9 μ g/ml concentrations against and *P. aeruginosa* *MraY*. The reaction mixture contained 30 μ M dansyl-labelled UDPMurNAc-pentapeptide, 30 μ g/ml heptaprenyl phosphate and 60 μ g protein in a total volume of 180 μ l in a buffer containing 83 mM Tris pH 7.5, 21 mM $MgCl_2$. A regression line was fitted to the data from a run of an individual inhibitor concentration between 140-190 seconds using GenStat. That provided an estimate for the slopes, e.g. the initial rates of the *MraY* reactions. The standard errors on the slopes resulting from the variations of the points (10 points/sec) were < 2%. The means of the slopes were then used to calculate % activity, the control lacking inhibitor taken as 100 % activity. A further non-linear regression was used to fit the activity against concentration: The calculation for 50 % activity with the standard error was estimated using GenStat with a curve fitting program. The

curve fitting program is the work of Dr. Julie Jones from the Quantitative Biology Centre (QuiBic) of the University of Warwick.

7.12 K_M determination for the dansyl-labelled UDPMurNAc-pentapeptide with *P. aeruginosa* MraY membranes

A range of different dansyl-labelled UDPMurNAc-pentapeptide concentrations were prepared in a volume of 40 μ l each. These solutions were added to a 500 μ l 85 mM Tris pH 7.5, 22 mM $MgCl_2$ buffer containing 20 μ g/ml heptaprenyl phosphate (total volume 540 μ l). A volume of 150 μ l of these solutions, containing different concentrations of the dansyl pentapeptide, was placed in a cuvette and the reactions were started each time with the addition of 15 μ l 60 μ g protein containing *P. aeruginosa* MraY membranes. Assays were carried out in duplicates.

Final concentrations of the dansyl-labelled UDPMurNAc-pentapeptide (165 μ l total volume) for the experiment: 8.8, 22, 44.1, 88.4 and 176 μ M. The fluorescence intensity was recorded in time in a PerkinElmer fluorimeter, excitation at 340 nm, emission at 530 nm. The rate of the reactions (v) was determined between 80 and 130 seconds on the curves. $1/[s]$, $1/v$ and $v/[s]$ and $[s]/v$ values were calculated in order to use the graphical methods such as plotting v vs. $[s]$, the Eadie-Hofstee ($v/[s]$ vs. v), the Lineweaver-Burk $1/v$ vs. $1/[s]$ and the Hanes-Woolf $[s]/v$ vs. $[s]$ for K_M determination (Table 7-6).

Table 7-6: Calculations for K_M determination with graphical methods

[s]	8.8	22	44.1	88.4	176
v	0.127	0.258	0.292	0.327	0.355
stdev on v	0.020	0.030	0.030	0.033	0.030
v/[s]	0.014	0.012	0.007	0.004	0.002
[s]/v	69.074	85.238	150.924	270.750	495.495
1/[s]	0.114	0.045	0.0227	0.011	0.006
1/v	7.849	3.874	3.422	3.062	2.815

7.13 Evidence for the presence of the dansyl-labelled lipid I by LC-MS

80 μ M dansyl-labelled UDPMurNAc-pentapeptide (3.75 mg/ml stock) was incubated with 200 μ g MraY membranes and 35 μ g/ml undecaprenyl or heptaprenyl phosphate (0.1 mg/ml stock in 50 mM Tris pH 7.5, 2 mM β -mercaptoethanol, 1 mM $MgCl_2$, 20 % glycerol and 0.5 % Triton X-100) in a buffer containing 100 mM Tris pH 7.5, 25 mM $MgCl_2$ in a total volume of 200 μ l. The mixture was vortexed and left for 30 minutes at room temperature to form the lipid products. The reaction was stopped by the addition of 50 % 6 M pyridinium acetate (200 μ l), and an additional 50 % (400 μ l) 1-butanol was added. The mixture was vortexed for 2 minutes and centrifuged at 12 000 x g for 4 minutes. The butanol extracted products were analysed by a run on a Dionex Ultramate3000 uHPLC with Bruker MaXis by Philip Aston as in Section 7.6.

7.14 Preparation of UDP-N-acetylmuramyl-L-Ala- γ -D-Glu-(N^ε-2,4-dinitrophenyl)-*m*-Dap-D-Ala-D-Ala (DNP-labelled UDPMurNAc-pentapeptide)

UDPMurNAc-pentapeptide (2.5 μ mol, 3 mg) was dissolved in 2.5 ml 0.5 M NaHCO₃ pH 9.0. 1-Fluoro-2,4-dinitrobenzene (100 mg) was dissolved in 2.5 ml acetone and added to the aqueous solution. The reaction mixture was stirred at room temperature in the dark for 24 hours. Acetone was removed by rotary evaporation. The labelled pentapeptide was purified by passage down a gel filtration Sephadex G25 column (80 x 3 cm) eluting with water, collecting 5 ml fractions. All fractions were monitored on a PerkinElmer UV/Vis spectrophotometer (absorbance maxima at 250 and 360 nm), enabling the isolation of the fractions of interest. The fractions of interest were pooled and lyophilised overnight. The dry powder was dissolved in water. Negative ion HR LC-MS was performed on a Dionex Ultramate3000 uHPLC with Bruker MaXis as in Section 7.6.

7.15 Preparation of UDP-N-acetylmuramyl-L-Ala- γ -D-Glu-(N^ε-fluorescamine)-*m*-Dap-D-Ala-D-Ala (fluorescamine-labelled UDPMurNAc-pentapeptide)

UDPMurNAc-pentapeptide (3.8 mg) was dissolved in 3 ml 0.5 M NaHCO₃ pH 9.0. Fluorescamine (84 mg) was dissolved in 3 ml acetone and added to the aqueous solution. The reaction mixture was stirred at room temperature in the dark for 25 minutes. Acetone was removed by rotary evaporation. The

fluorescamine-labelled pentapeptide was purified by passage down a gel filtration Sephadex G25 column (80 x 3 cm) eluting with water, collecting 5 ml fractions. All fractions were monitored on a PerkinElmer UV spectrophotometer (absorbance maxima at 250 and 390 nm) enabling the isolation of the fractions of interest. The fractions of interest were pooled and lyophilised overnight. The dry powder was dissolved in water to a 1 mg/ml stock solution. Negative ion HR LC-MS was performed on a Dionex Ultramate3000 uHPLC with Bruker MaXis as in Section 7.6.

7.16 Attempt to make an HPLC-based *MraY* assay

A 60 µl volume containing ~1 mg/ml UDPMurNAc-pentapeptide or one of the N-labelled pentapeptides (300 µg/ml final concentration) was incubated with 40 µl 0.1 mg/ml heptaprenyl phosphate in 50 mM Tris pH 7.5, 2 mM β-mercaptoethanol buffer, 1 mM MgCl₂, 20 % glycerol and 0.5 % Triton-X100 (20 µg/ml final concentration), with 40 µl of 5 mg/ml *MraY* membranes (overexpressed with various *MraY*s or *M. flavus* membranes) and with 60 µl buffer containing 200 mM Tris pH 7.5, 50 mM MgCl₂. The mixture of 200 µl was vortexed and incubated at 37 °C for 30 minutes at room temperature to form the lipid products. The reaction was stopped by the addition of 50 % 6 M pyridinium acetate (200 µl), and an additional 50 % (400 µl) 1-butanol was added. The mixture was vortexed for 4 minutes and centrifuged at 13,000 x g for 4 minutes. The butanol extracted products were analysed by LC-MS as it is described in Section 7.7.

7.17 Conversion of UDPMurNAc-tripeptide to UDPMurNAc-pentapeptide (before optimising the procedure)

A crude enzyme preparation (*E. coli* extract) having alanine racemase, D-Ala : D-Ala ligase and D-Ala-D-Ala adding activity (MurF) was made. The ingredients for a 500 μ l reaction (unlabelled) were the following:

Buffers: 0.25 M Tris-HCl, pH 8.4, 2.5 M Tris-HCl, pH 8.4

Reaction mixture:

250 mM Tris-HCl, pH 8.4	46 μ l
70.9 mM UDPMurNAc tripeptide	14 μ l (1 μ mol)
80 mM L-Ala	25 μ l (2 μ mol)
200 mM ATP	100 μ l, needs neutralising, then dissolved in buffer
800 mM MgCl ₂	50 μ l
2 M KCl	5 μ l
100 mM DTT (1 M stock diluted in 2.5 M buffer)	10 μ l
8 mM Pyridoxal phosphate	50 μ l

The last addition to the 2 ml Eppendorf was the 200 μ l enzyme extract (38.42 mg/ml protein concentration). The reaction mixture was incubated at 37 °C for ~3 hours. The sample was boiled for 3 minutes at 100 °C and microcentrifuged (12,000 x g for 2 minutes) to remove the denatured protein. The sample was purified through passage down a Sephadex G25 gel filtration column

and high molecular weight fractions showing absorbance maxima at 210 and 260 nm were collected, concentrated by freeze-drying and analysed by LC-MS (Section 7.7).

Preparation of an *E. coli* cell-free extract

CFE (Cell Free Extract) Medium contained 10 g casamino acids, 5 g yeast extract, 6 g Na_2HPO_4 , 1 g KH_2PO_4 in 900 ml water and was autoclaved. 20 g glucose in 100 ml water was sterilized separately and added to get 1 l media at pH 7. 100 ml CFE medium was inoculated with a single colony of *E. coli* K21 from an agar plate. The overnight culture was used to inoculate 2 x 2 l media at 2 %. These were shaken at 37 °C 180 rpm for 3.5 hours up to $\text{OD}_{600} \sim 0.4$ (mid log-phase). The cells were harvested at 12,000 x g, for 20 minutes at 4 °C. Pellet was re-suspended in 10 ml 0.02 M potassium phosphate buffer pH 7, 1 mM DTT and 1 mM EDTA. The suspension was sonicated for 4 x 30 secs (30 secs between bursts) on ice. The sonicated suspension was spun at 13,000 x g. The supernatant was dialysed overnight at 4 °C vs. 2 l 0.1 M potassium phosphate buffer containing 1 mM DTT at pH 7.

Preparation of 0.1 M and 0.02 M potassium phosphate buffers at pH 7:

Two solutions were prepared:

1. 0.5 l of 1 M K_2HPO_4 (174.18 g/mol)
2. 0.5 l of 1 M KH_2PO_4 (136.09 g/mol)

In order to prepare 0.1 M potassium phosphate buffer 61.5 ml 1 M K_2HPO_4 and 38.5 ml 1 M KH_2PO_4 was mixed and completed to 1 l with water. The 0.02 M potassium phosphate buffer was prepared by dilution of the 0.1 M potassium

phosphate buffer. The protein concentration was determined by the Bradford assay using albumin standards (38.42 mg/ml)¹³.

7.18 Radiochemical synthesis of the [¹⁴C]-UDPMurNAc-pentapeptide (optimised version)

The synthesis consists of a single overnight incubation at 37 °C of 1 µmol UDP-MurNAc-tripeptide with 3 µmol L-alanine (10 µCi/µmol), alanine racemase, DdlB, MurF, ATP and pyridoxal phosphate. The total volume of the reaction was 450 µl. The detailed composition is shown in Table 7-7. The reaction was first optimised without ¹⁴C-L-alanine.

Table 7-7: Reaction mixture (400 µl + 50 µl enzymes):

250 mM Tris HCl, pH 8.4	102 µl
160 mM L-Ala	19 µl
0.1 mCi/ml ¹⁴ CH ₃ ¹⁴ CH(NH ₂) ¹⁴ CO ₂ H	300 µl (freeze-dried and mixed with L-Ala)
200 mM ATP	100 µl
8 mM pyridoxal phosphate	50 µl
1 M MgCl ₂	50 µl
2 M KCl	10 µl
1M DTT	2 µl
UDPMurNAc-tripeptide	67 µl
7 mg/ml alanine racemase (<i>E. coli</i>)	20 µl
3.5 mg/ml DdlB (<i>E. coli</i>)	20 µl
24 mg/ml MurF (<i>P. aeruginosa</i>)	10 µl

The enzymes were removed by ultrafiltration with a centricon membrane (cut off 10,000 Da). The filtrate was purified by gel filtration (Sephadex G 25, 30 x 1 cm)

eluting with water collecting ~4 ml fractions. The fractions were monitored by a PerkinElmer UV-Vis Spectrophotometer. The highest molecular weight fractions (eluting first) with absorbance maxima at 210 and 260 nm were collected and counted in a scintillation counter (the neighbouring fractions that were collected before and after as well). The two fractions containing high counts (9,575 and 24,575 dpm/10 µl) were put away for the assays (Table 7-8). The non-labelled version of the radiochemical substrate synthesis was tested by LC-MS in order to confirm the presence of UDPMurNAc-pentapeptide.

Table 7-8: Radioactivity in fractions

fraction	radioactivity in 10 µl fraction (dpm)
3	28
4	9,575
5	24,575
6	3,827
7	2,241
8	44,747
9	25,979
10	518
11	46

7.19 General radiochemical MraY assay procedure

Assays were carried out as described by A. Lloyd *et al.* (2004)¹³⁰. A solution of [¹⁴C]-UDPMurNAc-pentapeptide (1-4 nCi/assay) was incubated for 30 minutes at 35 °C with 27 µg/ml undecaprenyl or heptaprenyl phosphate (0.1 mg/ml stock in buffer, see Section 7.10) and 30-50 µg overexpressed MraY membranes in a buffer containing 100 mM Tris pH 7.5, 17.5 mM MgCl₂, 4.0 % (vol/vol) glycerol, 2.3 % (vol/vol) DMSO, 0.1 % Triton X-100 a total volume of 100 µl. The mixture

was vortexed and left for 30 minutes at 35 °C to form the lipid products. The reaction was stopped by the addition of 50 % 6 M pyridinium acetate pH 4.2 (100 µl), and an additional 50 % (200 µl) 1-butanol was added. The mixture was vortexed for four minutes and centrifuged at 13,000 x *g* for 4 minutes. A volume of 200 µl of the upper butanol layer (the whole upper layer seems to be 250 µl) was placed in ~5 ml ScintiSafe scintillation liquid and quantified by liquid scintillation counting by a PerkinElmer scintillation counter (dpm). Mixtures for control experiments lacked *MraY* membranes (background) and measurements were corrected by subtracting the background radioactivity. Assays were carried out in duplicates at the presence of inhibitors at various concentrations. The negative control (no inhibitor) was prepared in quadruplets or sextuplets and inhibition by tunicamycin (125 or 250 µg/ml) or pacidamycin D (3 µg/ml) in duplicates was used as a positive control. IC₅₀ was measured from a plot of enzyme activity vs. inhibitor concentration where the negative controls lacking inhibitor was taken as 100 % activity, and error calculated by the same curve fitting program in GenStat that was used for the fluorescence measurements.

Typical composition of a 3 ml master mix:

- 1500 µl assay buffer (200 mM Tris pH 7, 50 mM MgCl₂)
- 1000 µl heptaprenyl or undecaprenyl phosphate (0.1 mg/ml stock in 50 mM Tris pH 7.5, 2 mM β-mercaptoethanol, 1 mM MgCl₂, 20 % glycerol and 0.5 % Triton-X100, see Section 7.10)
- 100 µl DMSO
- 120 µl ¹⁴C-labelled substrate (24,500 dpm/10 µl)
- 280 µl water

For the assays 80 µl master mix was placed into a 1.5 ml Eppendorf vial, then 10 µl inhibitor solution was added and the reaction was started with the addition of 10 µl MraY membranes (2-5 mg/ml protein stock) in 100 µl total volume.

7.19.1 Radiochemical assay for the wild type *E. coli* MraY

The general procedure applies as in Section 7.19. The total volume of 100 µl sample contained 1.7 µM ¹⁴C-labelled UDPMurNAc-pentapeptide (3.4 nCi, 7,500 dpm), 27 µg/ml heptaprenyl phosphate in 90 mM Tris pH 7.5, 23 mM MgCl₂, 4.0 % (vol/vol) glycerol, 2.3 % (vol/vol) DMSO, 0.1 % Triton X-100 and 40 µg protein containing overexpressed (C43) membranes or 40 µg wild type *E. coli* (C43) membranes. Known inhibitors were added such as tunicamycin (125 µg/ml), E peptide (100 µg/ml), pacidamycin D (3 µg/ml) and a capuramycin analogue, A-503083 B (1.2 µg/ml).

7.19.2 Investigation of D, D-carboxypeptidase activity

The general procedure applies as in Section 7.19. Each sample contained 1,800 dpm in total, 27 µg/ml heptaprenyl phosphate in 90 mM Tris pH 7.5, 23 mM MgCl₂, 4.0 % (vol/vol) glycerol, 2.3 % (vol/vol) DMSO, 0.1 % Triton X-100 and the reaction was started with the addition of 40 µg protein containing overexpressed C43 membranes. Samples containing 100 µg/ml ampicillin in order to stop D,D-carboxypeptidase activity were compared to samples with no ampicillin. 100 µg/ml tunicamycin was used for inhibition. Samples were prepared in duplicates.

7.19.3 Background activity from the endogenous undecaprenyl phosphate in *E. coli* C43 membranes

2.4 nCi (5,275 dpm) was the total radioactivity in each sample with no heptaprenyl phosphate in 90 mM Tris pH 7.5, 23 mM MgCl₂, 4.0 % (vol/vol) glycerol, 2.3 % (vol/vol) DMSO, 0.1 % Triton X-100. The MraY reaction was started with the addition of 40 µg protein containing (C43) membranes. Control samples were prepared in quadruplets also containing 27 µg/ml heptaprenyl phosphate.

7.19.4 The time-course of the MraY reaction by the radiochemical assay

The general procedure applies as in Section 7.19. The reaction was stopped at 1, 5 10 and 15 minutes after the membrane addition. Lipid products were extracted each time into butanol as described in Section 2.4.2.1 and radioactivity was measured by liquid scintillation counting. 100 µl total volume contained 1.7 µM ¹⁴C-labelled UDPMurNAc-pentapeptide (3.4 nCi, 7,500 dpm), 27 µg/ml heptaprenyl phosphate in 90 mM Tris pH 7.5, 23 mM MgCl₂, 4.0 % (vol/vol) glycerol, 2.3 % (vol/vol) DMSO, 0.1 % Triton X-100 and 40 µg protein containing overexpressed C43 membranes. The experiment was repeated with the addition of 40 µg protein overexpressed *B. subtilis*, 35 µg protein overexpressed *S. aureus*, 20 µg protein overexpressed *P. aeruginosa* in *E. coli* C43 membranes and 40 µg *M. flavus* membranes.

7.19.5 Overproduction of enzyme activity in the *E. coli* MraY membranes and comparison with the wild type *M. flavus*

The forming radiolabelled lipid products were quantified after 30 minutes reaction time using overexpressed MraY *E. coli* and *M. flavus* membranes. Lipid products were extracted each time into butanol as described in Section 2.4.2.1 and radioactivity of 200 µl butanol was measured by liquid scintillation counting. 100 µl total volume contained 1.7 µM ¹⁴C-labelled UDPMurNAc-pentapeptide (3.4 nCi), 27 µg/ml heptaprenyl phosphate in 90 mM Tris pH 7.5, 23 mM MgCl₂, 4.0 % (vol/vol) glycerol, 2.3 % (vol/vol) DMSO, 0.1 % Triton X-100 and 40 µg protein containing overexpressed *E. coli* (C43) membranes. The experiment was repeated with the addition of overexpressed *E. coli* (C43) membranes with MraY from *B. subtilis* (40 µg protein), *S. aureus* (35 µg protein), *P. aeruginosa* (20 µg protein) and *M. flavus* membranes (40 µg protein).

7.20 Fluorescence plate reader assays

The plate reader assays were performed at room temperature in a Tecan Genios Plate-Reader. The final volume in each micro-well was 100 µl (85 µl master mix, 5 µl test compound, 10 µl membranes). Measurements were taken before the start of the reaction, then over 20 minutes at 5 minute intervals, and once again at 30 minutes reaction time monitoring at a specified wavelength (excitation 340 nm, emission 535 nm).

Preparation of the undecaprenyl or heptaprenyl phosphate solution in a buffer:

A volume of 40 µl undecaprenyl or heptaprenyl phosphate (10 mg/ml stock) that was purchased from Larodan Fine Chemicals was placed in a tube and solvents

(chloroform/methanol (2:1) + 3 % (v/v) ammonia) removed with a stream of nitrogen. 4 ml of a buffer containing 50 mM Tris pH 7.5, 2 mM β -mercaptoethanol, 1 mM MgCl_2 , 20 % glycerol and 0.5 % Triton X-100 was added, vortexed and sonicated until the solution was clear (0.1 mg/ml).

Preparation of the master mix for the plate reader assays:

The master mix contains 13.1 μM dansyl-labelled UDPMurNAc-pentapeptide, 20 $\mu\text{g/ml}$ undecaprenyl or heptaprenyl phosphate in a buffer containing 100 mM Tris pH 7.5, 25 mM MgCl_2 (final concentrations in the master mix). Unless otherwise specified.

The typical composition of a 20 ml master mix and the final concentrations in the wells are shown in Table 7-9:

Table 7-9: Composition of a 30 ml master mix for the fluorescence MraY plate reader assays

	stock	volume	concentration in the master mix	final concentration in the assay (100 μl volume)
dansyl-labelled UDPMurNAc-pentapeptide (Mw: 1427.2)	3.75 mg/ml	100 μl	13.1 μM	11.2 μM
undecaprenyl or heptaprenyl phosphate	0.1 mg/ml	4 ml	20 $\mu\text{g/ml}$	17 $\mu\text{g/ml}$
assay buffer	200 mM Tris, 50 mM MgCl_2	10 ml	100 mM Tris, 25 mM MgCl_2	85 mM Tris, 21.25 mM MgCl_2
water		5.9 ml		

Note that the assay always contains 3 % glycerol and 0.1 % Triton X-100 at final concentrations from the buffer that the undecaprenyl or heptaprenyl phosphate solution was made. The presence of detergent is essential for the MraY assay.

A volume of 85 μ l of the master mix was used for the fluorescence assays in each well. The test compounds were added in 5 μ l volume. A volume of 5 μ l of a 2 mM stock solution of compounds from the diversity set (diluted in 100 mM Tris, 25 mM MgCl_2 from 10 mM stock in DMSO) were tested at 100 μ M final concentrations.

A volume of 5 μ l tunicamycin (2.5 mg/ml stock in DMSO, 25 μ g/ml final concentrations) was added as positive control (known inhibitor). A volume of 5 μ l 20 % (v/v) DMSO (diluted in 100 mM Tris, 25 mM MgCl_2) was added as negative control. Membranes were diluted to 4 mg protein/ml for *E. coli* membranes in 50 mM Tris pH 7.5, 2 mM β -mercaptoethanol, 1 mM MgCl_2 (membrane buffer).

A volume of 10 μ l of the membranes was added to start the reaction. For the negative control “no membranes” 10 μ l membrane buffer (50 mM Tris pH 7.5, 2 mM β -mercaptoethanol, 1 mM MgCl_2) was added instead of the membranes.

7.21 Testing hits from the initial fluorescence screen of the NCI diversity set by the continuous fluorescence assay

The hits from the microtitre fluorescence MraY assay were tested at 60 μ M concentration in a total volume of 170 μ l containing 20 μ M dansyl-labelled UDPMurNAc-pentapeptide, 35 μ g/ml heptaprenyl phosphate, 83 mM Tris pH 7.5,

21 mM MgCl₂, 6 % glycerol and 0.15 % Triton X-100. The reaction was started by the addition of 60 µg MraY membranes. 14.7 µg/ml tunicamycin was used as a positive control. See Section 7.10.

7.22 Testing low fluorescence and high fluorescence compounds from the NCI diversity set by the radiochemical MraY assay

The general procedure applies as in Section 7.19. The total volume of 100 µl sample contained 1.2 µM [¹⁴C]-labelled UDPMurNAc-pentapeptide (2.4 nCi), 27 µg/ml heptaprenyl phosphate in 90 mM Tris pH 7.5, 23 mM MgCl₂, 4.0 % (vol/vol) glycerol, 2.3 % (vol/vol) DMSO, 0.1 % Triton X-100 and 40 µg protein containing overexpressed MraY membranes. The test compounds were added in 5 µl volume at 100 and 500 µM concentrations. Assays were carried out in duplicates.

7.23 Testing michellamine B by the radiochemical MraY assay

The general procedure applies as in Section 6.19. The total volume of 100 µl sample contained 1.7 µM ¹⁴C-labelled UDPMurNAc-pentapeptide (3.2 nCi), 27 µg/ml heptaprenyl phosphate in 90 mM Tris pH 7.5, 23 mM MgCl₂, 4.0 % (vol/vol) glycerol, 2.3 % (vol/vol) DMSO, 0.1 % Triton X-100 and 40 µg protein containing overexpressed MraY membranes. The test compounds were added in 10 µl volume at 125, 250 and 500 µg/ml concentrations. Assays were carried out

in duplicates. IC₅₀ was determined by a plot of % activity inhibitor concentrations with the help of a curve fitting program in GenStat. See Section 2.2.6.

7.24 Antibacterial testing, microtitre broth dilution and agar plate filter disc methods

7.24.1 Microtitre broth dilution

Michellamine B was tested for antibacterial activity and minimal inhibitory concentration (MIC) against *E. coli* DH5 α , *B. subtilis* (W23) and *P. putida* (ATCC 33015). 3 x 10 ml LB medium was inoculated by a single colony picked from an LB agar plate overnight from each strain and incubated at 37 °C with shaking at 180 rpm. 100 μ l of this culture was used to inoculate 9.9 ml LB medium, incubated at 37 °C with shaking at 180 rpm until OD₆₀₀ was 0.6. The culture was diluted 100 fold and 95 μ l of this diluted culture was placed in 96-well plates and to each well 5 μ l inhibitor solution was added up to a total volume of 100 μ l. Michellamine B was tested at 125, 62.5, 31.3, 15.6, 7.81, 3.91 and 1.95 μ g/ml final concentrations. The 125 μ g/ml Michellamine B sample contained 2.5 % DMSO and further dilutions were made with water. Samples were carried out in triplicates. For the controls wells contained 100 μ l LB for checking bacterial contamination. For monitoring bacterial growth without antibiotics, 5 μ l water or 5 μ l DMSO containing solution was added. The concentration of DMSO for the negative controls was \leq 2.5 % in the samples, three different compositions were used for the 5 μ l solutions: DMSO:H₂O ratio: 1:2, 1:4 and 1:8. 5 μ l kanamycin solutions at 50, 25, 12.5, 6.25, 3.13, 1.56 0.781, and 0.391 μ g/ml final

concentrations was added for the positive controls. The plates were incubated and shaken at 37 °C and bacterial growth was monitored by the naked eye.

7.24.2 Agar plate filter disc method

3 x 10 ml LB medium was inoculated by a single colony of one of the three strains picked from an LB agar plate and incubated and shaken overnight at 37 °C. 100 µl of the overnight culture was used to inoculate 10 ml LB which was incubated at 37 °C and shaken at 180 rpm until OD₆₀₀ was 0.6. This culture was diluted 100 fold. 300 µl of the diluted culture was mixed and vortexed with 3 ml LB containing 0.7 % (w/v) agar, poured on top of an LB plate and spread evenly. Sterile filter discs were placed on the plates containing 25 µl michellamine B solutions at 0.05, 1.25 and 2.5 mg/ml concentrations. 25 µl of 1 mg/ml ampicillin and 2 mg/ml kanamycin was used as positive controls.

A small zone of inhibition was observed around the discs containing 50, 100 and 200 µg/ml michellamine B for the *B. subtilis* culture plates. No inhibition was observed against *E. coli* and *P. putida*.

7.25 Assay of *Streptomyces* culture supernatants

7.25.1 *Streptomyces* culture supernatants

7.25.1.1 Preparation of *Streptomyces* culture supernatants

Streptomyces strains were grown on MS agar plates for ten days. Spores were collected in sterile water and stocks were made in a 1 : 1 ratio of spore solution : 50 % glycerol/water. 10 ml ISP2 media was inoculated with 10 µl spore stock solutions and incubated at 30 °C for 2 days at 30 °C. Then, 50 µl of the cultures

were used to inoculate 10 ml ISP2 and Lac-MM media, and the cultures were incubated for 8 days at 30 °C. The cultures were centrifuged for 2 minutes at 5,000 x g and the supernatants were tested against MraY by the continuous and the micro-titre plate reader fluorescence MraY assay against *E. coli* MraY. 15 µl culture supernatant was added to a final volume of 180 µl for the continuous assays and 10 µl cultures were used for the plate reader assays in a total volume of 100 µl. See Sections 7.10 and 7.20.

MS agar:

agar: 20 g

mannitol: 20 g

soya flour: 20 g

completed to 1 l with water

ISP2:

4 g yeast extract

10 g malt extract

4 g glucose

Completed to 1 l with water, adjust pH to 7.3 with 1N NaOH, and autoclaved

Lac-MM

450 ml MM

50 ml 10 % lactose

MM:

2.14 g NH₄Cl 40 mM final conc.

0.6 g MgSO₄ 2.4 mM final conc.

1.74 g K₂HPO₄ 10 mM final conc.

20.99 g MOPS 100 mM final conc.

0.2 ml 50 mg/ml FeSO₄·2H₂O

0.2 ml 50 mg/ml $\text{MnCl}_2 \cdot 4\text{H}_2\text{O}$

0.2 ml 50 mg/ml $\text{ZnSO}_4 \cdot 7\text{H}_2\text{O}$

0.2 ml 50 mg/ml CaCl_2

water to 900 ml (or 950 ml for MM*), adjust pH to 7 with 10 N NaOH.

10 % lactose: dissolve 5 g lactose in a total volume of 50 ml distilled water. The procedure was based on Sabine Grischow's procedure (University of St. Andrews).

7.25.1.2 Testing *Streptomyces* culture supernatants by the fluorescence and radiochemical MraY assays

The general procedures apply. For the continuous fluorescence assays 15 μl culture supernatant was tested in a total volume of 180 μl (Section 7.10). For the fluorescence microtitre plate assays and the radiochemical assays 10 % (v/v) culture was used in the assays (10 μl in 100 μl). See Sections 7.19 and 7.20.

7.25.2 Preparation of *Streptomyces* cell extracts

10 μl of stock spore collections was spread on MS agar plates and grown for ten days or SMMS plates and incubated for 3 days at 30 °C. Plates were stored at 4 °C until the time of extraction, and then ethyl acetate was added (in equal volume to the volume of culture media used). The ethyl acetate layer was removed by filtration and evaporated under reduced pressure. The remaining residue was re-dissolved in 500 μl 50:50 HPLC grade methanol/water. Cell extracts interfered with fluorescence and were tested by the radiochemical MraY assay, where 10 μl cell extract was used in a total volume of 100 μl (see Section 7.25.2.1).

Modified Supplemented Minimal Medium Solid (SMMS):

Difco casaminoacids (2 g/l),

TES buffer (5.68 g/l)

Bacto agar (15 g/l) were dissolved in distilled water, the pH adjusted to 7.2 using 10 N NaOH and autoclaved.

At the time of use, the media was re-melted and the following ingredients were added:

$\text{NaH}_2\text{PO}_4 + \text{K}_2\text{HPO}_4$ (50 mM each, 10 ml per litre of culture),

$\text{MgSO}_4 \cdot 7\text{H}_2\text{O}$ (1 M, 5 ml per litre of culture),

glucose (50 % w/v, 18 ml per litre of culture),

trace element solution (2 ml per litre of culture)

Trace elements solution: 0.1 g/l each of $\text{ZnSO}_4 \cdot 7\text{H}_2\text{O}$, $\text{FeSO}_4 \cdot 7\text{H}_2\text{O}$, $\text{MnCl}_2 \cdot 4\text{H}_2\text{O}$,

$\text{CaCl}_2 \cdot 6\text{H}_2\text{O}$ and NaCl and the solution was stored at 4°C. The procedure was

based on John Sida's work (University of Warwick)²⁴⁰.

7.25.2.1 Testing *Streptomyces* cell extracts by the radiochemical MraY assay

The general procedure applies (Section 7.19). 10 µl cell extract was tested in a total volume of 100 µl.

7.26 Assay of P1 protein and halogenated fluorescein analogues by the radiochemical MraY assay

The general procedure applies (see Section 7.19). 100 µl assay contained 1.1 µM (2.12 nCi)/assay) [^{14}C]-UDPMurNAc-pentapeptide, 23.3 µg/ml undecaprenyl phosphate, 70 mM Tris pH 7.5, 17.5 mM MgCl_2 , 4.0 % (vol/vol) glycerol, 2.3 % (vol/vol) DMSO, 0.1 % Triton X-100, and the reaction was started by the addition

of 40 µg protein containing overexpressed *E. coli* MraY membranes. Assays were carried out in the presence of inhibitor at concentrations of 75-300 µg/ml, and inhibition by 125 µg/ml tunicamycin was used as a positive control. IC₅₀ was measured from a plot of enzyme activity vs. inhibitor concentration with the help of a curve fitting program in GenStat (Section 2.2.6). Dichloro- and dibromofluoresceins were tested in triplicates at 165 and 325 µg/ml final concentrations respectively, and phloxine B was tested in duplicate measurements in the range of 0-500 µg/ml.

7.27 Radiochemical MurG assay procedure

7.27.1 *E. coli* MraY-MurG procedure

Lipid I was generated from UDPMurNAc-L-Ala-γ-D-Glu-*m*-Dap-D-Ala-D-Ala and undecaprenyl phosphate by overexpressed *E. coli* MraY membranes and then converted in the presence of [³H]-UDPGlcNAc and *E. coli* MurG to give radiolabelled lipid II. Assays (total volume 100 µl) contained 100 µM UDPMurNAc-L-Ala-γ-D-Glu-*m*-Dap-D-Ala-D-Ala, 23.3 µg/ml undecaprenyl phosphate, 6.6 µM [³H]-UDPGlcNAc (2.53 nCi/assay), 70 mM Tris pH 7.5, 17.5 mM MgCl₂, 4.0 % glycerol (vol/vol), 2.3 % (vol/vol) DMSO, 0.1 % Triton X-100 to which was added 54 µg *E. coli* membranes containing overexpressed *E. coli* MraY, and 63 µg *E. coli* MurG solution. The mixture was incubated at 35 °C for 30 minutes and reactions were stopped by the addition of 100 µl 6 M pyridinium acetate, pH 4.2. The lipid products were extracted into 200 µl 1-butanol and quantified by liquid scintillation counting. Assays were carried out in duplicates in the presence of inhibitor at final concentrations of 18-300 µg/ml P1, 165 µg/ml di-chloro-fluorescein and 325 µg/ml di-bromo-

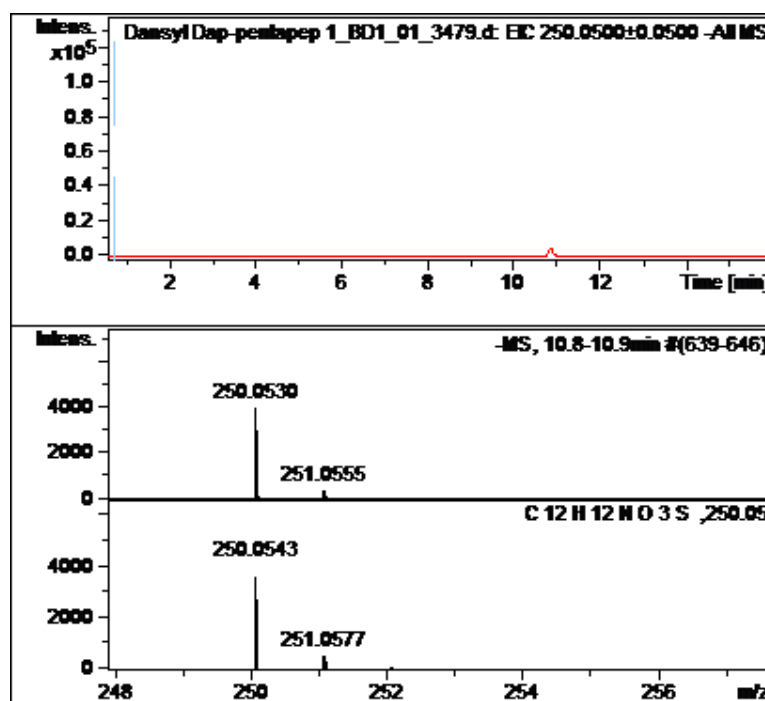
fluorescein. Inhibition by ramoplanin was used as a positive control. Mixtures for control experiments lacked *E. coli* MraY membranes and *E. coli* MurG²⁶⁷.

7.27.2 *M. flavus* MraY-MurG assay procedure

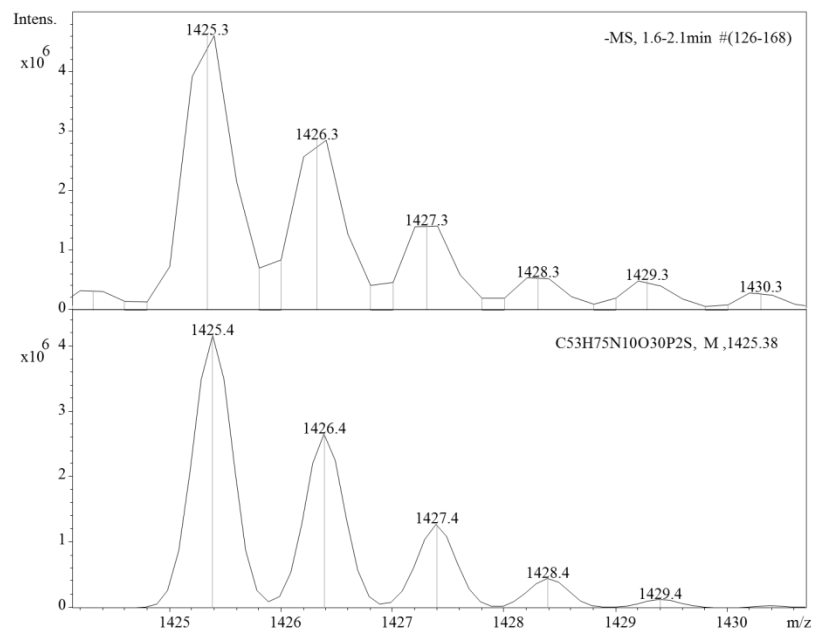
Lipid I was generated from UDPMurNAc-L-Ala- γ -D-Glu-*m*-Dap-D-Ala-D-Ala and undecaprenyl phosphate by *M. flavus* membranes naturally containing high level expression of MraY and MurG, and converted in the presence of [³H]-UDPGlcNAc to give radiolabelled lipid II. Assays (total volume 100 μ l) contained 100 μ M UDPMurNAc-L-Ala- γ -D-Glu-*m*-Dap-D-Ala-D-Ala, 23.3 μ g/ml undecaprenyl phosphate, 4.9 μ M [³H]-UDPGlcNAc (1.89 nCi/assay), 70 mM Tris pH 7.5, 17.5 mM MgCl₂, 4.0 % glycerol (vol/vol), 2.3 % (vol/vol) DMSO, 0.1 % Triton X-100 to which was added 23 μ g *M. flavus* membranes. The mixture was incubated at 35 °C for 30 minutes and reactions were stopped by the addition of 100 μ l 6 M pyridinium acetate, pH 4.2. The lipid products were extracted into 200 μ l 1-butanol and quantified by liquid scintillation counting. Assays were carried out in the presence of inhibitor concentrations at 75-300 μ g/ml for P1 peptide and phloxine B was tested at 500 μ g/ml. Inhibition by ramoplanin was used as a positive control. Mixtures for control experiments lacked *M. flavus* membranes²⁶⁷. Assays were carried out in triplicate. Activity or % inhibition was determined by taking the negative control lacking inhibitor as 100 % activity.

Appendices

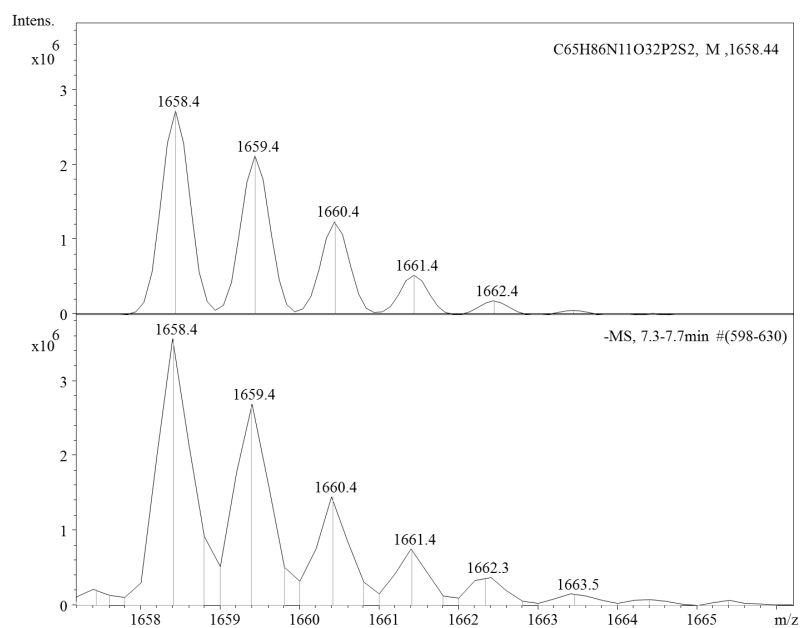
Appendix 1: Preparation of the dansyl-labelled UDPMurNAc-pentapeptide (Figures A 1 - A 3)



A 1: Isotopic pattern for dansic acid by HR LC-MS

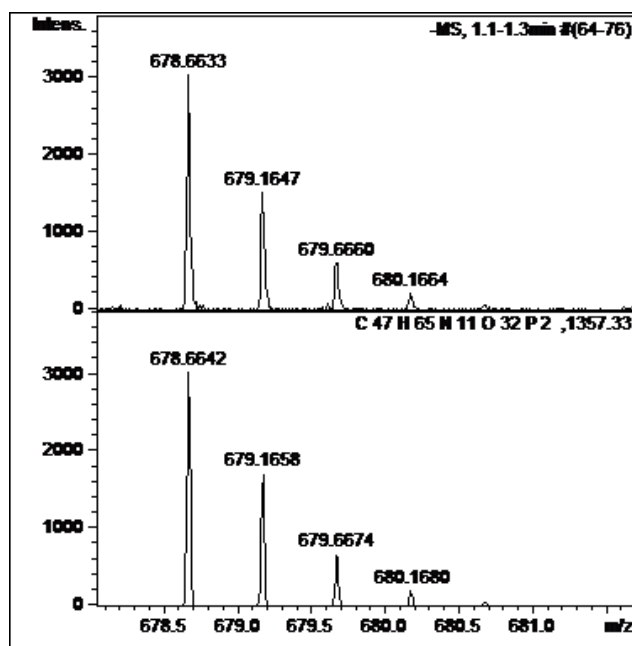


A 2: Isotopic pattern for the negatively charged ion of the dansyl-labelled UDPMurNAc-pentapeptide by LC-MS

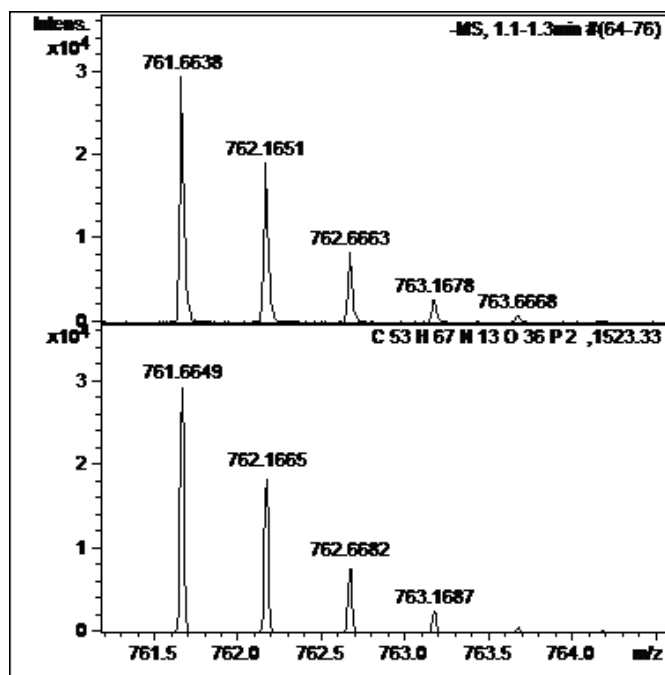


A 3: Isotopic pattern for the negatively charged ion of the didansyl-labelled UDPMurNAc-pentapeptide by LC-MS

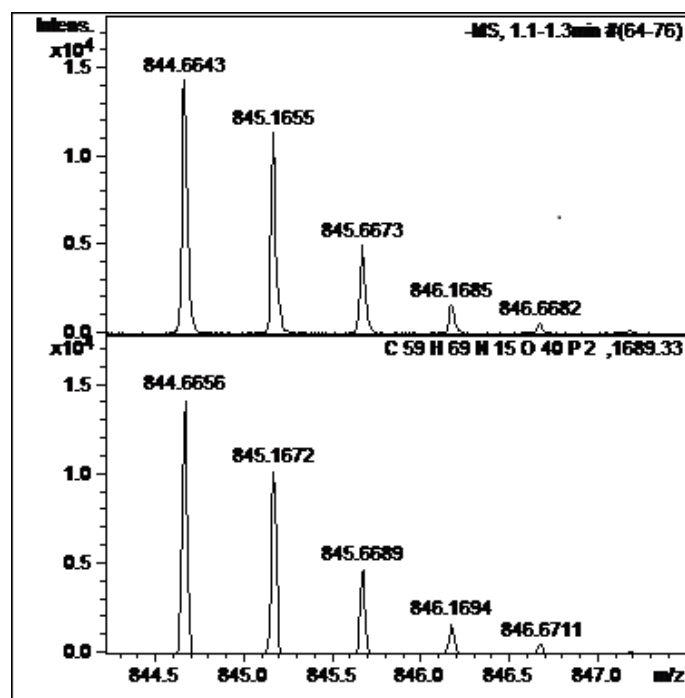
Appendix 2: LC-MS results for the attempted HPLC-based MraY assay (Figures A 4 - A 18)



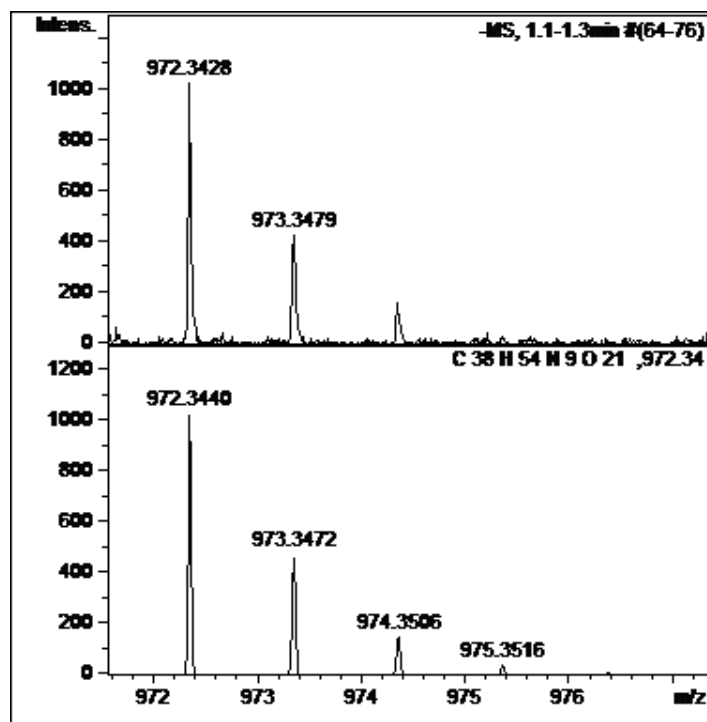
A 4: Isotopic pattern for the DNP-labelled UDPMurNAc-pentapeptide by HR LC-MS



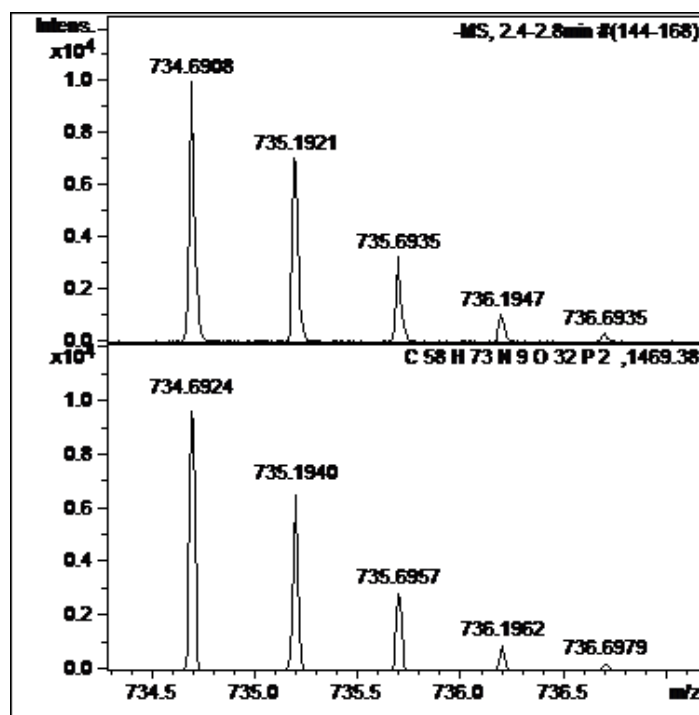
A 5: Isotopic pattern for the DNP-labelled UDPMurNAc-pentapeptide by HR-LC-MS (two DNP labels)



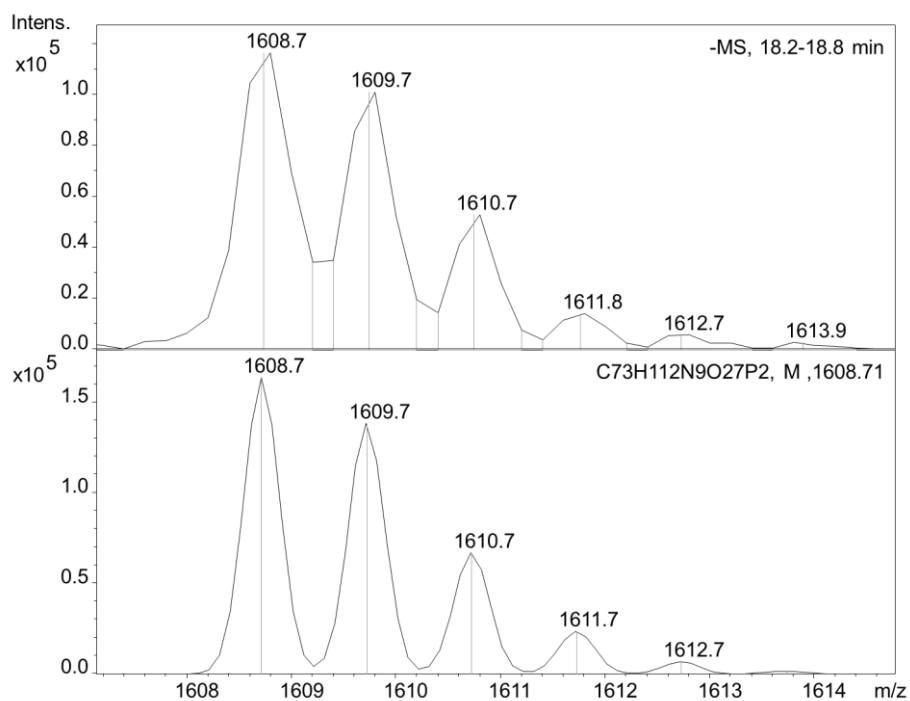
A 6: Isotopic pattern for the DNP-labelled UDPMurNAc-pentapeptide (three labels) by HR LC-MS



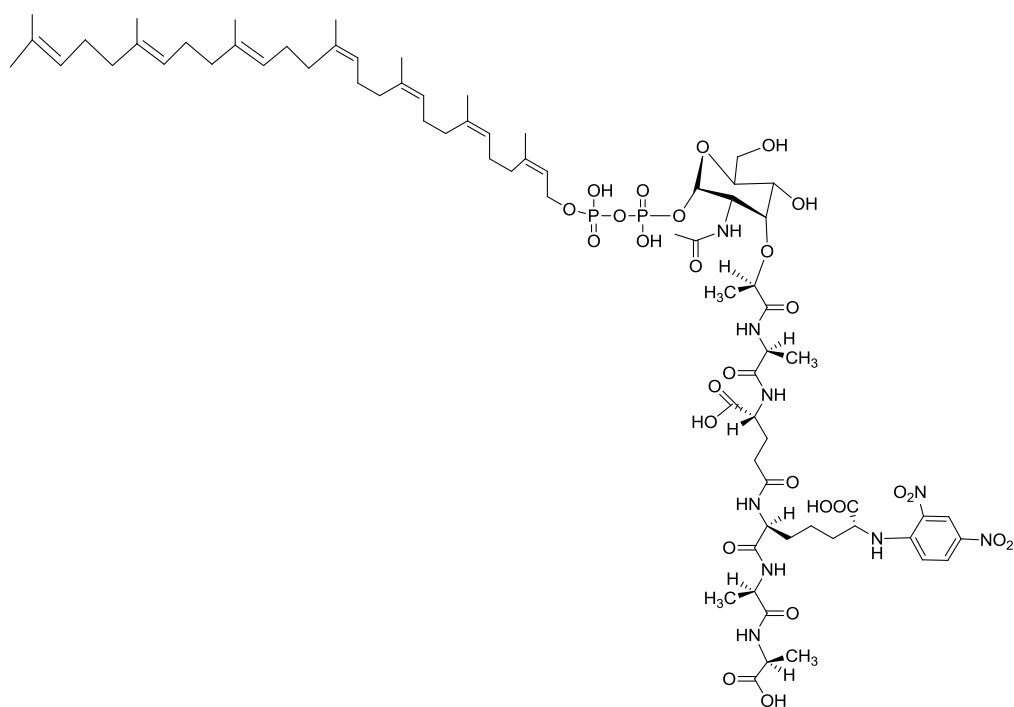
A 7: Isotopic pattern for a DNP-labelled UDPMurNAc-pentapeptide fragment



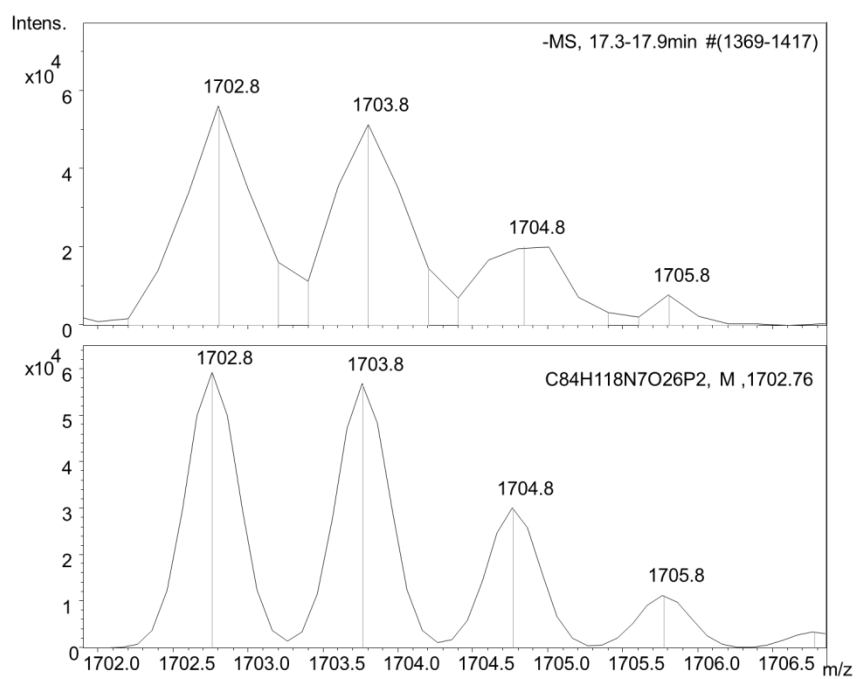
A 8: Isotopic pattern by HR LC-MS for the fluorescamine-labelled UDPMurAc-pentapeptide



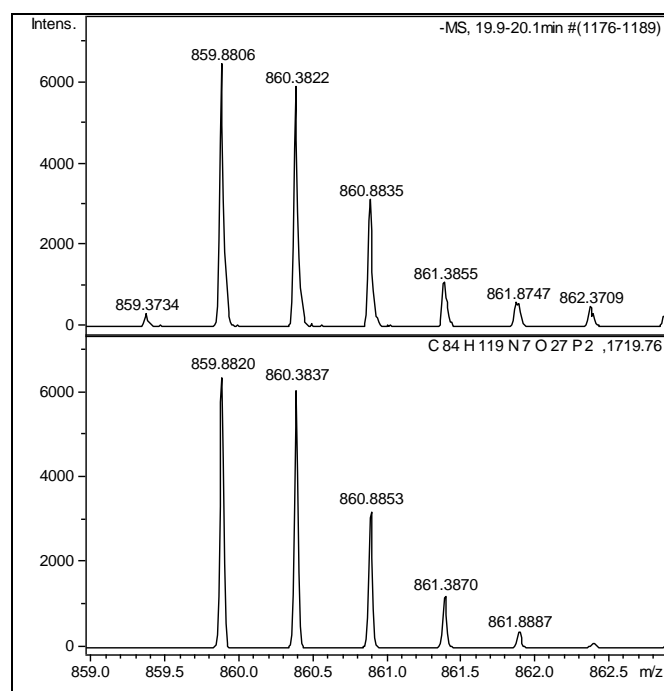
A 9: Isotopic pattern for the DNP-labelled C₃₅ lipid I



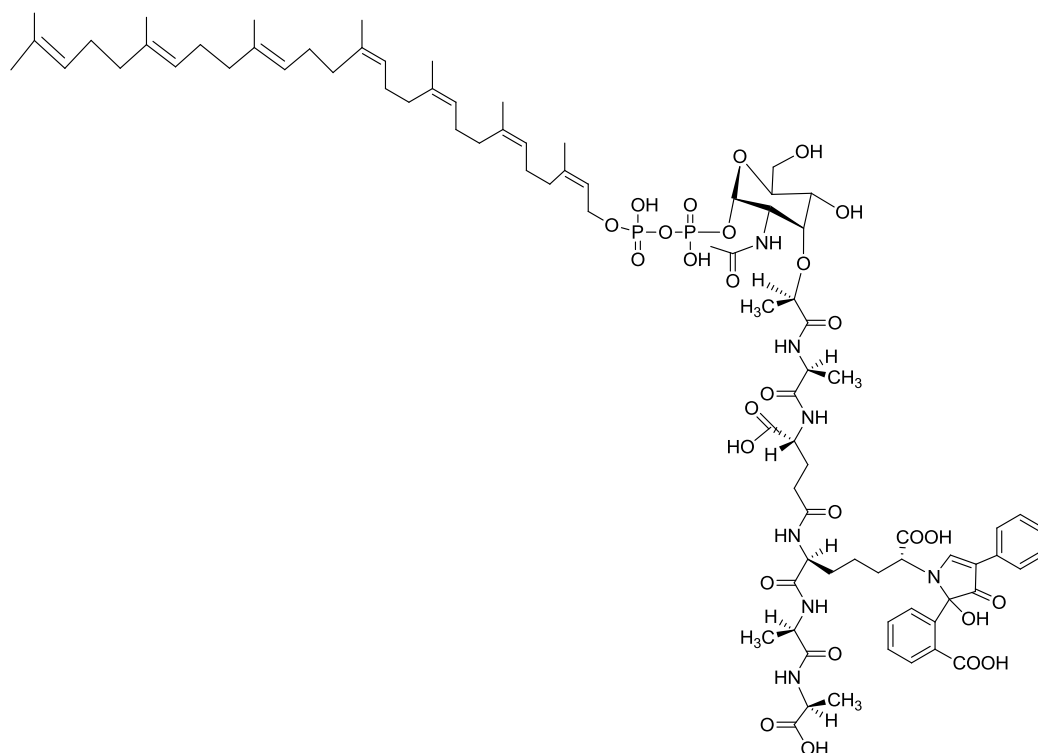
A 10: Chemical structure for the DNP-labelled C₃₅ lipid I



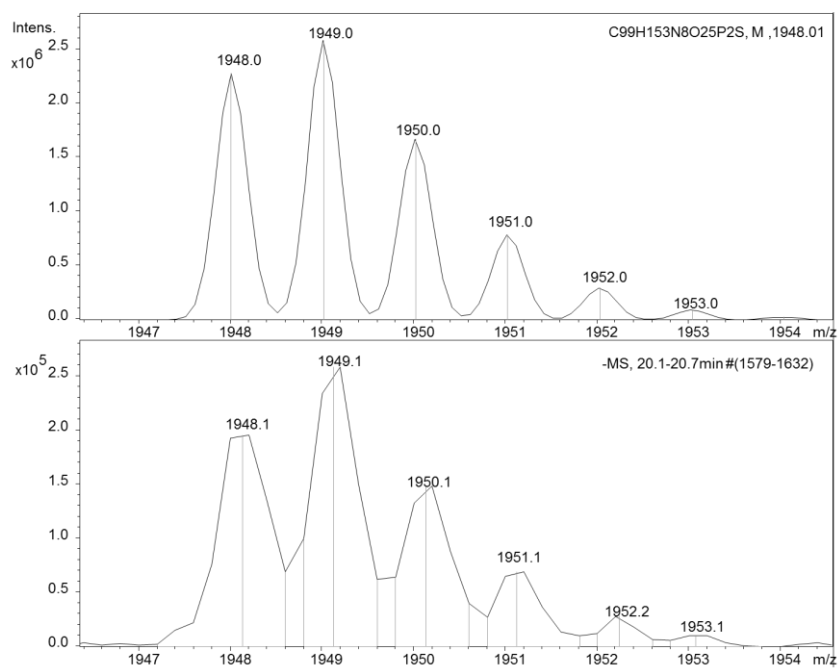
A 11: Isotopic pattern for the fluorescamine-labelled lipid I (-H₂O) by LC-MS



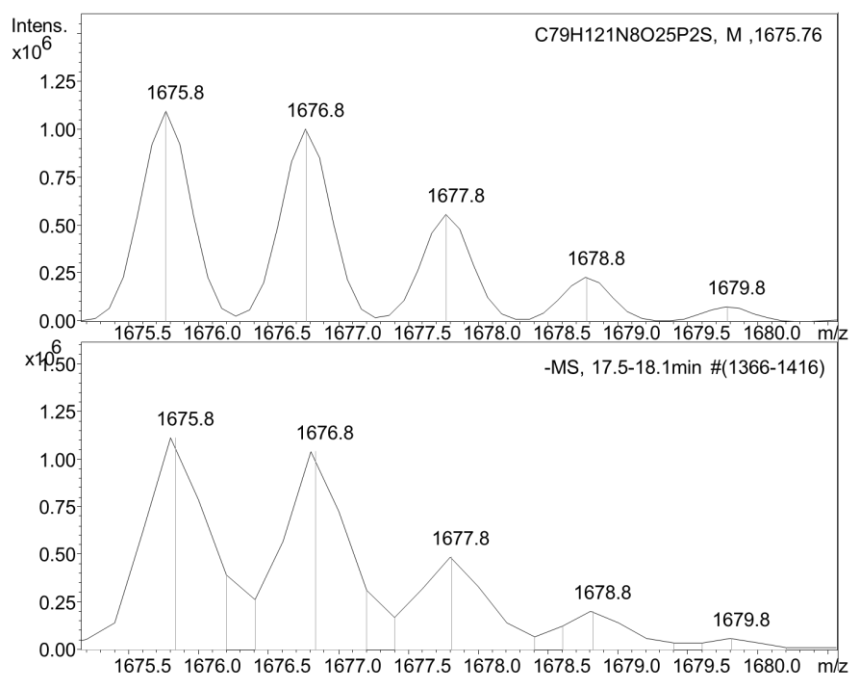
A 12: Isotopic pattern of the negatively and doubly charged ion of the fluorescamine-labelled lipid I (C₃₅) by HR LC-MS and the computer simulated isotopic pattern



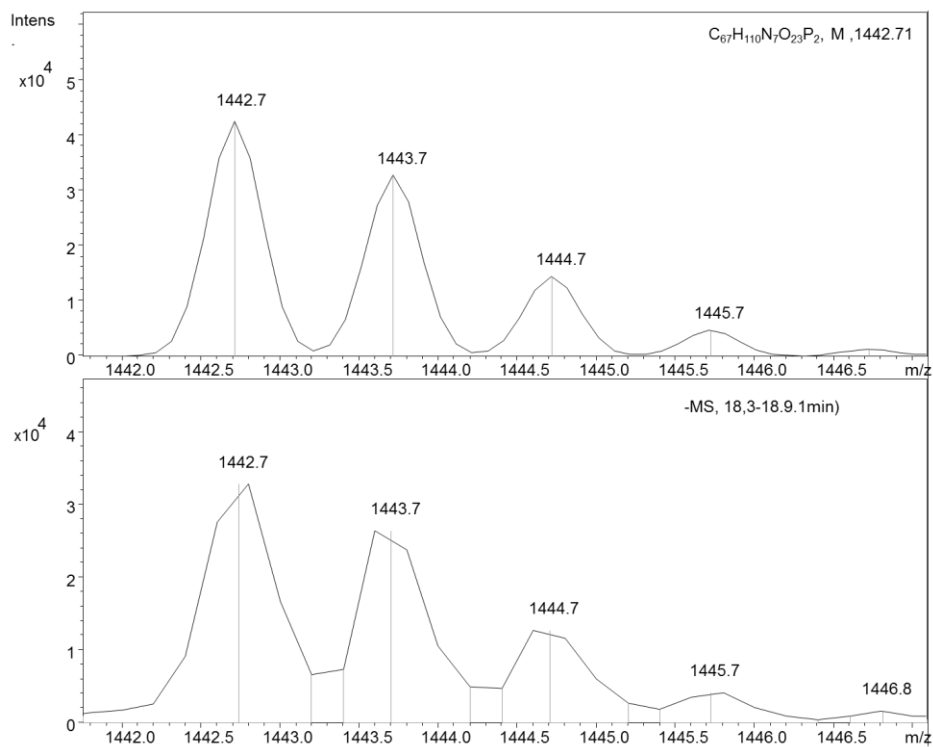
A 13: Chemical structure of the fluorescamine-labelled C₃₅ lipid I



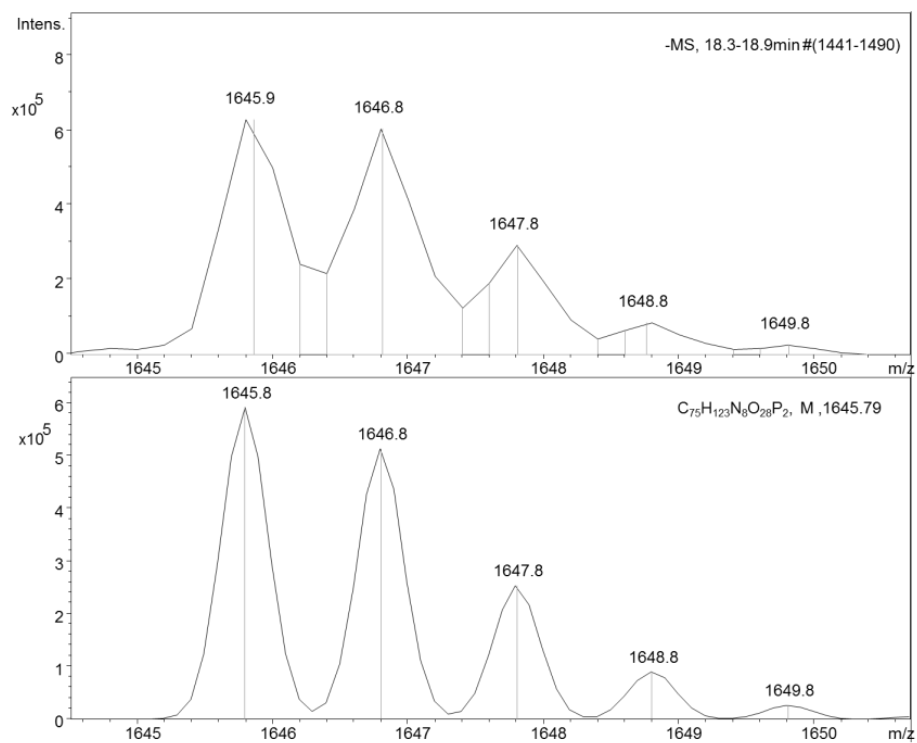
A 14: Isotopic pattern for dansyl-labelled lipid I (C_{55}) formed with MraY



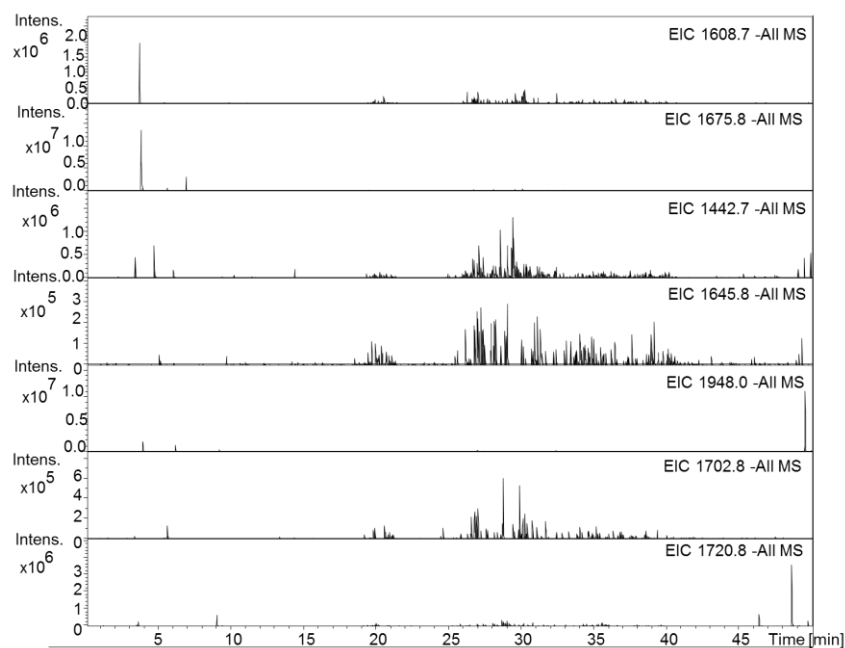
A 15: Isotopic pattern for the dansyl-labelled lipid I (C_{35}) formed with MraY



A 16: Isotopic pattern for lipid I (C_{35})

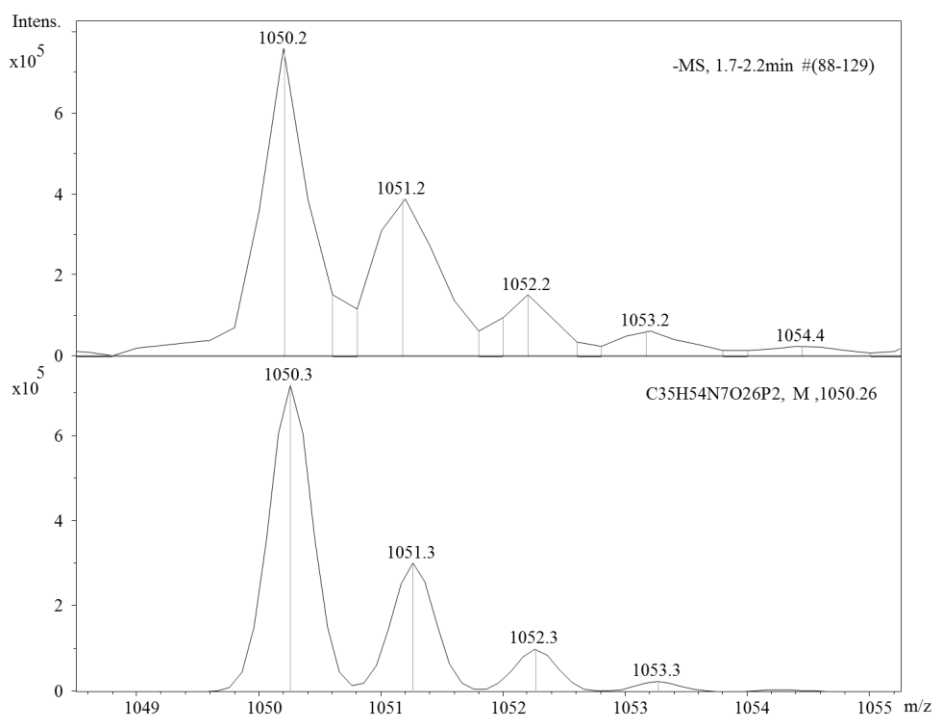


A 17: Isotopic pattern for lipid II (C_{35})

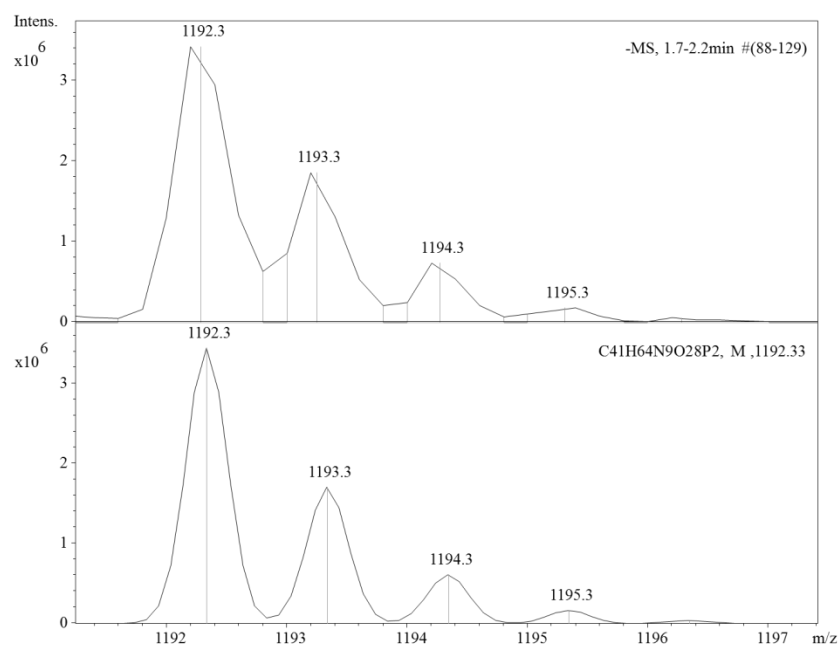


A 18: Control lacking the unlabelled or labelled UDPMurNAc-pentapeptides, no sign for the masses of lipid products (EICs)

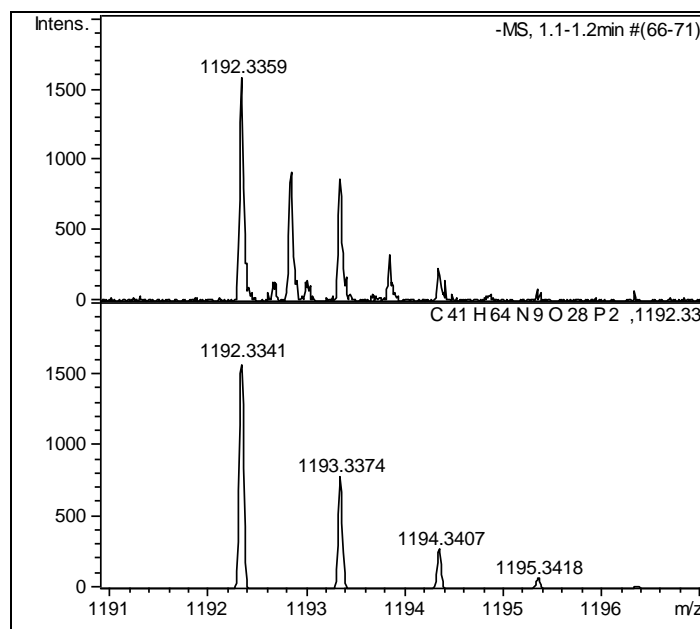
Appendix 3: Radiochemical synthesis of the [^{14}C]-UDPMurNAc-pentapeptide (Figures A 19 -A 22)



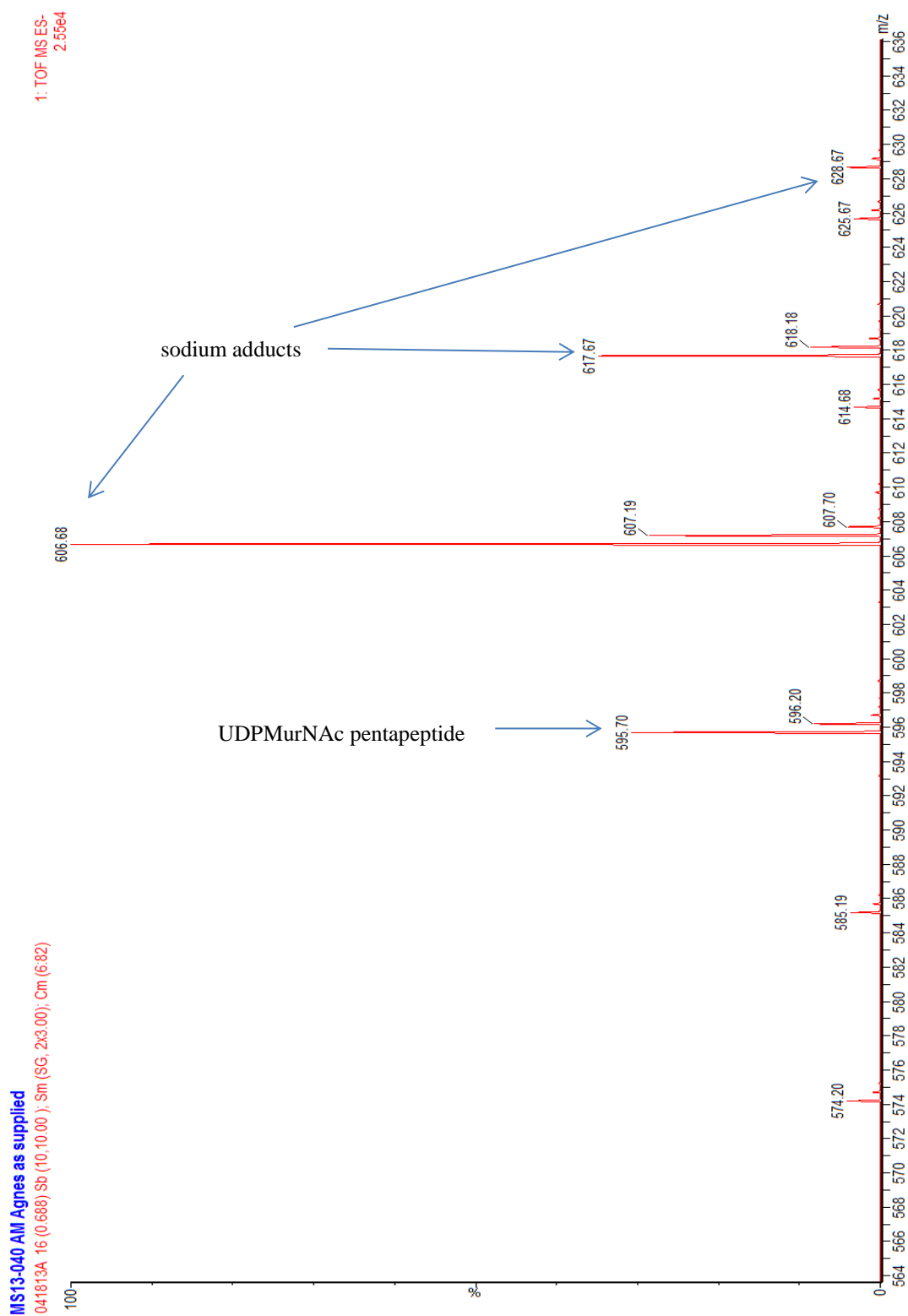
A 19: Isotopic pattern for the UDPMurNAc-tripeptide



A 20: Isotopic pattern for the UDPMurNAc-pentapeptide



A 21: Isotopic pattern for the UDPMurNAc-pentapeptide by HR LC-MS



A 22: ESI-MS for ^{14}C -labelled UDPMurNAc-pentapeptide m/z $[\text{M}-2\text{H}]^{2-}$: 595.70 for predicted 595.66, and sodium adducts, analysis was performed by Susan Slade

Appendix 4: Results from the NCI diversity set

Empty cells: no inhibition in fluorescence microtitre plate MraY assay

HF: high fluorescence in microtitre plate MraY assay

LFA: low fluorescence with fluorescence enhancement activity in the continuous MraY assay

LF: low fluorescence with no fluorescence enhancement activity in the continuous MraY assay

NCI diversity set III, plates 4737067/4720 - 4737067/4739:

20	2	3	4	5	6	7	8	9	10	11
A						HF				
B									LF	LFA
C				LFA						HF
D				LFA					HF	
E			LFA					HF		HF
F			LFA	LFA	LF	HF		LFA		
G						HF		LF		
H							HF			

21	2	3	4	5	6	7	8	9	10	11
A		LF				HF		HF		
B						HF				
C		HF								
D										
E		LF								
F		LF					HF		LF	
G									LF	
H										

22	2	3	4	5	6	7	8	9	10	11
A					HF					HF
B										
C			LFA							
D					LFA	HF	LF	LFA	HF	
E								HF		
F								LFA	HF	
G			LFA		HF		LFA			
H										HF

23	2	3	4	5	6	7	8	9	10	11
A	HF		LF		LF	HF	LFA	HF	HF	
B	HF	HF				LF	LF		LF	HF
C		LF				HF			LF	
D								HF		LF
E							LF		HF	
F		HF								
G		LFA	LF				HF			
H										

24	2	3	4	5	6	7	8	9	10	11
A		HF			LF					LFA
B	HF									
C							HF			
D				HF						
E				LFA	HF					HF
F										HF
G			LF				LF			
H								HF		

25	2	3	4	5	6	7	8	9	10	11
A		.							HF	
B	HF								HF	
C			HF		HF					
D					HF	HF			HF	LFA
E				HF				LF		
F		HF					HF			HF
G	HF		.				HF			
H				LF			HF	HF	HF	HF

26	2	3	4	5	6	7	8	9	10	11
A	HF		HF		HF		HF			
B		HF			HF		HF			LF
C				HF				HF		LF
D								HF		
E							HF	HF		
F	HF	HF							HF	LFA
G					HF					LFA
H	HF		HF					HF		

27	2	3	4	5	6	7	8	9	10	11
A	LFA									
B				HF		HF			HF	HF
C			HF							
D	HF				HF			HF		HF
E	HF				HF			HF	LF	HF
F										HF
G				HF			.		HF	LF
H			HF	LFA						

28	2	3	4	5	6	7	8	9	10	11
A										
B				HF	HF	LFA	LFA		LFA	
C	LFA									
D					LFA			HF		
E		HF		HF		LFA	HF			
F			LFA				LFA			
G			HF			HF			LFA	
H	LFA				LF					

29	2	3	4	5	6	7	8	9	10	11
A		HF				HF				
B										
C	HF			HF						
D	HF									HF
E	LFA	HF					LFA			
F		HF								
G		LFA					HF	HF		
H		HF								

30	2	3	4	5	6	7	8	9	10	11
A		HF				HF				
B				LFA		LFA				
C				HF						
D						LFA				
E										
F							LF			HF
G	HF								HF	HF
H		HF		HF		HF	HF		LFA	

31	2	3	4	5	6	7	8	9	10	11
A			HF	HF	HF					
B			HF				LFA			HF
C					HF				HF	
D						LFA	HF			HF
E						HF	LFA			
F									HF	
G	LFA									HF
H					HF			HF		

32	2	3	4	5	6	7	8	9	10	11
A										
B									HF	
C	LF				LFA					
D				LFA		HF		HF		
E	HF		HF			LFA		HF		
F	LF			HF			HF		HF	
G										
H						LF				

33	2	3	4	5	6	7	8	9	10	11
A			HF						HF	
B										
C										
D				LFA				HF		
E									HF	
F			LF	HF		HF	HF			
G			LFA		HF					HF
H	HF				HF			HF	LF	

34	2	3	4	5	6	7	8	9	10	11
A					HF		LF		HF	
B		HF	HF		LFA					
C	HF						HF			
D			HF	HF						
E								HF	HF	HF
F					HF					X
G							LFA		LFA	X
H				HF		HF	HF			X

35	2	3	4	5	6	7	8	9	10	11
A					HF					
B					LF					
C										
D			HF		HF					
E							LF	HF		HF
F										
G									LFA	
H	HF								HF	

36	2	3	4	5	6	7	8	9	10	11
A							HF			
B	HF							HF		LF
C		HF			LF					
D								HF		LFA
E	HF									
F						HF	HF			
G					LF		LFA			
H				HF	HF					

37	2	3	4	5	6	7	8	9	10	11
A	LF		HF	HF		LF				
B									HF	
C				LFA						
D		LFA			LFA					
E	HF		HF					HF		LF
F		LF	LFA		HF	LF	LF			
G		HF								
H				HF				HF		

38	2	3	4	5	6	7	8	9	10	11
A		HF							HF	HF
B			HF	LF			HF	LFA		
C									LFA	
D								LFA	LFA	HF
E	LFA				LFA				LFA	LFA
F						LFA	HF			
G			HF			HF	LFA	HF		
H		HF	HF			HF				HF

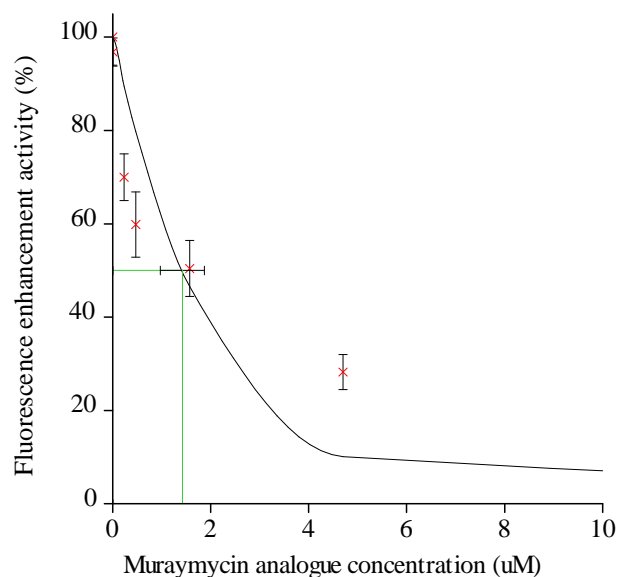
39	2	3	4	5	6	7	8	9	10	11
A	HF				LFA				LF	
B									HF	
C		LFA	HF		LFA					
D			HF				LF			HF
E										
F		LFA								
G						LF				
H										

NCI diversity set natural products set II, plates 130912**50** and 130912**51**:

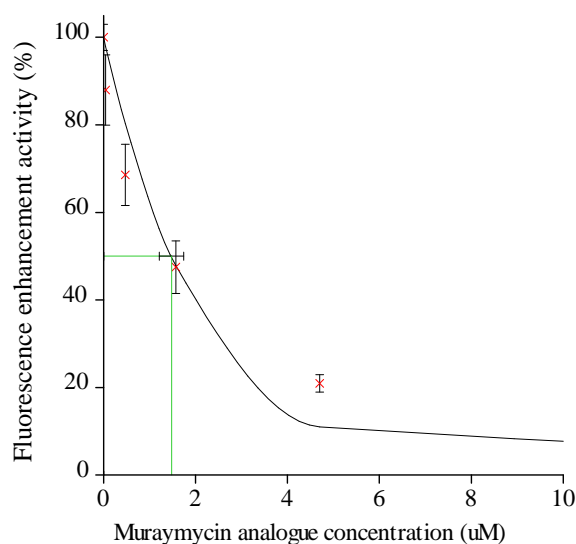
50	2	3	4	5	6	7	8	9	10	11
B	LFA		HF					LFA	HF	
C						LFA	LFA			
D				HF	HF	HF			LFA	LFA
E	HF			HF			HF			
F			HF	HF					LFA	HF
G				HF				HF		

51	2	3	4	5	6	7	8	9	10	11
B										
C	LFA									
D							HF	HF	HF	
E	HF									
F	HF					LFA	HF	HF		
G		LFA			HF					LFA

Appendix 5a: Inhibition of *E. coli* and *S. aureus* MraY by a synthetic muraymycin analogue (Figures A 23 and A 24)

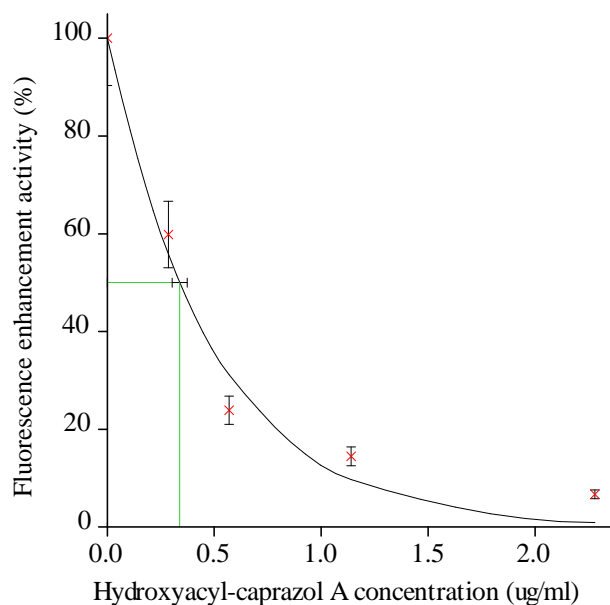


A 23: Muraymycin analogue inhibition against *E. coli* MraY, 50 μ M muraymycin gave 15 ± 2 % activity in the assay (missing from graph), IC₅₀: 1.6 ± 0.3 μ M

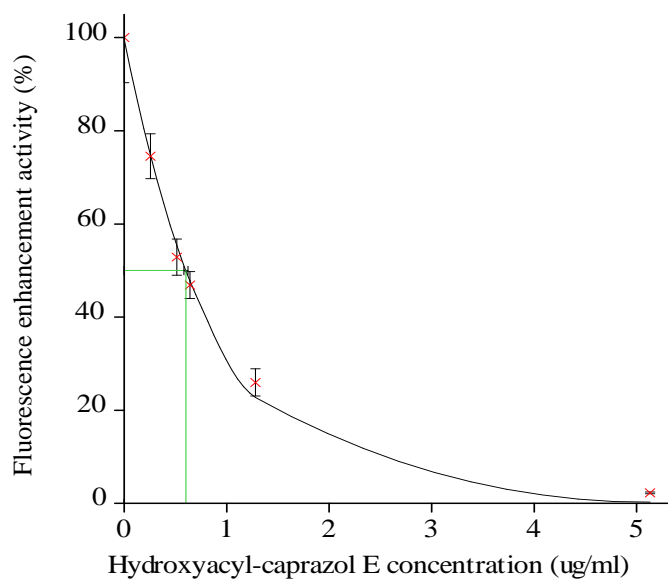


A 24: Muraymycin analogue inhibition against *S. aureus* MraY, 50 μ M gave 4.5 ± 0.5 % activity in the assay (missing from graph), IC₅₀: 1.6 ± 0.2 μ M

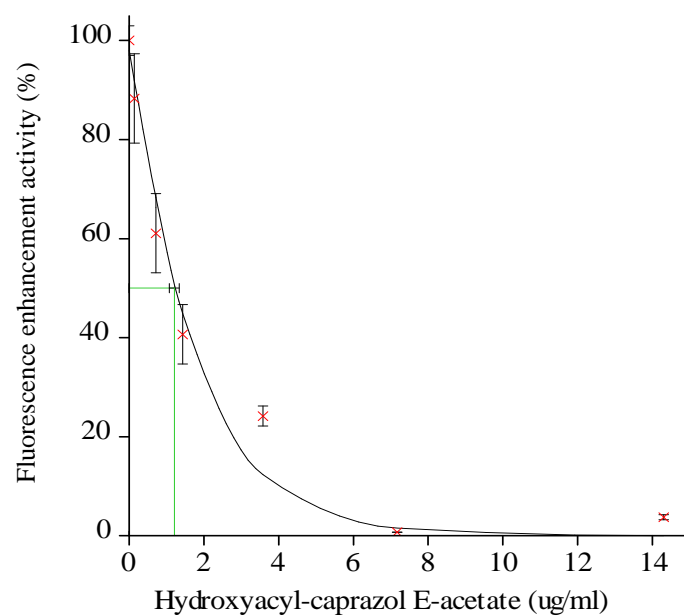
Appendix 5b: Inhibition of *E. coli* MraY by caprazamycin analogues (Figures A 25 - A 30)



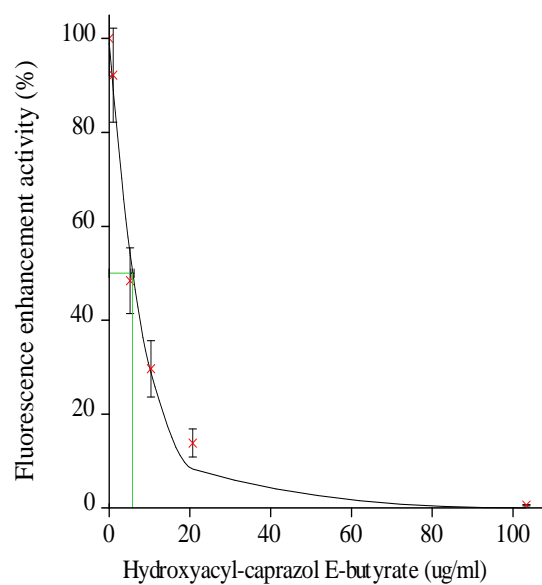
A 25: Hydroxyacyl-caprazol A inhibition against *E. coli* MraY, IC_{50} : 339 ± 35 ng/ml, $0.41 \mu M$



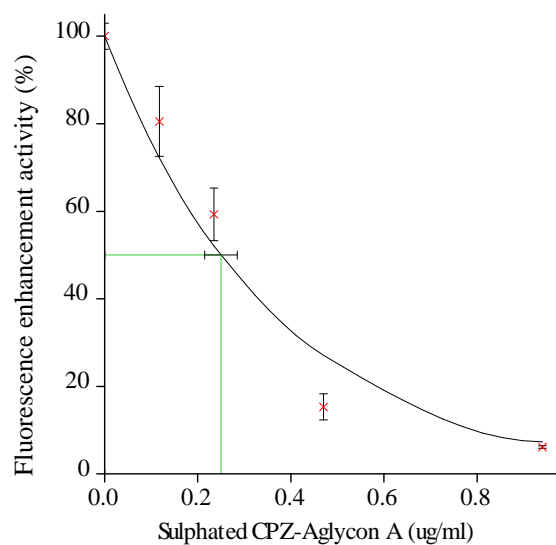
A 26: Hydroxyacyl-caprazol E inhibition against *E. coli* MraY, IC_{50} : 602 ± 19 ng/ml, $0.75 \mu M$



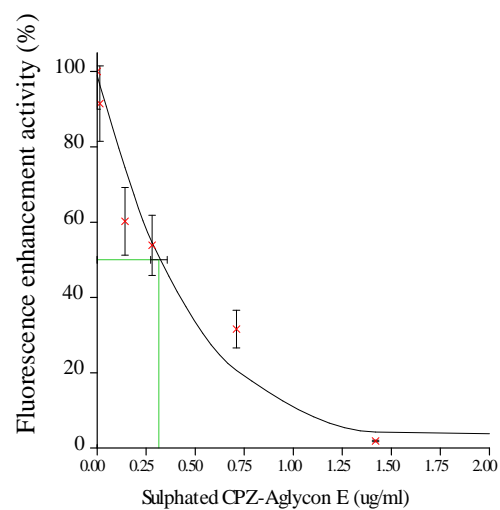
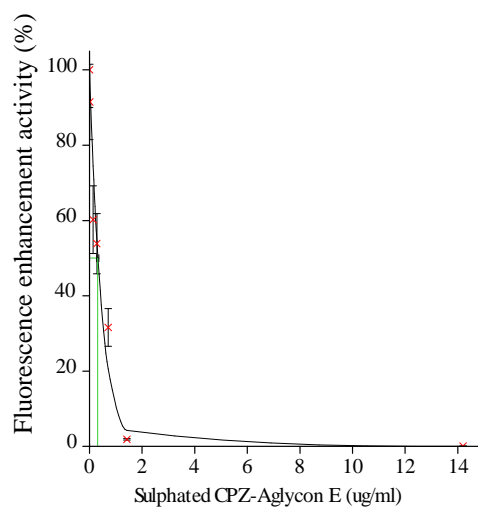
A 27: Hydroxyacyl-caprazol E-acetate inhibition against *E. coli* MraY, IC₅₀: 1.21 ± 0.13 µg/ml, 1.4 µM



A 28: Hydroxyacyl-caprazol E-butyrate inhibition against *E. coli* MraY, IC₅₀: 5.78 ± 0.41 µg/ml, 6.6 µM

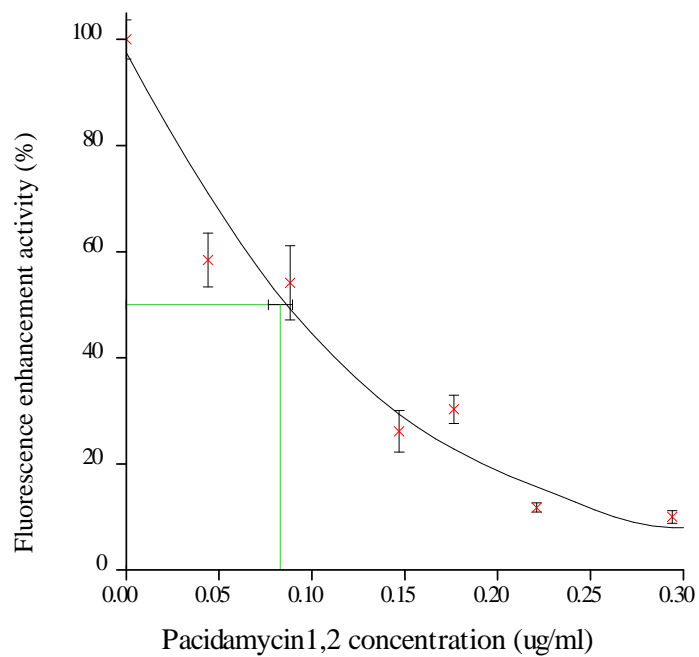


A 29: Sulphated CPZ-Aglycon A inhibition against *E. coli* MraY, IC_{50} : 250 ± 35 ng/ml, $0.24 \mu M$

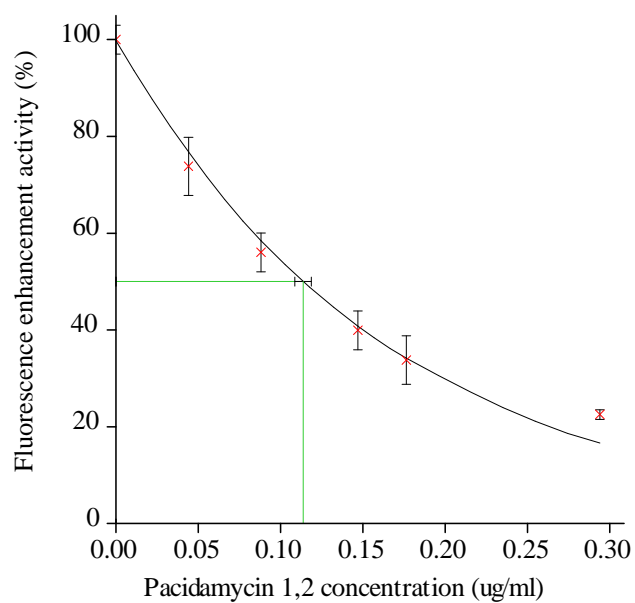


A 30: Sulphated CPZ-Aglycon E inhibition against *E. coli* MraY, IC_{50} : 314 ± 42 ng/ml, $0.31 \mu M$

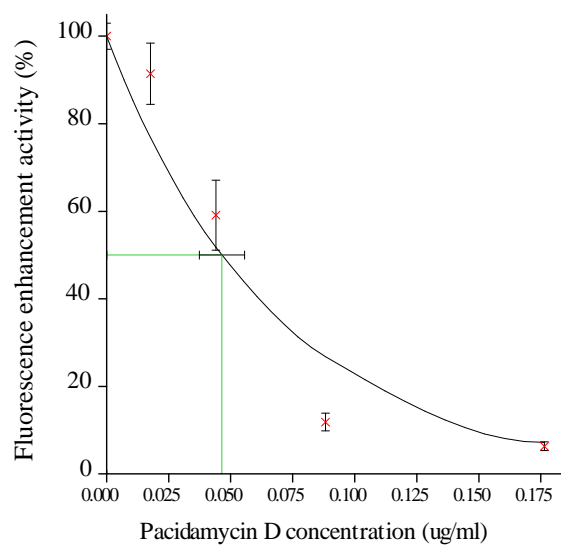
Appendix 5c: Inhibition of *E. coli* and *P. aeruginosa* MraY by pacidamycin 1,2 and pacidamycin D (Figures A 31 - A 34)



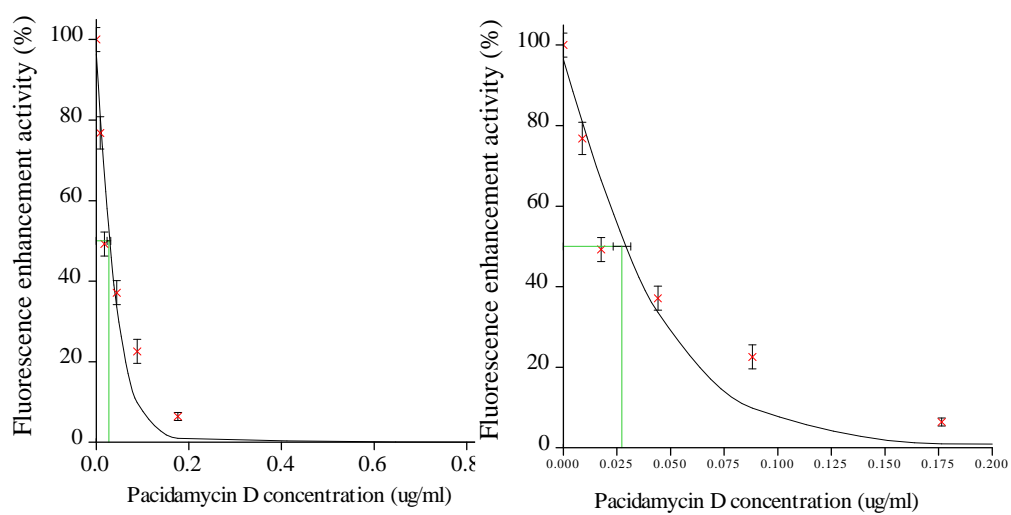
A 31: Pacidamycin 1,2 inhibition against *E. coli* MraY, IC_{50} : 83 ± 7 ng/ml



A 32: Pacidamycin 1,2 inhibition against *P. aeruginosa* MraY, IC_{50} : 114 ± 5 ng/ml

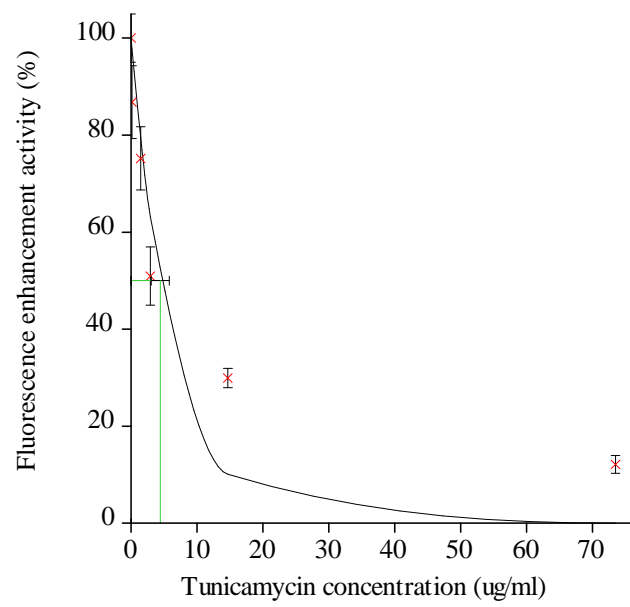


A 33: Pacidamycin D inhibition against *E. coli* MraY, IC_{50} : 46 ± 7 ng/ml



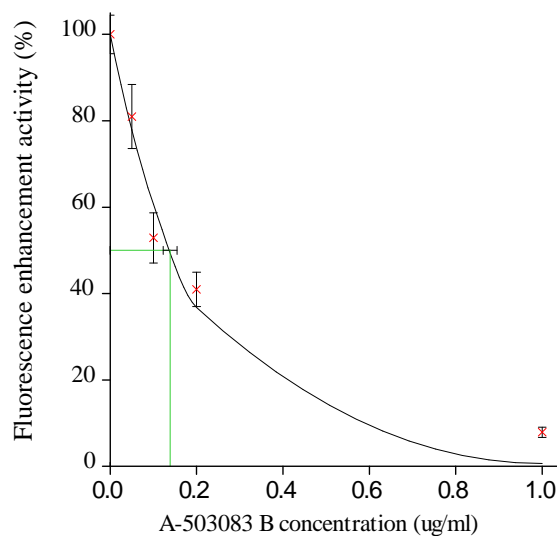
A 34: Pacidamycin D inhibition against *P. aeruginosa* MraY, IC_{50} : 27 ± 4 ng/ml

Appendix 5d: Inhibition of *P. aeruginosa* MraY by tunicamycin (Figure A 35)

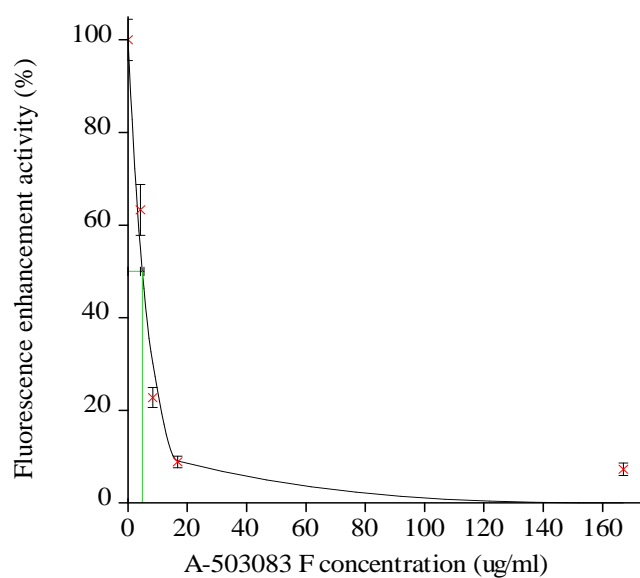


A 35: *P. aeruginosa* MraY inhibition by tunicamycin, IC₅₀: 4.44 ± 1.38 µg/ml

Appendix 5e: Inhibition of *E. coli* and *B. subtilis* MraY by capuramycin analogues (Figures A 36 and A 37)

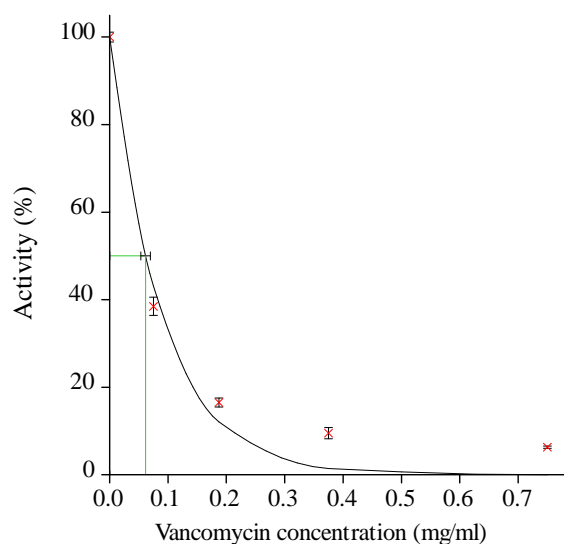


A 36: A-503083 B inhibition against *E. coli* MraY, IC_{50} : 139 ± 16 ng/ml

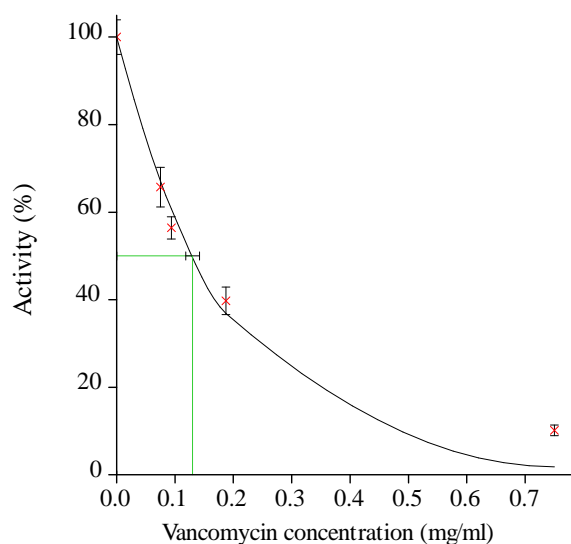


A 37: A-503083 F inhibition against *E. coli* MraY, IC_{50} : 4.8 ± 0.6 μ g/ml

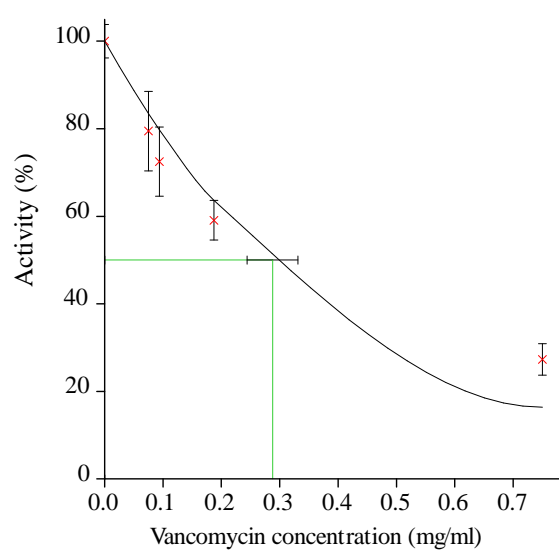
Appendix 6: Inhibition of *E. coli*, *S. aureus* and *P. aeruginosa* MraYs by the glycopeptide vancomycin (Figures A 38 - A 40)



A 38: Vancomycin inhibition against *E. coli* MraY, IC_{50} : $61.6 \pm 8 \mu\text{g/ml}$

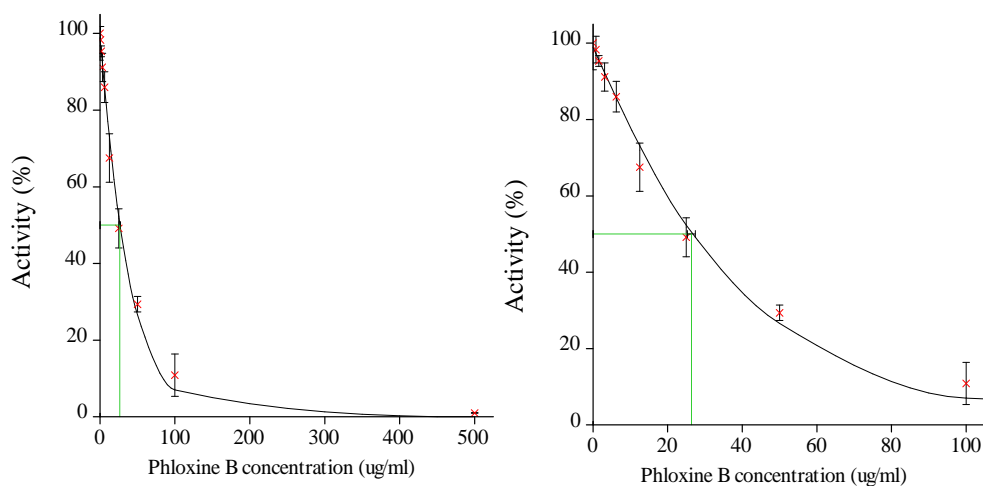


A 39: Vancomycin inhibition against *S. aureus* MraY, IC_{50} : $130 \pm 12 \mu\text{g/ml}$

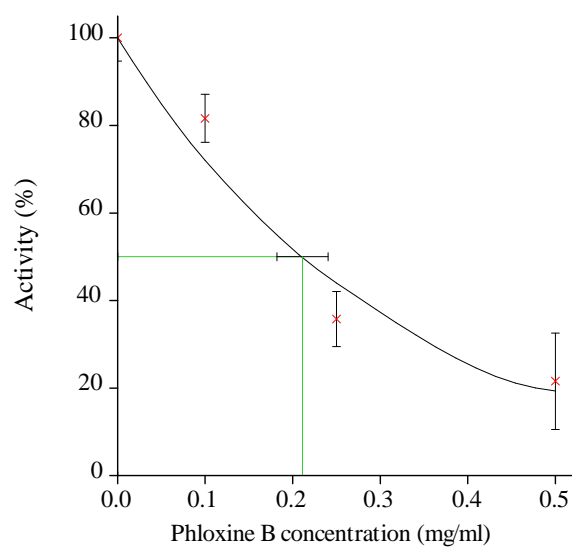


A 40: Vancomycin against *P. aeruginosa* MraY, IC₅₀: 288 ± 44 µg/ml

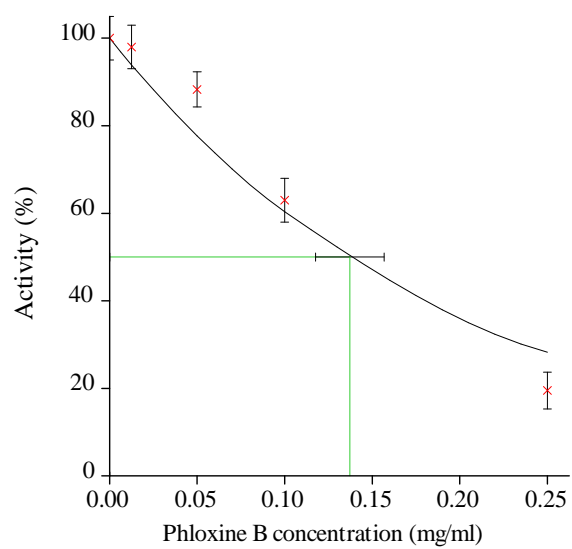
Appendix 7: Inhibition of *E. coli*, *S. aureus*, *B. subtilis*, *P. aeruginosa* and *M. flavus* MraYs by phloxine B (Figures A 41 - A 46)



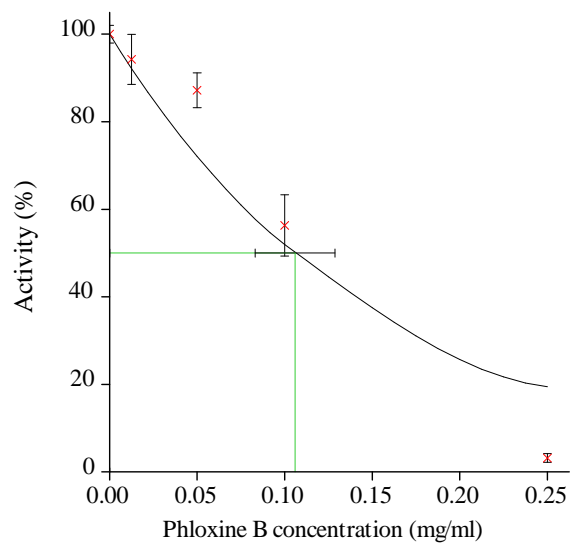
A 41: Phloxine B inhibition of *E. coli* MraY, IC₅₀: 26.4 ± 1.0 µg/ml



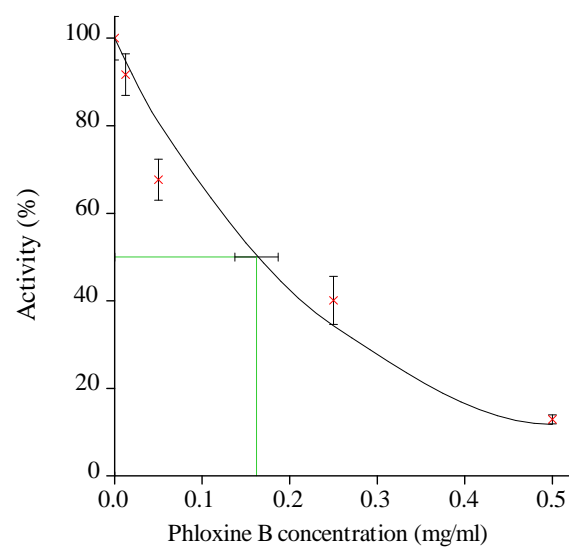
A 42: Phloxine B inhibition against *S. aureus* MraY, IC₅₀: 211 ± 29 µg/ml



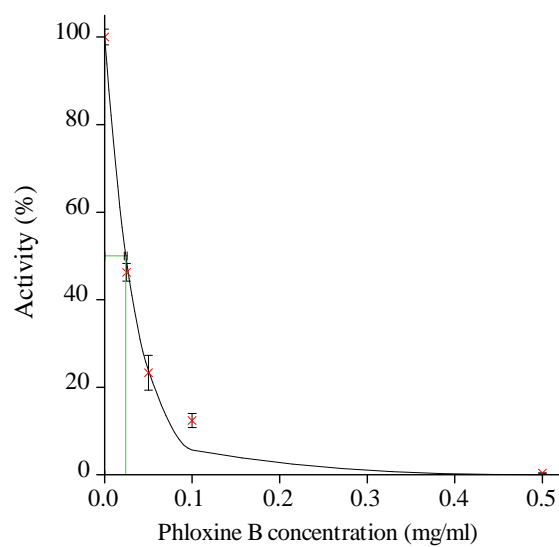
A 43: Phloxine B inhibition against *B. subtilis* MraY, IC_{50} : 137 ± 20 μ g/ml



A 44: Phloxine B inhibition against *P. aeruginosa* MraY, IC_{50} : 106 ± 23 μ g/ml



A 45: Phloxine B inhibition against *M. flavus* MraY, IC_{50} : 162 ± 25 μ g/ml



A 46: Phloxine B inhibition against *E. coli* MraY in the dark, IC_{50} : 24.2 ± 1.7 μ g/ml

8 References

1. E. Klein, D. L. Smith and R. Laxminarayan, *Emerg. Infect. Dis.*, 2007, **13**, 1840-1846.
2. B. E. Murray, *Braz. J. Infect. Dis.: an official publication of the Brazilian Society of Infectious Diseases*, 2000, **4**, 9-14.
3. Mesaros, P. Nordmann, P. Plesiat, M. Roussel-Delvallez, J. Van Eldere, Y. Glupczynski, Y. Van Laethem, F. Jacobs, P. Lebecque, A. Malfroot, P. M. Tulkens and F. Van Bambeke, *Clin. Microbiol. Infec.*, 2007, **13**, 560-578.
4. G. L. Patrick, *An Introduction to Medicinal Chemistry*, Oxford University Press, 2009.
5. J. Ziemska, A. Rajnisz and J. Solecka, *Cent. Eur. J. Biol.*, 2013, **8**, 943-957.
6. K. J. Williams and R. P. Bax, *Curr. Opin. Investig. Drugs*, 2009, **10**, 157-163.
7. T. J. Beveridge and J. A. Davies, *J. Bacteriol*, 1983, **156**, 846-858.
8. L. Maliničová, M. Piknová, P. Pristaš and P. Javorský, in *Current Research, Technology and Education Topics in Applied Microbiology and Microbial Biotechnology*. The Formatex Microbiology Book Series, ed. A. Mendez-Vilas, Formatex Research Center, Badajoz, 2010, **1**, 463-472.
9. A. Bouhss, A. E. Trunkfield, T. D. H. Bugg and D. Mengin-Lecreulx, *FEMS Microbiol. Rev.*, 2008, **32**, 208-233.
10. T. D. H. Bugg, A. J. Lloyd and D. I. Roper, *Infect. Disord. Drug Targets*, 2006, **6**, 85-106.
11. S. S. Hegde and T. E. Shrader, *J. Biol. Chem.*, 2001, **276**, 6998-7003.
12. K. H. Schleifer, *Current Contents/Life Sciences*, 1989, 19-19.
13. P. E. Brandish, *PhD thesis*, University of Southampton, 1995.
14. W. Vollmer and U. Bertsche, *Biochim. Biophys. Acta-Biomembranes*, 2008, **1778**, 1714-1734.
15. W. Vollmer, B. Joris, P. Charlier and S. Foster, *FEMS Microbiol. Rev.*, 2008, **32**, 259-286.

16. T. D. H. Bugg, D. Braddick, C. G. Dowson and D. I. Roper, *Trends Biotechnol.*, 2011, **29**, 167-173.
17. E. D. Brown, E. I. Vivas, C. T. Walsh and R. Kolter, *J. Bacteriol*, 1995, **177**, 4194-4197.
18. W. S. Du, J. R. Brown, D. R. Sylvester, J. Z. Huang, A. F. Chalker, C. Y. So, D. J. Holmes, D. J. Payne and N. G. Wallis, *J. Bacteriol*, 2000, **182**, 4146-4152.
19. K. L. Blake, A. J. O'Neill, D. Mengin-Lecreulx, P. J. F. Henderson, J. M. Bostock, C. J. Dunsmore, K. J. Simmons, C. W. G. Fishwick, J. A. Leeds and I. Chopra, *Mol. Microbiol.*, 2009, **72**, 335-343.
20. F. M. Kahan, J. S. Kahan, P. J. Cassidy and H. Kropp, *Ann. N.Y. Acad. Sci.*, 1974, **235**, 364-386.
21. J. L. Marquardt, E. D. Brown, W. S. Lane, T. M. Haley, Y. Ichikawa, C. H. Wong and C. T. Walsh, *Biochemistry*, 1994, **33**, 10646-10651.
22. K. A. L. De Smet, K. E. Kempseell, A. Gallagher, K. Duncan and D. B. Young, *Microbiology (Reading)*, 1999, **145**, 3177-3184.
23. H. Han, Y. Yang, S. H. Olesen, A. Becker, S. Betzi and E. Schonbrunn, *Biochemistry*, 2010, **49**, 4276-4282.
24. C. J. Dunsmore, K. Miller, K. L. Blake, S. G. Patching, P. J. F. Henderson, J. A. Garnett, W. J. Stubbings, S. E. V. Phillips, D. J. Palestrant, J. D. L. Angeles, J. A. Leeds, I. Chopra and C. W. G. Fishwick, *Bioorg. Med. Chem. Lett.*, 2008, **18**, 1730-1734.
25. A. Steinbach, A. J. Scheidig and C. D. Klein, *J. Med. Chem.*, 2008, **51**, 5143-5147.
26. J. Molina-Lopez, F. Sanschagrin and R. C. Levesque, *Peptides*, 2006, **27**, 3115-3121.
27. J. J. Bronson, K. L. DenBleyker, P. J. Falk, R. A. Mate, H. T. Ho, M. J. Pucci and L. B. Snyder, *Bioorg. Med. Chem. Lett.*, 2003, **13**, 873-875.
28. C. J. Andres, J. J. Bronson, S. V. D'Andrea, M. S. Deshpande, P. J. Falk, K. A. Grant-Young, W. E. Harte, H. T. Ho, P. F. Misco, J. G. Robertson, D. Stock, Y. X. Sun and A. W. Walsh, *Bioorg. Med. Chem. Lett.*, 2000, **10**, 715-717.

29. A. M. Gilbert, A. Failli, J. Shumsky, Y. Yang, A. Severin, G. Singh, W. Hu, D. Keeney, P. J. Petersen and A. H. Katz, *J. Med. Chem.*, 2006, **49**, 6027-6036.
30. P. J. Falk, K. M. Ervin, K. S. Volk and H. T. Ho, *Biochemistry*, 1996, **35**, 1417-1422.
31. T. D. H. Bugg and C. T. Walsh, *Nat. Prod. Rep.*, 1992, **9**, 199-215.
32. D. E. Ehmann, J. E. Demeritt, K. G. Hull and S. L. Fisher, *Biochim. Biophys. Acta Proteins Proteomics*, 2004, **1698**, 167-174.
33. L. E. Zawadzke, M. Norcia, C. R. Desbonnet, H. Wang, K. Freeman-Cook and T. J. Dougherty, *Assay Drug Dev. Technol.*, 2008, **6**, 95-103.
34. B. L. M. de Jonge, A. Kutschke, M. Uria-Nickelsen, H. D. Kamp and S. D. Mills, *Antimicrob. Agents Chemother.*, 2009, **53**, 3331-3336.
35. K. Strancar, D. Blanot and S. Gobec, *Bioorg. Med. Chem. Lett.*, 2006, **16**, 343-348.
36. N. Zidar, T. Tomasic, R. Sink, A. Kovac, D. Patin, D. Blanot, C. Contreras-Martel, A. Dessen, M. M. Premru, A. Zega, S. Gobec, L. P. Masic and D. Kikelj, *Eur. J. Med. Chem.*, 2011, **46**.
37. J. R. Horton, J. M. Bostock, I. Chopra, L. Hesse, S. E. V. Phillips, D. J. Adams, A. P. Johnson and C. W. G. Fishwick, *Bioorg. Med. Chem. Lett.*, 2003, **13**, 1557-1560.
38. J. D. Guzman, A. Gupta, D. Evangelopoulos, C. Basavannacharya, L. C. Pabon, E. A. Plazas, D. R. Munoz, W. A. Delgado, L. E. Cuca, W. Ribon, S. Gibbons and S. Bhakta, *J. Antimicrob. Chemother.*, 2010, **65**, 2101-2107.
39. C. Paradis-Bleau, A. Lloyd, F. Sanschagrin, H. Maaroufi, T. Clarke, A. Blewett, C. Dowson, D. I. Roper, T. D. H. Bugg and R. C. Levesque, *Biochem. J.*, 2009, **421**, 263-272.
40. H. Im, M. L. Sharpe, U. Strych, M. Davlieva and K. L. Krause, *BMC Microbiol.*, 2011, **11**.
41. P. LeMagueres, H. Im, A. Dvorak, U. Strych, M. Benedik and K. L. Krause, *Biochemistry*, 2003, **42**, 14752-14761.
42. P. LeMagueres, H. Im, J. Ebalunode, U. Strych, M. J. Benedik, J. M. Briggs, H. Kohn and K. L. Krause, *Biochemistry*, 2005, **44**, 1471-1481.

43. U. Strych, M. Davlieva, J. P. Longtin, E. L. Murphy, H. Im, M. J. Benedik and K. L. Krause, *BMC Microbiol.*, 2007, **7**.
44. D. Wu, T. Hu, L. Zhang, J. Chen, J. Du, J. Ding, H. Jiang and X. Shen, *Protein Sci.*, 2008, **17**, 1066-1076.
45. J.-L. Liu, X.-Q. Liu and Y.-W. Shi, *World J. Microbiol. Biotechnol.*, 2012, **28**, 267-274.
46. M. P. Lambert and F. C. Neuhaus, *J. Bacteriol*, 1972, **110**, 978-&.
47. J. L. Lynch and F. C. Neuhaus, *J. Bacteriol*, 1966, **91**, 449-460.
48. E. Wang and C. Walsh, *Biochemistry*, 1978, **17**, 1313-1321.
49. M. Ciustea, S. Mootien, A. E. Rosato, O. Perez, P. Cirillo, K. R. Yeung, M. Ledizet, M. H. Cynamon, P. A. Aristoff, R. A. Koski, P. A. Kaplan and K. G. Anthony, *Biochem. Pharmacol.*, 2012, **83**, 368-377.
50. C. Fan, P. C. Moews, C. T. Walsh and J. R. Knox, *Science*, 1994, **266**, 439-443.
51. C. Fan, I. S. Park, C. T. Walsh and J. R. Knox, *Biochemistry*, 1997, **36**, 2531-2538.
52. B. A. Ellsworth, N. J. Tom and P. A. Bartlett, *Chemistry & Biology*, 1996, **3**, 37-44.
53. M. Sova, G. Cadez, S. Turk, V. Majce, S. Polanc, S. Batson, A. J. Lloyd, D. I. Roper, C. W. G. Fishwick and S. Gobec, *Bioorg. Med. Chem. Lett.*, 2009, **19**, 1376-1379.
54. F. C. Neuhaus and J. L. Lynch, *Biochemistry*, 1964, **3**, 471-480.
55. G. A. Prosser and L. P. S. de Carvalho, *FEBS J.*, 2013, **280**, 1150-1166.
56. Y. G. Gu, A. S. Florjancic, R. F. Clark, T. Y. Zhang, C. S. Cooper, D. D. Anderson, C. G. Lerner, J. O. McCall, Y. N. Cai, C. L. Black-Schaefer, G. F. Stamper, P. J. Hajduk and B. A. Beutel, *Bioorg. Med. Chem. Lett.*, 2004, **14**, 267-270.
57. E. Z. Baum, S. M. Crespo-Carbone, A. Klinger, B. D. Foleno, I. Turchi, M. Macielag and K. Bush, *Antimicrob. Agents Chemother.*, 2007, **51**, 4420-4426.
58. E. Z. Baum, S. M. Crespo-Carbone, B. D. Foleno, L. D. Simon, J. Guillemont, M. Macielag and K. Bush, *Antimicrob. Agents Chemother.*, 2009, **53**, 3240-3247.

59. S. Sandhu, *PhD thesis*, University of Warwick, 2010.
60. C. Paradis-Bleau, A. Lloyd, F. Sanschagrin, T. Clarke, A. Blewett, T. D. H. Bugg and R. C. Levesque, *BMC Biochem.*, 2008, **9**.
61. Y. W. Yan, S. Munshi, B. Leiting, M. S. Anderson, J. Chrzas and Z. G. Chen, *J. Mol. Biol.*, 2000, **304**.
62. K. L. Longenecker, G. F. Stamper, P. J. Hajduk, E. H. Fry, C. G. Jakob, J. E. Harlan, R. Edalji, D. M. Bartley, K. A. Walter, L. R. Solomon, T. F. Holzman, Y. G. Gu, C. G. Lerner, B. A. Beutel and V. S. Stoll, *Protein Sci.*, 2005, **14**.
63. J. A. Bertrand, E. Fanchon, L. Martin, L. Chantalat, G. Auger, D. Blanot, J. van Heijenoort and O. Dideberg, *J. Mol. Biol.*, 2000, **301**.
64. O. O. Coker and P. Palittapongarnpim, *Afr. J. Microbiol. Res.*, 2011, **5**, 2555-2565.
65. C. M. Apfel, S. Takacs, M. Fountoulakis, M. Stieger and W. Keck, *J. Bacteriol*, 1999, **181**, 483-492.
66. Willough.E, Stroming.Jl and Y. Highasi, *J. Biol. Chem.*, 1972, **247**, 5113-&.
67. K. J. Stone and Stroming.Jl, *Proc. Natl. Acad. Sci. U.S.A.*, 1971, **68**, 3223-&.
68. R. Bernard, A. Guiseppi, M. Chippaux, M. Foglino and F. Denizot, *J. Bacteriol*, 2007, **189**, 8636-8642.
69. L. E. Zawadzke, P. Wu, L. Cook, L. Fan, M. Casperson, M. Kishnani, D. Calambur, S. J. Hofstead and R. Padmanabha, *Anal. Biochem.*, 2003, **314**, 243-252.
70. A. L. Lovering, S. S. Safadi and N. C. J. Strynadka, *Annu. Rev. Biochem*, 2012, **81**, 451-478.
71. M. Crouvoisier, D. Mengin-Lecreulx and J. van Heijenoort, *FEBS Lett.*, 1999, **449**, 289-292.
72. L. Chen, H. Men, S. Ha, X. Y. Ye, L. Brunner, Y. Hu and S. Walker, *Biochemistry*, 2002, **41**, 6824-6833.
73. S. Ha, D. Walker, Y. G. Shi and S. Walker, *Protein Sci.*, 2000, **9**, 1045-1052.

74. Y. N. Hu, L. Chen, S. Ha, B. Gross, B. Falcone, D. Walker, M. Mokhtarzadeh and S. Walker, *Proc. Natl. Acad. Sci. U.S.A.*, 2003, **100**, 845-849.
75. K. Brown, S. C. M. Vial, N. Dedi, J. Westcott, S. Scally, T. D. H. Bugg, P. A. Charlton and G. M. T. Cheetham, *Protein Pept. Lett.*, 2013, **20**, 1002-1008.
76. X. Fang, K. Tiyanont, Y. Zhang, J. Wanner, D. Boger and S. Walker, *Mol. Biosyst.*, 2006, **2**, 69-76.
77. M. C. Lo, H. Men, A. Branstrom, J. Helm, N. Yao, R. Goldman and S. Walker, *J. Am. Chem. Soc.*, 2000, **122**, 3540-3541.
78. J. S. Helm, L. Chen and S. Walker, *J. Am. Chem. Soc.*, 2002, **124**, 13970-13971.
79. C. C. Johnson, S. Taylor, P. Pitsakis, P. May and M. E. Levison, *Antimicrob. Agents Chemother.*, 1992, **36**, 2342-2345.
80. W. Brumfitt, P. A. C. Maple and J. M. T. Hamiltonmiller, *Drugs under Experimental and Clinical Research*, 1990, **16**, 377-383.
81. T. Pelaez, L. Alcala, R. Alonso, A. Martin-Lopez, V. Garcia-Arias, M. Marin and E. Bouza, *Antimicrob. Agents Chemother.*, 2005, **49**, 1157-1159.
82. J. W. Schmidt, A. Greenough, M. Burns, A. E. Luteran and D. G. McCafferty, *FEMS Microbiol. Lett.*, 2010, **310**, 104-111.
83. J. S. Helm, Y. N. Hu, L. Chen, B. Gross and S. Walker, *J. Am. Chem. Soc.*, 2003, **125**, 11168-11169.
84. Y. Hu, J. S. Heim, L. Chen, C. Ginsberg, B. Gross, B. Kraybill, K. Tiyanont, X. Fang, T. Wu and S. Walker, *Chemistry & Biology*, 2004, **11**, 703-711.
85. A. E. Trunkfield, S. S. Gurcha, G. S. Besra and T. D. H. Bugg, *Bioorg. Med. Chem.*, 2010, **18**, 2651-2663.
86. J. J. Li and T. D. H. Bugg, *Chem. Commun.*, 2004, 182-183.
87. D. Patin, H. Barreteau, G. Auger, S. Magnet, M. Crouvoisier, A. Bouhss, T. Touze, M. Arthur, D. Mengin-Lecreulx and D. Blanot, *Biochimie*, 2012, **94**, 985-990.

88. T. Touze, H. Barreteau, M. El Ghachi, A. Bouhss, A. Barneoud-Arnoulet, D. Patin, E. Sacco, D. Blanot, M. Arthur, D. Duche, R. Lloubes and D. Mengin-Lecreulx, *Biochem. Soc. Trans.*, 2012, **40**, 1522-1527.
89. E. Breukink, H. E. van Heusden, P. J. Vollmerhaus, E. Swiezewska, L. Brunner, S. Walker, A. J. R. Heck and B. de Kruijff, *J. Biol. Chem.*, 2003, **278**, 19898-19903.
90. T. Schneider, T. Kruse, R. Wimmer, I. Wiedemann, V. Sass, U. Pag, A. Jansen, A. K. Nielsen, P. H. Mygind, D. S. Ravents, S. Neve, B. Ravn, A. Bonvin, L. De Maria, A. S. Andersen, L. K. Gammelgaard, H. G. Sahl and H. H. Kristensen, *Science*, 2010, **328**, 1168-1172.
91. K. Mandal, B. L. Pentelute, V. Tereshko, V. Thammavongsa, O. Schneewind, A. A. Kossiakoff and S. B. H. Kent, *Protein Sci.*, 2009, **18**, 1146-1154.
92. A. J. Lloyd, A. M. Gilbey, A. M. Blewett, G. De Pascale, A. El Zoeiby, R. C. Levesque, A. C. Catherwood, A. Tomasz, T. D. H. Bugg, D. I. Roper and C. G. Dowson, *J. Biol. Chem.*, 2008, **283**, 6402-6417.
93. G. De Pascale, A. J. Lloyd, J. A. Schouten, A. M. Gilbey, D. I. Roper, C. G. Dowson and T. D. H. Bugg, *J. Biol. Chem.*, 2008, **283**, 34571-34579.
94. S. R. Filipe and A. Tomasz, *Proc. Natl. Acad. Sci. U.S.A.*, 2000, **97**, 4891-4896.
95. U. Kopp, M. Roos, J. Wecke and H. Labischinski, *Microbial Drug Resistance*, 1996, **2**, 29-41.
96. E. Cressina, A. J. Lloyd, G. De Pascale, D. I. Roper, C. G. Dowson and T. D. H. Bugg, *Bioorg. Med. Chem. Lett.*, 2007, **17**, 4654-4656.
97. M. Chemama, M. Fonvielle, R. Villet, M. Arthur, J.-M. Valery and M. Etheve-Quelquejeu, *J. Am. Chem. Soc.*, 2007, **129**, 12642-12643.
98. V. van Dam, R. Sijbrandi, M. Kol, E. Swiezewska, B. de Kruijff and E. Breukink, *Mol. Microbiol.*, 2007, **64**, 1105-1114.
99. A. L. Lovering, L. H. de Castro, D. Lim and N. C. J. Strynadka, *Science*, 2007, **315**, 1402-1405.

100. R. C. Goldman, E. R. Baizman, A. A. Branstrom and C. B. Longley, *Bioorg. Med. Chem. Lett.*, 2000, **10**, 2251-2254.
101. Y. Van Heijenoort, M. Derrien and J. Van Heijenoort, *FEBS Lett.*, 1978, **89**, 141-144.
102. H.-W. Shih, K.-T. Chen, S.-K. Chen, C.-Y. Huang, T.-J. R. Cheng, C. Ma, C.-H. Wong and W.-C. Cheng, *Org. Biomol. Chem.*, 2010, **8**, 2586-2593.
103. E. R. Baizman, A. A. Branstrom, C. B. Longley, N. Allanson, M. J. Sofia, D. Gange and R. C. Goldman, *Microbiology-Uk*, 2000, **146**, 3129-3140.
104. K. Hiramatsu and H. Hanaki, *Curr. Opin. Infect. Dis.*, 1998, **11**, 653-658.
105. L. Z. Cui, A. Iwamoto, J. Q. Lian, H. M. Neoh, T. Maruyama, Y. Horikawa and K. Hiramatsu, *Antimicrob. Agents Chemother.*, 2006, **50**, 428-438.
106. L. Chen, D. Walker, B. Sun, Y. Hu, S. Walker and D. Kahne, *Proc. Natl. Acad. Sci. U.S.A.*, 2003, **100**, 5658-5663.
107. R. S. Roy, P. Yang, S. Kodali, Y. S. Xiong, R. M. Kim, P. R. Griffin, H. R. Onishi, J. Kohler, L. L. Silver and K. Chapman, *Chemistry & Biology*, 2001, **8**, 1095-1106.
108. B. Glauner, J. V. Holtje and U. Schwarz, *J. Biol. Chem.*, 1988, **263**, 10088-10095.
109. Y. Michelbriand, *Comptes Rendus Des Seances De La Societe De Biologie Et De Ses Filiales*, 1978, **172**, 609-627.
110. D. F. J. Brown and P. E. Reynolds, *FEBS Lett.*, 1980, **122**, 275-278.
111. D. A. Leonard, R. A. Bonomo and R. A. Powers, *Acc. Chem. Res.*, 2013, **46**, 2407-2415.
112. J. C. J. Barna and D. H. Williams, *Annu. Rev. Microbiol.*, 1984, **38**, 339-357.
113. V. Vinatier, C. B. Blakey, D. Braddick, B. R. G. Johnson, S. D. Evans and T. D. H. Bugg, *Chem. Commun.*, 2009, 4037-4039.
114. J. S. Anderson and J. L. Strominger, *Biochem. Biophys. Res. Commun.*, 1965, **21**, 516-521.

115. W. G. Struve and F. C. Neuhaus, *Biochem. Biophys. Res. Commun.*, 1965, **18**, 6-12.
116. W. G. Struve, R. K. Sinha and F. C. Neuhaus, *Biochemistry*, 1966, **5**, 82-&.
117. M. Ikeda, M. Wachi, H. K. Jung, F. Ishino and M. Matsushashi, *J. Bacteriol*, 1991, **173**, 1021-1026.
118. J. M. C. Mondego, J. L. Simoes-Araujo, D. E. de Oliveira and M. Alves-Ferreira, *Plant Science*, 2003, **164**, 323-331.
119. D. S. Boyle and W. D. Donachie, *J. Bacteriol*, 1998, **180**, 6429-6432.
120. J. A. Thanassi, S. L. Hartman-Neumann, T. J. Dougherty, B. A. Dougherty and M. J. Pucci, *Nucleic Acids Res.*, 2002, **30**, 3152-3162.
121. Y. Van Heijenoort, M. Gomez, M. Derrien, J. Ayala and J. Van Heijenoort, *J. Bacteriol*, 1992, **174**, 3549-3557.
122. B. Soldo, V. Lazarevic and D. Karamata, *Microbiology-Sgm*, 2002, **148**, 2079-2087.
123. J. Lehrer, K. A. Vigeant, L. D. Tatar and M. A. Valvano, *J. Bacteriol*, 2007, **189**, 2618-2628.
124. M. S. Anderson, S. S. Eveland and N. P. J. Price, *FEMS Microbiol. Lett.*, 2000, **191**, 169-175.
125. T. D. H. Bugg and P. E. Brandish, *FEMS Microbiol. Lett.*, 1994, **119**, 255-262.
126. M. A. Lehrman, *Glycobiology*, 1994, **4**, 768-771.
127. A. R. Dal Nogare, N. Dan and M. A. Lehrman, *Glycobiology*, 1998, **8**, 625-632.
128. M. G. J. Heydanek and F. C. Neuhaus, *Biochemistry*, 1969, **8**, 1474-1481.
129. A. Bouhss, D. Mengin-Lecreulx, D. Le Beller and J. van Heijenoort, *Mol. Microbiol.*, 1999, **34**, 576-585.
130. A. J. Lloyd, P. E. Brandish, A. M. Gilbey and T. D. H. Bugg, *J. Bacteriol*, 2004, **186**, 1747-1757.
131. M. G. J. Heydanek, W. G. Struve and F. C. Neuhaus, *Biochemistry*, 1969, **8**, 1214-1221.

132. M. G. Heydanek, R. Linzer, D. D. Pless and F. C. Neuhaus, *Biochemistry*, 1970, **9**, 3618-&.
133. A. Bouhss, M. Crouvoisier, D. Blanot and D. Mengin-Lecreulx, *J. Biol. Chem.*, 2004, **279**, 29974-29980.
134. P. F. Marrero, C. D. Poulter and P. A. Edwards, *J. Biol. Chem.*, 1992, **267**, 21873-21878.
135. D. D. Pless and F. C. Neuhaus, *J. Biol. Chem.*, 1973, **248**, 1568-1576.
136. B. Al-Dabbagh, X. Henry, M. El Ghachi, G. Auger, D. Blanot, C. Parquet, D. Mengin-Lecreulx and A. Bouhss, *Biochemistry*, 2008, **47**, 8919-8928.
137. B. C. Chung, J. Zhao, R. A. Gillespie, D.-Y. Kwon, Z. Guan, J. Hong, P. Zhou and S.-Y. Lee, *Science*, 2013, **341**, 1012-1016.
138. A. O. Amer and M. A. Valvano, *Microbiology-Sgm*, 2001, **147**, 3015-3025.
139. Y. Ma, D. Muench, T. Schneider, H.-G. Sahl, A. Bouhss, U. Ghoshdastider, J. Wang, V. Doetsch, X. Wang and F. Bernhard, *J. Biol. Chem.*, 2011, **286**, 38844-38853.
140. W. P. Hammes and F. C. Neuhaus, *J. Biol. Chem.*, 1974, **249**, 3140-3150.
141. W. A. Weppner and F. C. Neuhaus, *J. Biol. Chem.*, 1977, **252**, 2296-2303.
142. P. E. Brandish, M. K. Burnham, J. T. Lonsdale, R. Southgate, M. Inukai and T. D. H. Bugg, *J. Biol. Chem.*, 1996, **271**, 7609-7614.
143. P. E. Brandish, K. Kimura, M. Inukai, R. Southgate, J. T. Lonsdale and T. D. H. Bugg, *Antimicrob. Agents Chemother.*, 1996, **40**, 1640-1644.
144. T. Stachyra, C. Dini, P. Ferrari, A. Bouhss, J. van Heijenoort, D. Mengin-Lecreulx, D. Blanot, J. Biton and D. Le Beller, *Antimicrob. Agents Chemother.*, 2004, **48**, 897-902.
145. S. Bagga, *PhD thesis*, University of Warwick, 2004.
146. J. A. Schouten, S. Bagga, A. J. Lloyd, G. Pascale, C. G. Dowson, D. I. Roper and T. D. H. Bugg, *Mol. Biosystems*, 2006, **2**, 484-491.

147. S. M. Solapure, P. Raphael, C. N. Gayathri, S. P. Barde, B. Chandrakala, K. S. Das and S. M. de Sousa, *J. Biomol. Screen.*, 2005, **10**, 149-156.
148. A. A. Branstrom, S. Midha, C. B. Longley, K. Han, E. R. Baizman and H. R. Axelrod, *Anal. Biochem.*, 2000, **280**, 315-319.
149. S. Ravishankar, V. P. Kumar, B. Chandrakala, R. K. Jha, S. M. Solapure and S. M. de Sousa, *Antimicrob. Agents Chemother.*, 2005, **49**, 1410-1418.
150. Takatsuk.A, K. Arima and G. Tamura, *J. Antibiot.*, 1971, **24**, 215-&.
151. Takatsuk.A and G. Tamura, *J. Antibiot.*, 1971, **24**, 224-&.
152. A. Banerjee, J.-Y. Lang, M.-C. Hung, K. Sengupta, S. K. Banerjee, K. Baksi and D. K. Banerjee, *J. Biol. Chem.*, 2011, **286**, 29127-29138.
153. A. Heifetz, R. W. Keenan and A. D. Elbein, *Biochemistry*, 1979, **18**, 2186-2192.
154. A. G. Myers, D. Y. Gin and D. H. Rogers, *J. Am. Chem. Soc.*, 1994, **116**, 4697-4718.
155. F. J. Wyszynski, S. S. Lee, T. Yabe, H. Wang, J. P. Gomez-Escribano, M. J. Bibb, S. J. Lee, G. J. Davies and B. G. Davis, *Nature Chemistry*, 2012, **4**, 539-546.
156. M. Winn, R. J. M. Goss, K. Kimura and T. D. H. Bugg, *Nat. Prod. Rep.*, 2010, **27**, 279-304.
157. M. Inukai, F. Isono, S. Takahashi, R. Enokita, Y. Sakaida and T. Haneishi, *J. Antibiot.*, 1989, **42**, 662-666.
158. F. Isono, M. Inukai, S. Takahashi, T. Haneishi, T. Kinoshita and H. Kuwano, *J. Antibiot.*, 1989, **42**, 667-673.
159. F. Isono, T. Katayama, M. Inukai and T. Haneishi, *J. Antibiot.*, 1989, **42**, 674-679.
160. F. Isono and M. Inukai, *Antimicrob. Agents Chemother.*, 1991, **35**, 234-236.
161. M. Inukai, F. Isono and A. Takatsuki, *Antimicrob. Agents Chemother.*, 1993, **37**, 980-983.
162. F. Isono, Y. Sakaida, S. Takahashi, T. Kinoshita, T. Nakamura and M. Inukai, *J. Antibiot.*, 1993, **46**, 1203-1207.

163. J. P. Karwowski, M. Jackson, R. J. Theriault, R. H. Chen, G. J. Barlow and M. L. Maus, *J. Antibiot.*, 1989, **42**, 506-511.
164. R. H. Chen, A. M. Buko, D. N. Whittern and J. B. McAlpine, *J. Antibiot.*, 1989, **42**, 512-520.
165. P. B. Fernandes, R. N. Swanson, D. J. Hardy, C. W. Hanson, L. Coen, R. R. Rasmussen and R. H. Chen, *J. Antibiot.*, 1989, **42**, 521-526.
166. R. M. Fronko, J. C. Lee, J. G. Galazzo, S. Chamberland, F. Malouin and M. D. Lee, *J. Antibiot.*, 2000, **53**, 1405-1410.
167. V. J. Lee and S. J. Hecker, *Med. Res. Rev.*, 1999, **19**, 521-542.
168. C. G. Boojamra, R. C. Lemoine, J. C. Lee, R. Leger, K. A. Stein, N. G. Vernier, A. Magon, O. Lomovskaya, P. K. Martin, S. Chamberland, M. D. Lee, S. J. Hecker and V. J. Lee, *J. Am. Chem. Soc.*, 2001, **123**, 870-874.
169. W. Zhang, B. Ostash and C. T. Walsh, *Proc. Natl. Acad. Sci. U.S.A.*, 2010, **107**, 16828-16833.
170. S. Chatterjee, S. R. Nadkarni, E. K. S. Vijayakumar, M. V. Patel, B. N. Ganguli, H. W. Fehlhaber and L. Vertesy, *J. Antibiot.*, 1994, **47**, 595-598.
171. Y. Xie, R. Chen, S. Si, C. Sun and H. Xu, *J. Antibiot.*, 2007, **60**, 158-161.
172. Y. Xie, H. Xu, S. Si, C. Sun and R. Chen, *J. Antibiot.*, 2008, **61**, 237-240.
173. B. Gust, K. Eitel and X. Tang, *Biol. Chem.*, 2013, **394**, 251-259.
174. S. Siebenberg, L. Kaysser, E. Wemakor, L. Heide, B. Gust and B. Kammerer, *Rapid Commun. Mass Spectrom.*, 2011, **25**, 495-502.
175. K. Isono, M. Uramoto, H. Kusakabe, K. I. Kimura, K. Izaki, C. C. Nelson and J. A. McCloskey, *J. Antibiot.*, 1985, **38**, 1617-1621.
176. M. Muroi, K. I. Kimura, H. Osada, M. Inukai and A. Takatsuki, *J. Antibiot.*, 1997, **50**, 103-104.
177. L. Kaysser, L. Lutsch, S. Siebenberg, E. Wemakor, B. Kammerer and B. Gust, *J. Biol. Chem.*, 2009, **284**, 14987-14996.
178. L. Kaysser, S. Siebenberg, B. Kammerer and B. Gust, *Chembiochem*, 2010, **11**, 191-196.

179. L. Kaysser, E. Wemakor, S. Siebenberg, J. A. Salas, J. K. Sohng, B. Kammerer and B. Gust, *Appl. Environ. Microbiol.*, 2010, **76**, 4008-4018.
180. S. Hirano, S. Ichikawa and A. Matsuda, *J. Org. Chem.*, 2008, **73**, 569-577.
181. Y. Ishizaki, C. Hayashi, K. Inoue, M. Igarashi, Y. Takahashi, V. Pujari, D. C. Crick, P. J. Brennan and A. Nomoto, *The J. Biol. Chem.*, 2013, **288**, 30309-30319.
182. Y. Takahashi, M. Igarashi, T. Miyake, H. Soutome, K. Ishikawa, Y. Komatsuki, Y. Koyama, N. Nakagawa, S. Hattori, K. Inoue, N. Doi and Y. Akamatsu, *J. Antibiot.*, 2013, **66**, 171-178.
183. J. Engohang-Ndong, *Expert Opin. Invest. Drugs*, 2012, **21**, 1789-1800.
184. J. C. Palomino and A. Martin, *Curr. Med. Chem.*, 2013, **20**, 3785-3796.
185. J. J. Salomon, P. Galeron, N. Schulte, P. R. Morow, D. Severynse-Stevens, H. Huwer, N. Daum, C.-M. Lehr, A. J. Hickey and C. Ehrhardt, *Therapeutic delivery*, 2013, **4**, 915-923.
186. L. A. McDonald, L. R. Barbieri, G. T. Carter, E. Lenoy, J. Lotvin, P. J. Petersen, M. M. Siegel, G. Singh and R. T. Williamson, *J. Am. Chem. Soc.*, 2002, **124**, 10260-10261.
187. T. Tanino, B. Al-Dabbagh, D. Mengin-Lecreulx, A. Bouhss, H. Oyama, S. Ichikawa and A. Matsuda, *J. Med. Chem.*, 2011, **54**, 8421-8439.
188. H. Yamaguchi, S. Sato, S. Yoshida, K. Takada, M. Itoh, H. Seto and N. Otake, *J. Antibiot.*, 1986, **39**, 1047-1053.
189. H. Seto, N. Otake, S. Sato, H. Yamaguchi, K. Takada, M. Itoh, H. S. M. Lu and J. Clardy, *Tetrahedron Lett.*, 1988, **29**, 2343-2346.
190. Y. Muramatsu, T. Ohnuki, M. M. Ishii, M. Kizuka, R. Enokita, S. Miyakoshi, T. Takatsu and M. Inukai, *J. Antibiot.*, 2004, **57**, 639-646.
191. H. Hotoda, M. Furukawa, M. Daigo, K. Murayama, M. Kaneko, Y. Muramatsu, M. M. Ishii, S. Miyakoshi, T. Takatsu, M. Inukai, M. Kakuta, T. Abe, T. Harasaki, T. Fukuoka, Y. Utsui and S. Ohya, *Bioorg. Med. Chem. Lett.*, 2003, **13**, 2829-2832.
192. Y. Muramatsu, M. M. Ishii and M. Inukai, *J. Antibiot.*, 2003, **56**, 253-258.

193. Y. Muramatsu, S. Miyakoshi, Y. Ogawa, T. Ohnuki, M. M. Ishii, M. Arai, T. Takatsu and M. Inukai, *J. Antibiot.*, 2003, **56**, 259-267.
194. H. Hotoda, M. Daigo, M. Furukawa, K. Murayama, C. A. Hasegawa, M. Kaneko, Y. Muramatsu, M. M. Ishii, S. Miyakoshi, T. Takatsu, M. Inukai, M. Kakuta, T. Abe, T. Fukuoka, Y. Utsui and S. Ohya, *Bioorg. Med. Chem. Lett.*, 2003, **13**, 2833-2836.
195. R. Young, I. N. Wang and W. D. Roof, *Trends Microbiol.*, 2000, **8**, 120-128.
196. A. Witte, U. Blasi, G. Halfmann, M. Szostak, G. Wanner and W. Lubitz, *Biochimie*, 1990, **72**, 191-200.
197. T. G. Bernhardt, W. D. Roof and R. Young, *Proc. Natl. Acad. Sci. U.S.A.*, 2000, **97**, 4297-4302.
198. T. G. Bernhardt, D. K. Struck and R. Young, *J. Biol. Chem.*, 2001, **276**, 6093-6097.
199. T. G. Bernhardt, W. D. Roof and R. Young, *Mol. Microbiol.*, 2002, **45**, 99-108.
200. S. Mendel, J. M. Holbourn, J. A. Schouten and T. D. H. Bugg, *Microbiology*, 2006, **152**, 2959-2967.
201. H. Tanaka, R. Oiwa, S. Matsukura and S. Omura, *Biochem. Biophys. Res. Commun.*, 1979, **86**, 902-908.
202. H. Tanaka, Y. Iwai, R. Oiwa, S. Shinohara, S. Shimizu, T. Oka and S. Omura, *Biochim. Biophys. Acta*, 1977, **497**, 633-640.
203. D. K. Banerjee, *J. Biol. Chem.*, 1989, **264**, 2024-2028.
204. L. Vertesy, E. Ehlers, H. Kogler, M. Kurz, J. Meiwes, G. Seibert, M. Vogel and P. Hammann, *J. Antibiot.*, 2000, **53**, 816-827.
205. M. Saidijam, G. Psakis, J. L. Clough, J. Meuller, S. Suzuki, C. J. Hoyle, S. L. Palmer, S. M. Morrison, M. K. Pos, R. C. Essenberg, M. C. J. Maiden, A. Abu-Bakr, S. G. Baumberg, A. A. Neyfakh, J. K. Griffith, M. J. Stark, A. Ward, J. O'Reilly, N. G. Rutherford, M. K. Phillips-Jones and P. J. F. Henderson, *FEBS Lett.*, 2003, **555**, 170-175.
206. A. Adebisuyi and J. Foght, *Res. Microbiol.*, 2013, **164**, 172-180.
207. T. D. H. Bugg, *An Introduction to Enzyme and Coenzyme Chemistry*, Blackwell Science Ltd, 1997.

208. A. B. Shapiro, H. Jahic, N. Gao, L. Hajec and O. Rivin, *J. Biomol. Screen.*, 2012, **17**, 662-672.
209. G. Bringmann, R. Zagst, M. Schajfer, Y. E. Hallock, J. Cardellina IZ and M. R. Boyd, *Angew. Chem. Int. Ed. Engl*, 1993, **32**, 1190-1191.
210. K. P. Manfredi, J. W. Blunt, J. H. Cardellina, J. B. McMahon, L. L. Pannell, G. M. Cragg and M. R. Boyd, *J. Med. Chem.*, 1991, **34**, 3402-3405.
211. R. N. Okigbo, C. L. Anuagasi and J. E. Amadi, *Journal of Medicinal Plants Research*, 2009, **3**, 86-95.
212. E. L. White, W. R. Chao, L. J. Ross, D. W. Borhani, P. D. Hobbs, V. Upender and M. I. Dawson, *Arch. Biochem. Biophys.*, 1999, **365**, 25-30.
213. J. D. Deschamps, J. T. Gautschi, S. Whitman, T. A. Johnson, N. C. Gassner, P. Crews and T. R. Holman, *Bioorg. Med. Chem.*, 2007, **15**, 6900-6908.
214. J. M. Andrews, *J. Antimicrob. Chemother.*, 2001, **48**, 5-16.
215. M. R. Boyd, Y. F. Hallock, K. P. Manfredi, J. W. Blunt, J. B. McMahon, R. W. Buckheit, G. Bringmann, M. Schaffer, G. M. Cragg, D. W. Thomas, J. G. Jato and J. H. Cardellina, *J. Med. Chem.*, 1994, **37**, 1740-1745.
216. Y. F. Hallock, K. P. Manfredi, J. R. Dai, J. H. Cardellina, R. J. Gulakowski, J. B. McMahon, M. Schaffer, M. Stahl, K. P. Gulden, G. Bringmann, G. Francois and M. R. Boyd, *J. Nat. Prod.*, 1997, **60**, 677-683.
217. S. Huang, T. B. Petersen and B. H. Lipshutz, *J. Am. Chem. Soc.*, 2010, **132**, 14021-14023.
218. G. Francois, G. Timperman, T. Steenackers, L. A. Assi, J. Holenz and G. Bringmann, *Parasitol. Res.*, 1997, **83**, 673-679.
219. G. Bringmann, G. Zhang, T. Buettner, G. Bauckmann, T. Kupfer, H. Braunschweig, R. Brun and V. Mudogo, *Chem. Eur. J.*, 2013, **19**, 916-923.
220. T. R. Hoye, M. Z. Chen, B. Hoang, L. Mi and O. P. Priest, *J. Org. Chem.*, 1999, **64**, 7184-7201.

221. V. Upender, D. J. Pollart, J. Liu, P. D. Hobbs, C. Olsen, W. R. Chao, B. Bowden, J. L. Crase, D. W. Thomas, A. Pandey, J. A. Lawson and M. I. Dawson, *J. Heterocycl. Chem.*, 1996, **33**, 1371-1384.
222. J. B. McMahon, M. J. Currens, R. J. Gulakowski, R. W. Buckheit, C. Lackmansmith, Y. F. Hallock and M. R. Boyd, *Antimicrob. Agents Chemother.*, 1995, **39**, 484-488.
223. T. A. Steitz, L. A. Kohlstaedt, J. Wang, J. M. Friedman and P. A. Rice, *Science*, 1993, **259**, 295-295.
224. J. G. Supko and L. Malspeis, *Proceedings of the American Association for Cancer Research Annual Meeting*, 1994, **35**, 423-423.
225. G. M. Cragg, F. Katz, D. J. Newman and J. Rosenthal, *Nat. Prod. Rep.*, 2012, **29**, 1407-1423.
226. E. L. White, L. J. Ross, P. D. Hobbs, V. Upender and M. I. Dawson, *Anticancer Res.*, 1999, **19**, 1033-1035.
227. H. K. Wang, J. X. Xie, J. J. Chang, K. M. Hwang, S. Y. Liu, L. M. Ballas, J. B. Jiang and K. H. Lee, *J. Med. Chem.*, 1992, **35**, 2717-2721.
228. H. Mellor and P. J. Parker, *Biochem. J.*, 1998, **332**, 281-292.
229. E. Skrzypczak-Jankun, J. Jankun and A. Al-Senaidy, *Curr. Med. Chem.*, 2012, **19**, 5122-5127.
230. G. Bringmann, B. K. Lombe, C. Steinert, K. N. Ioset, R. Brun, F. Turini, G. Heubl and V. Mudogo, *Org. Lett.*, 2013, **15**, 2590-2593.
231. R. E. de Lima Procopio, I. R. da Silva, M. K. Martins, J. L. de Azevedo and J. M. de Araujo, *Braz. J. Infect. Dis.*, 2012, **16**, 466-471.
232. K. F. Chater, *Philos. Trans. R. Soc. London, Ser. B*, 2006, **361**, 761-768.
233. S. D. Bentley, K. F. Chater, A. M. Cerdeno-Tarraga, G. L. Challis, N. R. Thomson, K. D. James, D. E. Harris, M. A. Quail, H. Kieser, D. Harper, A. Bateman, S. Brown, G. Chandra, C. W. Chen, M. Collins, A. Cronin, A. Fraser, A. Goble, J. Hidalgo, T. Hornsby, S. Howarth, C. H. Huang, T. Kieser, L. Larke, L. Murphy, K. Oliver, S. O'Neil, E. Rabinowitsch, M. A. Rajandream, K. Rutherford, S. Rutter, K. Seeger, D. Saunders, S. Sharp, R. Squares, S. Squares, K. Taylor, T. Warren, A. Wietzorrek, J. Woodward, B. G. Barrell, J. Parkhill and D. A. Hopwood, *Nature*, 2002, **417**, 141-147.

234. Z. Tian, Q. Cheng, F. K. Yoshimoto, L. Lei, D. C. Lamb and F. P. Guengerich, *Arch. Biochem. Biophys.*, 2013, **530**, 101-107.
235. T. Kieser, M. J. Bibb, M. J. Buttner, K. F. Chater and D. A. Hopwood, *Practical Streptomyces Genetics*, The John Innes Foundation, 2000.
236. S. Horinouchi and T. Beppu, *Mol. Microbiol.*, 1994, **12**, 859-864.
237. D. W. Hood, R. Heidstra, U. K. Swoboda and D. A. Hodgson, *Gene*, 1992, **115**, 5-12.
238. R. Murakami, Y. Fujita, M. Kizuka, T. Kagawa, Y. Muramatsu, S. Miyakoshi, T. Takatsu and M. Inukai, *J. Antibiot.*, 2008, **61**, 537-544.
239. Y. Fujita, M. Kizuka, M. Funabashi, Y. Ogawa, T. Ishikawa, K. Nonaka and T. Takatsu, *J. Antibiot.*, 2011, **64**, 495-501.
240. J. D. Sidda and C. Corre, *Natural Product Biosynthesis by Microorganisms and Plants*, Pt C, 2012, **517**, 71-87.
241. A. P. Spork and C. Ducho, *Synlett*, 2013, 343-346.
242. L. Kaysser, K. Eitel, T. Tanino, S. Siebenberg, A. Matsuda, S. Ichikawa and B. Gust, *J. Biol. Chem.*, 2010, **285**, 12684-12694.
243. D. I. Roper, T. Huyton, A. Vagin and G. Dodson, *Proc. Natl. Acad. Sci. U.S.A.*, 2000, **97**, 8921-8925.
244. K. Bupp and J. Vanheijenoort, *J. Bacteriol*, 1993, **175**, 1841-1843.
245. V. L. Healy, I. A. D. Lessard, D. I. Roper, J. R. Knox and C. T. Walsh, *Chemistry & Biology*, 2000, **7**, R109-R119.
246. T. D. H. Bugg, S. Dutkamalen, M. Arthur, P. Courvalin and C. T. Walsh, *Biochemistry*, 1991, **30**, 2017-2021.
247. S. M. Solapure, C. N. Gayathri, K. Das, B. Chandrakala and S. M. De Sousa, *Abstr. InterSci. Conf. Antimicrob. Agents and Chemother.*, 2003, **43**, 252.
248. D. Maratea, K. Young and R. Young, *Gene*, 1985, **40**, 39-46.
249. K. J. Buckley and M. Hayashi, *Molecular & General Genetics*, 1986, **204**, 120-125.
250. S. Tanaka and W. M. Clemons, Jr., *Mol. Microbiol.*, 2012, **85**.
251. A. Cherkasov, K. Hilpert, H. Jenssen, C. D. Fjell, M. Waldbrook, S. C. Mullaly, R. Volkmer and R. E. W. Hancock, *ACS. Chem. Biol.*, 2008, **4**, 65-74.

252. J. L. Fox, *Nat. Biotechnol.*, 2013, **31**, 379-382.
253. M. A. Apponyi, T. L. Pukala, C. S. Brinkworth, V. M. Maselli, J. H. Bowie, M. J. Tyler, G. W. Booker, J. C. Wallace, J. A. Carver, F. Separovic, J. Doyle and L. E. Llewellyn, *Peptides*, 2004, **25**, 1035-1054.
254. K. A. Brogden, M. Ackermann, P. B. McCray and B. F. Tack, *Int. J. Antimicrob. Agents.*, 2003, **22**, 465-478.
255. R. E. W. Hancock, *Lancet. Infect. Dis.*, 2001, **1**, 156-164.
256. R. E. W. Hancock and H.-G. Sahl, *Nat. Biotechnol.*, 2006, **24**, 1551-1557.
257. R. E. W. Hancock, K. L. Brown and N. Mookherjee, *Immunobiology*, 2006, **211**, 315-322.
258. B. Findlay, G. G. Zhanel and F. Schweizer, *Antimicrob. Agents Chemother.*, 2010, **54**, 4049-4058.
259. E. A. Groisman, *Trends Microbiol.*, 1994, **2**, 444-449.
260. A. K. Marr, W. J. Gooderham and R. E. W. Hancock, *Curr. Opin. Pharmacol.*, 2006, **6**, 468-472.
261. M. Kesting, C. Pautke, D. Loeffelbein, F. Hoelzle, T. Muecke, K. D. Wolff, R. Hasler and L. Steinstraesser, *Journal of Cranio-Maxillofacial Surgery*, 2008, **36**, S39-S39.
262. R. S. Bullard, W. Gibson, S. K. Bose, J. K. Belgrave, A. C. Eaddy, C. J. Wright, D. J. Hazen-Martin, J. M. Lage, T. E. Keane, T. A. Ganz and C. D. Donald, *Molecular Immunology*, 2008, **45**, 839-848.
263. T. J. Falla, D. N. Karunaratne and R. E. W. Hancock, *J. Biol. Chem.*, 1996, **271**, 19298-19303.
264. B. Bommarius, H. Jenssen, M. Elliott, J. Kindrachuk, M. Pasupuleti, H. Gieren, K. E. Jaeger, R. E. W. Hancock and D. Kalman, *Peptides*, 2010, **31**, 1957-1965.
265. M. T. Rodolis, *PhD thesis*, University of Warwick, 2013.
266. J. Klovins, G. P. Overbeek, S. H. E. van den Worm, H. W. Ackermann and J. van Duin, *Journal of General Virology*, 2002, **83**, 1523-1533.
267. A. E. Trunkfield, *PhD thesis*, University of Warwick, 2008.

- 268. J. J. Roy, A. Lau and D. G. McFee, *Can. Med. Assoc. J.*, 1998, **158**, 471-471.
- 269. A. Rasooly and A. Weisz, *Antimicrob. Agents Chemother.*, 2002, **46**, 3650-3653.
- 270. M. H. Lyttle, T. G. Carter and R. M. Cook, *Org. Process Res. Dev.*, 2001, **5**, 45-49.
- 271. J. R. Heitz, *ACS Symposium Series; Light-activated pest control*, 1995, **616**, 1-16.
- 272. K. O. Willeford, T. A. Parker and S. V. Diehl, *J. Agric. Food. Chem.*, 1998, **46**, 1637-1641.
- 273. R. Rasooly, *FEMS Immunol. Med. Microbiol.*, 2005, **45**, 239-244.
- 274. D. A. Bergsten, *Light-Activated Pest Control*, 1995, **616**, 54-69.